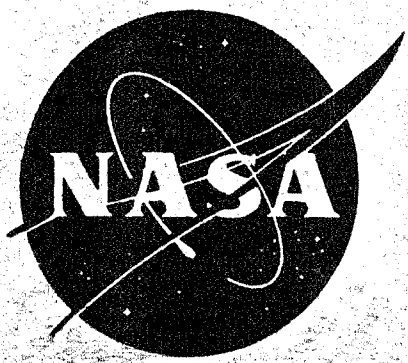


UNCLASSIFIED

AD NUMBER
ADB209341
NEW LIMITATION CHANGE
TO Approved for public release, distribution unlimited
FROM Distribution authorized to U.S. Gov't. agencies and their contractors; Administrative/Operational Use; 01 APR 1966. Other requests shall be referred to National Aeronautics and Space Administration, Attn: AFSS-A, Washington, DC 20546.
AUTHORITY
NASA TR Server Website

THIS PAGE IS UNCLASSIFIED

T  
NASA CR-54471  
4176-6014-S0000



INVESTIGATION OF RESIN SYSTEMS  
FOR  
IMPROVED ABLATIVE MATERIALS

by

"DTIC USERS ONLY"

H. R. Lubowitz, E. A. Burns and B. Dubrow

Prepared for

NATIONAL AERONAUTICS AND SPACE ADMINISTRATION

Contract NAS3-4188

19960419 036

DTIC QUALITY INSPECTED 1

**TRW** SYSTEMS

DEPARTMENT OF DEFENSE  
PLASTICS TECHNICAL EVALUATION CENTER  
ELCATON, MARYLAND, U.S.A.

89972

## NOTICE

This report was prepared as an account of Government sponsored work. Neither the United States, nor the National Aeronautics and Space Administration (NASA), nor any person acting on behalf of NASA:

- A.) Makes any warranty or representation, expressed or implied, with respect to the accuracy, completeness, or usefulness of the use of any information, apparatus, method, or process disclosed in this report may not infringe privately owned rights; or
- B.) Assumes any liabilities with respect to the use of, or for damages resulting from the use of any information, apparatus, method or process disclosed in this report.

As used above, "person acting on behalf of NASA" includes any employee or contractor of NASA, or employee of such contractor, to the extent that such employee or contractor of NASA, or employee of such contractor prepares, disseminates, or provides access to, any information pursuant to his employment or contract with NASA, or his employment with such contractor.

Requests for copies of this report should be referred to

National Aeronautics and Space Administration  
Office of Scientific and Technical Information  
Attention: AFSS-A  
Washington, D. C. 20546

FINAL REPORT

INVESTIGATION OF RESIN SYSTEMS  
FOR  
IMPROVED ABLATIVE MATERIALS

by

H. R. Lubowitz, E. A. Burns and B. Dubrow

Prepared for  
NATIONAL AERONAUTICS AND SPACE ADMINISTRATION

1 April 1966

CONTRACT NAS3-4188

Technical Management  
NASA Lewis Research Center  
Cleveland, Ohio  
Liquid Rocket Technology Branch  
Stephen M. Cohen

**TRW** SYSTEMS

## FOREWORD

This document constitutes the final report for the work accomplished between 19 June 1964 and 31 July 1965 by TRW Systems (formerly TRW Space Technology Laboratories) for the National Aeronautics and Space Administration, Lewis Research Center, under Contract NAS3-4188 on the Investigation of Resin Systems for Improved Ablative Materials.

The work was under the technical direction of Mr. Stephen M. Cohen of the Lewis Research Center, Cleveland, Ohio and the NASA Headquarters Project Manager was Mr. Frank E. Compitello.

The Chemistry Department of the Propulsion Laboratory, Mechanics Division was responsible for the work performed on this program. Mr. B. Dubrow, Manager, Chemistry Department provided overall program supervision, Dr. E. A. Burns was Program Manager and Mr. H. R. Lubowitz was Principal Investigator. Acknowledgement is made of the technical assistance provided during this program by the following TRW Systems personnel:

### Members of the Technical Staff

J. L. Blumenthal	Chemistry Department
P. I. Gold	Chemistry Department
M. H. Goodrow	Chemistry Department
H. M. Hoffman	Materials Engineering Department
J. R. Kliegel	Chemical Propulsion Technology Department
J. L. Reger	Chemistry Department
F. E. Romie	Propulsion Laboratory
M. C. Starr	Chemical Propulsion Technology Department
L. J. Van Nice	Chemistry Department

### Technical Support

G. G. Brown	Chemistry Department
G. B. Charlan	Chemistry Department
W. P. Kendrick	Chemistry Department
C. T. Weekley	Chemistry Department

INVESTIGATION OF RESIN SYSTEMS  
FOR  
IMPROVED ABLATIVE MATERIALS

by

H. R. Lubowitz, E. A. Burns and B. Dubrow

ABSTRACT

This final report describes the work performed to advance the state-of-the-art of resin matrices required for improved ablative materials for use with high energy fluorine-containing liquid propellant systems. This was accomplished through a comprehensive theoretical and experimental study which a) defined critical parameters controlling the effectiveness of resins in ablative systems, b) synthesized new resins and determined critical properties of new and modified resins, and c) recommended resins for future use.

The critical resin properties which influence the effectiveness of ablative composites were determined analytically in order that criteria could be established for the synthesis and property testing of new and modified resins. As a result of these studies, criteria were provided for directing and selecting promising areas of resin synthesis and modification. Several new polymer systems with improved properties were proposed, evaluated and recommended for future study. Poly(cyclized 1,2-polybutadiene) tolyl urethane ladder polymers, poly alkaline earth metal acrylates, phosphate bonded oxides, modified polyimides and several other organic and inorganic systems were conceived and/or evaluated during this program to meet the property requirements identified analytically.

CONTENTS

	Page
FOREWORD . . . . .	iii
ABSTRACT . . . . .	v
SUMMARY . . . . .	xvii
1.0 INTRODUCTION . . . . .	1
2.0 DEFINITION OF PROPERTIES FOR SELECTION OF RESINS . . . . .	3
2.1 General Thermophysical Evaluation of Ablator Performance . . . . .	3
2.2 Analytical Evaluation of Critical Thermal Properties . . . . .	7
2.3 Initial Selection of Candidate Resin Classes . . . . .	11
2.4 Analytical Determination of the Chemical Compatibility Between Candidate Resin Systems and Propellant Combustion Products . . . . .	12
2.4.1 Equilibrium Thermal Decomposition Studies . . . . .	12
2.4.2 Physical Properties of the Residues . . . . .	14
2.4.3 Definition of Engine Environment . . . . .	14
2.4.4 Equilibrium Reactions of Resin Residues with Propellant Gases . . . . .	15
2.4.4.1 The F <sub>2</sub> /H <sub>2</sub> Propellant Class . . . . .	18
2.4.4.2 The OF <sub>2</sub> /B <sub>2</sub> H <sub>6</sub> Propellant Class . . . . .	19
2.4.5 Equilibrium Considerations of Internal Chemical Reactions . . . . .	19
2.5 Guidelines and Criteria for Selection of Resins . . . . .	20
2.5.1 Equilibrium Propellant Considerations . . . . .	20
2.5.1.1 F <sub>2</sub> /H <sub>2</sub> Propellant Class . . . . .	20
2.5.1.2 OF <sub>2</sub> /B <sub>2</sub> H <sub>6</sub> Propellant Class . . . . .	21
2.5.2 Thermophysical Property Considerations . . . . .	22
2.5.3 Nonequilibrium Reaction Rate Considerations . . . . .	23
2.6 Selection of Candidate Resins for Synthesis . . . . .	24
3.0 SYNTHESIS AND PROPERTY DETERMINATION OF NEW RESINS . . . . .	27
3.1 High Carbon Epoxy Reference Formulations . . . . .	27
3.2 Carbon Rich Resins for F <sub>2</sub> /H <sub>2</sub> Propellant Class . . . . .	28
3.2.1 Selection of Cyclized Polybutadiene Urethane Ladder Polymers as a Candidate "Stiff" Hydrocarbon Resin Class . . . . .	28

	Page
3.2.2 Preparation of Poly (Cyclized 1,2-Polybutadiene) Tollyl Urethane . . . . .	31
3.3 Organo-Metallic and Inorganic Resins for Use with OF <sub>2</sub> /B <sub>2</sub> H <sub>6</sub> Propellant Class . . . . .	31
3.3.1 Poly Alkaline Earth Metal Acrylates . . . . .	33
3.3.2 Phosphate Bonded Oxides. . . . .	33
3.4 Additional Promising Candidate Resin Systems . . . . .	34
3.4.1 Polybenzimidazoles . . . . .	34
3.4.2 Polyimide Esters . . . . .	35
3.4.3 Polyimide Ethers . . . . .	36
3.4.4 Zirconium-Boron Polymers . . . . .	39
3.5 Property Determination . . . . .	40
3.5.1 Test Methods. . . . .	40
3.5.2 Property Test Results. . . . .	40
3.5.3 Discussion of Test Results. . . . .	46
4.0 RECOMMENDATIONS OF RESINS FOR FUTURE USE . . . . .	49
4.1 Methods of Preparation and Scale Up of Synthesis . . . . .	50
4.1.1 Cyclized Polybutadiene-Urethane Resins and Composites . . . . .	50
4.1.2 Poly Alkaline Earth Metal Acrylate Resins and Composites . . . . .	51
4.1.3 Phosphate Bonded Oxides. . . . .	52
4.1.4 "Stiff" Polymers . . . . .	52
4.2 Reproducibility of Preparation and Compatibility of New Resins with Fillers . . . . .	52
4.3 Recommendation for the Application of Selected Resins . . . . .	53
5.0 CONCLUSIONS. . . . .	55
6.0 NEW TECHNOLOGY . . . . .	57
6.1 Cyclized Polybutadiene Urethanes . . . . .	57
6.2 Cyclized Polyisoprene Urethanes . . . . .	58
6.3 Reinforced Structural Plastics . . . . .	58
6.4 High Temperature Adhesives . . . . .	59
6.5 Protective Coatings . . . . .	59
6.6 Polyimide Esters and Polyimide Ethers . . . . .	60
6.7 Poly Alkaline Earth Metal Acrylates . . . . .	60

CONTENTS (Continued)

	Page
APPENDICES	
A. THE CHARRING-RECESSION COMPUTER PROGRAM . . . . .	61
B. CRITERIA FOR INITIAL SELECTION OF CANDIDATE RESINS . . . . .	69
C. EQUILIBRIUM THERMAL DECOMPOSITION STUDIES OF CANDIDATE RESINS . . . . .	81
D. HIGH CARBON SPECIES ASSESSMENT . . . . .	95
E. GAS COMPOSITIONS AND FLAME TEMPERATURES FOR SELECTED PROPELLANT SYSTEMS . . . . .	103
F. EQUILIBRIUM CHEMICAL COMPATIBILITY EVALUATIONS . . . . .	115
G. SYNTHESIS OF CANDIDATE ABLATIVE RESINS . . . . .	129
H. PROPERTY DETERMINATION METHODS . . . . .	159
I. SYNTHESIS ROUTES AND STRUCTURE OF SELECTED STIFF POLYMERS . . . . .	177
J. PARAMETERS AFFECTING DRY BONDING ADHESION. . . . .	187
REFERENCES . . . . .	195
DISTRIBUTION . . . . .	197

ILLUSTRATIONS

	Page
1. Dependency of Backwall Temperature and Recession Rate on Significant Engine and Ablator Parameters . . . . .	4
2. Carbon Residue as a Function of Temperature for the Equilibrium Decomposition of Hydrocarbon and Fluorocarbon Systems. . . . .	16
3. Synthesis of Poly (Cyclized 1, 2-Polybutadiene) Tolyl Urethane . . . . .	30
4. Preparation of Poly Magnesium Acrylate . . . . .	34
5. Hypothesized Pyrolysis Intermediate Reaction of Polyimide Ester . . . . .	37
6. Proposed Synthesis Route to Polyimide-Polyester Copolymer Resins . . . . .	38
C-1. Equilibrium Total Condensables for a B-N Resin Containing Borazine Rings as a Function of Temperature. . . . .	83
C-2. Equilibrium Total Condensables for a Polysilarylene-siloxane Resin as a Function of Temperature . . . . .	87
C-3. Equilibrium Total Condensables for a Phenyl Silsesquioxane Resin as a Function of Temperature . . . . .	88
C-4. Equilibrium Total Condensables for a Silazine Resin as a Function of Temperature . . . . .	90
D-1. Heat Capacity and Enthalpy of H <sub>2</sub> as a Function of Temperature . . . . .	98
D-2. Heat Capacity and Enthalpy of C <sub>2</sub> H as a Function of Temperature. . . . .	99
D-3. Heat Capacity and Enthalpy of C <sub>3</sub> H as a Function of Temperature . . . . .	100
D-4. Heat Capacity and Enthalpy of C <sub>4</sub> H as a Function of Temperature . . . . .	101
D-5. Heat Capacity and Enthalpy of C <sub>2</sub> H <sub>2</sub> as a Function of Temperature . . . . .	102
G-1. Synthesis of Poly (Cyclized 1, 2-Polybutadiene) Tolyl Urethane . . . . .	136

ILLUSTRATIONS (Continued)

	Page
G-2. Infrared Spectrum of 1, 2-Polybutadiene Diol. . . . .	139
G-3. Infrared Spectrum of Poly (Cyclized 1, 2-Polybutadiene) Tolyl Urethane Mixture No. 28C. . . . .	140
G-4. Infrared Spectrum of Poly (Cyclized 1, 2-Polybutadiene) Tolyl Urethane Mixture No. 25B. . . . .	141
G-5. Infrared Spectrum of Poly (Cyclized 1, 2-Polybutadiene) Tolyl Urethane Mixture No. 18A . . . . .	142
G-6. Differential Calorimetric Scan of Poly (Cyclized 1, 2- Polybutadiene) Tolyl Urethane . . . . .	146
G-7. Schematic Diagram of the Vacuum Hot Press . . . . .	154
G-8. Interior View of the Hot Press Die Assembly . . . . .	155
G-9. Hot Press Die Assembly in the Press and Associated Controlling and Monitoring Equipment . . . . .	156
H-1. Schematic Diagram of the Thermal Conductivity Apparatus . . . . .	160
H-2. Thermal Conductivity Apparatus with Top Insulation Removed and Main Sample Heater in Hand . . . . .	161
H-3. Perkin-Elmer Model DSC-1 Differential Scan Calorimeter . . . . .	163
H-4. Propellant Exhaust Environmental Test (PEET) Apparatus . . . . .	165
H-5. Assembled PEET Sample Holder and Inert Gas Chamber. . . . .	167
H-6. Disassembled PEET Sample Holder and Inert Gas Chamber Showing a Target Specimen . . . . .	168
H-7. F <sub>2</sub> /H <sub>2</sub> Flame Temperatures as a Function of Volume Mixture Ratio . . . . .	171
H-8. Beckman Model 930 Air Comparison Pycnometer. . . . .	174
H-9. Principle of Operation of the Air Comparison Pycnometer . . . . .	175
J-1. Dependence of Joint Strength on Temperature of Joint Formation of a Copolymer System . . . . .	190
J-2. Dependence of Joint Strength on Temperature of Joint Formation of a Homopolymer System . . . . .	191

TABLES

	Page
I Effect of 20% Increase in Selected Variables on Backwall Temperature and Total Recession . . . . .	10
II Candidate Resin Classes Under Consideration . . . . .	13
III Representative Empirical Formulae of Typical Resin Compounds Used in Analytical Equilibrium Thermal Decomposition Studies . . . . .	15
IV Estimated Density and Porosity of Residues . . . . .	17
V Equilibrium Reaction of Carbon, Silicon Carbide and Boron Nitride with HF . . . . .	18
VI Additive Consumption . . . . .	21
VII Enthalpy Changes Due to Material Addition at 5500 <sup>o</sup> R and 100 psia . . . . .	26
VIII Carbon Content of Various Resins . . . . .	31
IX Candidate Resin Properties . . . . .	29
X Properties of Laminates . . . . .	42
XI Filled Resin Properties . . . . .	44
XII Metal Acrylate-Epon 828 Properties . . . . .	45
XIII Refractory Filler Material Properties . . . . .	47
XIV Preparation Format of Candidate Resins and Composites . . . . .	51
A-I Reference Case Parameter Values . . . . .	65
A-II Preliminary Results from the Charring Ablation Computer Program . . . . .	66
A-III Influence Coefficients . . . . .	67
C-I Equilibrium Decomposition Products Molar Composition for a B-N Type Resin with Empirical Formula C <sub>6</sub> H <sub>15</sub> B <sub>2</sub> N <sub>3</sub>	82
C-II Equilibrium Decomposition Products Molar Composition for a Si-O Type Resin with Empirical Formula C <sub>8</sub> H <sub>10</sub> SiO <sub>2</sub>	85

TABLES (Continued)

	Page
C-III Equilibrium Decomposition Products Molar Composition for a Si-O Type Resin with Empirical Formula of $C_{12}H_{10}Si_2O_3$ . . . . .	86
C-IV Equilibrium Decomposition Products Molar Composition for an Si-N Type Resin with Empirical Formula of $C_{13}H_{13}SiN$ . . . . .	89
C-V Equilibrium Decomposition Products Molar Composition for a Hydrocarbon Type Resin with Empirical Formula of $C_5H_4O$ . . . . .	91
C-VI Equilibrium Decomposition Products Molar Composition for a Hydrocarbon Type Resin with Empirical Formula of $C_5H_3N$ . . . . .	91
C-VII Equilibrium Decomposition Products Molar Composition for a Hydrocarbon Type Resin with Empirical Formula of $C_8H_3O_2N$ . . . . .	92
C-VIII Equilibrium Decomposition Products Molar Composition for a Hydrocarbon Type Resin with Empirical Formula of $C_{84}H_{120}O_2N$ . . . . .	93
C-IX Equilibrium Decomposition Products Molar Composition for a Fluorocarbon Type Resin with Empirical Formula of $CF_2$ . . . . .	94
C-X Equilibrium Decomposition Products Molar Composition for a Fluorocarbon Type Resin with Empirical Formula of $C_3F_2$ . . . . .	94
D-I Heat Capacity Maxima in the Data of Duff and Bauer . . . . .	97
E-I Propellant System: FLOX (20 $F_2$ - 80 $O_2$ )/MMH . . . . .	104
E-II Propellant System: FLOX (40 $F_2$ - 60 $O_2$ )/MMH . . . . .	105
E-III Propellant System: FLOX (60 $F_2$ - 40 $O_2$ )/MMH . . . . .	106
E-IV Propellant System: FLOX (80 $F_2$ - 20 $O_2$ )/MMH . . . . .	107
E-V Propellant System: $F_2$ /MMH . . . . .	108
E-VI Propellant System: $F_2$ /MMH . . . . .	109
E-VII Propellant System: $F_2/N_2H_4$ . . . . .	110
E-VIII Propellant System: $F_2/NH_3$ . . . . .	111

TABLES (Continued)

	Page
E-IX Propellant System: $F_2/H_2$ . . . . .	112
E-X Propellant System: $F_2/H_2$ . . . . .	113
E-XI Propellant System: $OF_2/B_2H_6$ . . . . .	114
F-I Equilibrium Reactions of Carbon and Silicon Carbide with $OF_2/B_2H_6$ Gases with $OF_2/B_2H_6$ at MR = 3.5, P = 100 psia . . . . .	116
F-II Equilibrium Reaction of Carbon, Silicon Carbide and Boron Nitride with BOF. . . . .	117
F-III Gas Composition for 50 Grams of Propellant Gas Only and in Equilibrium with Metal Oxides at 5500 °R and 100 psia . . . . .	119
F-IV Gas Composition for 50 Grams of Propellant Gas Only and in Equilibrium with 50 Grams of Ablator at 5500 °R and 100 psia . . . . .	120
F-V Net Reactions of Alumina with $OF_2/B_2H_6$ Propellant Gas (MR = 3.5) at 5500 °R and 100 psia . . . . .	122
F-VI Net Reactions of Magnesia with $OF_2/B_2H_6$ Propellant Gas (MR = 3.5) at 5500 °R and 100 psia . . . . .	123
F-VII Net Reactions of Beryllia with $OF_2/B_2H_6$ Propellant Gas (MR = 3.5) at 5500 °R and 100 psia . . . . .	124
F-VIII Net Reactions of Calcia with $OF_2/B_2H_6$ Propellant Gas (MR = 3.5) at 5500 °R and 100 psia . . . . .	125
F-IX Net Reactions of Zirconia with $OF_2/B_2H_6$ Propellant Gas (MR = 3.5) at 5500 °R and 100 psia . . . . .	126
F-X Net Reactions of Tungsten with $OF_2/B_2H_6$ Propellant Gas (MR = 3.5) at 5500 °R and 100 psia . . . . .	127
F-XI Net Reactions of Titania with $OF_2/B_2H_6$ Propellant Gas (MR = 3.5) at 5500 °R and 100 psia . . . . .	128
G-I Modified Novalac Epoxy Formulations . . . . .	132
G-II Infrared Examination of Vinyl Consumption in Various Poly (Cyclized 1, 2-Polybutadiene) Tollyl Urethane Formulations. . . . .	144
G-III Poly (Cyclized 1, 2-Polybutadiene) Tollyl Urethane Properties . . . . .	145

TABLES (Continued)

	Page
H-I Hydrogen-Fluorine Flame Composition and Temperature as a Function of Volume Composition . . . . .	170
H-II Variation of Ablation Parameters in Standard Novalac Resin Samples . . . . .	172
I-I Monomers for Polypyromellitimide Preparations . . . . .	181
I-II Monomers for Polybenzimidazoles . . . . .	183
I-III Monomers for Polyquinoxalines . . . . .	186

INVESTIGATION OF RESIN SYSTEMS  
FOR  
IMPROVED ABLATIVE MATERIALS

by

H. R. Lubowitz, E. A. Burns and B. Dubrow

SUMMARY

This report is the final program report describing the work performed by TRW Systems (formerly TRW Space Technology Laboratories) for the National Aeronautics and Space Administration, Lewis Research Center, under Contract NAS3-4188. The principal objective of the program was the preparation of new resin matrices for improved ablative materials for use with high energy fluorine-containing liquid propellant systems. This objective was accomplished with support of detailed studies which:

- a) Defined critical parameters controlling the effectiveness of resins in ablative systems,
- b) Synthesized new resins and determined the critical properties of new and modified resins, and
- c) Recommended resins for future use.

The first phase of the work determined the critical resin properties which influence the effectiveness of ablative composites in order that criteria could be established for the synthesis and property testing of new and modified resins.

The thermophysical factors which influence surface recession, backwall temperature, and the chemical compatibility of the resin and char matrix in the engine environment were defined and assessed. A thermophysical evaluation of ablative resin performance was accomplished using computer techniques to determine the relative importance of thermophysical parameters, such as density, thermal conductivity, specific heat, energy of reaction, etc. Thermochemical analysis, using an equilibrium computer program, was employed to select the

elemental species which could survive in the high energy fluorine-containing propellant environment.

In addition, the chemical properties of the resin which relate to thermal and oxidative stability, resistance to erosion, nature of pyrolysis gases, and dimensional stability of the char residue were evaluated for a large number of thermally stable polymers.

Two general classes of high energy fluorine-containing propellant environments were identified which presented distinct differences in their reactivity with resins. One class consists of fluorine-containing propellant systems whose combustion products do not include oxygen in any free or combined form (e. g., fluorine/hydrogen) and the other class includes propellant combinations which have fluorine and oxygen-containing exhaust species (e. g.,  $\text{OF}_2/\text{B}_2\text{H}_6$ ).

The chemical and thermal considerations associated with the use of resins in each of these propellant combustion environments resulted in the identification of the following guidelines for synthesis. For the fluorine/hydrogen propellant class, resin systems whose decomposition products yield a carbon char matrix are most desirable. With such a resin system a high char density appears to be the most significant thermophysical property for reduced surface recession. The backwall temperature is significantly influenced by additional thermophysical considerations, such as the effective decomposition activation energy, resin density and thermal conductivity of both the virgin and char material. Near the flame temperature, the  $\text{OF}_2/\text{B}_2\text{H}_6$  combustion products were found to be reactive with all candidate materials examined when equilibrium conditions were imposed. For survival, endothermic reactions may provide adequate heat sinks to lower the surface temperature and maintain dimensional stability of the ablative material. Resins which appear attractive to survive exposure to the  $\text{OF}_2/\text{B}_2\text{H}_6$  combustion products are those which have a minimum carbon content and contain elements which yield refractory oxides on pyrolysis and form high melting fluorides. The thermophysical properties which apply to the fluorine/hydrogen propellant class also apply to the  $\text{OF}_2/\text{B}_2\text{H}_6$  propellant class.

The primary candidate resin synthesized for the fluorine/hydrogen propellant class was poly (cyclized 1,2-polybutadiene) tolyl urethane. This resin has the highest carbon content of any structural plastic (85.9%). Its ladder structure results in high thermal stability (incipient decomposition temperature of 457°C) and oxidative resistance. It also can be readily processed. Other organic resins having high carbon content examined in this program included the polybenzimidazoles, polypyromellitimides, polyimide-amides, polyimide esters and polyimide ethers. The latter two resins are new materials conceived during the program but not synthesized.

Poly alkaline earth metal acrylate resins containing magnesium, calcium, or barium were synthesized for use with the  $\text{OF}_2/\text{B}_2\text{H}_6$  propellant class. These resins satisfy the criteria of yielding high melting oxides and fluorides on decomposition. Phosphate bonded oxides also were prepared for use with this propellant class. In addition, zirconium boride polymers were postulated as a promising resin for the  $\text{OF}_2/\text{B}_2\text{H}_6$  propellant combination.

Thermophysical properties and the resistance to a fluorine/hydrogen torch environment were determined for the synthesized polymers as well as selected commercially available materials, including polyimide-amides, polypyromellitimides, and zirconium diboride. These studies confirmed that 1) a high carbon content, and 2) a high degree of aromaticity which leads to a dense carbon char, contribute to the resistance of the resin to the fluorine/hydrogen flame. The poly calcium acrylate and phosphate bonded oxides also were resistant to the fluorine/hydrogen environment, however, the phosphate bonded oxide was not sufficiently ductile to withstand the thermal shock imposed by the flame.

The factors affecting the potential scale up, synthesis and production of composites from candidate resins were reviewed. Poly (cyclized 1,2-polybutadiene) tolyl urethane resins can use conventional resin processing art. Poly alkaline earth metal acrylate resins are prepared by compression molding techniques at moderate temperatures. The other organic resins can be classed as stiff polymers and, although

presenting processing difficulties, can be prepared by hot pressing with concurrently applied vacuum and heat. The thermophysical properties and resistance to fluorine/hydrogen torch of these resins indicate that they could be prepared in a reproducible manner. From chemical consideration, compatibility problems between the resins and candidate fillers are not anticipated.

The poly (cyclized 1,2-polybutadiene) tolyl urethane, poly calcium and magnesium acrylate and phosphate bonded oxides are in a stage of development where optimization of the resin is recommended. Additional synthesis and property determinations are necessary for the polyimide ether, polyimide ester, and zirconium borides. Property determinations are also needed to complete the information required for polybenzimidazole resins. A systematic experimental evaluation of processing ablative composites using the candidate resins is required prior to engine testing.

In summary, the parameters which govern the effectiveness of ablative resins in high energy propellant classes were identified. Applying this technical basis, new and improved resins for use as ablative matrices for advanced propellants were synthesized, evaluated and recommended for future use.

## 1.0 INTRODUCTION

This report presents the work accomplished by TRW Systems (formerly TRW Space Technology Laboratories) for the National Aeronautics and Space Administration, Lewis Research Center, under Contract NAS3-4188. This program, which represents a one year effort, was comprised of analytical and laboratory studies on new or improved resin systems suitable for use as a matrix material in ablative composites for liquid rocket engine thrust chambers. The overall program objective was to evaluate and prepare ablative resin matrices which could be utilized under the more severe conditions imposed by future engine systems using high energy propellants, such as fluorine/hydrogen and oxygen difluoride/diborane. Ablative composites employing these resins are required to offer advantages over existing resin systems, such as reduced ablation rates, greater resistance to severe chemical environments, ability to withstand extremely high temperatures for extended durations, and capability to perform successfully when subjected to engine duty cycles of varying durations.

In order to accomplish this objective, the analytical and experimental effort was organized in a manner which would make it possible to address the investigation of new and improved resins to their effectiveness in the use environment. Thus, the program first determined the parameters which control the effectiveness of resins considered for use in ablative composites. The resin performance was related to the intrinsic properties of the composite and to the thermal and chemical engine environment. The desirable properties of the resin for use in an ablative matrix then were interpreted in terms of elemental composition and chemical structure. These factors provided the guidelines for selection and synthesis of new and improved materials. Thus, the resins were tailored with consideration given to the thermophysical criteria and chemical reactions which occur in the engine environment.

The initial part of the program represented an integrated effort of individuals proficient in heat transfer, fluid mechanics, thermochemistry, and polymer chemistry to provide a definition of properties which critically influence the performance of resins as the matrix of

ablative composites for liquid rocket thrust chambers. The major portion of the program was devoted to the preparation of new or modified resins and the experimental determination of their properties. Finally, the use factors for these resins were assessed giving consideration to methods of formulation or synthesis, techniques for fabrication of ablative composite structures, and the compatibility of the resin with reinforcing fibers or other structural materials. The principal contribution of the overall effort was the synthesis of several novel resins which were based on their compliance with the analytical use criteria generated in this program for fluorine-containing propellants. These resins also show promise of being readily processed into composite ablative materials for comprehensive engine evaluation.

The report is divided into three principal sections covering each of the three following consecutive program tasks:

- Task I - Definition of critical properties influencing the ablation effectiveness of resin systems and selection of resins for Task II;
- Task II - Synthesis and property determination of the more promising resin systems; and
- Task III - Evaluation and recommendation of resins for future use.

This report identifies in a separate section the new concepts originating from the program. The information presented in the main body of the report is supplemented by appendices covering detailed descriptions of procedures, equipment and underlying theoretical considerations.

## 2.0 DEFINITION OF PROPERTIES FOR SELECTION OF RESINS

Ablation of rocket combustion chambers and nozzles is a complex thermal, chemical and mechanical process. Definition of the more important properties and their interrelationships is required before new or improved resins may be selected or studied. In order to establish guidelines for synthesis of new ablative resins, the thermophysical factors which influence surface recession and backwall temperature and the chemical compatibility of the resin and char matrix in the engine environment were defined and assessed.

The thermophysical evaluation of ablative resin performance utilized computer techniques which provided influence coefficients or relative importance of thermophysical parameters such as, density, thermal conductivity, specific heat, energy of reaction, etc. The thermochemical analyses, using an equilibrium computer program, was employed to select the elemental species which could survive in the high energy fluorine-containing propellant environment.

The information derived from these two analytical sources, and consideration of the reaction kinetics in the resin interior and on the surface, provide the necessary identification of the resin properties which are critical in controlling the rate of ablation in specific thrust chamber environments. In addition, consideration was given to the interaction of resin fillers in the overall analytical evaluation. This comprehensive analytical assessment permitted the screening and evaluation of a number of resin systems based on selected thermal and chemical properties. A description of this effort and the recommendation of resins for synthesis and property determination are presented in this section.

### 2.1 GENERAL THERMOPHYSICAL EVALUATION OF ABLATOR PERFORMANCE

A schematic representation showing the interrelationship among engine geometry, propellants, and engine parameters, reinforcements and fillers and the resin itself on the ablation rate is shown in Figure 1.

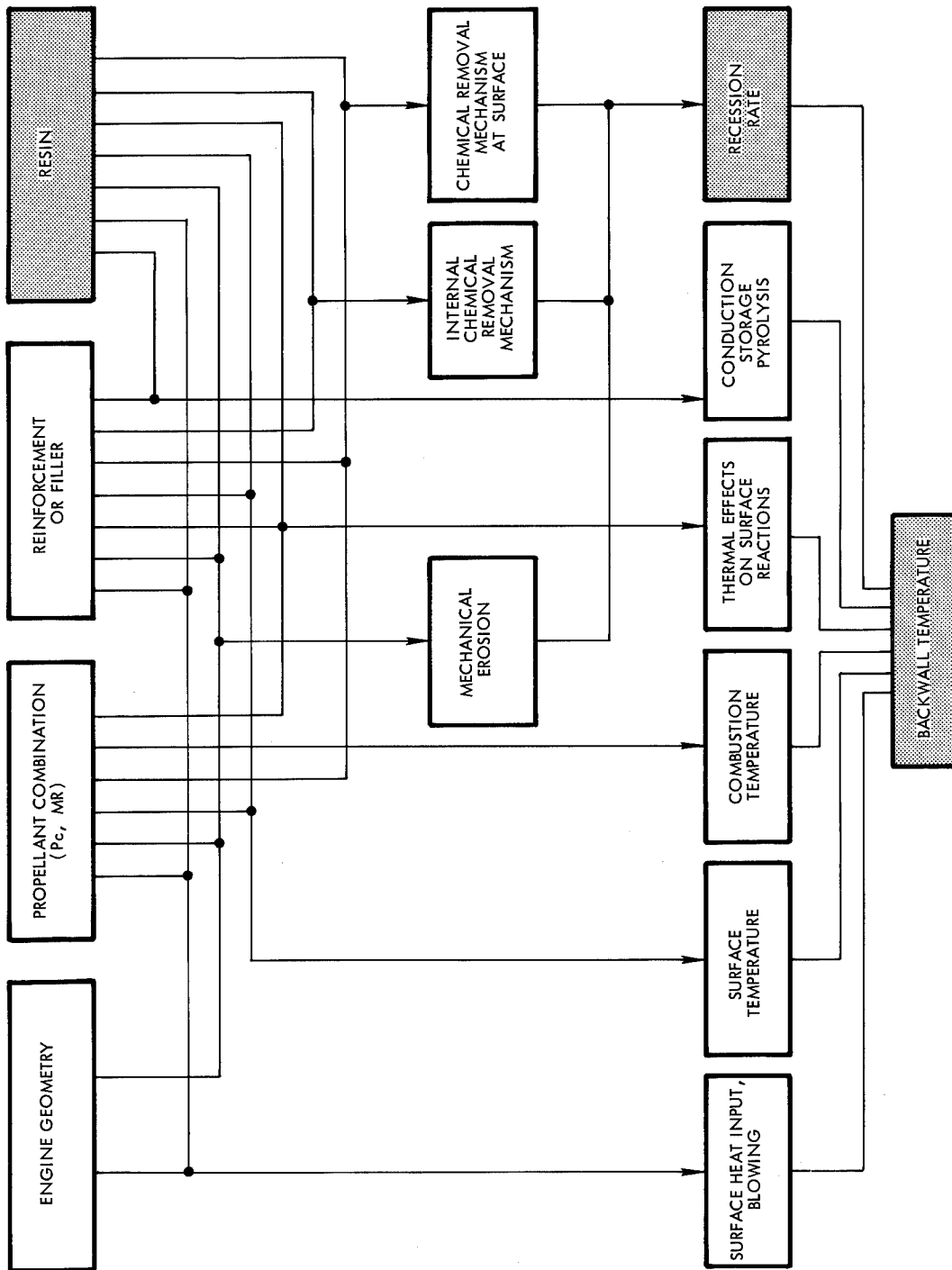


Figure 1. Dependency of Backwall Temperature and Recession Rate on Significant Engine and Ablator Parameters

This flow diagram shows the relative importance of each parameter to the two common criteria used to evaluate the rate of ablation, namely the backwall temperature and surface recession rate.

The resin affects the ablative recession rate by the following mechanism:

- Mechanical Erosion - In conjunction with the reinforcement, the resistance of the char structure to shear is dependent on its physical structure and is a partial result of the charring mechanism occurring within the composite.
- Internal Chemical Removal Mechanisms - The generation rate and chemical nature of the pyrolysis gases determine the extent and type of reaction occurring with the composite char material.
- External Chemical Removal Mechanisms - The pyrolysis gases and char material can react chemically with the propellant environment.

The resin influences the ablative backwall temperature through the following parameters:

- Surface Heat Input - The injection of pyrolysis gases into the turbulent boundary layer causes a thickening of the boundary layer, and a reduction in the convective heat input.
- Surface Temperature - Endothermic reactions occurring between the pyrolysis gases, char structure and propellant environment, can limit the surface temperature.
- Thermal Effect on Surface Reactions - The reactions, described above, can effectively remove heat from the surface of the ablator.
- Conduction, Storage, Pyrolysis - With a surface temperature and heat input specified, the conduction of heat to the backwall will depend on the thermophysical properties of the composite char and virgin materials: density, specific heat, and thermal conductivity. In addition, the pyrolysis process itself provides an internal mechanism for heat removal. The flow of pyrolysis gases through the material can also remove an appreciable amount of heat.
- Surface Recession - The effect of the resin on surface recession has been described previously. The recession influences the backwall temperature through the continual reduction in ablator thermal resistance as recession proceeds.

A criterion often used for the useful life of an ablative material is the "time to char through", or the time required for the virgin-char interface to recede completely through the ablative material. This occurrence can create two undesirable situations: a greatly decreased thermal resistance between the ablating surface and the backwall; and a possible loss in strength of the ablative material. The length of time for this to occur is determined by both the ablative material and the engine environment.

As can be seen from Figure 1, one of the parameters involved in the determination of backwall temperature is the surface recession rate. The surface recession rate is, itself, a more significant factor in the throat region of a nozzle where dimensional changes would cause performance degradation. The mechanisms for propellant combustion heat utilization within phenolic refrasil were explored for the cases of quasi-steady erosion, and a non-eroding semi-infinite solid (Reference 1). "Quasi-steady erosion" of an ablative material refers to the situation where the recession rate of the ablating surface is identical with the recession rate of the char-virgin interface. This assumption does not reflect the fact that most ablative materials in current rocket use exhibit a higher char-virgin interface recession rate than ablating surface recession rate; however, it does permit an exact solution to the energy equations in the char and virgin materials, and these results can be used to estimate the relative importance of ablative heating steps.

Using physical data for phenolic-silica, and assuming a surface temperature of 3000°F with a quasi-steady erosion rate of 0.1 in/minute, the following utilization of heat is obtained:

Heat Required To:

	<u>%</u>
Pyrolyze Plastic	5.3
Heat Pyrolysis Gases	26.0
Heat Char Layer	49.0
Heat Virgin Material	<u>19.7</u>
	100.0

Heat utilization through surface chemical reactions has been eliminated here, through the assumption of a given surface temperature. However, such reactions must be considered to determine the true surface temperature under desired conditions. The major contribution of the above analysis is its indication of the relatively small contribution made by the material's heat of pyrolysis to the total heat utilization problem.

Although both the backwall temperature and recession rate are of significance to the problem, it is apparent that the recession rate aspect should receive prime consideration since it represents a more formidable engineering problem.

## 2.2 ANALYTICAL EVALUATION OF CRITICAL THERMAL PROPERTIES

Whereas the quasi-steady state analysis provided a general description of the ablative process, the TRW Systems Charring-Recession Computer Program was used for the quantitative evaluation of the relative importance of ablator material properties on the backwall temperature and recession rate. The Charring-Recession Computer Program permits determination of the thermal response and surface recession of a charring ablative material backed by a non-ablative material. The ablator is assumed to consist of two components: one which decomposes into a gas and the other which remains to form a char structure.

The key equations solved by the computer program consider:

- The energy balance at each node within the material.
- The energy balance at the interior "heated" surface.
- The energy balance at the exterior "cooled" surface.
- The rate of decomposition.

A description of these equations and the required temperature functions, time functions, initial variables and constants in the program is presented in Appendix A. The program solves for the following unknown quantities as a function of time:

s	(ft)	Distance from time zero surface ( $x = 0$ ) to ablating surface
---	------	--

$\dot{s}$	(ft/sec)	Surface recession rate
T	(°F)	Temperature through the ablative material
W	(lb/ft <sup>2</sup> -sec)	Mass flux of gas at the surface
$\rho_a$	(lb/ft <sup>3</sup> )	Density of decomposable component through the ablative material.

If endothermic chemical reactions occur at or near the surface, the surface temperature will reach a maximum ( $T_s$ ) at which temperature quasi-steady surface recession will occur and the surface recession rate will be determined by the surface energy balance.

Following a coordinate transformation to a non-receding coordinate system, the equations are solved in finite difference form by the method of Crank and Nicholson (Reference 2).

A reference case was chosen in the parametric study in which resin parameters were varied. In this case phenolic refrasil properties were used with the convective heat input typical of that experienced under the TRW LEM Descent Engine firing conditions. In this manner the parameters for the analysis could be examined in the light of test experience. To perform the parametric survey a computer run was made for each of two values bracketing the reference value of the variable under investigation. Details of this parametric study also are presented in Appendix A. The resin parameters investigated were:

<u>Symbol</u>	<u>Parameter</u>
$\lambda_a$	Heat of decomposition
J	Endothermic surface heat of reaction
$k_b$	Char thermal conductivity
$k_o$	Virgin material thermal conductivity
$c_g$	Pyrolysis gas specific heat
$c_a$	Specific heat of decomposable portion
$\gamma_a$	Decomposition rate constant

$\Gamma$	Decomposition parameter (related to activation energy of the resin decomposition)
$\rho_a$	Density of the decomposable portion
$\rho_b$	Char density

The effects of the changes in specific physical and thermal properties of the ablator on the backwall temperature and surface recession are given in Table I where the percent change in the backwall temperature and thermal recession are tabulated for a 20% increase in each property.

Table I. Effect of 20 Percent Increase in Selected Variables on Backwall Temperature and Total Recession

Variable	Percent Increase In Backwall Temperature	Percent Increase In Total Recession
Decomposition Parameter, $\Gamma$	+26.0	+4.5
Char Density, $\rho_b$	-5.8	-17.0
Surface Endothermic Heat of Reaction, J	-0.6	-18.8
Density, Decomposable Portion, $\rho_a$	-12.9	-2.2
Char Conductivity, $k_b$	+11.6	-4.6
Virgin Conductivity, $k_o$	+7.2	-0.2
Pyrolysis Gas Specific Heat, $c_g$	-6.8	-4.3
Heat of Decomposition, $\lambda_a$	-5.3	-1.0
Decomposition Constant, $\gamma$	-2.6	0.0
Specific Heat, Decomposable Portion, $c_a$	-2.5	+1.3

The decomposition parameter,  $\Gamma$ , displays the largest affect on backwall temperature of any of the properties investigated. The density of the decomposable material and the char conductivity follow in importance.

Surface recession, on the other hand, is seen to be most strongly influenced by the surface heat of reaction,  $J$ . Of other ablative material properties, the char density follows in order of importance.

For some parameters it is observed that an increase in the property decreases one ablation criterion, e. g., backwall temperature, but increases the other. Where these conflicts exist, as with the char conductivity, the direction of change to favor the more sensitive of the two ablative criteria is indicated. The resin parameters, in order of importance, are listed below, together with the respective direction of desired property change to improve the ablator.

<u>Parameter</u>	<u>Desired Property Change</u>
Decomposition parameter, $\Gamma$	Decrease
Char density, $\rho_b$	Increase
Surface endothermic heat of reaction, $J$	Increase
Density of decomposable portion, $\rho_a$	Increase
Char thermal conductivity, $k_b$	Decrease
Virgin material thermal conductivity, $k_o$	Decrease
Pyrolysis gas specific heat, $c_g$	Increase
Heat of decomposition, $\lambda_a$	Increase
Decomposition rate constant, $\gamma_a$	Increase
Specific heat of decomposable portion, $c_a$	Increase

### 2.3 INITIAL SELECTION OF CANDIDATE RESIN CLASSES

For the purpose of performing detailed thermal and chemical evaluations of ablative resin matrices in the engine environment, criteria were chosen for the initial selection of candidate resins. These

initial selection criteria were established prior to the performance of thermophysical property evaluations, and consequently, were based only on past knowledge and experience concerning material factors believed to be important. Consideration was also given to the inclusion of a polymer that leaves a residue other than carbon and the use of a polymer that deposits a residue in addition to carbon. The general engineering criteria that was used for initial resin selection were:

- Thermal and oxidative stability
- Low thermal conductivity
- Resistance to erosion
- Capability of generating low molecular weight gases on pyrolysis
- Dimensional stability of char residue
- High heat distortion temperature.

In addition, in the selection of inorganic resins, particular attention was given to resins that:

- Exhibit a high degree of plasticity
- Have a high molecular weight
- Can be synthesized into chain structures
- Do not readily undergo molecular rearrangement or scission of the polymer chain.

The processing criteria for the resins included, among other factors, high tractibility so that useful and viable objects could be fabricated. Appendix B discusses the chemical considerations related to the synthesis of materials which comply with the above criteria. The relations between structural chemistry and properties are included in this discussion.

The resin classes examined in light of the above criteria are given in Table II.

Table II. Candidate Resin Classes Under Consideration

Polymers Containing Boron	B-N: linear, condensed rings, linear chain of rings Carboranes B-P Resins
Polymers Containing Silicon	Si-O Si-C Si-N
Furan Derivatives	Furfural Base Furfural Alcohol Base
Fluorocarbons	Aliphatic Backbones Aromatic Backbones
Polybenzimidazoles	Aromatic Backbone Aliphatic Backbone Polybenzothiazoles
Phosphate Bonded Oxides	
Other Systems	Polymetalosiloxanes Phenylsilsesquioxanes Phosphonitrilic Polymers Phosphoranes Polyimides (polypyromellitimides)

#### 2.4 ANALYTICAL DETERMINATION OF THE CHEMICAL COMPATIBILITY BETWEEN CANDIDATE RESIN SYSTEMS AND PROPELLANT COMBUSTION PRODUCTS

The chemical compatibility between resin systems and propellant combustion products was determined using equilibrium thermochemical computer methods. This analysis was intended to distinguish the inherently inactive chemical elements or species from the active ones. The overall thermochemical evaluation processing included:

- The determination of amount and nature of the solid residue and gases formed in equilibrium decomposition of candidate resins.
- Estimation of the physical properties of the residues.

- Definition of engine environment.
- Reactions of the ablators with the propellant gases in the engine environment.

Chemical reactions occurring below the ablator-propellant combustion gas interface and which limit the rate of surface recession warranted separate analysis. Brief discussions of these studies are presented below.

#### 2.4.1 Equilibrium Thermal Decomposition Studies

Representative compounds and empirical formulae were selected from the resin classes listed in Table II, Section 2.3. The selected compounds are shown in Table III and were evaluated by calculating the species which would exist at thermal equilibrium at a total pressure of 100 psia over 100 °R intervals from 4500 °R to 7000 °R. In general, the only solid matter which remained in these studies existed as carbon and in some instances as silicon carbide or boron nitride. The detailed results of this study are listed in Appendix C in both graphical and tabular form.

Table III. Representative Empirical Formulae of Typical Resin Compounds Used in Analytical Equilibrium Thermal Decomposition Studies

Class	Compound	Empirical Formula
B-N	Borazine-Containing	$C_6H_{15}B_2N_3$
Si-O	Polysilarylenesiloxane	$C_8H_{10}SiO_2$
Si-O	Phenyl Silsesquioxanes	$C_{12}H_{10}Si_2O_3$
Si-N	Silazine	$C_{13}H_{13}SiN$
C-O	Furans	$C_5H_4O$
C-N-O	Polyimides	$C_8H_3O_2N$
C-N	Polybenzimidazoles	$C_5H_3N$
C-F	Polytetrafluorethylene	$CF_2$
C-F	Perfluoro Polyphenylene	$C_3F_2$
C-H	Poly (Cyclized 1, 2-Polybutadiene) Tollyl Urethane (CPBU)	$C_{84}H_{120}O_2N$

Recently Duff and Bauer reported some thermochemical data for high carbon species not considered in the TRW computer program which could exist in the high temperature environment applicable in these thermal decomposition studies. Their data also were evaluated, but considered to be nonapplicable to the particular study in hand. This evaluation is discussed in detail in Appendix D.

A summary of the total solid matter which exists for the selected classes of polymers is shown in Figure 2 as a function of temperature. From this study it is evident that at temperatures above 5500 °R polymers which contain little oxygen and have a high hydrocarbon content are the more stable thermally.

#### 2.4.2 Physical Properties of the Residues

Theoretical equilibrium calculations indicate that all resins included in the survey have a solid residue which is partly or entirely carbon, except polytetrafluoroethylene which has no solid residue. At the lower temperature, those resin systems containing silicon have silicon carbide in addition to carbon and the boron-containing resin has solid boron nitride in addition to carbon.

A preliminary estimate of the porosity of the residue can be made based on the calculated equilibrium composition, an assumed resin density and the observation that many resins undergo little bulk volume change during pyrolysis. This estimate of the char porosity contains considerable uncertainty, but it provides initial data for estimating thermal conductivity, density and strength of the residue. Table IV gives the estimates of the room temperature porosity and bulk density of the char present for each resin system.

The porosity may be considered to provide an estimate of relative strength of the residue. From the estimate of char strength, it is anticipated that the B-N resins, the silazine type and the polybenzimidazoles would hold the greatest promise for unfilled ablators. The fluorocarbons would not be expected to retain any char layer while the other resins would fall between these two groups.

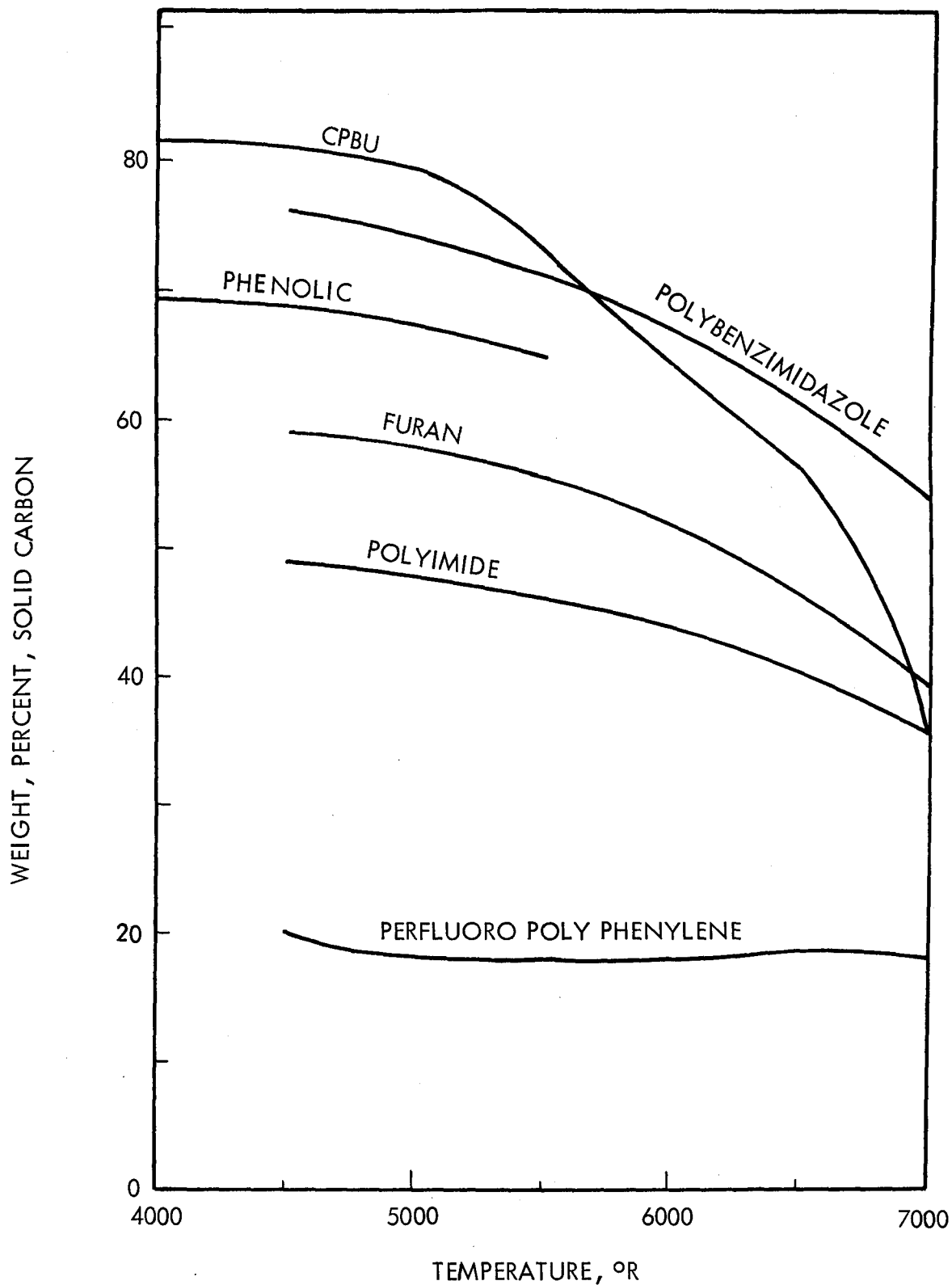


Figure 2. Carbon Residue as a Function of Temperature for the Equilibrium Decomposition of Hydrocarbon and Fluorocarbon Systems

Table IV. Estimated Density and Porosity of Residues

Polymer	Porosity (%)	Bulk Density (g/cc)
$C_6H_{15}B_2N_3$ (B-N resin)	55	1.0
$C_8H_{10}SiO_2$ (polysilarylenesiloxane)	70	0.8
$C_{12}H_{10}Si_2O_3$ (phenyl silsesquioxane)	65	0.8
$C_{13}H_{13}SiN$ (silazine)	55	1.1
$C_5H_4O$ (furan)	65	0.8
$C_5H_3N$ (polybenzimidazole)	55	1.0
$C_8H_3O_2N$ (polyimide)	70	0.6
$CF_2$ (polytetrafluoroethylene)	100	No Residue
$C_3F_2$ (perfluoropolyphenylene)	90	0.3

#### 2.4.3 Definition of Engine Environment

In order to define the chemical and thermal conditions seen by the ablator surface it is necessary to determine the chemical composition and adiabatic flame temperatures of advanced propellant combinations. These data are required to aid in evaluation of surface reactions and chemical attack and to supply the thermal environment for calculations of the enthalpy potential. The chemical composition of the exhaust gases at various mixture ratios, expansion ratios, and chamber pressures have been determined utilizing the TRW Systems AP2A Computer Program and the results of these studies are found in Appendix E.

The propellant combinations examined were; fluorine/hydrazine, fluorine/monomethylhydrazine, fluorine/hydrogen, fluorine/ammonia, oxygen difluoride/diborane, and FLOX/MMH. The propellant exhaust gases for these systems contain one or several of the following major chemical constituents: boron oxyfluoride (BOF), hydrogen fluoride (HF), hydrogen, water, carbon monoxide and carbon dioxide. Estimates of the reactions of some of these active exhaust species with residue from ablated resins are presented in the following section.

#### 2.4.4 Equilibrium Reactions of Resin Residues with Propellant Gases

Chemical stability of the residues in the presence of the propellant exhaust gases has been investigated. Necessary background for this analysis was the definition of engine environment with primary emphasis on the systems oxidized with fluorine, FLOX and  $\text{OF}_2$  presented in Section 2.4.3.

Flame temperatures above  $7000^\circ\text{R}$  and exhaust gases containing large amounts of HF and  $\text{H}_2$  are characteristic of the advanced propellants under consideration. Systems of FLOX or  $\text{OF}_2$  with  $\text{NH}_3$  or  $\text{N}_2\text{H}_4$  also contained  $\text{N}_2$  and  $\text{H}_2\text{O}$ , while monomethylhydrazine or the hydrazine-unsymmetrical dimethylhydrazine blend added CO to the exhaust products. Except for HF, these gases are those most important in the exhaust of current state-of-the-art propellants.

The  $\text{OF}_2/\text{B}_2\text{H}_6$  propellant combination introduces several additional combustion species. From the data presented in Table E-XI (Appendix E) the relative importance of BOF as a major combustion product is shown. Because this molecule contains both oxygen and fluorine, it is very important in reactions with walls susceptible to chemical attack by either oxygen or fluorine.

The compatibility of candidate resin residues (carbon, silicon carbide and boron nitride) with propellant gases was determined by equilibrium calculations. Details of these calculations are reported in Appendix F.

From these studies it is possible to separate the advanced propellant systems under consideration into two classes. The first class consists of fluorine-containing propellant systems whose combustion products do not include oxygen in any free or combined form. Specific examples of these systems are fluorine-hydrogen, fluorine-hydrazine, fluorine-monomethylhydrazine and fluorine-ammonia.

The second class consists of fluorine-containing propellants which also have oxygen in the system. Specific examples of this class are propellant combinations which have FLOX or oxygen difluoride as an oxidizer (e. g., FLOX-monomethylhydrazine and  $\text{OF}_2/\text{B}_2\text{H}_6$ ). Although both classes have high flame temperatures (e. g.,  $6000\text{-}8000^\circ\text{R}$ ), over usable mixture ratios, chamber pressures and expansion ratios, the fluorine-oxygen containing propellant class exposes the ablator to the more extreme chemical environment.

2.4.4.1 The F<sub>2</sub>/H<sub>2</sub> Propellant Class

Equilibrium calculations were performed to estimate the chemical compatibility of solid residues with the HF combustion product of the F<sub>2</sub>/H<sub>2</sub> propellant class. These results are typical of the propellant class as any nitrogen or carbon containing exhaust gases have little affect on the removal of solid residue through chemical reaction. Table V shows the weight of solid C, SiC, and BN removed by equilibrium reaction with a unit weight of HF at temperatures from 4500°R to 7000°R.

Table V. Equilibrium Reaction of Carbon, Silicon Carbide and Boron Nitride with HF

Temperature, °R	Solid Removed per Unit Weight of HF				
	C	SiC			BN
	Total	Total	Liquid	Gas	Total
4500	0.004	0.355	0	0.355	>1.0* (all gas)
5000	0.010	0.350	0	0.350	>1.0
5500	0.021	0.730	0.351	0.379	>1.0
6000	0.041	0.751	0.244	0.507	>1.0
6500	0.079	0.779	0	0.779	>1.0
7000	0.177	0.861	0	0.861	>1.0

\*Highest ratio included in this survey.

These results clearly demonstrate the superior chemical resistance of carbon over silicon carbide and boron nitride in this environment. At 5500°R, for example, only 2 percent of carbon is removed, per gram of HF, whereas SiC and BN have very high amounts removed.

2.4.4.2 The OF<sub>2</sub>/B<sub>2</sub>H<sub>6</sub> Propellant Class

The results of equilibrium calculations on the chemical compatibility of the OF<sub>2</sub>/B<sub>2</sub>H<sub>6</sub> propellant class presented in Appendix F indicate that a large fraction of solid residue (carbon, silicon carbide and boron nitride) is removed in this environment. Carbon is still the best of the residues, however, it does not appear to be a prime candidate for this propellant class. For an ablator to withstand this environment it is evident that additional elements and/or compounds must be included in the system, either as part of the chemical structure or in the form of a filler, to provide a protective endothermic chemical reaction or protective coating.

### 2.4.5 Equilibrium Considerations of Internal Chemical Reactions

Several high melting candidate additives were evaluated for their chemical compatibility with the  $\text{OF}_2/\text{B}_2\text{H}_6$  propellant class combustion environment. The candidate additives evaluated were alumina, beryllia, magnesia, calcia, zirconia, tungsten and titania. A detailed description of these theoretical compatibility evaluations is presented in Appendix F.

The consumption of additives, calculated assuming 50 g of propellant gas ( $\text{OF}_2/\text{B}_2\text{H}_6$ , MR = 3.5) in equilibrium with 50 g of additive at  $5500^\circ\text{R}$  and 100 psia, is listed in Table VI. It is seen that tungsten metal is by far the least reactive of the additives considered, followed by zirconia, alumina, magnesia and beryllia. Calcia and titania are completely consumed at equilibrium.

Table VI. Additive Consumption

Additive	Consumption	
	Moles	Grams
$\text{Al}_2\text{O}_3$ (l)	0.088	8.9
BeO (l)	1.34	33.4
MgO (s)	0.41	16.4
CaO (l)*	0.89	50.0
$\text{ZrO}_2$ (l)	0.042	5.1
W (s)	0.00002	0.0037
$\text{TiO}_2$ (l)*	0.63	50.0

\* Complete consumption.

Endothermic reactions are important in providing lower wall temperatures required for less refractory materials. The data for the additives were analyzed to determine the enthalpy change during the reaction of the additive and the propellant gases at  $5500^\circ\text{R}$  and 100 psia. A summary of the results is shown in Table VII. In general, the reaction process is less effective (per gram of additive removed) than the vaporization process. The exception to this rule is tungsten metal.

Table VII. Enthalpy Changes Due to Material Addition  
at 5500°R and 100 psia

Change	Mode	MgO (s)	BeO (l)	Al <sub>2</sub> O <sub>3</sub> (l)	ZrO <sub>2</sub> (l)	CaO (l)	W (s)	TiO <sub>2</sub> (l)
Enthalpy absorbed per gram of material removed, Kcal/g	Reaction	2.000	1.470	1.220	1.150	0.500	1.630	0.190
	Vaporization	3.430	5.960	3.120	1.200	1.530	1.110	1.500
Weight removed per unit weight of propellant gas	Reaction	0.327	0.669	0.178	0.102	*	0.00007	*
	Vaporization	0.006	0.002	0.000	0.002	0.103	0.000	0.005

\* Completely consumed.

It should be noted that, while equilibrium data are useful for general comparison, a kinetic analysis is necessary for more precise interpretations.

The ideal additive material is that which is not affected by the conditions of temperature, pressure and reactive atmosphere to which it is subjected. If, however, the material is reactive with its surroundings at any particular temperature and pressure, it is important that the reaction be endothermic. Thus, if the reaction of the additive and propellant gases results in an absorption of heat, a corresponding temperature decrease in the neighborhood of the ablating surface will occur thereby decreasing the reactivity of the ablator-propellant gas combination. In the absence of reaction rate data, the enthalpy absorbed per gram of material reacted, and weight removed by the reaction, provide a means of ranking the effectiveness of the additive.

From Table VII it would appear that tungsten metal, magnesia, alumina and zirconia are relatively more effective additives than beryllia, calcia and titania. For example, the tungsten metal-propellant gas system is quite unreactive; only 0.00007 g of tungsten is consumed per gram of propellant gas. Moreover, the reaction is endothermic to the extent of 1.63 kcal/g of tungsten removed.

## 2.5 GUIDELINES AND CRITERIA FOR SELECTION OF RESINS

Guidelines and criteria for selection of resin systems for synthesis studies were established by consideration of the equilibrium analytical studies (Section 2.4), the results of the Charring-Recession Computer Program (Section 2.2) and also evaluation of the nonequilibrium reaction rate factors. Feasible synthesis routes also were assessed to attain the desired objectives. These considerations are discussed and summarized below.

### 2.5.1 Equilibrium Propellant Considerations

#### 2.5.1.1 F<sub>2</sub>/H<sub>2</sub> Propellant Class

The criteria for guiding the selection and synthesis of new resins for the F<sub>2</sub>/H<sub>2</sub> propellant systems indicate resin systems whose decomposition products yield large quantities of carbon are most desirable. Carbon is relatively unreactive at temperatures approaching the flame temperature. Surface recession is controlled more by evaporation from the surface than by reaction at the surface. From these studies it has been seen that truly inorganic systems such as Si-O and B-N systems, although introducing strong chemical bonds in the ablator, are not expected to survive the chemical exposure as well as the high-carbon species.

#### 2.5.1.2 OF<sub>2</sub>/B<sub>2</sub>H<sub>6</sub> Propellant Class

Propellants in the OF<sub>2</sub>/B<sub>2</sub>H<sub>6</sub> class are found to be reactive at temperatures near the flame temperature with all candidate materials examined when equilibrium conditions are imposed. For survival the surface probably must be maintained at lower temperatures. As the wall temperature is reduced to meet this condition, the heat input to the wall increases but the conduction from the surface toward the backwall and the radiation from the surface decreases. Thus, if the lower temperature is to be maintained, an endothermic process must occur.

Several processes can be envisioned which could absorb the heat. At the surface, evaporation and reaction of the propellant combustion gases with the ablator or its residue may provide adequate heat sinks if the processes are sufficiently endothermic. Beneath the surface, reactions of resin with a filler, of the resin with itself, or of resin decomposition products with the filler could be a useful means of absorbing heat.

Resin systems which appear attractive to survive exposure to the propellant combustion products are those which have a minimum carbon content, contain elements yielding refractory oxides on pyrolysis and form high melting fluorides (e. g., calcium and magnesium oxides). Other additives, either in combined form or as a filler, that would appear to provide chemical stability to the system are tungsten, alumina and zirconia.

#### 2.5.2 Thermophysical Property Considerations

Based on the thermal parameters surveyed in Section 2.2, the char density and surface endothermic heat of reaction were identified as having the greatest influence on surface recession. The resin decomposition parameter which is related to activation energy of decomposition and also the density of the virgin material were found to have the greatest influence on backwall temperature.

The material properties guidelines are as follows. The density of the char should be maximized in order to decrease total surface recession. Highly endothermic reactions should take place preferably below the surface in order to maintain the high surface temperature yet absorb heat, thereby acting as a thermal barrier. In order to minimize backwall temperature, the decomposition parameter (rate of change of thermal decomposition with temperature) should be at a minimum and the density of the ablative material should be as high as possible. Char and resin thermal conductivity should be minimized and gases having high specific heat should be produced. It should be noted that increased thermal conductivity decreases surface recession somewhat, but appreciably increases backwall temperature.

The activation energy of decomposition, the most significant thermophysical property, is not expected to be greatly different for most of the organic resin systems. The char density is related to the aromaticity of the resin compounds. The resin composition can influence thermal conductivity and the properties of the gases produced upon decomposition (e. g., hydrogen being a desirable gas).

In terms of criteria, the thermophysical properties provide a valuable set of guidelines to superimpose on the basic chemical compatibility criteria and as a means of theoretically assessing the resin performance data.

### 2.5.3 Nonequilibrium Reaction Rate Considerations

For purposes of analysis, chemical reactions have been conveniently separated into reactions at the surface and those beneath the surface. Sub-surface endothermic reactions have a lesser effect on the surface temperature per unit of heat absorbed. They are much more likely to be kinetically controlled. An example of such an endothermic reaction in current ablative materials is that between silica and carbon. At 5500°R, this reaction absorbs about 140 kcal/mole or 3,500 BTU per pound of reactants in producing SiO and CO. The reaction absorbs about the same heat as absorbed by vaporization at 5500°R of a pound of silica (3,600 BTU/lb). Other reactions of oxides, borides, nitrides, silicides or carbides with polymer residues or decomposition products were screened and none were located that had as highly an endothermic reaction which also was thermodynamically favored at elevated temperatures. This would indicate that a resin with a high carbon content, together with silica, provides the most favorable chemical conditions for an internal endothermic reaction.

Surface reactions, those between residues and the propellant gases, also were studied. For those systems studied the heat absorbed by reaction was considerably less than the heat of vaporization of the oxide (see Table VII). In addition, these surface reactions are expected to be partially, if not completely, diffusion controlled, thus limiting their rate of reaction, and hence, their relative importance as a means of cooling the surface layer.

## 2.6 SELECTION OF CANDIDATE RESINS FOR SYNTHESIS

On the basis of guidelines and criteria established in Section 2.5, two primary candidate resins were identified for synthesis. Each of these resins represented new materials which were intended to meet the chemical compatibility criteria previously discussed. The primary candidate resins selected were:

- Poly (Cyclized 1, 2-Polybutadiene) Tollyl Urethane - This ladder polymer was selected for its high carbon content which indicated promise for use with the fluorine/hydrogen propellant class. The synthetic chemistry considerations indicated that this polymer also would have high thermal and oxidative stability and would be readily processable.
- Poly Alkaline Earth Metal Acrylates - This organometallic polymer incorporates elements which on decomposition of the resin form high melting oxides and fluorides, and thus indicates promise for use with the oxygen difluoride/diborane propellant class.

Two other resin systems also were selected for preparation in this program:

- Epoxy-Based Materials - Novalac epoxy formulations selected to represent the commercial materials having high carbon content and high temperature resistance were selected for preparation and use as a desirable reference material.
- Phosphate Bonded Oxides - This inorganic matrix provides a backup material to satisfy the synthesis criteria for the oxygen difluoride/diborane propellant class. The synthesis route reported in the literature for the phosphate bonded oxides provided a means of introducing highly refractory inorganic materials prepared in the form of a ductile matrix for ablative composites.

Three organic resins were selected as additional promising materials which offer advantages for use as a resin matrix with the fluorine/hydrogen propellant class:

- Polybenzimidazoles - The high carbon content and aromaticity of this resin system, in addition to the high thermal and oxidative stability, indicate its utility as an ablative composite matrix. This material is difficult to process, and consequently, plans were made to modify the processing techniques to permit the practical utilization of the polybenzimidazoles.

- Polyimide Esters - This new organic polymer system provides an approach to introduce high aromaticity and, at the same time, good processing characteristics. These resins should be tough, stiff, materials having high carbon content.
- Polyimide Ethers - The advantages of this resin system are similar to those for the polyimide esters, however, it is anticipated that this polymer would be more stable since the ether bond is substituted for the ester bond.

A third inorganic polymer selected in addition to the poly alkaline earth metal acrylates and phosphate bonded oxides was:

- Zirconium Boride Polymers - These polymers, although considered difficult to prepare, provided the interesting means of introducing the stable zirconium diboride into the resin structure and thus provided a promising approach to a novel resin for the oxygen difluoride/diborane propellant class.

Commercially available resins were examined in terms of the criteria for each propellant class and the following materials were selected for specimen preparation and laboratory testing: Proprietary Monsanto phenolic-based resin (used in state-of-the-art ablative materials), DuPont's polyimide (modified polypyromellitimide) and Amoco polyimide-amide homopolymer.

The synthesis and property determination of these polymers are described in the following section.

### 3.0 SYNTHESIS AND PROPERTY DETERMINATION OF NEW RESINS

In this section specific descriptions of the synthesis of high carbon epoxy reference formulations, cyclized polybutadiene urethane ladder polymers, poly alkaline earth metal acrylates, and phosphate bonded oxides are presented. In addition, other candidate materials which were not explored experimentally in this program are discussed, such as polyimide esters, polyimide ethers, and zirconium boride polymers. Included in the description of the specific resin systems are discussions of the underlying philosophy which guided the synthesis effort. Also reported are the results of property determinations of synthesized and commercially available resins, composites, carbon filled systems, and high temperature materials. The details of the synthesis approach and experimental procedures are presented in Appendix G. The property determination procedures are located in Appendix H.

#### 3.1 HIGH CARBON EPOXY REFERENCE FORMULATIONS

In order to permit meaningful evaluation of candidate resin systems it was necessary to prepare a standard class of resins for use as a reference. The organic acid anhydride-cured Novalac epoxides were chosen as representative of a conventional high temperature polymer system. This class of epoxides has the highest reported heat distortion temperature (265°C) of epoxides which are rich in carbon.

In the course of this work the following two modified acid anhydride-cured Novalac epoxides were prepared:

- 1) A system employing a recently developed anhydride (cyclopentane tetracarboxylic acid dianhydride) which, in theory, contributes higher chemical functionality to the epoxy system. This is related to increased crosslinking and thereby improves the chemical passiveness, and
- 2) A system utilizing a chlorine-containing anhydride (chlorendic anhydride) which provides the means to incorporate the stabilizing influence of chlorine atoms into resins and to increase resin density (reduced backwall temperature).

The details of the synthetic approach for preparation of neat epoxide resin and carbon-filled specimens are described in Appendix G.1.

The results of the property determinations of these systems are presented in Section 3.5 and Appendix G.1.

### 3.2 CARBON RICH RESINS FOR F<sub>2</sub>/H<sub>2</sub> PROPELLANT CLASS

A resin having a high carbon content, low molecular weight pyrolysis products, and thermal stability was sought for the fluorine/hydrogen propellant systems (see criteria in Section 2). Hydrocarbons comply with this basic chemical criteria. An exploratory survey of current polymer art showed that presently available hydrocarbon resins are not suitable for the preparation of ablative materials because they lack sufficient stiffness and thermal stability. Conventional hydrocarbon systems (e.g., polyethylene, polypropylene, and polystyrene) have flexural moduli in the range of 10,000 to 60,000 psi and heat distortion temperatures less than 125°C which are considerably less than that desired for ablative resins (e.g., 150,000 psi and 300°C, respectively).

Plastics which do exhibit desired mechanical properties and thermal stability (polyesters, phenolics, silicones, furans, and epoxides) contain elements such as oxygen and/or silicon which are chemically reactive in the high temperature corrosive environment which exists for the fluorine/hydrogen propellant class.

Recently, new polymers called "stiff" polymers\* have been introduced to polymer art. These polymers have a modulus of approximately 500,000 psi and are thermally stable at temperatures unusually high for organic resins. Polyphenylene are one class of a stiff hydrocarbon polymer (See Appendix I for discussion). Others (e.g., polybenzimidazoles, polyimides, polysilsequioxalenes, etc.) have a high hydrocarbon content, but normally contain nitrogen and oxygen atoms which could be sites of thermal decomposition.

#### 3.2.1 Selection of Cyclized Polybutadiene Urethane Ladder Polymers as a Candidate "Stiff" Hydrocarbon Resin Class

Because of the limitations of the available high hydrocarbon resins, a new hydrocarbon rich polymer was conceived and synthesized in this

---

\*"Stiff" polymers contain molecular backbones characterized mainly by cyclic chemical groups rather than singly bonded groups which are common to most polymers.

program. The resin system developed is based on poly (cyclized 1, 2-polybutadiene) tolyl urethane. The synthesis route and idealized structure of this resin are given in Figure 3.

Poly (cyclized 1, 2-polybutadiene) tolyl urethane is viewed as a modified "ladder" polymer resin system. The "ladder" configuration is desirable because it enhances the thermal and oxidative stability of hydrocarbons (See Appendix B). In addition, the system should yield resins that are stiff and tough, thus exhibiting the mechanical properties required for preparation of useful laminates.

Because the toughness of resins increases with increasing molecular weight of the prepolymer used in its preparation, chain extension of the low molecular weight prepolymer was considered to be desirable prior to formation of the ladder configuration. Consequently, the prepolymer was fitted with chemically functional primary hydroxyl groups, which on reaction with a diisocyanate form high molecular weight chain extended polyurethane polymers at moderate temperature, i. e., room temperature to 160°F. After chain extension, a free radical mechanism will induce cyclization, e. g., formation of the ladder structure-cyclized 1, 2-polybutadiene groups, as shown in Figure 3.

The candidate member of the cyclized polybutadiene urethanes chosen for synthesis in this program, poly (cyclized 1, 2-polybutadiene) tolyl urethane, is rich in carbon in compliance with the criteria established for resin stability in the F<sub>2</sub>/H<sub>2</sub> propellant class combustion environment. The weight percent of carbon and hydrocarbon in this polymer are listed in Table VIII together with comparable data for other laminating resin systems. This table shows that the selected resin has a carbon/oxygen atom ratio six times larger than phenol-formaldehyde currently employed as an ablative resin.

Table VIII. Carbon Content of Various Resins

Resin System	Empirical Formula	C atoms/- O atoms	Weight % Carbon	Weight % Hydrocarbon
Epoxide	C <sub>19</sub> H <sub>20</sub> O <sub>4</sub>	19/4	73.1	79.5
Phenol-Formaldehyde	C <sub>7</sub> H <sub>7</sub> O	7/1	78.5	85.0
Furans	C <sub>11</sub> H <sub>8</sub> O <sub>2</sub>	11/2	76.7	81.4
Cyclized 1, 2- Polybutadiene (Urethane Extended)	C <sub>84</sub> H <sub>120</sub> O <sub>2</sub> N	42/1	85.9	96.1

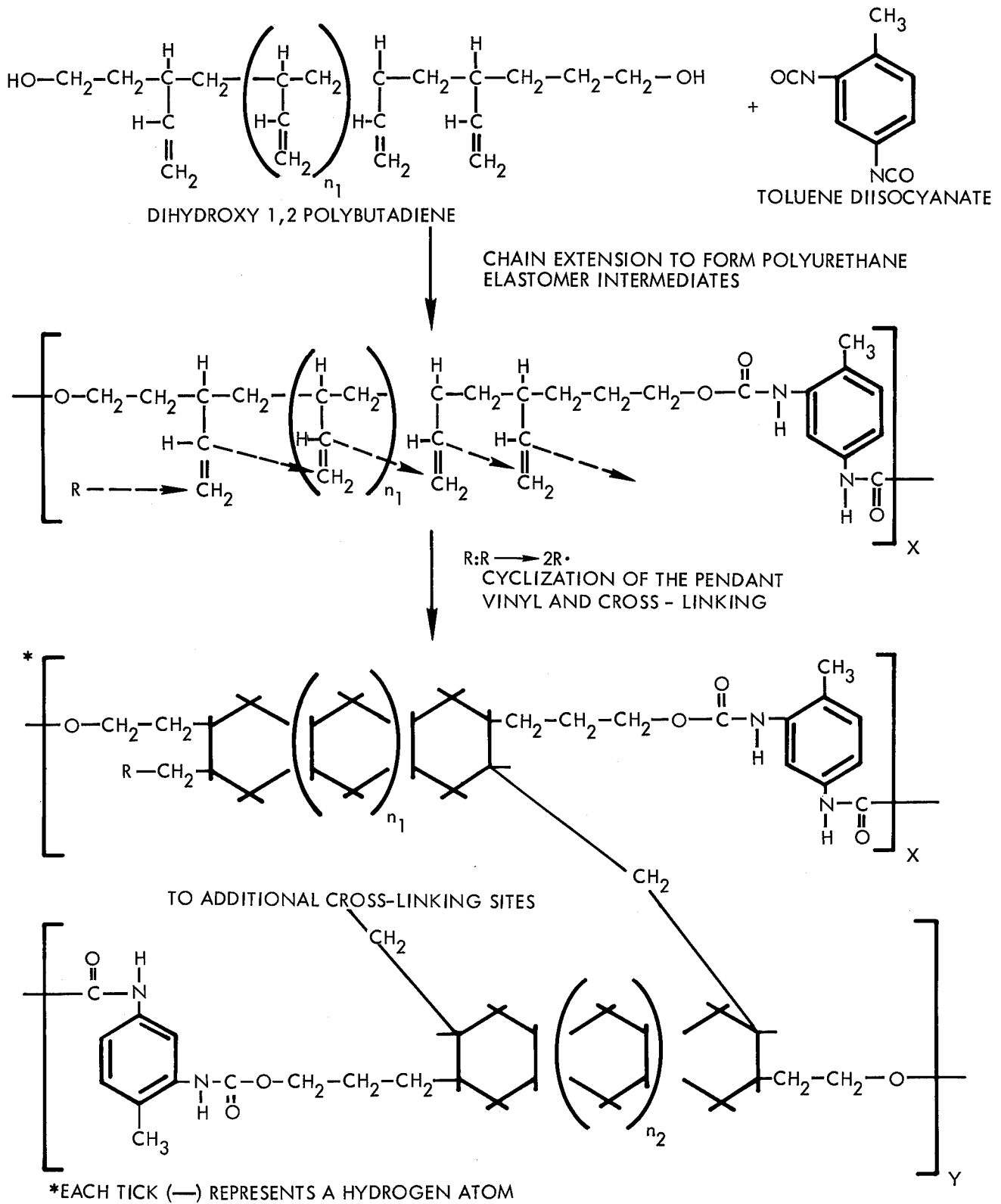


Figure 3. Synthesis of Poly (Cyclized 1,2-Polybutadiene) Toly Urethane

### 3.2.2 Preparation of Poly (Cyclized 1, 2-Polybutadiene) Tollyl Urethane

An extensive synthetic effort was devoted to the preparation of poly (cyclized 1, 2-polybutadiene) tolyl urethane. From this effort it was found that a stiff hard plastic could be formed using 1, 2-polybutadiene diol prepolymer, toluene diisocyanate and ditertiary butyl peroxide in the manner depicted in Figure 3. Details concerning the studies which covered free radical initiator optimization, curing conditions, mode of polymerization, experimental property determinations, comparison of the synthesis approach to related work, and a discussion concerning the mechanism of polymerization are presented in Appendix G-2. Physical and thermal properties of this newly synthesized material are listed in Section 3.5, Table IX.

### 3.3 ORGANO-METALLIC AND INORGANIC RESINS FOR USE WITH OF<sub>2</sub>/B<sub>2</sub>H<sub>6</sub> PROPELLANT CLASS

The thermochemical criteria for resins most suitable for use in the highly reactive OF<sub>2</sub>/B<sub>2</sub>H<sub>6</sub> propellant combustion environment indicate that the formation of resins, which on decomposition, yield high melting oxides and fluoride residual species are desirable. Such a residue can form a stable matrix which, when considered in combination with the filler, permits the formation of a protective surface coating during ablation and provides an approach for incorporation of materials which will cause internal endothermic reactions. It is preferable to incorporate the high melting oxide, fluoride-metallic elements directly in the resin structure as opposed to blending them into the matrix as separate compounds. As separate compounds, the species would be subject to substantial erosion by the exhaust stream. The use of metal oxides and fluorides per se as ablative resins is undesirable because these materials are devoid of "plastic" properties, consequently, they are sensitive to mechanical and thermal shock.

Two approaches which appeared attractive for preparing resins containing suitable metallic elements were: 1) the synthesis of polymers containing alkaline earth metal oxides, and 2) the formulation of phosphate bonded oxides which were reported by Wehr and Lauchner (Reference 4) to be ductile.

Primary emphasis in this program was placed on the preparation of alkaline earth metal containing polymers. This work and also the laboratory effort on phosphate bonded oxides are discussed below.

### 3.3.1 Poly Alkaline Earth Metal Acrylates

Polymers containing alkaline earth metal oxides were synthesized in order to prepare resins with a decomposition matrix chemically resistant to the  $OF_2/B_2H_6$  propellant exhaust composition. Poly alkaline earth metal acrylate resins represent such a polymer system.

In poly alkaline earth metal acrylates, the alkaline earth metals are positioned pendant to the carbon-carbon backbone, the flexible carbon-carbon backbone gives the resins stability to thermal-mechanical shock.

Of various polymeric system backbones considered for incorporation of alkaline earth metal oxides, the alkaline metal acrylates contained the greatest amount of alkaline earth metal oxide. In addition, these polymers appeared capable of exhibiting processing properties which make them suitable for the preparation of laminates.

The specific poly alkaline earth metal acrylates selected for synthesis and evaluation were the magnesium, calcium and barium salts of poly acrylic acid. These polymers were prepared by free radical polymerization of anhydrous alkaline earth acrylates according to the reaction shown in Figure 4. The details concerning the synthesis, isolation, and chemical considerations of these candidate resins are given in Appendix G.3. The results obtained on property testing are given in Section 3.5.

### 3.3.2 Phosphate Bonded Oxides

Wehr and Lauchner (Reference 4) formulated phosphate bonded oxides to yield inorganic polymers which exhibit ductility and oxidative stability. As a result, these polymers were proposed as matrices of

ablator compositions for use with the  $\text{OF}_2/\text{B}_2\text{H}_6$  propellant system. These materials offer the best available route to form matrices without organic matter. They are prepared from alumina, cobalt oxide, zinc oxide, phosphoric acid and water. The hard material obtained on reacting these constituents at  $200^\circ\text{C}$  is crushed and ball milled. The resulting powder is pressed into desired shapes at elevated pressure and temperatures. In the synthesis studies described in Appendix G. 4, the phosphate bonded oxides of Wehr and Lauchner were prepared for evaluation and physical property determinations. The results of the property testing are recorded in Section 3. 5.

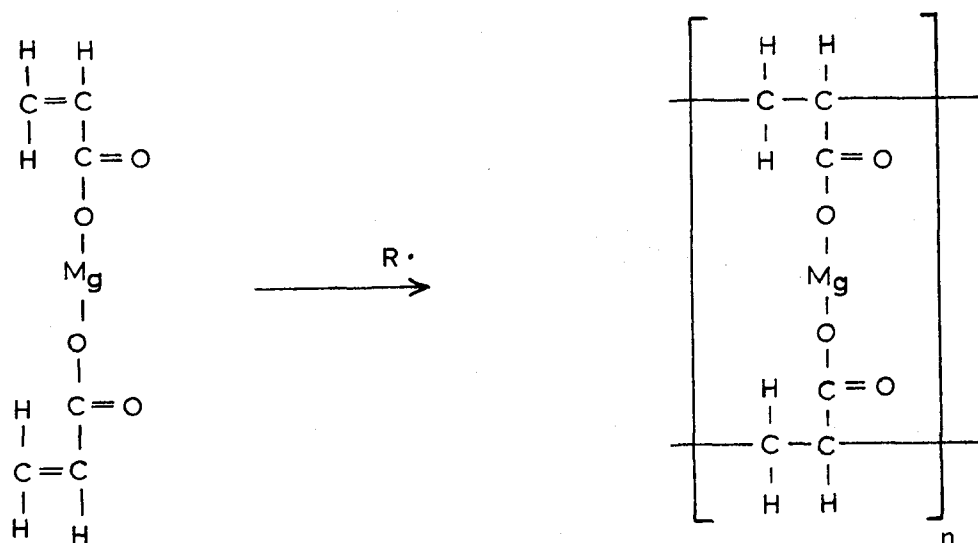


Figure 4. Preparation of Poly Magnesium Acrylate

### 3. 4 ADDITIONAL PROMISING CANDIDATE RESIN SYSTEMS

Several promising resin systems for fluorine containing propellants were found to offer specific advantages and therefore were reviewed in detail. These resin systems which include polybenzimidazoles, polyimide esters and polyimide ethers for the fluorine/hydrogen propellant class and zirconium boron polymers for the  $\text{OF}_2/\text{B}_2\text{H}_6$  propellant class, are discussed below.

#### 3. 4. 1 Polybenzimidazoles

Polybenzimidazoles represent the most thermally stable commercially available polymer class. Their highly aromatic ladder-type structure should produce dimensionally stable char residues.

Furthermore, they contain a high carbon content. These properties make it attractive for use with the fluorine/hydrogen propellant class. The disadvantage of polybenzimidazoles is that they are difficult to process since they require high temperature, high pressure and long handling time in their formation. During processing volatile products are evolved.

The availability of this material from a commercial source occurred during the latter part of the program, and consequently, tests of this general class of materials could not be performed. Modification of polybenzimidazole resins and the use of dry bonding techniques described in Appendix J are recommended for future study. The synthesis techniques and structure of the polybenzimidazoles are presented in Appendix I.

### 3.4.2 Polyimide Esters

One of the new stiff organic polymer systems which was conceived during the program and was not reduced to practice is that of the polyimide ester as shown in Figure 5. A probable synthesis route for preparation of polyimide ester resins is shown in Figure 6. These polymers are an initial determination of resins whose cyclic chemical groups will aromatize under curing and/or ablative conditions. A discussion of other classes and types of selected stiff polymers is presented in Appendix I.

The new polymer systems are representative of a class of "stiff" polymers which should exhibit, upon aromatization, high second order transition temperatures, yet differ from current "stiff" polymers shown in Appendix I in that they provide processing advantages. Because resins do not thermally distort below their second order transition temperature, a high value of this property is attractive for applications where dimensional stability at high temperatures is required. In ablation, it is desirable that the resin be dimensionally stable to a temperature which is greater than the temperature determining the onset of its pyrolysis. In this manner, the resin has improved resistance to erosion by gases of a rocket engine (see Appendix B). Because the pyrolysis rate of organic resins proceeds appreciably at temperatures of 350 °C and greater, the high thermal stability of "stiff" polymers assures that pyrolysis of the resin will occur without significant loss of its mechanical integrity.

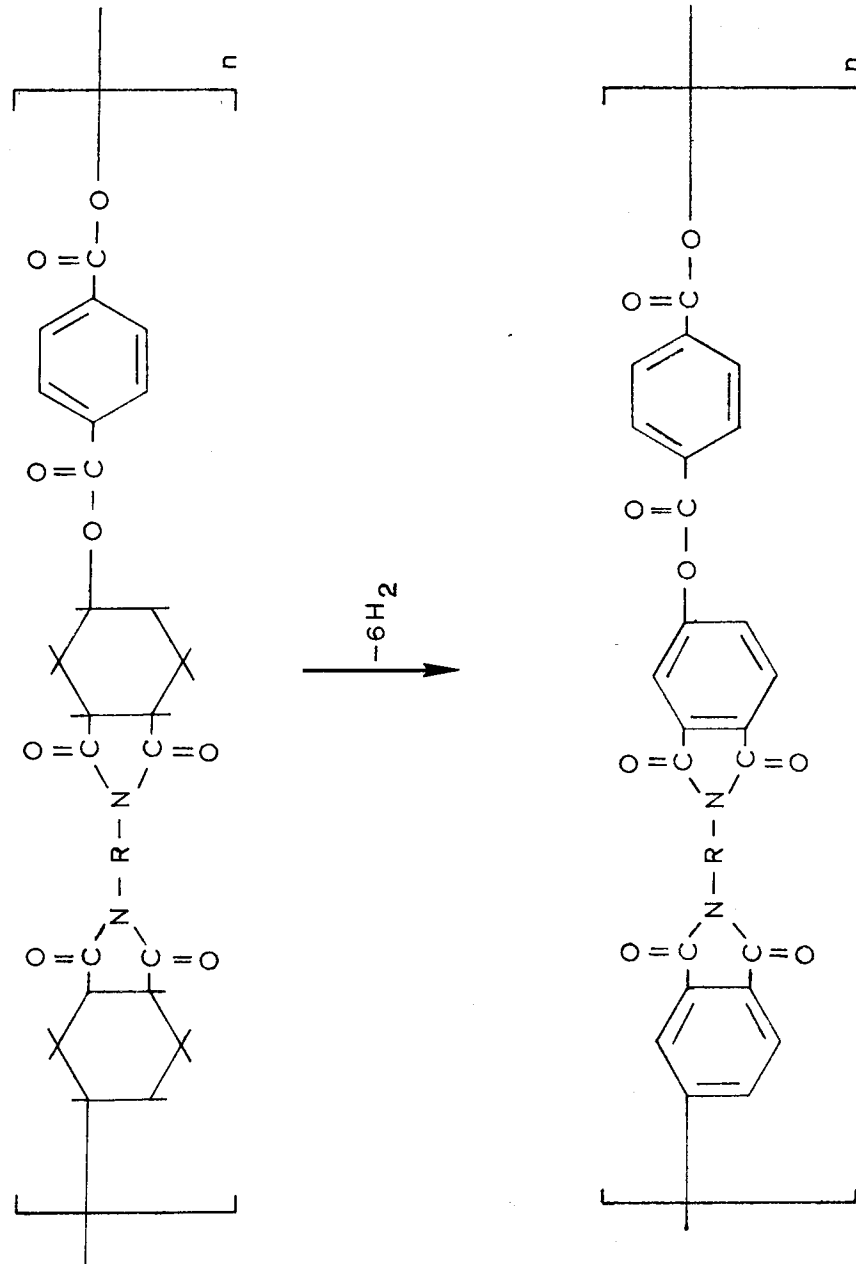


Figure 5. Hypothesized Pyrolysis Reaction Intermediate of Polyimide Esters

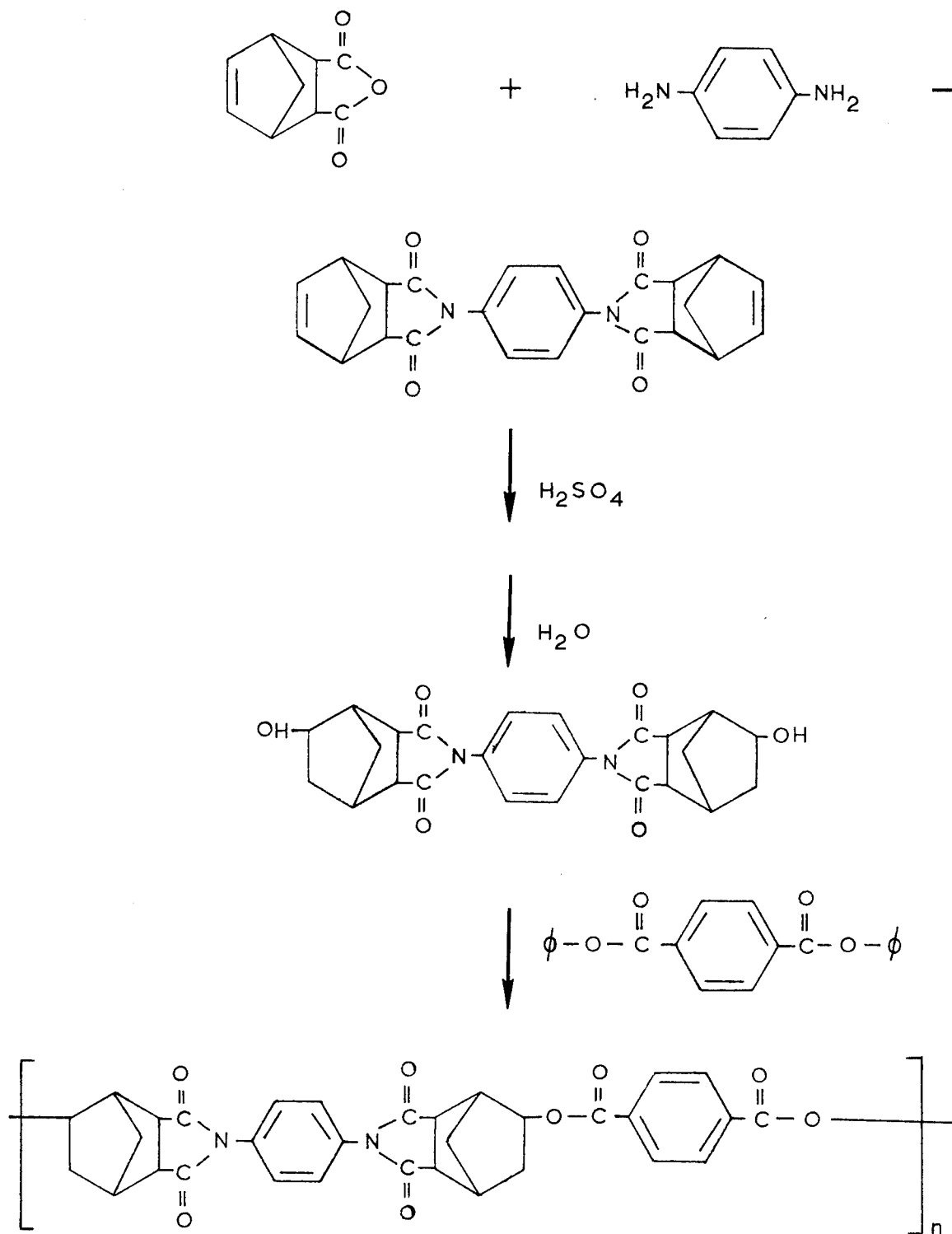


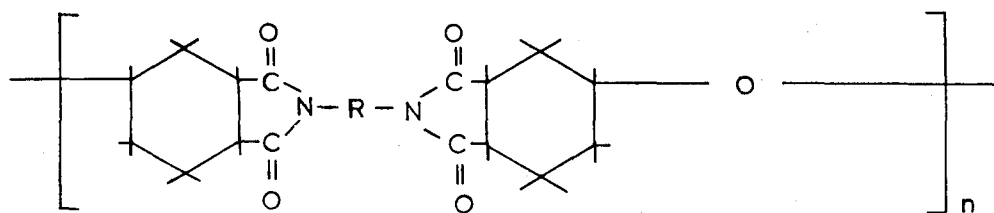
Figure 6. Proposed Route to Polyimide-Polyester Copolymer Resins

The fact that these polymer systems contain initially non-aromatized cyclic groups, their second order transition temperature is expected to be significantly lower than that of the analogous aromatic polymers. Thereby, these polymers are expected to "dry bond" at convenient laminating temperatures (see Appendix J).

In addition, the saturated and/or partially unsaturated cyclic chemical groups of the polymers are expected to aromatize during ablative use conditions. This aromatization is expected to occur through the liberation of hydrogen (methane for the polymer in Figure 6) from the cyclic groups. In order to facilitate the expulsion of hydrogen, the cyclic groups are chemically tailored with electron withdrawing chemical substituents, e. g., carbonyl groups. Upon the loss of chemical compounds from the polymer, their second order transition temperature will undergo a marked increase. This phenomenon occurs with minimum loss of volatiles evolving from a stable nonsolvated polymeric precursor. The phenomenon may be viewed as constituting resin curing, and as such is a distinct and novel chemical mechanism when it is utilized for the curing of resin masses.

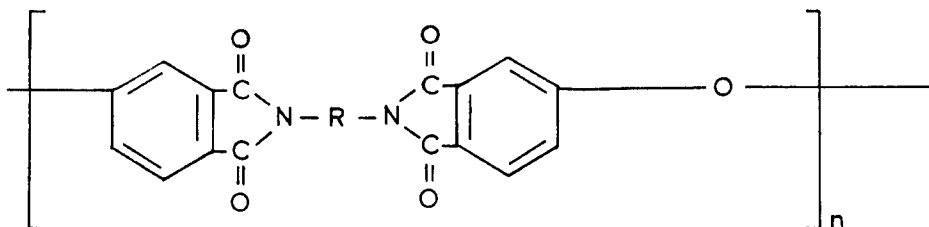
### 3.4.3 Polyimide Ethers

Another example of the modified polyimide polymer class described above that has been conceived during this program is that of polyimide ethers. The synthesis is exemplified in Figure 6; in this case a sulfuric acid derivative of a diimide would be reacted with a molar equivalent amount of water. Reaction conditions are required which minimize the hydrolysis of the imide groups. The expected products of this reaction are ether polymers of theoretically infinite molecular weight. In practice, the molecular weight of the polymers would be adjusted by careful control of the amount of water reacted with the sulfuric acid derivative. The chemical structure of a typical polyimide ether is shown below.



Polyimide Ether

In the pyrolysis of polyimide ethers, hydrogen gas (which has a high heat capacity) should be evolved initially leaving dimensionally stable polymers having the following structure:



Initial Polyimide Ether Pyrolysis Product

This polymer is considered to be even more dimensionally stable than the analogous intermediate formed on pyrolysis of polyimide esters.

#### 3.4.4 Zirconium-Boron Polymers

Inorganic polymers consisting of boron and zirconium were considered for development and evaluation. One method of synthesis of these materials consists of reacting zirconium or zirconium hydride with suitable proportions of boron. Reaction products of the formula  $ZrB_2$ , and  $ZrB_{12}$  have been separated (References 5 through 7). Zirconium diboride is extremely stable at all temperatures up to the melting point (about  $5430^{\circ}F$ ) in contact with carbon, while  $ZrB_{12}$  tends to decompose at elevated temperatures when carbon is present.  $ZrB_2$  is commercially available. Investigation of the products of the reaction of zirconium or zirconium hydride and boron in the presence of refractory metals, e.g., titanium, hafnium, tantalum, tungsten, and molybdenum may yield higher melting materials exhibiting enhanced chemical passivity. The borides of selected refractory metals were proposed for evaluation and comparison with zirconium diboride and mixed metal borides.

The formation of boron-zirconium polymers differing structurally from  $ZrB_2$ , - the structure of which consists of alternating layers of zirconium and boron atoms - may be obtained through the reactions described in Appendix G.5.

Preliminary evaluation of zirconium diboride was considered advisable prior to committing an effort to the difficult synthesis of zirconium-boride polymers. Pressed zirconium diboride samples, therefore, were tested with the Propellant Exhaust Environment Test (PEET) apparatus and showed excellent resistance to the  $F_2/H_2$  environment. The result of this test is included in Section 3.5.2. Continued interest in this resin system concept appears warranted.

### 3.5 PROPERTY DETERMINATION

Thermophysical properties and resistance to a fluorine/hydrogen combustion environment were computed or determined for the candidate resins, related materials such as composites employing these resins, and materials that may be used in conjunction with the resins. Specific properties determined included thermal decomposition temperature, density, thermal conductivity, specific heat and resistance to the Propellant Exhaust Environment Test (PEET).

#### 3.5.1 Test Methods

The methods used for the property determinations are presented in Appendix H. All tests were performed in replicate with a minimum test number of 2, and often as many as 5. The results of these tests are reported in the following section.

#### 3.5.2 Property Test Results

The physical properties of candidate resins and zirconium diboride are summarized in Table IX. Test information is shown for poly (cyclized 1, 2-polybutadiene) tolyl urethane together with the reference Novalac epoxy resin and other commercially available materials including an epoxy (EPON 828), a thermally stable proprietary phenolic resin from Monsanto (SC-1008), polypyromellitimide from DuPont (SP-1) and polyimide-amide resin obtained from Amoco. Table IX also presents data for the organometallic and inorganic materials poly calcium acrylate, phosphate bonded oxide and zirconium diboride.

The compilation of data in Table IX shows that the poly (cyclized 1, 2-polybutadiene) tolyl urethane represents the lowest density structural plastic tested. With the exception of CPBU, the thermal conductivity of the organic materials appears to be a direct function of aromaticity.

Table IX. Candidate Resin Properties

Material	Density, g/cm <sup>3</sup>	Thermal Conductivity, cal/cm-sec-°C x 10 <sup>4</sup>	Decomposition Temperature, °C	Specific Heat, cal/g°C	PEET Evaluation	
					Weight Loss, g	Volume Loss, cm <sup>3</sup>
Epon 828 Epoxy	1.23	5.98	303	0.224	0.58	0.47
Novalac Epoxy	1.45	4.69	351	0.282	0.55	0.38
CPBU <sup>a</sup>	1.05	7.54	457	0.470	0.50	0.48
Monsanto SC-1008 <sup>b</sup>	1.21	7.50	>500	0.328	0.38	0.31
SP-1 <sup>c</sup>	1.51	9.38	>500	0.253	0.21	0.14
Amoco <sup>d</sup>	1.37	9.32	>500	0.280	0.11	0.080
Polycalcium Acrylate	1.86	9.92	498	0.245	0.30	0.16
Phosphate Bonded Oxides	3.12	76.5	>500	0.093	0.025 <sup>f</sup>	0.008
Zirconium Diboride	6.10	1030 <sup>e</sup>	>500	0.15 <sup>e</sup>	Nil	Nil

a. Cyclized polybutadiene-urethane

b. Phenolic resin used in preparation of ablative resins

c. Dupont's modified polypyromellitimide

d. Pressed Amoco Chemical polyimide-amide resin

e. Literature values

f. Sample cracked

The phosphate bonded oxides have thermal conductivities approximately an order of magnitude higher than the organic resins. Poly calcium acrylate has thermal conductivity comparable to the highly aromatic organic compounds. It should be noted that the resins selected for evaluation generally have high decomposition temperatures. The reference epoxy resins have somewhat lower values. It also is interesting to note that the poly (cyclized 1, 2-polybutadiene) tolyl urethane has the highest specific heat of the resins considered, whereas the phosphate bonded oxides have the lowest specific heat.

The phosphate bonded oxides and zirconium diboride showed excellent resistance to the fluorine/hydrogen flame environment. The resins having high aromaticity demonstrated improved resistance to the flame environment. The weight or volume lost for the samples tested in the flame environment generally correlated with the thermal conductivity of the sample (the higher the thermal conductivity the lower the weight or volume loss). As identified in Section 2.2, it is desired to decrease thermal conductivity to decrease back wall temperature and increase the thermal conductivity to decrease the recession rate. The pronounced apparent relationship to thermal conductivity is partially attributed to the fact that steady state was probably not attained in the 10 seconds PEET evaluation. Further, it should be pointed out that thermal conductivity is a strong function of aromaticity for the organic materials. Because surface recession rate is a strong function of char density, the results of these tests indirectly support the thermophysical evaluation of relative importance of properties. The flame evaluation tests indicate that the properties of poly (cyclized 1, 2-polybutadiene) tolyl urethane, when employed as the resin matrix from which the principal char residue must be formed, should be modified to produce a more stable char. This may be accomplished by the use of catalytic additives which have been demonstrated to increase significantly the char density of aliphatic polymers (polyisoprene and polybutadiene) employed as insulators in solid rocket chambers.

Laminates of refrasil and carbon cloth with poly (cyclized 1, 2-polybutadiene) tolyl urethane were prepared. The physical properties and resistance to the fluorine/hydrogen flame were determined for these composites and compared with commercially available phenolic composites also containing refrasil and carbon cloth. These data and that for the Monsanto SC-1008 phenolic resin (without filler) are summarized in Table X.

Table X. Properties of Laminates

Material		Density, g/cm <sup>3</sup>	Thermal Conductivity, cal/cm-sec-°C x 10 <sup>4</sup>	PEET Evaluation	
Resin	Filler			Wt. Loss, g	Volume Loss, cm <sup>3</sup>
Cyclized Polybutadiene-Urethanes	None	1.05	7.54	0.50	0.48
	Refrasil <sup>a</sup>	1.71		0.26	0.15
	Carbon Cloth <sup>b</sup>	1.26	23.1	0.16	0.13
Phenolic	None <sup>c</sup>	1.21	7.50	0.38	0.31
	Refrasil <sup>d</sup>	1.85	10.9	0.19	0.10
	Carbon Cloth <sup>e</sup>	1.45	30.1	0.12	0.083

a = 38% w/w resin,

b = 35% w/w resin,

c = Monsanto SC-1008

d = Fiberite MX2600, Monsanto SC-1008 resin, 29% w/w

e = HITCO CCA-1, Monsanto SC-1008 resin, 38% w/w

The use of carbon cloth, which increases the overall carbon content of the composite, improves the resistance of the composite to the fluorine/hydrogen flame environment. This improvement can be attributed either to the higher thermal conductivity of the sample which reduced the temperature of the surface reaction zone during the 10 second test exposure or to the inherently less reactive nature of carbon in the fluorine/hydrogen environment.

An evaluation was performed of the influence of the passive filler carbon on the behavior of resins. Initially the interaction of carbon filler with the reference Novalac epoxy was studied to determine general trends. The results of these tests are tabulated in Table XI. In general, increasing the carbon content, as expected, increased the thermal conductivity of the sample. There was an indication that the incorporation of carbon also tends to increase the resistance of the epoxy resins to the fluorine/hydrogen environment. An acetylenic carbon, RHC, was selected for use with poly (cyclized 1, 2-polybutadiene) tolyl urethane since chemical bonding between the carbon and the polymer would be expected. The test results indicate, however, that the addition of carbon to this high carbon content polymer decreases the resistance to the flame environment. This trend also was noted for polypyromellitimides containing graphite.

The poly alkaline earth metal acrylates are synthesized in the form of a powder which then is fused into a specimen suitable for property determination. The conditions for preparing a suitable fused specimen were not determined until late in the program. Consequently, early physical property testing of the poly alkaline earth metal acrylates was conducted in specimens using EPON 828 epoxy as a binder. It was postulated that the poly alkaline earth metal acrylates would cross-link with the epoxy resin. Physical property data for the metal acrylate-epoxy resins are presented in Table XII. Results for neat EPON 828 epoxy resin and a fused specimen of calcium polyacrylate prepared during the later part of the program are included in Table XII for comparison. The most significant result shown is the resistance imparted to the epoxy by the use of poly alkaline earth metal acrylates. The calcium and magnesium poly acrylates appeared comparable; the barium poly acrylates appeared to be less resistant to the fluorine/hydrogen flame.

Table XI. Filled Resin Properties

Material		Density, g/cm <sup>3</sup>	Thermal Conductivity, cal/sec-cm <sup>2</sup> C x 10 <sup>4</sup>	PEET Evaluation	
Resin	Filler			Wt. Loss, g	Volume Loss, cm <sup>3</sup>
Novalac Epoxy	None	1.45	4.69	0.55	0.38
	4.6% P-33	1.54	6.90	0.31	0.20
	16% P-33	1.36	7.61	0.24	0.18
	23% P-33	1.40	8.19	0.22	0.16
	27% P-33	1.44	9.62	0.28	0.19
	5% Statex F-12	1.30		0.55	0.42
	10% Statex F-12	1.33		0.27	0.20
	20% Statex F-12	1.35		0.27	0.20
	5% Molacco H	1.30		0.61	0.47
	10% Molacco H	1.30		0.61	0.47
	20% Molacco H	1.34		0.33	0.25
	5% Statex B-12	1.33		0.61	0.46
	10% Statex B-12	1.36		0.34	0.29
	20% Statex B-12	1.33		0.31	0.23
Cyclized Polybutadiene-Urethane	None	1.05	7.54	0.50	0.48
	10% RHC <sup>a</sup>	1.08		0.67	0.66
Polypyromellitimide	None	1.51	9.38	0.21	0.14
	Graphite	1.58	11.39	0.36	0.23

a. Acetylenic carbon black

Table XII. Metal Acrylate-EPON 828 Properties

Additive	Density, g/cm <sup>3</sup>	Thermal Conductivity, cal/cm-sec-°C x 10 <sup>4</sup>	PEET Evaluation	
			Wt. Loss, g	Volume Loss, cm <sup>3</sup>
None (100% Epon 828)	1.23	5.98	0.58	0.47
Calcium Polyacrylate (fused)	1.86	9.92	0.30	0.16
65% Ca Polyacrylate	1.43	8.74	0.37	0.26
55% Ca Polyacrylate	1.45		0.29	0.20
55% Ca Polyacrylate 2:1 Epoxy:MNA	1.46		0.29	0.20
70% Mg Polyacrylate	1.44	9.87	0.26	0.18
60% Mg Polyacrylate	1.48		0.29	0.20
60% Mg Polyacrylate 2:1 Epoxy:MNA	1.50		0.23	0.15
65% Ba Polyacrylate	2.02		0.38	0.19
60% Ba Polyacrylate	1.95		0.47	0.24
60% Ba Polyacrylate 2:1 Epoxy:MNA	1.67		0.40	0.24

In order to establish guidelines for the use of refractory filler materials which may be employed in conjunction with resins, thermophysical properties of the materials shown in Table XIII were compiled from the literature. Fluorine/hydrogen flame resistance of these materials was also determined and the data are summarized in Table XIII. The materials are listed in order of their reactivity with the fluorine/hydrogen environment. The data show that carbon-type fillers are the most resistant to the fluorine/hydrogen environment. This confirms the general conclusion for the use of high carbon content composites with this propellant class. Tungsten showed a higher relative reactivity than would be anticipated from equilibrium calculations. Tantalum is considerably more reactive than the resins. Melting of the pyrolytic graphite was observed. This information is of interest since it indicates that the temperature of the graphite was at least  $3923^{\circ}\text{K}$ , which substantiates the calculated adiabatic flame temperature of  $3984^{\circ}\text{K}$  at the experimental mixture ratio for the fluorine/hydrogen combination.

### 3.5.3 Discussion of Test Results

The candidate resins and related composites and materials were characterized in terms of three thermophysical properties of the unreacted specimens which are theoretically related to the specimen performance in a high temperature environment. These properties are density, thermal conductivity, and specific heat. The heat of decomposition also was determined.

The thermophysical properties of the decomposition products were not directly measured. The determination of these properties requires a comprehensive effort which includes special techniques for preparation of samples which would be representative of those obtained in an engine environment. Consequently a use test was devised which would assess, in a semi-quantitative manner, the reactivity of materials to the fluorine/hydrogen flame environment at a mixture ratio producing a theoretical combustion temperature of  $3984^{\circ}\text{K}$ . The limitations of this test must be recognized in the interpretation of the results, namely:

1. The gas dynamic conditions in the engine are not simulated.

Table XIII. Refractory Filler Material Properties

Material	Density, g/cm <sup>3</sup>	Thermal Conductivity, <sup>a</sup> cal/cm-sec-°C x 10 <sup>4</sup>	Specific Heat, <sup>a</sup> cal/g-°C	PEET Evaluation	
				Wt. Loss, g	Volume Loss, cm <sup>3</sup>
Tantalum-10% Tungsten	16.8	1350		0.79	0.047
Tantalum	16.7	1300		0.74	0.044
Zircon (ZrO <sub>2</sub> -SiO <sub>2</sub> )	4.64	124	0.14	0.18	0.038
FS85 <sup>b</sup>	10.8	910		0.37	0.034
Tantalum-10% Tungsten (carburized)	16.8	1350		0.55	0.033
Hafnium Carbide-Carbon	10.2			0.30	0.030
Tantalum (Carburized)	16.6	1300		0.28	0.017
Zirconium Carbide	6.80	530	0.08	0.10	0.016
Tantalum Carbide	14.4	505		0.16	0.011
TZM <sup>c</sup>	10.1	2790	0.063	0.11	0.011
Tungsten	19.3	3940	0.032	0.19	0.010
JTA <sup>d</sup>	3.0	1780-2690 <sup>f</sup>		0.030	0.010
Pyrolytic Graphite	2.27	41 (C-direction)	0.215	0.020	0.009
CFZ <sup>e</sup>	1.9	1000-5000 <sup>f</sup>		0.004	0.002
P-2003 Graphite	2.07	1000-5000 <sup>f</sup>	0.215	0.002	0.001
Extruded Graphite	2.19	1000-5000 <sup>f</sup>	0.215	Nil	Nil
ATJ Graphite	1.73	1000-5000 <sup>f</sup>	0.215	Nil	Nil

- a. Literature values  
b. Cb - 29 Ta - 12 W - 1.1 Zr (Fansteel)  
c. Mo - 0.5 Ti - 0.8 Zr - 0.03 C (Climax Molybdenum)  
d. Calcined petroleum coke, zirconium diboride and silicon graphite composite (National Carbon)  
e. Molded, medium grain graphite (National Carbon)  
f. Anisotropic - depends on orientation

2. The flame conditions were limited to that produced by the fluorine/hydrogen propellant combination at one mixture ratio for a fixed duration. A flame containing oxygen in addition to fluorine as the oxidizer was not utilized in this program.
3. Optimum composites employing new resins are not available at this time for test. Thus, the interaction of the resin and the filler is not suitably evaluated.

Nevertheless, the following data trends could be determined which influence the choice of resins for fluorine-containing propellant systems:

1. As indicated in the thermochemical evaluation, Section 2.4, high carbon content provides a matrix that is resistant to the fluorine/hydrogen flame.
2. Organic compounds having high aromaticity which should produce a dense carbon char are most resistant to ablation by a fluorine/hydrogen flame.
3. The poly calcium acrylate resin, although synthesized primarily for use in  $OF_2$ /diborane propellant class, was resistant to reaction in the fluorine/hydrogen environment.
4. The phosphate bonded oxides were not sufficiently ductile to withstand the thermal shock imposed by the flame, however, these materials showed excellent chemical resistance.
5. Although poly (cyclized 1, 2-polybutadiene) tolyl urethane contains the highest carbon content, there is indication that the formation of a higher density char would improve its utility as an ablative resin matrix. This can be compensated partially by the selection of carbon fabric fillers which reinforce the char residue. Since the density of the char is a function of the decomposition kinetics for materials such as poly (cyclized 1, 2-polybutadiene) tolyl urethane, catalytic additives which produce more dense chars in linear hydrocarbon polymers show promise of improving the ablative resistance of this resin system.

#### 4.0 RECOMMENDATIONS OF RESINS FOR FUTURE USE

The analytical and laboratory efforts described in the previous sections of this report establish a sound technical basis for determining the potential of resins for future ablative applications. This effort also can serve to direct continued studies toward the solution of identical problem areas.

The investigation of new resins in this program was based on satisfying specific property criteria required for the resins to be useful in future ablative applications. The underlying theme for the use of resins with the fluorine/hydrogen propellant class, namely, the generation of carbon as the decomposed resin matrix in the engine environment, was determined from equilibrium chemistry considerations. Superimposing thermophysical considerations, a high density char evolved as the primary factor to minimize surface recession.

A number of resins were found to satisfy these foremost criteria. A tradeoff appears to exist, however, between processing difficulty and the capacity of the resin to contain high carbon content and produce dense chars. These processing factors are discussed in this section.

The criteria for resins to be employed for future propellant systems containing oxygen as well as fluorine in the oxidizer, e. g.,  $OF_2$ , can not be based chemically on the relatively straightforward equilibrium considerations of reactivity between the resin and the propellant combustion environment. It is necessary to rely on the less predictable chemical kinetic considerations to provide a stable matrix for survival in the oxygen containing propellant environment. The interaction between the resin and the filler is of considerable importance to the final choice of resin. Based on the inherent resin characteristics, polymers containing elements that form high melting fluorides and oxides are most promising because they can form a stable matrix in the propellant combustion environment. Polymers of this type are not readily available, consequently, continued synthesis effort, property determination and materials testing are needed to resolve this technical difficulty.

The analytical and laboratory investigations have identified a number of resins which show promise of improving the effectiveness of ablative composites in the environments of advanced liquid rocket propellants. In this section the methods of preparation of the resins and potential composites are evaluated. Also discussed are the reproducibility of the resin formulations and the compatibility of the most promising resins with reinforcing fabrics. Finally, the choice of resins offering the most potential for future ablative applications is summarized.

#### 4.1 METHODS OF PREPARATION AND SCALE UP OF SYNTHESIS

The factors affecting potential scale up of synthesis and production of composites from candidate resins are discussed below. The general preparation format of candidate systems is shown in Table XIV.

##### 4.1.1 Cyclized Polybutadiene-Urethane Resins and Composites

Cyclized polybutadiene-urethane resins are composed of a prepolymer, a chain extender, and a cyclization catalyst. Of the three components in the system, the prepolymer is the single component which is not available commercially. However, the prepolymer is formed from chemical components which are inexpensive and available in large quantities, namely, butadiene and ethylene oxide. The catalyst employed in the preparation of the prepolymer, lithium, is commercially available. Lithium would be a recoverable by-product of the prepolymer synthesis.

Scale up synthesis of cyclized polybutadiene-urethane resins should not entail any unusual difficulties. In addition, the fabrication of laminates with cyclized polybutadiene-urethane resins does not represent any special problems. Standard laminating art employed in the preparation of epoxide and polyester laminates may be utilized.

The cyclized polybutadiene-urethane ladder polymers are considered to be particularly applicable to the preparation of carbon and graphite laminates. The low surface free energy that is expected in this hydrocarbon rich resin contributes to enhanced wetting of carbonaceous fibers. In addition, on curing this resin may be expected to interact chemically with sites of unsaturation that exist on the surface of carbonaceous fibers.

Table XIV. Preparation Format of Candidate Resins and Composites

Resins	Resin Preparation Method	Laminate Formation
Cyclized Polybutadiene Urethanes	Casting, degassing then curing	Wet "layups", or prepregging, followed by curing with minimal mechanical pressure
Calcium- and Magnesium - Containing Polymers Phosphate-Bonded Oxides "Stiff" Polymers Polybenzimidazoles Polyimides Polyimide Esters Polyimide Ethers Polyimide-Amides	Hot pressing, concurrently applied vacuum, mechanical pressure, heat	Powder-fabric fusion with vacuum and mechanical pressure. With "stiff" polymers: prepregging, followed by "dry bonding"*
Zirconium Diboride Titanium Diboride	Consecutively applied mechanical pressure, sintering	Compact powder-fabric with mechanical pressure, followed by sintering.

\*See Appendix J

#### 4.1.2 Poly-Alkaline Earth Metal Acrylate Resins and Composites

All of the constituents of poly-alkaline earth metal acrylate resins are prepared from commercially available materials. The chemical constituents are inexpensive, no component of the resin system should cost more than one dollar per pound.

The preparation of laminates with this polymer system will not present any difficulty. The resin cures at moderate temperature, e. g., 120°C, at mechanical pressures of around 15,000 psia. During the curing process it is not considered to be necessary to protect the laminate from the action of air because oxygen and moisture are believed to have only a slight effect upon the curing character. No volatiles are eliminated during the cure of the resin.

The major shortcoming of this resin is its tendency to absorb water to form the dihydrate. Special protective handling and storage procedures may be required.

#### 4.1.3 Phosphate Bonded Oxides

The phosphate bonded oxide resin system is composed of basically very inexpensive materials. If refractory materials are added to this system, the cost will increase somewhat. All of the constituents for preparing satisfactory materials are commercially available. The preparation of laminates of this polymer system will not present any major difficulties. Use can be made of techniques, such as, powder-fabric vacuum fusion, and mechanical pressure. Incorporation of short brittle fiber materials may necessitate certain modifications in processing techniques which require high mechanical pressures.

#### 4.1.4 "Stiff" Polymers

The processing techniques to be used for preparation of large resin specimens and composite materials are very similar for polybenzimidazoles, polyimides and polyimide-amides. These techniques for resin synthesis consist of hot pressing with concurrently applied vacuum, mechanical pressure and heat. Polyimide ester and polyimide ether resins and composites should be capable of preparation by the same general techniques but at less severe conditions. To prepare laminates of stiff polymers, the readily amenable processing method consists of prepregging the filler, followed by curing, and then dry bonding the impregnated material. A detailed discussion of the techniques of dry bonding is presented in Appendix J.

The starting materials for preparation of these stiff polymers are available only in moderate quantities and for very large scale synthesis it would be necessary to have special batches prepared.

### 4.2 REPRODUCIBILITY OF PREPARATION AND COMPATIBILITY OF NEW RESINS WITH FILLERS

By using consistent amounts of starting materials and processing conditions, it has been possible to prepare reproducibly all the resins synthesized during this program. The measure of reproducibility was both 1) the thermophysical property measurements and 2) the resistance

to the fluorine/hydrogen torch. No detailed studies were made concerning the reproducibility of the mechanical properties in the preparation of the candidate resins. The resin materials should be chemically compatible at ambient temperatures with the potential filler systems. At engine firing temperatures, desired endothermic chemical reactions between the charred resin products and the filler can occur through proper selection of the filler. This was discussed in detail in Section 2.4.

#### 4.3 RECOMMENDATION FOR THE APPLICATION OF SELECTED RESINS

As stated previously the candidate resin systems can be segregated into classes for application with two specific propellant systems as follows:

- Fluorine/hydrogen propellant class - poly (cyclized 1,2-polybutadiene) tolyl urethane, polyimide-amide, polybenzimidazoles, polyimide ether, and polyimide ester resins.
- $\text{OF}_2/\text{B}_2\text{H}_6$  propellant class - poly calcium and magnesium acrylates, phosphate bonded oxides, and zirconium boride resins.

The candidate resins are in various states of development. The poly (cyclized 1, 2-polybutadiene) tolyl urethane, poly calcium and magnesium acrylates, and phosphate bonded oxides are in a stage of development where optimization of the resin for use as an ablative matrix should be emphasized. The resin optimization would examine such factors as varying the cure cycles, catalysts, chain extenders and aromatization promoters. Additional synthesis and property determination are necessary for the polyimide ether-polyimide ester resin class and zirconium boride resins. Property determinations also are required to complete the information on polybenzimidazole resins. Furthermore, all candidate resins for the  $\text{OF}_2/\text{B}_2\text{H}_6$  propellant class require screening with a flame use test employing oxygen as well as fluorine as the oxidizer. Standard reinforcing agents such as graphite, silica cloth and new fiber systems which may be in short lengths and extremely brittle require processing optimization with the resins. Therefore, a systematic experimental evaluation of fabricating ablative composites using the candidate resins is required prior to engine test of the composites. The methods to

evaluate the composites, analytically and experimentally, which were developed under this program should be used for screening and selecting the most promising composites for scale up and final engine test evaluation. This sequence of steps provides a sound technical approach for the introduction of the new resins as ablative matrices for use with advanced liquid rocket engine propellants.

## 5.0 CONCLUSIONS

Summarized below are the conclusions reached during the analytical and experimental effort to study new or improved resin systems suitable for use as a matrix material in ablative composites for liquid rocket combustion chambers.

1. On the basis of analytical study, the thermophysical properties which govern the surface recession rate, listed in order of importance, are: surface heat of reaction, char density, char conductivity, decomposition parameter (effective decomposition activation energy), pyrolysis gas specific heat, resin density, resin specific heat, heat of decomposition, virgin conductivity and the decomposition constant.

The properties which govern the backwall temperature, listed in order of importance, are: the decomposition parameter (effective decomposition activation energy), resin density, char conductivity, virgin conductivity, pyrolysis gas specific heat, char density, heat of decomposition, decomposition constant, resin specific heat, and surface heat of reaction.

2. On the basis of equilibrium thermochemical calculations the principal criteria for guiding the selection and synthesis of new resins for the fluorine/hydrogen propellant system is the capability of the resin to yield a carbon matrix upon decomposition. High carbon content in the resin therefore is desirable.
3. Propellants of the  $\text{OF}_2/\text{B}_2\text{H}_6$  class were found to be reactive at temperatures near the flame temperature with all candidate materials examined when equilibrium conditions were imposed. For survival, the ablative surface should be maintained at lower temperatures. If the lower temperature is to be maintained, an endothermic process must occur. Resins which appear attractive to survival in the presence of the  $\text{OF}_2/\text{B}_2\text{H}_6$  propellant combustion products are those which have a minimum carbon content and contain elements yielding refractory oxides on pyrolysis and form high melting fluorides (e. g., calcium and magnesium oxides).
4. Poly (cyclized 1,2-polybutadiene) tolyl urethane, a new resin system having 86% carbon by weight, represents a candidate resin for use with the fluorine/hydrogen propellant class. This resin is readily processable into a tough, stiff material having an incipient thermal decomposition temperature of  $457^\circ\text{C}$ .

5. Poly alkaline earth metal acrylates can be prepared containing 24.2, 30.8 and 54.9 equivalent oxide weight percents of magnesium, calcium and barium, respectively. These resins are candidates for use with the  $\text{OF}_2/\text{B}_2\text{H}_6$  propellant class.
6. Phosphate bonded oxides represent a second candidate resin for the  $\text{OF}_2/\text{B}_2\text{H}_6$  propellant class. However, process optimization and possible modifications are required to obtain a material having improved ductility.
7. Polybenzimidazoles, polyimide-amides, and the polyimide esters - polyimide ethers resin system are additional candidate resins for the fluorine/hydrogen propellant class. Zirconium boride polymers offer an approach for the synthesis of a material resistant to  $\text{OF}_2/\text{B}_2\text{H}_6$  propellants.

## 6.0 NEW TECHNOLOGY

In this section are presented discussions of the new resin concepts generated in the course of this program. These concepts, covering both compositions of matter and applications, are believed to be of sufficient novelty that invention disclosures have been submitted to the TRW Systems Patent Department. The subject of these disclosures are listed below:

<u>Docket No.</u>	<u>Title</u>
3232	Cyclized Polybutadiene Urethanes
3339	Polyimide Esters, a New Class of Polymers
3306	Polyimide Ethers, a New Class of Polymers
3329	Cyclized Polyisoprene Urethanes
3395	Poly Alkaline Earth Metal Acrylates
3357	New High Temperature Adhesives
3381	Reinforced Structural Plastics
3382	Protective Coatings

A separate report covering these disclosures is in the process of being submitted to NASA, but a discussion of these inventions, their novel features, and applications is deemed appropriate herein.

### 6.1 CYCLIZED POLYBUTADIENE URETHANES

A series of polymers based on the cyclized polybutadiene urethane structure has been conceived during this program. Specifically, this class of resin compounds is characterized by fused, linear cyclohexane structures interconnected by polyurethane groups and cross-linked between the molecular assemblages. As discussed in Section 3.2, this resin class is formed by reacting a long chain 1,2-polybutadiene diol with a diisocyanate at moderate temperatures and then initiation of the free radical induced cyclization of the pendant vinyl groups. The invention disclosure also covers the use of 1,2-polybutadiene diols which have a variety of molecular weights.

This polymer system has several unique features such as:

- Low density
- High chemical resistance
- Easily processed
- High thermal stability
- Resistance to water absorption
- High resistance to UV exposure
- High compressive strength
- High carbon content

It is believed that this polymer system can be used as a high temperature adhesive, a matrix for reinforced structural plastics, and preparation of plastic parts which have chemical and moisture resistance.

## 6.2 CYCLIZED POLYISOPRENE URETHANES

This class of resins is very similar to the cyclized polybutadiene urethanes. A 3,4-polyisoprene diol is employed instead of the 1,2-polybutadiene diol. The resultant polymer is characterized by a series of linear, fused 1-methyl cyclohexane groups. It is believed that features and applications of the cyclized polyisoprene urethanes would be very similar to the cyclized polybutadiene urethanes.

A potential advantage of the methyl cyclohexane basic structure that has been postulated is that on pyrolysis of the cyclized polyisoprene urethanes, the first step of decomposition could be formation of methane. This would introduce unsaturation in the cyclic structure which subsequently could be converted to a highly aromatic structure which would be favorable for producing high char yields.

## 6.3 REINFORCED STRUCTURAL PLASTICS

An invention disclosure was submitted concerning the application of the cyclized polybutadiene urethanes and cyclized polyisoprene urethanes for use as a resin in reinforced structural plastics.

The reinforced structures prepared using this class of resins exhibited high thermal, oxidative, hydrolytic and chemical stability. Structural plastics prepared using this resin system show promise for use in ablative materials, deep submergence ocean vessels, and

lightweight structural plastics. The use of cyclized polybutadiene urethane resin systems permit preparation of composite structures by vacuum bag layup methods, preimpregnation and pressing, tape winding and curing, and filament winding procedures. The reinforced structural plastic can be prepared without the elimination of volatile matter, thus permitting use of processing techniques which require relatively low mechanical pressures. The reinforced structural plastic has a lower density than comparable materials using other resin matrices. The mechanical properties of the reinforced structural plastic are not degraded appreciably on boiling in water.

#### 6.4 HIGH TEMPERATURE ADHESIVES

An invention disclosure was submitted to the TRW Patent Department covering the application of cyclized polybutadiene urethanes and cyclized polyisoprene urethanes as high temperature adhesives. These adhesives have thermal stability in excess of 400°C, yet can be processed in a manner similar to epoxides. In addition, it is possible to apply the adhesives by formation of separate tack-free films on the surface of adherends which can be subsequently pressed together at moderate temperatures to affect adhesive bonding. Adhesives with comparable high temperature stability, such as, polypyromellitimides, polybenzimidazoles, and polyphenylenes are extremely difficult to process. The adhesive also exhibits excellent oxidative and chemical stability.

#### 6.5 PROTECTIVE COATINGS

An invention disclosure was submitted to the TRW Systems Patent Department covering the applications of cyclized polybutadiene urethanes and cyclized polyisoprene urethanes as protective coatings. These coatings show exceptional chemical resistance in particular, resistance to chemical attack by nitrogen tetroxide. It is possible to apply the coating in the form of an aerosol, paint and dip either in a carrier or in the neat liquid uncured form. The protective coating is practically colorless, consequently, pigments or dyes can be formulated into the mixture to provide desirable colors.

## 6.6 POLYIMIDE ESTERS AND POLYIMIDE ETHERS

Two new classes of polymers (polyimide esters and polyimide ethers) which are suspected to exhibit high temperature stability were conceived during this program. These polymers constitute new compositions of matter and are described in detail in Section 3.4

In addition to application as an ablative resin matrix it is believed that the high thermal and oxidative stability, toughness and impact strength of this polymer system are properties which would permit application of the plastic to fibers, films, re-entry glider nose caps, leading edges, fins, high performance nose cones, and hot structures.

The ether and ester groups in the polymer backbone of the polyimide ethers and polyimide esters should increase the flexibility and impact resistance of the polymers without sacrificing thermal and oxidative stability. The polymers of these inventions can be prepared by mild heating of a solution of monomer components. Hence, the processing of these polymers is considerably easier than required in the preparation of other stiff, high temperature polymers, such as polypyromellitimides, polybenzimidazoles, and polyimide-amides.

## 6.7 POLY ALKALINE EARTH METAL ACRYLATES

The application of poly alkaline earth metal acrylates for use in ablative materials was conceived during this program. The polymer system consists of the alkaline earth adducts of poly acrylic acid. The polymers can be prepared into compact resin specimens by hot pressing at 350°C under vacuum and applied mechanical pressure around 15,000 psi.

Detailed discussion concerning the preparation, isolation and evaluation of these polymers is presented in Appendix G.3. These polymers have use in ablative materials which are exposed to the combustion products of the OF<sub>2</sub>/B<sub>2</sub>H<sub>6</sub> propellant class.

The poly alkaline earth metal acrylates can be prepared into compact specimens containing alkaline earth metals molecularly dispersed and chemically bound within their matrices. They exhibit resistance to fluorine/hydrogen combustion environments.

APPENDIX A

THE CHARRING-RECESSION COMPUTER PROGRAM

The Charring-Recession Computer Program permits determination of the thermal response and surface recession of a charring, ablative material backed by a non-ablative material. The ablator is assumed to consist of two components; one which decomposes into a gas, and the other which remains to form a char structure.

The key equations\* solved by the program are as follows:

- a) Energy balance at each node within the material -

$$\begin{aligned} (\rho_a c_a + \rho_b c_b) \frac{\partial T}{\partial t} = k \frac{\partial^2 T}{\partial x^2} + \left( \frac{\phi k}{x} + \frac{\partial k}{\partial x} + W c_g \right) \frac{\partial T}{\partial x} \\ + \left[ \lambda_a + \int_0^T (c_g - c_a) dT \right] \frac{\partial \rho_a}{\partial t} \end{aligned} \quad (A-1)$$

- b) Energy balance at the interior (heated) surface -

$$\begin{aligned} -k \frac{\partial T}{\partial x} = h_1 (T_{oc} - T) + \sigma F_1 (T^4 - T_{or}^4) + Q_1 \\ - M \left[ W + (E\rho_b + F\rho_a) \dot{s} \right] (G - T) - \\ (J\rho_b + K\rho_a) \dot{s} \end{aligned} \quad (A-2)$$

- c) Energy balance at the exterior (cooled) surface -

$$-k \frac{\partial T}{\partial x} = h_2 (T - T_{2c}) + \sigma F_2 (T^4 - T_{2r}^4) + Q_2 \quad (A-3)$$

- d) Rate of decomposition -

$$\frac{\partial \rho_a}{\partial t} = -\gamma \rho_a^\epsilon e^{-\Gamma/T} = \frac{\partial W}{\partial x} + \frac{\phi W}{x} \quad (A-4)$$

\*Definition of symbols is given on pages 62 and 63

The following are prescribed as functions of temperature in the program input:

$c_a$	(BTU/lb- $^{\circ}$ F)	Specific heat of decomposable component
$c_b$	(BTU/lb- $^{\circ}$ F)	Specific heat of non-decomposable component
$c_g$	(BTU/lb- $^{\circ}$ F)	Specific heat of gas
$c_w$	(BTU/lb- $^{\circ}$ F)	Specific heat of backwall material
$k_o$	(BTU/ft-sec- $^{\circ}$ F)	Conductivity of virgin ablator
$k_b$	(BTU/ft-sec- $^{\circ}$ F)	Conductivity of non-decomposable component
$k_w$	(BTU/ft-sec- $^{\circ}$ F)	Conductivity of backwall material

The following are prescribed as functions of time in the program input:

$h_1$	(BTU/ft <sup>2</sup> -sec- $^{\circ}$ F)	Interior convective coefficient
$Q_1$	(BTU/ft <sup>2</sup> -sec)	Arbitrary heat input
$M$	(BTU/lb- $^{\circ}$ F)	Heat blocking factor

The prescribed initial variables are:

$T_o(x)$	( $^{\circ}$ F)	Initial temperature distribution in ablator
$\rho_o(x)$	(lb/ft <sup>3</sup> )	Initial density distribution in ablator

The following constants are prescribed in the input:

$E$	(Dimensionless)	Empirical constant in surface energy balance
$F$	(Dimensionless)	Empirical constant in surface energy balance
$F_1, F_2$	(Dimensionless)	Radiation shape factors
$G$	( $^{\circ}$ F)	Reference temperature
$h_2$	(BTU/ft <sup>2</sup> -sec- $^{\circ}$ F)	Exterior surface convective coefficient
$J$	(BTU/lb)	Surface heat of reaction (non-decomposable)
$K$	(BTU/lb)	Surface heat of reaction (decomposable)
$p$	(Dimensionless)	Number of intervals in ablator
$q$	(Dimensionless)	Number of intervals in backwall

$Q_2$	(BTU/ft <sup>2</sup> -sec)	Arbitrary heat input at backwall
$R_1$	(ft)	Distance from $x = 0$ to ablator-backwall interface
$R_2$	(ft)	Distance from $y = 0$ to outside surface of backwall
$s_o$	(ft)	Distance from $x = 0$ to initial position of ablator surface
$T_{max}$	(°F)	Control temperature for decomposition
$T_{oc}, T_{2c}$	(°F)	Convective driving temperatures
$T_{min}$	(°F)	Control temperature for decomposition
$T_{or}, T_{2r}$	(°F)	Radiative driving temperatures
$T_s$	(°F)	Control temperature for recession
$\rho_b$	(lb/ft <sup>3</sup> )	Density of non-decomposable component
$\rho_w$	(lb/ft <sup>3</sup> )	Density of backwall material
$\phi$	(Dimensionless)	Constant having a value of zero or one
$\lambda_a$	(BTU/lb)	Heat of decomposition
$\gamma_a$	(1/sec)	Empirical constant in decomposition equation
$\epsilon$	(Dimensionless)	Empirical constant in decomposition equation
$\Gamma$	(°F)	Empirical constant in decomposition equation

The program solves for the following unknown quantities as a function of time:

$s$	(ft)	Distance from $X = 0$ to ablating surface
$\dot{s}$	(ft/sec)	Surface recession rate
$T$	(°F)	Temperatures through the ablative material
$W$	(lb/ft <sup>2</sup> -sec)	Mass flux of gas at the surface
$\rho_a$	(lb/ft <sup>3</sup> )	Density of decomposable component through the ablative material

For the reference case, phenolic refrasil properties were used, with a convective heat input typical of that experienced under LEM Descent Engine firing conditions. This case was chosen for reference since considerable reported and test firing data were available for comparison with analytical predictions. The input quantities used for the reference run are tabulated in Table A-I. Surface recession was calculated by the surface energy balance, Equation A-2. The results obtained to date do not take into account the effect of boundary layer gas injection on the convective heat transfer coefficient. This effect reduces the convective heating in LEMDE by only 4%.

To perform the parametric survey, a computer run was made for each of two values bracketing the reference value of the variable being investigated. The driving temperatures were 5000, 6000 and 7000 °F. The total recession and backwall temperatures were obtained for a simulated firing duration of 300 seconds. In all cases, the original material thickness was 0.8 inch, the starting temperature was 70 °F, and the backwall was assumed to be adiabatic. The backwall temperature and recession obtained for each run are tabulated in Table A-II.

In order to evaluate the effect of changes in the physical properties of the ablator or changes in the engine thermal environment on the back-wall temperature and the surface recession, two influence coefficients  $\alpha$  and  $\beta$  were calculated by the following equations:

$$\frac{T}{T_R} = 1 + \alpha_1 \left( \frac{X - X_R}{X_R} \right) + \beta_1 \left( \frac{X - X_R}{X_R} \right)^2 \quad (A-5)$$

and

$$\frac{S}{S_R} = 1 + \alpha_2 \left( \frac{X - X_R}{X_R} \right) + \beta_2 \left( \frac{X - X_R}{X_R} \right)^2 \quad (A-6)$$

where

- X = Value of parameter being considered
- $X_R$  = Value of parameter in reference case
- T = Back-face temperature
- $T_R$  = Reference case back-face temperature
- S = Total recession
- $S_R$  = Total recession for reference case

Table A-I. Reference Case Parameter Values

Variable	Value	Units	Virgin Material Thermal Conductivity	
			$k_o \times 10^5$ BTU-ft <sup>-1</sup> sec <sup>-1</sup> °F <sup>-1</sup>	T/°F
$\rho_b$	78.4	lb/ft <sup>3</sup>	5.27	0
$\lambda_a$	500	BTU/lb	6.11	100
$\gamma_a$	10 <sup>6</sup>	1/sec	6.66	200
$\epsilon$	1	-	6.84	300
$\Gamma$	20,000	°F	7.78	400
$T_s$	4,000	°F	7.48	500
$T_{oc}$	5,000	°F	7.48	1000
J	22,000	BTU/lb	7.48	6000
$C_a$	0.48	BTU/lb°F		
$C_b$	0.136	BTU/lb°F		
$C_g$	0.4	BTU/lb°F		
$k_b$	$7.48 \times 10^{-5}$	BTU/ft-sec°F		
$\rho_o$	112	lb/ft <sup>3</sup>		
$h_1$	0.0475	BTU/ft <sup>2</sup> sec°F		
$T_o$	70	°F		

All other values set equal to 0.

The magnitude of the influence coefficient  $\alpha$  indicates the importance of a given percentage change in the parameter considered and the magnitude of the influence coefficient  $\beta$  is a measure of the nonlinearity of the effect of variations in the given parameter. The values of these influence coefficients are tabulated in Table A-III.

Table A-II. Preliminary Results From the Charring Ablation  
Computer Program

Case	Variable	Reference Value	Case Value	Backwall Temperature, °F	Recession, ft
14	Reference Case (Table A-I)	-	-	517.4	0.00530
17	$\lambda_a$	500	1000	430.8	0.00519
18			250	607.1	0.00550
19	$T_s$	4000	4500	520.5	0.00137
20			3500	512.6	0.00968
21	$T_{oc}$	5000	6000	554.7	0.01320
22			7000	589.6	0.02090
23	J	22,000	33,000	512.3	0.00356
24			14,700	525.4	0.00783
26	$h_1$	0.0475	0.024	505.2	0.00170
27	$k_o$	TV <sup>a</sup>	$1.5 \times TV^b$	563.7	0.00531
28			$0.5 \times TV^b$	312.5	0.00539
29	$k_b$	$7.48 \times 10^{-5}$	$11.22 \times 10^{-5}$	662.8	0.00478
30			$3.74 \times 10^{-5}$	357.1	0.00610
31	$c_g$	0.4	0.8	392.5	0.00431
32			0.2	628.7	0.00594
33	$\gamma_a$	$1 \times 10^6$	$1.5 \times 10^6$	505.9	0.00535
34			$0.5 \times 10^6$	550.7	0.00542
35	$c_a$	0.48	0.528	552.8	0.01329
36			0.432	551.0	0.01300
37	$\Gamma$	20,000	22,000	633.7	0.01328
38			18,000	469.2	0.01320
39	$\rho_o$	112	134	454.0	0.00523
40	$\rho_b$	78.4	94.1	490.6	0.00446

a.  $TV = K_o$  vs T Reference Table Values (see Table A-I).

b. Each value of TV was multiplied by factor shown.

Table A-III. Influence Coefficients

Variable	Backwall Temperature		Recession	
	$\alpha_1$	$\beta_1$	$\alpha_2$	$\beta_2$
Heat of Decomposition - $\lambda_a$	-0.2870	0.1200	-0.0572	0.0365
Surface Temperature - $T_s$	0.0611	-0.1050	-6.2700	2.7200
Convective Driving Temperature - $T_{oc}$	0.3720	-0.0580	7.5500	-0.4720
Surface Heat of Reaction - J	-0.0359	0.0323	-1.1300	0.9400
Virgin Thermal Conductivity - $k_o$	0.4840	-0.6120	-0.0150	0.0378
Char Conductivity - $k_b$	0.5910	-0.0576	-0.2490	0.1060
Gas Specific Heat - $c_g$	-0.3670	0.1260	-0.2230	0.0365
Decomposition Constant - $\gamma_a$	-0.0866	0.0843	-0.0132	0.0641
Convective Coefficient - $h_1$	0.0480	-	1.3600	-
Resin Specific Heat - $c_a$	0.0100	-	0.095	0.150
Decomposition Parameter - $\Gamma$	1.49	-0.3	0.02	0.8

## APPENDIX B

### CRITERIA FOR INITIAL SELECTION OF CANDIDATE RESINS

In order to guide the synthesis of new resins for ablation it is necessary to relate the thermophysical and thermochemical properties to chemical structure. The synthesis effort, thus, can be implemented in a manner consistent with the guidelines for resin selection. This appendix discusses property-chemical structure relationships for the criteria used for initial selection of the candidate resins.

#### B.1 THERMAL AND OXIDATIVE STABILITY OF ORGANIC POLYMERS

The chemical structure of modified polymers which yield resins of enhanced thermal and oxidative stability over state-of-the-art resins are:

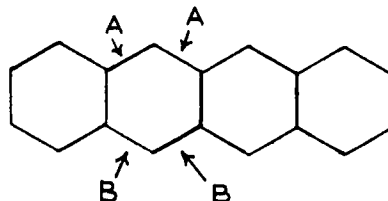
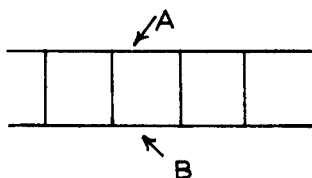
- Molecular assemblages containing a minimum of hydrogen atoms, and a maximum of stable chemical units with
- Linkages between stable units being nearly as stable as those in the units, and
- Offering no ready mode of depolymerization or chain scission.

Thermally stable polymers are mainly condensation polymers-- polymers formed by the elimination of chemical compounds upon condensation of monomers. Thus, they cannot depolymerize to the starting monomers. Both thermal and oxidative chain scission, however, are important modes of polymer decomposition as well as polymer re-arrangements. As a result, polymers containing aromatic groups are preferred because they have fewer hydrogen atoms, which are potential sites for oxidation, and they are stabilized through resonance. Furthermore, resonance stabilization of the chemical bonds linking the aromatized groups through conjugation with these groups is desirable, because it equilibrates the stability of the chemical bonds in the backbone of the molecular assemblage, thereby increasing bond strength of the connecting chemical links over that of their non-conjugated analogues.

Where additional bond strength of chemical linkages is not available by resonance stabilization, then the bond strengths per se should be as

high as possible. However, the selection of atom pairs based on bond strengths alone may yield undesirable results. For example, the carbon-carbon bond strength in the backbone of organic polymers is ~80 Kcal, whereas boron-oxygen is ~130 Kcal, and boron-nitrogen is ~100 Kcal. Nevertheless, despite their high bond strengths, the boron-oxygen and boron-nitrogen bonds, are labile to chain scission by attack of many chemical agents, in particular oxygen and water. As a result, the carbon-carbon bond is particularly attractive - especially when reinforced by resonance and/or augmented by an arrangement of atoms wherein a bond scission does not result in the rupture of the polymer backbone.

In those cases where aromatic polymers are not desired e. g. , because these polymers generally exhibit higher thermal conductivities than analogous aliphatic polymers, the "ladder" polymers of singly bonded atoms provide an interesting alternative to achieve thermal and oxidative stability. The "ladder" polymers are stable materials because the "ladder" structure of the polymer backbone prevents scission of the polymer chain even though one of its chemical bonds may be broken. The "ladder" configuration of atoms is shown as follows:



A break of this arrangement at point A must be followed by a break at point B in order to rupture the chain. This is an unlikely event; in a high molecular weight assemblage in which all of the chemical bonds have similar strength, the overriding possibility of bond scission is at a point other than B. As a result, the "ladder" configuration of atoms preserves the integrity of the polymer backbone when bond scission occurs, thereby making the polymer stable to thermal and oxidative degradation.

## B. 2 DIMENSIONAL STABILITY AT ELEVATED TEMPERATURES

Polymers having chemically equivalent molecular assemblages can yield resin masses exhibiting different degrees of dimensional stability at elevated temperatures. The dimensional stability of resin classes have been advanced to higher temperatures by two general methods: crystallization and chemical crosslinking. Polyethylene prepared by free radical catalysis, for example, contains polymer chain branches which interfere with crystallization, and thus, this resin exhibits a low heat distortion temperature ( $\sim 80^{\circ}\text{C}$ ) because of its low degree of crystallinity. In contrast, polyethylene prepared by anionic catalysis is linear, thus, this resin exhibits a higher heat distortion temperature ( $120^{\circ}\text{C}$ ) because of its high degree of crystallinity. On the other hand, phenolic resins which exhibit high heat distortion temperatures contain a greater amount of chemical crosslinks than "ordinary" phenolic resins. The above methods, nevertheless, have not yielded resins exhibiting heat distortion temperatures greater than  $250^{\circ}\text{C}$ . Although chemically crosslinked resins will not melt, in contrast to non-crosslinked crystalline resins, the amount of crosslinking effected even in highly crosslinked resins is not sufficient to prevent low range distortions.

Resins distort dimensionally as a result of the thermal disruption of forces of attraction between their polymer chains. The heat distortion temperatures of resins are generally lower (e. g., less than  $250^{\circ}\text{C}$ ) than the temperature where they degrade chemically (e. g., carbon-carbon bond scission at  $450 - 500^{\circ}\text{C}$ ) because the intermolecular forces between polymer chains is less than those which characterizes the chemical bonds of the polymer chain. The energy of intermolecular interaction in resins is about  $1-6 \text{ Kcal mol}^{-1}$ , whereas the energy of chemical bonds, which characterize most polymer backbones is about  $70 - 100 \text{ Kcal mol}^{-1}$ .

**Resins in which the heat distortion temperature is determined** by the rupture of chemical bonds will exhibit significantly enhanced dimensional stability. Increasing the heat distortion temperature by inducing additional chemical crosslinking of three dimensional polymers, however, is accomplished with the sacrifice of mechanical properties. The resin becomes brittle, and although there may be an increase in its tensile strength, the elongation of the resin to break is severely reduced thus resulting in loss of toughness.

The dimensional stability of resins can be increased, together with an advancement of toughness, by preparing resins containing linear polymers which are characterized by "stiff" backbones. In this report, these materials are called "stiff" polymers. In substance, "stiff" polymers have backbones characterized by cyclic chemical groups.

"Stiff" polymers are characterized by significantly greater heat distortion temperatures than that of ordinary polymers (i. e., polymers with backbones characterized by singly bonded atoms), because the energy required to surmount the potential barrier opposing rotation about a great number of chemical bonds of their backbone is equivalent to the energy of chemical bonds. In contrast the energy of free rotation in ordinary polymers is about 1 - 6 Kcal mol<sup>-1</sup>, which is the same order as the energy of cohesion i. e., the energy required in thermal disruption of forces of attraction between polymer chains.

The above consideration may be appreciated by visualizing the zero strength temperature of a resin to be the temperature at which the structure of the resin approaches that of an isotropic liquid. In this state, the polymer chain segments are disposed randomly, this phenomenon necessitates an unconstrained polymer chain. Constraints on the flexibility of a polymer chain involve the energy barrier for free rotation of chemical groups about the chemical bonds of the chain in addition to molecular forces of attraction between chains. The cohesive energy of stiff polymers and that of ordinary polymers are approximately the same. The energy of free rotation of stiff polymers and those of ordinary polymers, on the other hand, are markedly different, i. e., 70 - 100 Kcal mol<sup>-1</sup> vs 1 - 6 Kcal mol<sup>-1</sup>. Thus the thermal stability of resins consisting of "stiff" polymers may be compared to logs in a pond, wherein the general parallel alignment of logs is maintained despite agitation of the surface of the water. The resistance of "stiff" polymers to exhibit isotropy at elevated temperature arises essentially from the elongated nature and stiffness of the polymer chains, and as in the case of the logs in the pond, not from enhanced attraction between them.

The consequence of this analysis is that the parameters which define molecular assemblages with improved thermal stability also define polymers of improved dimensional stability provided these

molecular assemblages are in the backbone of the polymer. This concept is illustrated in Appendix I concerning new "stiff" polymers as ablative resins proposed for synthesis by TRW Systems. Such polymers provide ideal char forming ablative resins. Chain scission of the chemical bonds not in the polymer backbone contributes to the formation of char. This phenomenon occurs while the integrity of the backbone of the polymer is preserved, thereby the resin maintains its mechanical strength during the process of initial pyrolysis.

### B.3 CHAR RESIDUE AND PYROLYSIS GASES

In the case of high charring materials, the quantity of the residue is a parameter determining the strength of the char formed. The erosion resistance of the ablator in propellant combustion environments is directly related to its strength. In addition the availability of char promotes the highly desirable endothermic reaction between carbon and silica of glass reinforced composites. Consequently, it is desirable in providing high charring materials to improve the material by enhancing its char yield.

In the absence of selected catalysts, organic resins may be expected to char in relation to the carbon-carbon bond strength to that of other chemical bonds in the resin. Organic polymers containing resonance hybrid carbon-carbon bonds are more stable thermally than hydrogen saturated organic polymers. The extent of thermal degradation of any particular bond as a function of temperature can be expressed in the form of the Arrhenius equation, i. e., the rate of decomposition as a function of temperature varies exponentially with the activation energy, which is approximately equal to the bond energy. Consequently, the difference in the relative rates of thermal scission of chemical bonds is markedly dependent upon the magnitude of the difference between bond energies. Because char formation, in the case of hydrocarbons, will depend on pyrolytic scission of the carbon-hydrogen bond in preference to scission of the carbon-carbon bonds, appreciably more char may be expected from the more stable conjugated polyolefins than from polyalkanes, the latter resulting in chain cleavage forming mainly low molecular weight volatile products. An example of a low char yield organic resin is polyperfluoroethylene. The bond strength of the carbon-fluorine bond is greater than that of carbon-carbon. Consequently, the resin, on pyrolysis, favors the formation of volatile compounds

rather than the formation of char.

Another characteristic of a resin which mitigates against the formation of volatile products, is high molecular weight; in addition, cross-linked polymers and ladder polymers favor char formation. Furthermore, resins containing higher carbon contents are preferred polymer compositions for char formation. According to the analysis arising from this program, another requirement for a resin to generate a high char content is dimensional stability at elevated temperatures (see Section B.1). This stability is required so that thermal distortion of the resin does not occur at a temperature lower than that required for initiation of pyrolysis -- consequently, the polymer will resist flow under high shearing forces.

The important properties of resins which determine the maximum amount of carbonaceous pyrolyzed char residue are summarized below:

- Resonance stabilized polymer backbones
- High molecular weight
- High carbon content
- High dimensional stability.

In addition to a high char yield, the nature and quantity of pyrolysis gases are important. A given weight of lower molecular weight pyrolysis gas generally requires more heat for the same degree of expansion than that of higher molecular weight gases. Thus, heat will be dissipated more effectively at the surface of the ablator resin by a low molecular weight gas. Hydrogen gas is preferred as the major portion of ablative pyrolysis gases.

#### B.4 RESIN PLASTICITY AND LOW TEMPERATURE STABILITY

Brittle resins are not suitable as resin binders for composites. Useful composites must have resin matrices having a lower modulus of elasticity than that of the reinforcing filler. Thus, when a composite is strained, most of the resulting stresses are transmitted to the high modulus filler. The resin component of the composite, in other words, must be capable of some plastic deformation so that more of the inherent strength of the fibers can be realized.

Plasticity in resins arises from the arrangements of chemical bonds between atoms. The plastic resin is characterized by polymers having linear arrangements of atoms bonded together by chemical bonds which are directionally oriented in space. Weaker, non-directional bonds "cement" together the linear arrangements of atoms of the polymer chains. Upon straining plastic resins, these weaker bonds permit distribution of stresses within the resin, thereby preventing structural failure of the material. In crosslinked, (or three-dimensional) resins, the number of chemical bonds between polymer chains is less than the number of chemical bonds in the chain. Although plastic properties are thereby retained, as a class, crosslinked polymers are more brittle than non-crosslinked polymers, and become more brittle with increasing degree of crosslinking.

Although resins containing polymers having a linear arrangement of atoms exhibit plasticity, this plastic property is generally lost at temperatures below the glass transition temperature,  $T_g$ . The value of  $T_g$  depends mainly upon the chemical structure of the polymers. Resins containing polymers having linear arrangements of singly bonded atoms, which yield "flexible" chain segments at temperatures above  $T_g$ , lose their plasticity at temperatures lower than  $T_g$ . However, resins containing polymers having linear arrangements of atoms which are "stiff" maintain plasticity at temperatures far below their  $T_g$ 's. Du Pont's polyimide "H" film, for example, is plastic at room temperature and at very low temperatures ( $< -200^\circ\text{C}$ ) yet the  $T_g$  of this resin ( $\sim 700^\circ\text{C}$ ) is appreciably greater than room temperature.

"Stiff" polymers, consequently, are very interesting because they exhibit high temperature stability and low temperature flexibility. Because the  $T_g$  and the heat distortion temperature of resins, generally, are about the same temperature, one may presume that dimensional stability in a resin is gained at the expense of low temperature flexibility. For "stiff" polymers, however, this is not the case; in fact, these materials exhibit flexibility at temperatures where many resins become brittle.

## B.5 THERMAL CONDUCTION

The basis for modification in chemical structure to produce desired change in thermal conductivity is not as clear-cut as that for other physical, chemical and mechanical properties. A certain amount of theoretical foundation exists; however, its application to organic structures has not been implicitly confirmed.

Thermal conduction through a material is governed by two separate processes:

- 1) thermal transport by electron conduction, and
- 2) thermal transport by molecular vibrations.

In the case of non-conductors, e g., organic resins, the molecular vibrations are normally considered as the most important mode of thermal conduction. However, when the temperature becomes sufficiently high, many materials exhibit surprisingly high electrical conductivities because of their intrinsic semiconductor nature. The electrical conductivity may then contribute to the thermal conductivity, and thereby enhance the overall thermal conduction at elevated temperatures.

Generally, resonance stabilized polymers, i. e., aromatic polymers, are comparatively better conductors than non-resonance stabilized polymers. Molecular vibrations also become increasingly more effective in thermal transfer as the structure of the material becomes more regular, i. e., the material approaches crystalline form. Thus, the amount of crystallinity, and the phenomenon of thermal ionization play important roles in the thermal conduction that any given material possesses.

## B.6 EROSION RESISTANCE

Erosion resistance of a class of resins can be improved by:

- Preparation of polymers with higher molecular weights,
- High heat distortion temperatures, and
- Intimate adhesion of polymers to fillers or reinforcing fabrics.

Higher molecular weight polymers of a given class yield resins that are invariably tougher than those of lower molecular weight, and in

conjunction with the greater viscosity of their melts are expected to be more resistant to erosion. The melt viscosity of resin classes containing "stiff" polymers may be expected to be greater than those containing "flexible" polymers because of their higher heat distortion temperature.

Improved adhesion of resins to fabric results in not only tougher laminates, but also improved resistance to the erosive action of the atmosphere upon the surface of space vehicles. The parameters which determine adhesion between materials are given in Appendix J.

## B. 7 CRITERIA FOR INORGANIC POLYMERS AS LAMINATING RESINS

### B. 7. 1 Plasticity

The plastic character required of resins for use in laminates (see Section B. 4) is not evident in the preponderant number of inorganic polymers. Most inorganic compositions exhibit brittle ceramic properties. The ceramic, in contrast to the plastic is characterized by an arrangement of atoms chemically bonded three-dimensionally in space. The ceramic is devoid of plasticity because no mechanism exists for the alleviation of stresses induced upon straining the material. Stress concentrations at points of flaw augment failure of the material. Ionic solids having a cubic crystal structure, however, possess some plasticity, indicating that there are exceptions to the above generalizations.

### B. 7. 2 Molecular Weight

Resins must consist of high molecular weight polymers, as well as mainly linear polymers, in order to exhibit mechanical properties useful in laminates. The molecular weight of polymers is one of the most significant parameters determining the mechanical properties of resins. In a given system, tougher resins result from higher molecular weight polymers, although the advancement in toughness may not be as significant in one molecular weight range as in another. Although processing requirements of resins may dictate the use of lower molecular weight polymers, this does not mitigate the desirability for resins to consist of high molecular weight polymers.

The formation of high molecular weight polymers involves an equilibrium between the reactants and the products. The position of the equilibrium dictates the degree of reaction, however, not necessarily the degree of polymerization. The arrangement of the atoms in the product, for example, may be in the form of small rings rather than the desirable, linear macromolecules, because small rings are favored thermodynamically.

At a given temperature, the free energy in passing from a macromolecule to small rings and vice versa depends on enthalpy and entropy according to the well-known relationship

$$\Delta F = \Delta H - T\Delta S$$

For inorganic resins, entropy effects play a dominate role (although the degree of polymerization is also affected by enthalpy changes). As a result, the reversion of macromolecules to a large number of small ring molecules is favored thermodynamically because of an increase in entropy.

Fortunately, the process of reversion is governed by kinetic effects as well as thermodynamic effects. If reversion requires considerable activation energy, then the rate of reversion is slow relative to that of polymerization. Thereby, polymeric systems can be synthesized with sufficient molecular weight to make them useful resins.

For organic systems the activation energy is high, while for inorganic ones it is low. This fact shows why a greater variety of organic polymers have been prepared than inorganic ones. In addition, the greater likelihood of chemical attack upon inorganic bonds by processes requiring low activation energies make inorganic polymers, generally, more susceptible than organic polymers to chemical degradation. As a result, some successfully synthesized inorganic polymers may not be useful despite the higher energies of their chemical bonds than those which characterize organic polymers. (Higher bond energies may be considered to give improved thermal stability to polymers when chemical degradative processes are not operable.)

### B.7.3 Criteria Determining Inorganic Polymer Synthesis

Successful synthesis of inorganic polymers, therefore, depends upon methods for devising the synthesis of chain structures rather than rings, and for preventing molecular rearrangements and/or scission of polymer chains once they are formed. By the utilization of steric effects, and the selection of the types of bonding which do not favor ring formation, linear, high molecular weight polymers have been realized.

A survey of the inorganic polymer literature shows that organic chemical groups are utilized to provide steric interference to the depolymerization of inorganic polymers. If carbon-containing groups are to be minimized from the chemical composition, then the types of bonding which do not favor ring formation offer the best possibility for synthesizing linear inorganic polymers.

## APPENDIX C

EQUILIBRIUM THERMAL DECOMPOSITION STUDIES  
OF CANDIDATE RESINS

In this appendix the detailed results of equilibrium thermal decomposition studies of candidate resin classes are reported. The equilibrium calculations were performed using the TRW Rocket Chemistry Computer Program (AP2A) incorporating JANAF thermochemical data. The only program input required for these studies was the empirical formula. Sufficient variations in the results of these calculations were found between classes that discussion of each individual class is required.

## C.1 B-N CLASS OF RESINS

Selected as representative of the B-N resin systems was a polymer containing borazine rings with an empirical formula of  $C_6H_{15}B_2N_3$ . Equilibrium calculations at 100 psia total pressure were made at 100 °R intervals from 4500 °R to 7000 °R. An examination of the abstracted results (500 °R intervals) presented in Table C-I showed that at low temperatures (below 4500 °R) essentially all the boron was present in the residue as BN and the majority of the carbon was present as solid carbon.

The gas was principally hydrogen with small amounts of nitrogen, hydrogen cyanide and acetylene. At temperatures well below those shown, methane replaced acetylene as the hydrocarbon in the gas phase, but at the resin decomposition temperature, or above, it was in low concentration.

As the temperature was raised, the boron nitride was converted to liquid boron carbide ( $B_4C$ ) over a narrow temperature range near 5000 °R. The liquid  $B_4C$  was stable to about 6200 °R where a dissociation to liquid elemental boron and several gaseous carbon species occurred. The amount of residue (both solid and liquid plus solid) present at each temperature is displayed graphically in Figure C-1, while the changes in the gas composition are most readily observed by reference to Table C-I.

Table C-I. Equilibrium Decomposition Products Molar Composition For  
a B-N Type Resin with Empirical Formula of  $C_6H_{15}B_2N_3$

Decomposition Product	Temperature, °R					
	4500	5000	5500	6000	6500	7000
B (g)	0	0	0	0	0.37	1.51
CN (g)	0	0	0	0.17	0.45	0.92
C <sub>3</sub> (g)	0	0	0	0	0	0.21
H (g)	0	0.23	0.55	1.10	1.97	3.39
H <sub>2</sub> (g)	7.27	6.87	6.25	5.41	4.40	3.55
HCN (g)	0.17	0.47	0.77	1.00	1.13	1.05
HCCH (g)	0.09	0.25	0.53	0.94	1.41	1.53
N <sub>2</sub> (g)	0.42	1.03	1.09	0.91	0.71	0.51
B (l)	0	0	0	0	1.52	0.31
B <sub>4</sub> C (l)	0	0.39	0.49	0.46	0	0
C (s)	5.64	4.63	3.61	2.43	1.40	0
BN (s)	1.99	0.44	0	0	0	0
Liquid, % W/W	0	14.1	17.9	17.0	10.9	2.3
Solid, % W/W	77.7	44.1	28.7	19.4	11.1	0

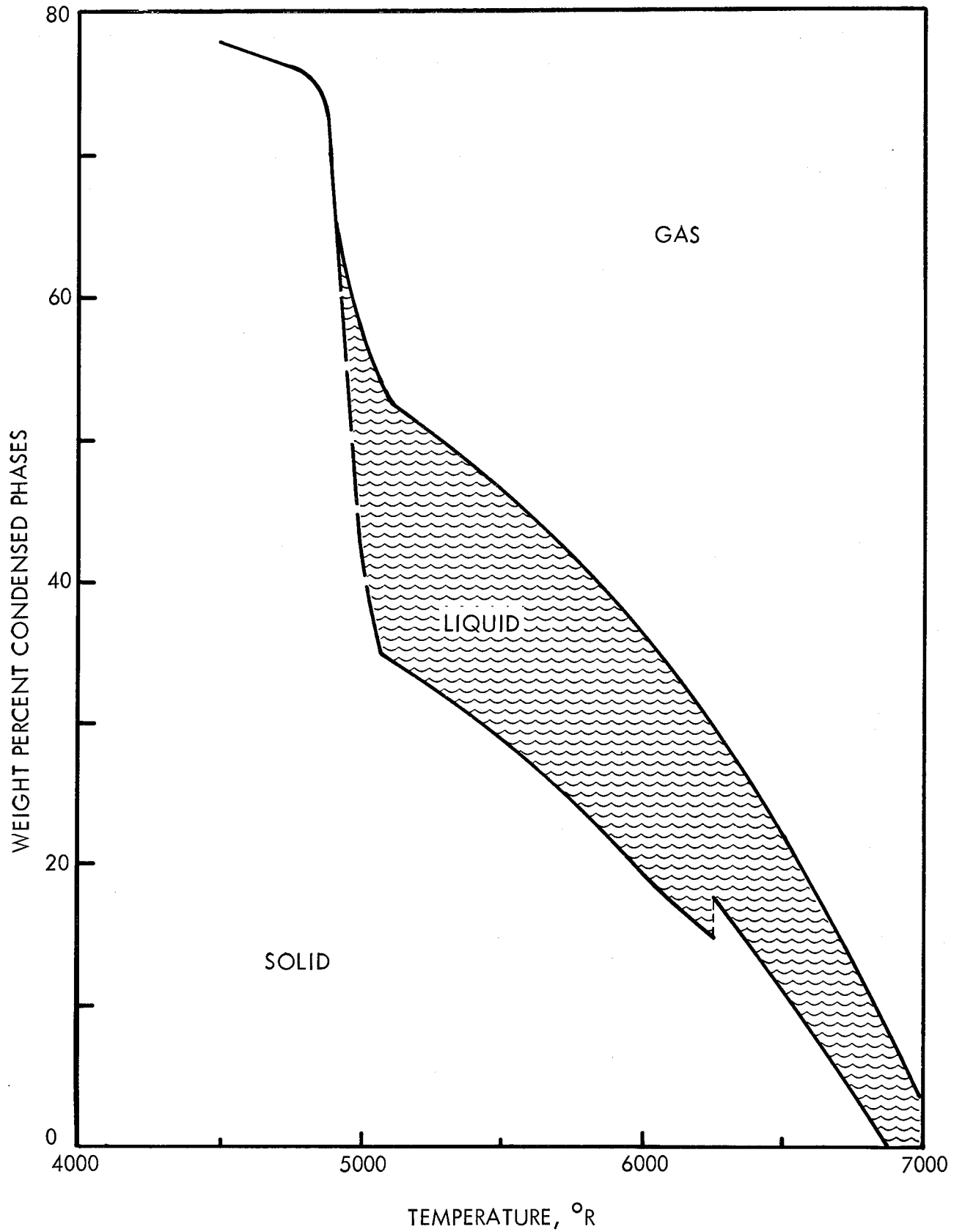


Figure C-1. Equilibrium Total Condensables for a B-N Resin Containing Borazine Rings as a Function of Temperature

## C.2 Si-O CLASS OF RESINS

The Si-O system was represented by two resins: a polysilarylene-siloxane ( $C_8H_{10}SiO_2$ ) and a phenyl silsesquioxane ( $C_{12}H_{10}Si_2O_3$ ). The results of equilibrium calculations at 100 psia total pressure and temperatures from 4500 °R to 7000 °R are shown in Tables C-II and C-III.

The characteristics of these two resins are similar with respect to the decomposition products. At low temperatures, essentially all the silicon is retained in the residue as solid silicon carbide, but carbon is retained in the char only to the extent that the atoms of carbon exceed the atoms of oxygen. It is apparent that oxygen in the resin theoretically removes carbon to the gas phase almost quantitatively as carbon monoxide.

An examination of the effect of temperature on the composition and quantity of residue from each of the Si-O resins shows that the carbon and silicon carbide content continuously decrease as temperatures increase from 4500 °R to about 5200 °R. Between 5200 °R and 5300 °R the Si-C decomposes to solid carbon and liquid silicon. Both the carbon and silicon decrease in amount with further increase in temperature until 6300 to 6400 °R at which temperature the liquid silicon has completely vaporized. Figures C-2 and C-3 show the weight percent of solid and liquid present as a function of temperature for the polysilarylenesiloxane resin and the phenyl silsesquioxane resin, respectively.

## C.3 Si-N CLASS OF RESINS

The silazine resins were of potential interest since these materials contained no oxygen and would not lose carbon to the gas phase as CO. A silazine with the empirical formula  $C_{13}H_{13}SiN$  was selected as representative of this resin class. The equilibrium decomposition products have been computed at temperatures from 4500 °R to 6600 °R at 100 psia total pressure. These data are abstracted in Table C-IV.

An examination of the equilibrium compositions shows that the residue responds to temperature in the same way as the Si-O system. The amount of carbon was much greater than in the Si-O systems, and in fact, the total residue exceeded that of any other resin system included in this analysis. Figure C-4 shows the percent of solid and liquid present at equilibrium for temperatures from 4500 °R to 6600 °R.

Table C-II. Equilibrium Decomposition Products Molar Composition  
for a Si-O Type Resin with Empirical Formula of  
 $C_8H_{10}SiO_2$

Decomposition Product	Temperature, °R					
	4500	5000	5500	6000	6500	7000
CO (g)	1.94	1.92	1.91	1.92	1.96	1.98
C <sub>3</sub> (g)	0	0	0	0	0	0.21
H (g)	0	0.17	0.41	0.84	1.51	2.40
H <sub>2</sub> (g)	4.90	4.73	4.41	3.88	3.19	2.44
HCCH (g)	0	0.17	0.37	0.67	1.02	1.31
Si (g)	0	0	0.11	0.43	0.78	0.89
SiO (g)	0.05	0.08	0.09	0.08	0.04	0.02
Si <sub>2</sub> (g)	0	0	0.02	0.07	0.08	0.04
Si (l)	0	0	0.77	0.33	0	0
C (s)	4.99	4.83	5.33	4.70	3.84	2.44
SiC (s)	0.94	0.90	0	0	0	0
Liquid, % W/W	0	0	13.0	5.7	0	0
Solid, % W/W	58.7	56.6	38.5	33.9	27.8	17.6

Table C-III. Equilibrium Decomposition Products Molar Composition  
for a Si-O Type Resin with Empirical Formula of  
 $C_{12}H_{10}Si_2O_3$

Decomposition Product	Temperature, °R					
	4500	5000	5500	6000	6500	7000
CO (g)	2.92	2.88	2.88	2.88	2.92	2.96
C <sub>3</sub> (g)	0	0	0	0	0.06	0.23
C <sub>5</sub> (g)	0	0	0	0	0	0.02
H (g)	0.06	0.18	0.44	0.90	1.82	2.61
H <sub>2</sub> (g)	4.90	4.74	4.40	3.86	2.98	2.38
HCCH (g)	0.06	0.16	0.28	0.68	1.06	1.28
Si (g)	0	0.02	0.12	0.50	1.50	1.70
SiO (g)	0.08	0.12	0.12	0.12	0.08	0.04
Si <sub>2</sub> (g)	0	0	0.02	0.08	0.20	0.12
Si (l)	0	0	1.70	1.22	0	0
C (s)	7.04	6.92	8.38	7.74	6.68	5.34
SiC (s)	1.92	1.86	0	0	0	0
Liquid, % W/W	0	0	18.6	13.2	0	0
Solid, % W/W	62.5	61.0	38.9	36.0	31.0	24.8

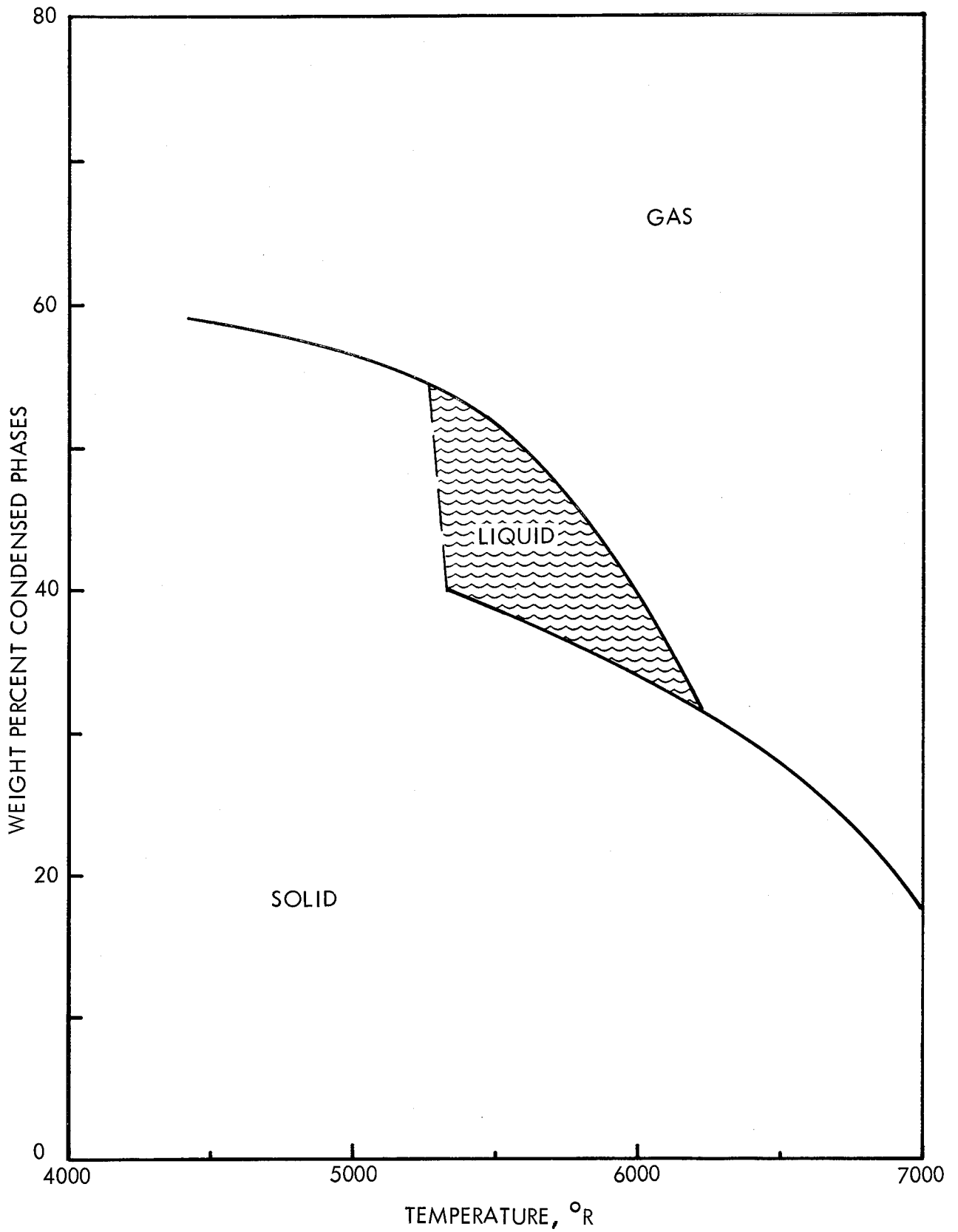


Figure C-2. Equilibrium Total Condensables for a Polysilarylenesiloxane Resin ( $C_8H_{10}SiO_2$ ) As a Function of Temperature

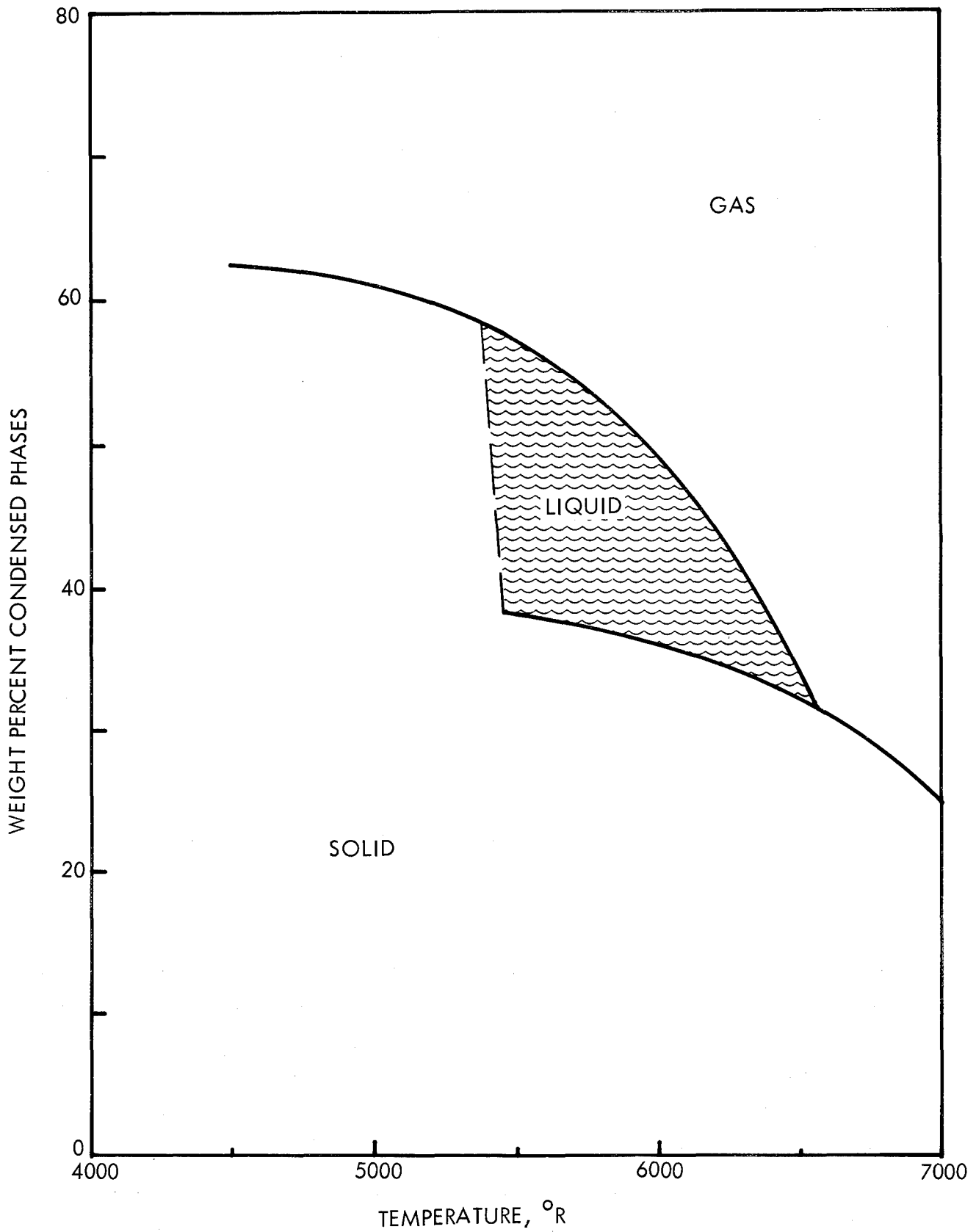


Figure C-3. Equilibrium Total Condensables for a Phenyl Silsesquioxane Resin ( $C_{12}H_{10}Si_2O_3$ ) as a Function of Temperature

Table C-IV. Equilibrium Decomposition Products Molar Composition for an Si-N Type Resin with Empirical Formula of  $C_{13}H_{13}SiN$

Decomposition Product	Temperature, °R				
	4500	5000	5500	6000	6500
CN (g)	0	0	0	0	0.19
H (g)	0	0.19	0.46	0.95	1.73
H <sub>2</sub> (g)	6.30	6.04	5.59	4.91	4.05
HCN (g)	0.16	0.26	0.38	0.47	0.50
HCCH (g)	0.08	0.22	0.47	0.85	1.29
N <sub>2</sub> (g)	0.42	0.36	0.30	0.22	0.15
Si (g)	0	0	0.11	0.44	0.81
Si <sub>2</sub> (g)	0	0	0.02	0.08	0.09
Si (l)	0	0	0.86	0.40	0
C (s)	11.68	11.31	11.63	10.70	9.55
SiC (s)	1.00	0.98	0	0	0
Liquid, % W/W	0	0	11.4	5.3	0
Solid, % W/W	85.3	82.9	66.1	60.8	54.3

#### C. 4 HYDROCARBON CLASS OF RESINS

Numerous examples of this class of resin are known encompassing a wide range of carbon-hydrogen ratios and may contain oxygen or nitrogen singly or together. Four high temperature materials were selected as representative, namely: furan-containing oxygen ( $C_5H_4O$ ), polybenzimidazole containing nitrogen ( $C_5H_3N$ ), and polyimide ( $C_8H_3O_2N$ ) and poly(cyclized 1, 2 polybutadiene) tolyl urethane (CPBU) ( $C_{84}H_{120}O_2N$ ) containing both oxygen and nitrogen.

Equilibrium calculations over the temperature range 4500 °R to 7000 °R at a total pressure of 100 psia are presented in Tables C-V, C-VI, C-VII, and C-VIII. Again it was observed that oxygen in the resin

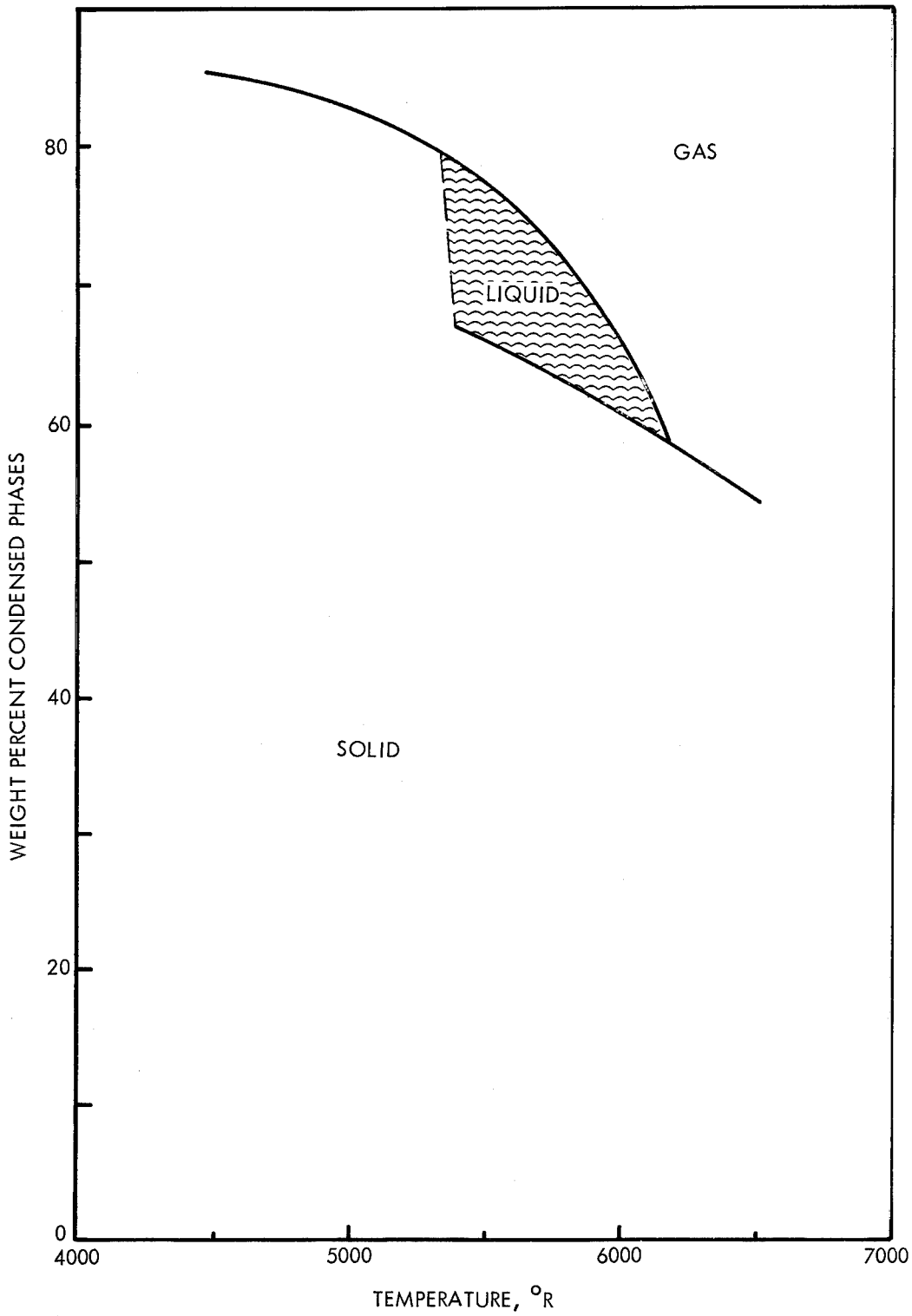


Figure C-4. Equilibrium Total Condensables for a Silazine Resin (C<sub>13</sub>H<sub>13</sub>SiN) as a Function of Temperature

Table C-V. Equilibrium Decomposition Products Molar Composition for a Hydrocarbon Type Resin with Empirical Formula of  $C_5H_4O$

Decomposition Products	Temperature, °R					
	4500	5000	5500	6000	6500	7000
CO (g)	1.00	1.00	1.00	1.00	1.00	1.00
C <sub>3</sub> (g)	0	0	0	0	0	0.08
H (g)	0.02	0.07	0.17	0.34	0.59	0.94
H <sub>2</sub> (g)	1.96	1.89	1.76	1.55	1.28	0.99
HCCH (g)	0.02	0.07	0.15	0.27	0.41	0.53
C (s)	3.95	3.86	3.70	3.45	3.12	2.58
Solid % W/W	59.2	57.9	55.4	51.7	46.8	38.7

Table C-VI. Equilibrium Decomposition Products Molar Composition for a Hydrocarbon Type Resin with Empirical Formula of  $C_5H_3N$

Decomposition Product	Temperature, °R					
	4500	5000	5500	6000	6500	7000
CN (g)	0	0	0.015	0.05	0.13	0.29
C <sub>3</sub> (g)	0	0	0	0	0.01	0.06
H (g)	0.02	0.05	0.11	0.23	0.40	0.65
H <sub>2</sub> (g)	1.43	1.36	1.23	1.06	0.86	0.66
HCN (g)	0.08	0.14	0.21	0.27	0.31	0.32
HCCH (g)	0.02	0.05	0.11	0.19	0.28	0.35
N <sub>2</sub> (g)	0.46	0.43	0.39	0.34	0.28	0.20
C (s)	4.89	4.76	4.57	4.30	3.96	3.43
Solid, % W/W	76.10	74.18	71.2	67.0	61.7	53.5

Table C-VII. Equilibrium Decomposition Products Molar Composition for a Hydrocarbon Type Resin with Empirical Formula of  $C_8H_3O_2N$

Decomposition Product	Temperature, °R					
	4500	5000	5500	6000	6500	7000
CN (g)	0	0.005	0.02	0.07	0.18	0.37
CO (g)	2.00	2.00	2.00	2.00	2.00	2.00
C <sub>3</sub> (g)	0	0	0	0	0.015	0.105
H (g)	0.025	0.07	0.16	0.32	0.55	0.85
H <sub>2</sub> (g)	1.43	1.35	1.22	1.03	0.82	0.60
HCN (g)	0.08	0.14	0.20	0.27	0.30	0.28
HCCH (g)	0.02	0.05	0.10	0.18	0.26	0.33
N <sub>2</sub> (g)	0.46	0.43	0.39	0.34	0.26	0.18
C (s)	5.98	5.76	5.57	5.30	4.93	4.23
Solid, % W/W	48.7	47.7	46.1	43.8	40.8	35.0

quantitatively removes carbon to the gas phase as CO. The remaining carbon is present as solid residue at low temperatures with gradually increasing amounts present in the gas phase as the temperature is raised.

A phenolic resin with an empirical formula closely approximating that of the furan resin was investigated as part of another program. Equilibrium calculations were performed in a lower temperature range (1900 °R to 5500 °R). At lower temperatures, methane and water become more stable thermodynamically, and small amounts of CO<sub>2</sub> are found in the equilibrium gas composition. Acetylene, ethylene and monatomic species effectively disappear at the low temperatures.

The solid residue from all the hydrocarbon resins (furan, polybenzimidazole, polyimide, CPBU and phenolic) contains carbon only at all temperatures.

Table C-VIII. Equilibrium Decomposition Products Molar Composition for a Hydrocarbon Type Resin with Empirical Formula of  $C_{84}H_{120}O_2N$

Decomposition Product	Temperature, °R					
	4500	5000	5500	6000	6500	7000
C (g)	0	0	0	0	0.07	0.40
C <sub>2</sub> (g)	0	0	0	0	0.07	0.60
C <sub>3</sub> (g)	0	0	0	0	0.28	1.71
C <sub>5</sub> (g)	0	0	0	0	0	0.08
C <sub>2</sub> H <sub>2</sub> (g)	0.75	2.03	4.45	8.15	12.6	16.5
CO (g)	2.00	2.00	2.00	2.00	2.00	2.00
H (g)	0.56	1.70	4.20	8.48	15.15	24.3
H <sub>2</sub> (g)	58.7	56.7	52.9	47.1	39.3	30.7
HCN (g)	0.38	0.57	0.78	0.85	0.85	0.86
N <sub>2</sub> (g)	0.31	0.20	0.11	0.07	0.07	0.07
C (s)	80.1	77.3	72.2	64.6	54.8	40.5
Solid, % W/W	81.8	78.9	73.8	66.0	56.0	41.3

### C.5 FLUOROCARBON CLASS OF RESINS

The fluorocarbon resins were represented by polytetrafluoroethylene (CF<sub>2</sub>) and a fully fluorinated polyphenylene (C<sub>3</sub>F<sub>2</sub>). This selection provided fluorine to carbon ratios at the extremes of the range which can probably be obtained. The results of equilibrium calculations at a pressure of 100 psia for temperatures from 4500 °R to 7000 °R are presented in Tables C-IX and C-X.

Difluoroacetylene, (C<sub>2</sub>F<sub>2</sub>), is the major gaseous species at these temperatures and, as a consequence, no solid carbon remains for the CF<sub>2</sub> resin because of its low C/F ratio. Only a small percent of char remains in the C<sub>3</sub>F<sub>2</sub> system. The percent of carbon residue for the C<sub>3</sub>F<sub>2</sub> resin was found to be only a weak function of temperature.

Table C-IX. Equilibrium Decomposition Products Molar Composition for a Fluorocarbon Type Resin with Empirical Formula of  $CF_2$

Decomposition Product	Temperature, °R					
	4500	5000	5500	6000	6500	7000
$CF_2$ (g)	0.05	0.10	0.17	0.21	0.19	0.14
$CF_3$ (g)	0.21	0.25	0.23	0.14	0.05	0.02
$CF_4$ (g)	0.17	0.11	0.06	0.01	0	0
F (g)	0.01	0.06	0.20	0.47	0.71	0.83
FCCF (g)	0.28	0.27	0.27	0.32	0.38	0.41

Table C-X. Equilibrium Decomposition Products Molar Composition for a Fluorocarbon Type Resin with Empirical Formula of  $C_3F_2$

Decomposition Product	Temperature, °R					
	4500	5000	5500	6000	6500	7000
CF (g)	0	0	0	0	0.01	0.01
$C_3$ (g)	0	0	0	0	0.01	0.02
$CF_2$ (g)	0.04	0.05	0.05	0.05	0.05	0.05
$CF_3$ (g)	0.07	0.02	0.01	0	0	0
$CF_4$ (g)	0.02	0	0	0	0	0
F (g)	0	0	0.03	0.06	0.11	0.19
FCCF (g)	0.80	0.90	0.92	0.91	0.88	0.84
C (s)	1.25	1.13	1.11	1.13	1.16	1.13
Solid, % W/W	20.4	18.3	18.0	18.3	18.8	18.3

APPENDIX D  
HIGH CARBON SPECIES ASSESSMENT

The thermochemical properties of 70 gaseous carbon-hydrogen species and solid carbon have been reported by Duff and Bauer (Reference 3). These data are in the form of Equations (D-1) and (D-2)

$$\frac{H - H_o}{RT} = a + b T + c T^2 + d T^3 + e T^4 \quad (D-1)$$

$$\begin{aligned} \frac{F - H_o}{RT} = & a (1 - \ln T) - b T - c T^2/2 \\ & - d T^3/3 - e T^4/4 - k \end{aligned} \quad (D-2)$$

for which constants a through e, k and the standard heat of formation,  $H_o$ , at 0 °K are given.

The TRW Rocket Chemistry Program requires as input  $H_{298}$  and tables of  $H - H_{298}$  and  $S$  as a function of  $T$  which are least squares curve fit with a ninth order orthogonal polynomial. The enthalpy and entropy tables required are generated from the enthalpy and free energy functions given by Equations (D-3) and (D-4),

$$H - H_{298} = RT \left( \frac{H - H_o}{RT} \right) - (298.15)R \left[ \frac{H - H_o}{RT} \right]_{298} \quad (D-3)$$

$$S = R \left( \frac{H - H_o}{RT} - \frac{F - H_o}{RT} \right) \quad (D-4)$$

where  $[ ]_{298}$  signifies that the term is evaluated at 298.15 °K. The heat capacity is also computed from Equation (D-5)

$$C_p = \frac{d \left[ RT \left( \frac{H - H_o}{RT} \right) \right]}{d T} \quad (D-5)$$

Equations (D-1) through (D-5) were programmed for the IBM 7094 digital computer. The tabular output was examined and found to contain some

values not considered to be normal. The 27 species given in Table D-1 showed maxima in the calculated heat capacity curves at temperatures between 1600 and 3300 °K. Generally, the heat capacity calculated at 6000 °K was highly negative.

Machine plots of heat capacity and  $H - H_{298}$  for five species reported by Duff and Bauer are shown in Figures D-1 through D-5. JANAF values for heat capacity of  $H_2$  (Figure D-1) and acetylene (Figure D-5) are plotted on the same graphs for comparison. In view of the uncertainty as to the meaning of these data, JANAF thermochemical data will be used although they contain only 12 of the 71 species reported.

Table D-1. Heat Capacity Maxima in the Data of Duff and Bauer

Species Number	Compound	Temperature for Maximum $C_p$ , °K
1	H <sub>2</sub>	3300
5	C <sub>3</sub>	2200
6	C <sub>4</sub>	2100
7	C <sub>5</sub>	2000
8	C <sub>6</sub>	2000
9	C <sub>7</sub>	1900
10	C <sub>8</sub>	1900
11	C <sub>9</sub>	1900
12	C <sub>10</sub>	1900
14	C <sub>2</sub> H	2300
15	C <sub>3</sub> H	2700
16	C <sub>4</sub> H	1800
17	C <sub>5</sub> H	1900
18	C <sub>6</sub> H	1700
19	C <sub>7</sub> H	1700
20	C <sub>8</sub> H	1700
21	C <sub>9</sub> H	1700
22	C <sub>10</sub> H	1700
24	C <sub>2</sub> H <sub>2</sub>	1600
25	C <sub>3</sub> H <sub>2</sub>	1900
26	C <sub>4</sub> H <sub>2</sub>	1800
27	C <sub>5</sub> H <sub>2</sub>	1800
28	C <sub>6</sub> H <sub>2</sub>	1700
29	C <sub>7</sub> H <sub>2</sub>	1800
30	C <sub>8</sub> H <sub>2</sub>	1700
31	C <sub>9</sub> H <sub>2</sub>	1800
32	C <sub>10</sub> H <sub>2</sub>	1700

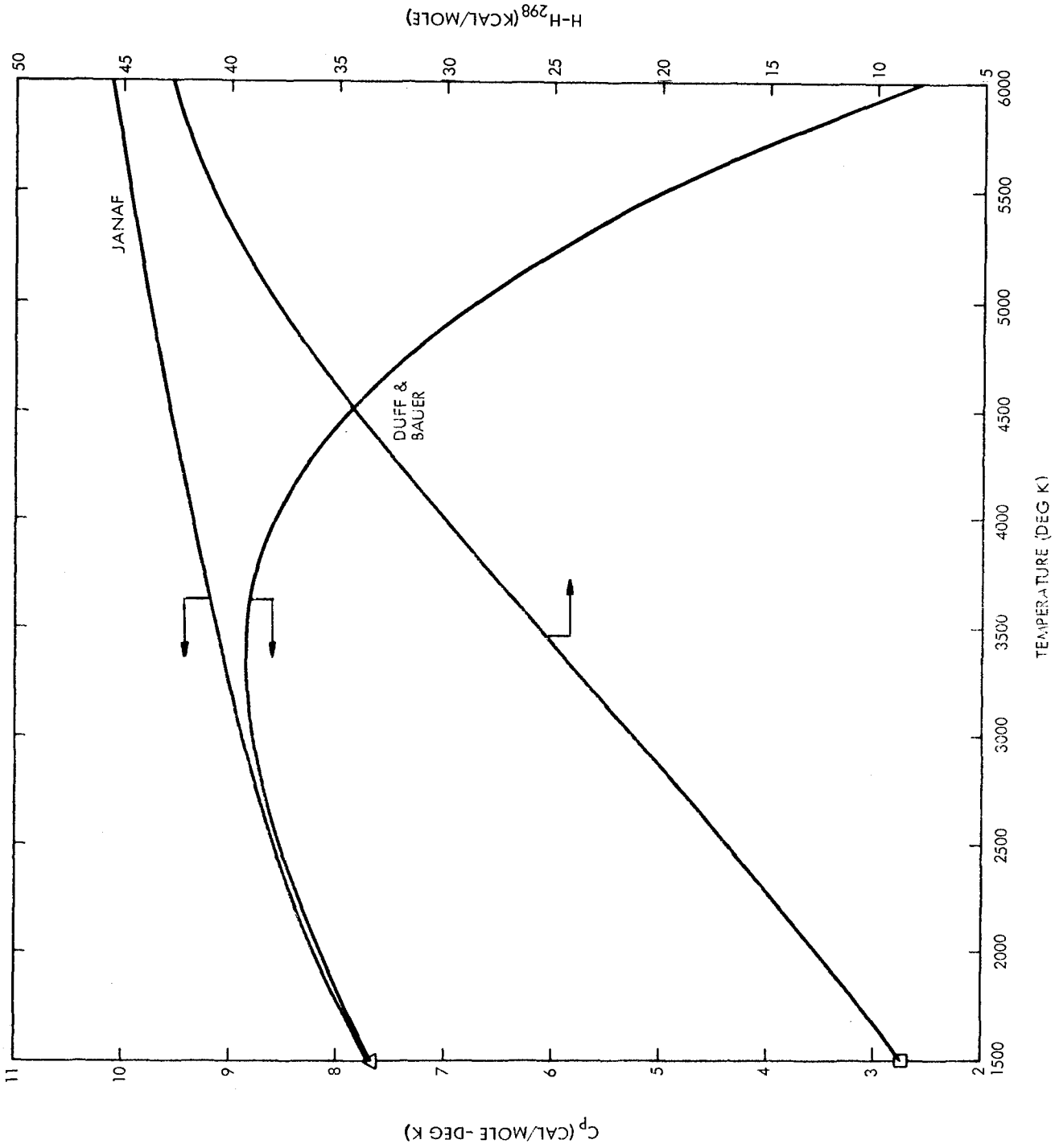


Figure D-1. Heat Capacity and Enthalpy of H<sub>2</sub> as a Function of Temperature

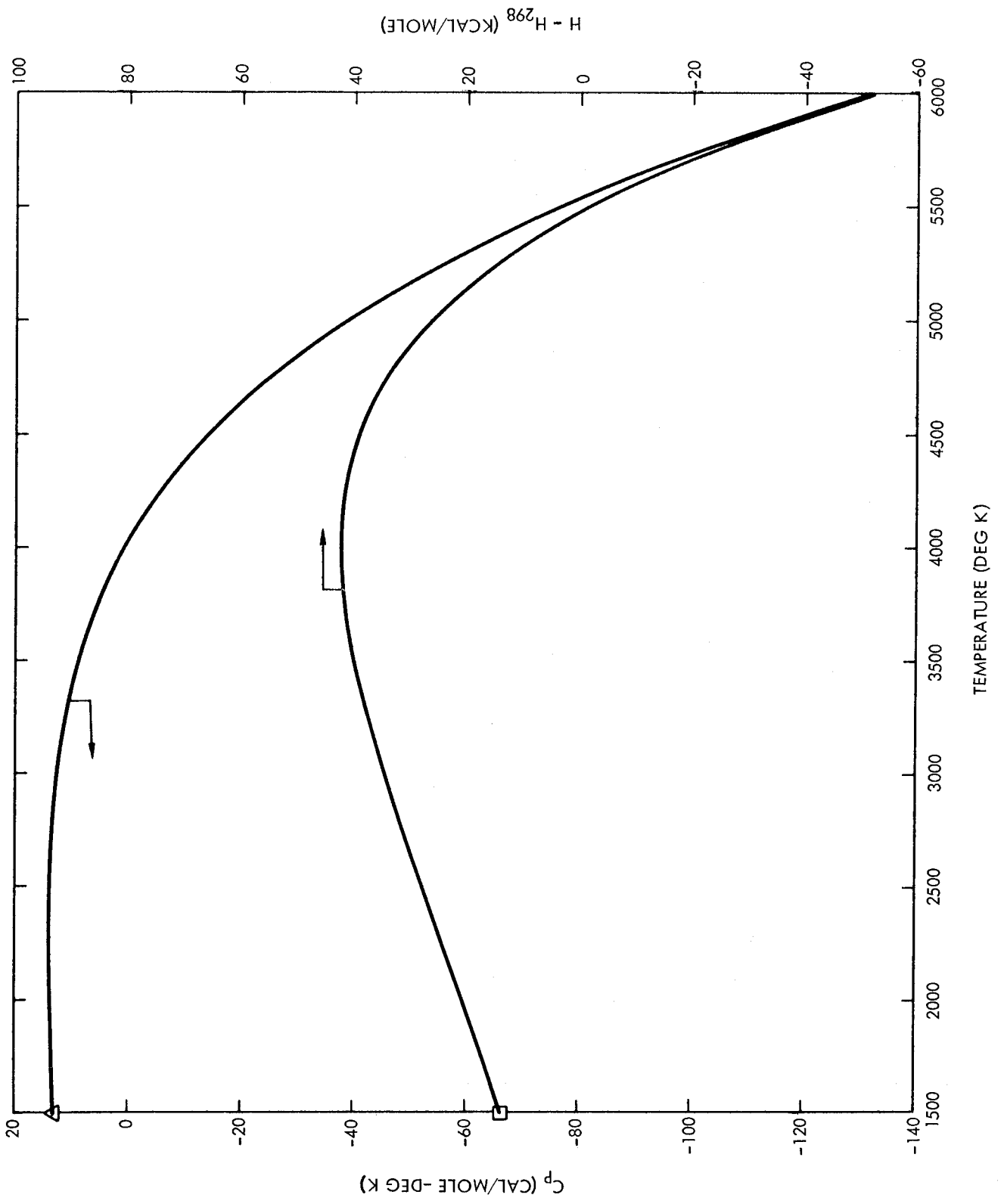


Figure D-2. Heat Capacity and Enthalpy of C<sub>2</sub>H as a Function of Temperature

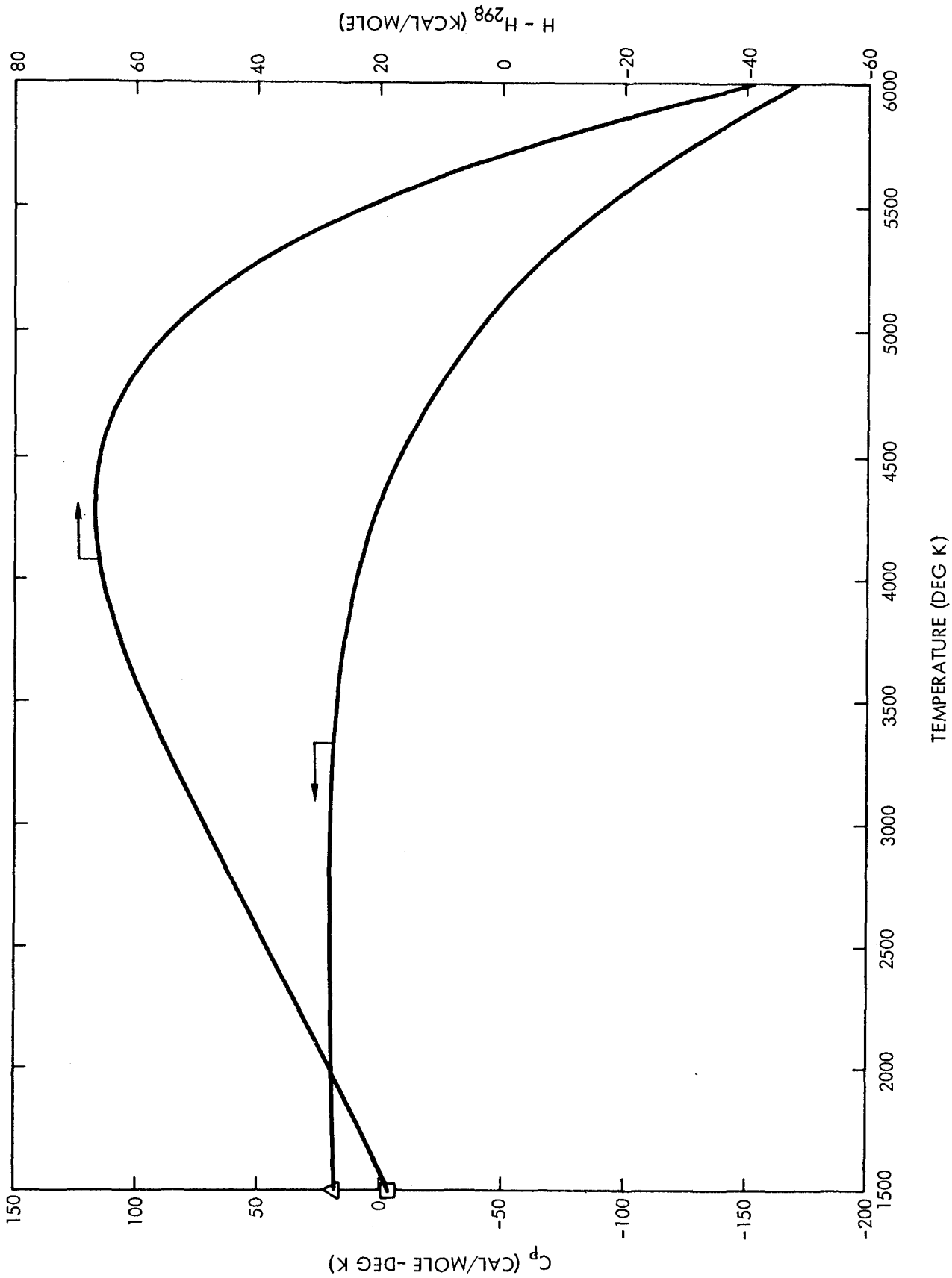


Figure D-3. Heat Capacity and Enthalpy of C<sub>3</sub>H as a Function of Temperature

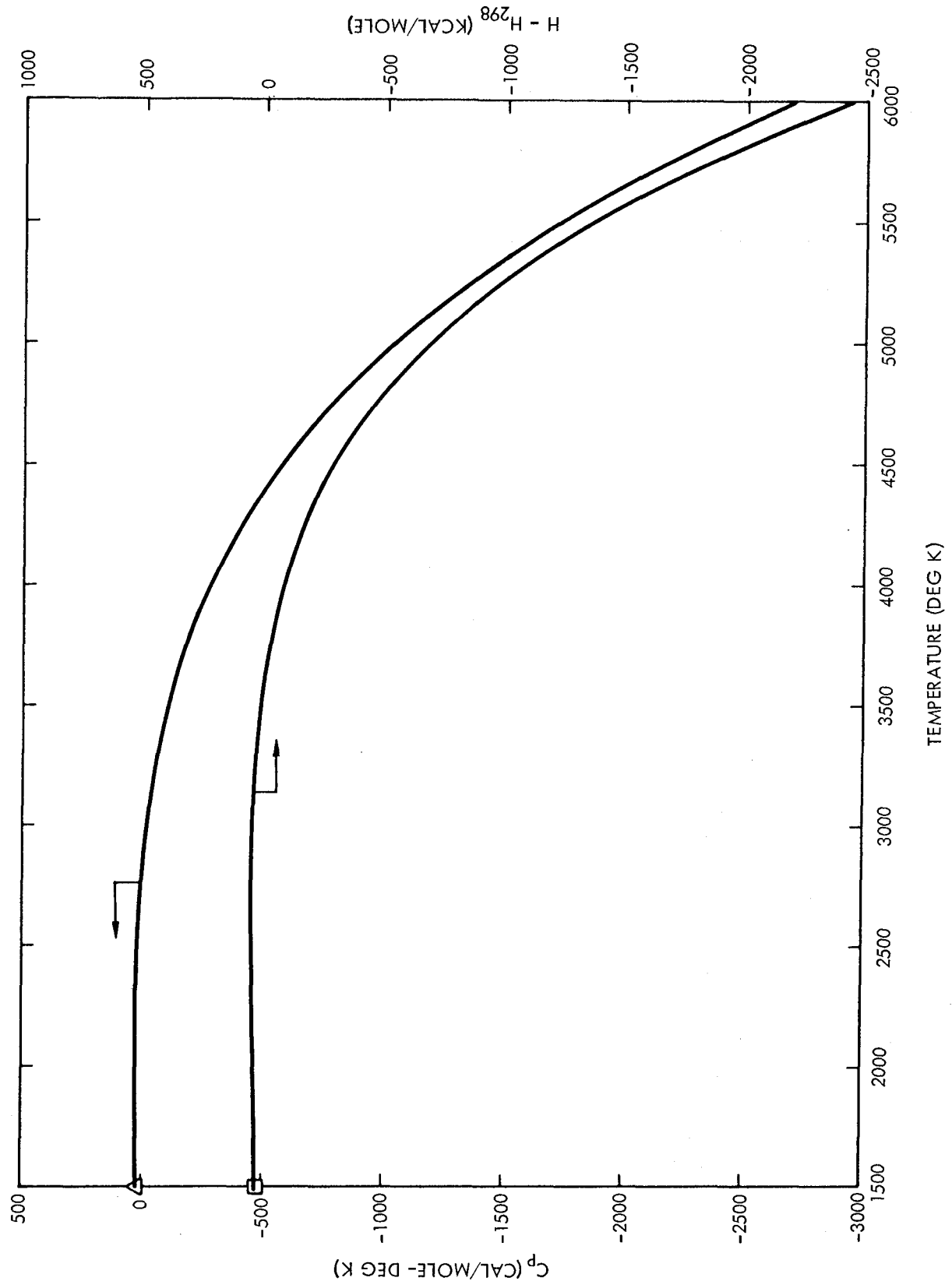


Figure D-4. Heat Capacity and Enthalpy of C<sub>4</sub>H as a Function of Temperature

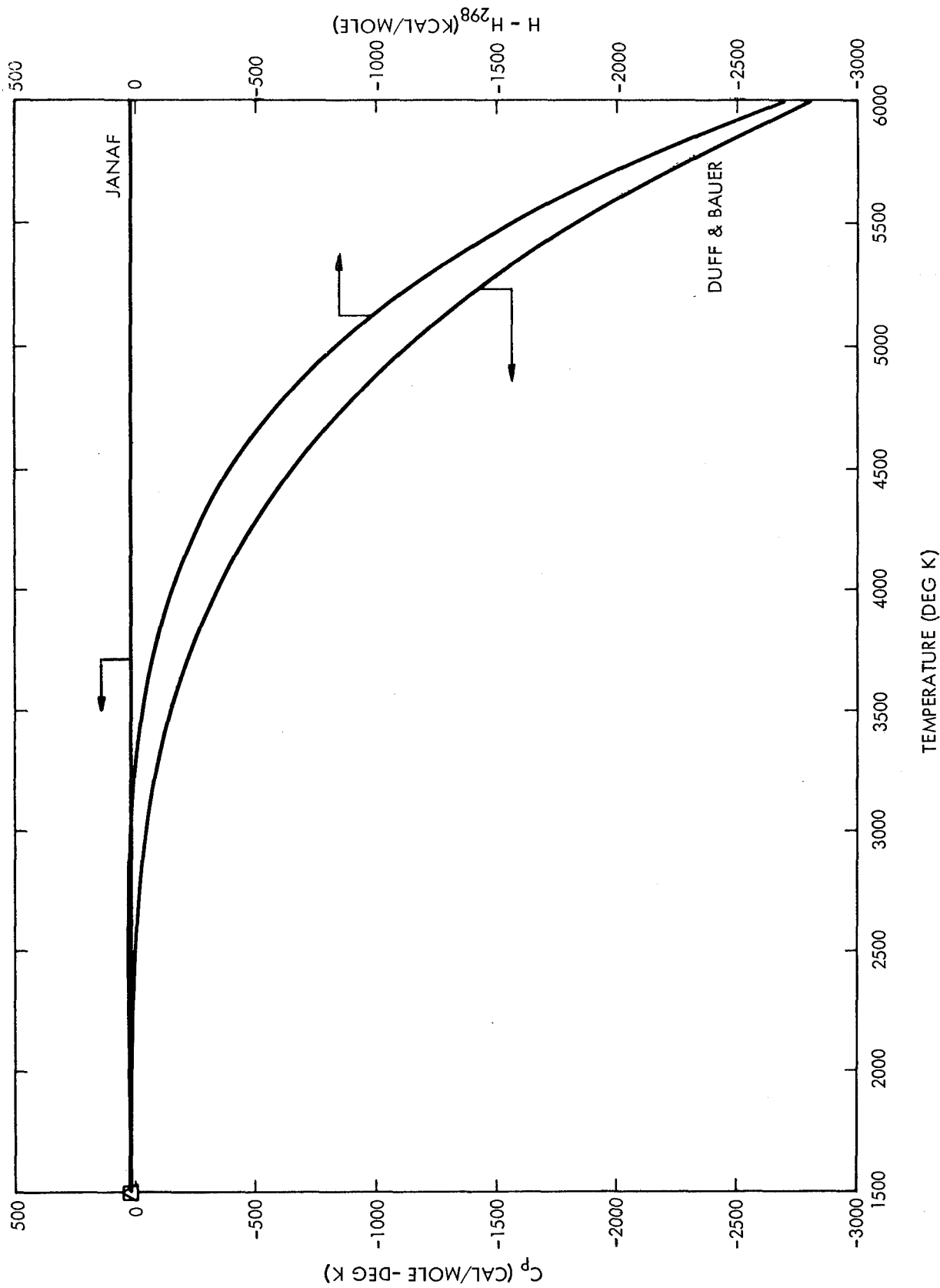


Figure D-5. Heat Capacity and Enthalpy of C<sub>2</sub>H<sub>2</sub> as a Function of Temperature

APPENDIX E

GAS COMPOSITIONS AND FLAME TEMPERATURES  
FOR SELECTED PROPELLANT SYSTEMS

Data presented in this appendix are previously unpublished calculations made at TRW Systems in support of other studies. The flame temperature and gas composition of monomethylhydrazine (MMH) with liquid fluorine-liquid oxygen mixtures at 100 psia chamber pressures and several mixture ratios are shown in Tables E-I to E-V. Fluorine/oxygen ratios were varied from 20/80 to 100/0. Table E-VI presents the  $F_2$ /MMH system at chamber pressure of 300 psia for comparison to Table E-V at 100 psia chamber pressure. Tables E-VII to E-X show the compositions and flame temperatures of fluorine/hydrazine ( $N_2H_4$ ) at 100 psia chamber pressure, fluorine/ammonia ( $NH_3$ ) at 300 psia chamber pressure, fluorine/hydrogen at chamber pressures at 100 psia and at 300 psia. Table E-XI shows the composition and flame temperatures of oxygen difluoride/diborane propellant system at a chamber pressure of 300 psia.

Data which have been published previously are not repeated here. Collections of propellant performance are generally available, but relatively few collections of propellant gas composition are available. The Aerospace Corporation, "Propellant Performance and Gas Composition Handbook" includes a compilation of flame temperatures and gas compositions, but generally the data must be retrieved from scattered sources.

Table E-1. Propellant System: FLOX (20 F<sub>2</sub> - 80 O<sub>2</sub>)/MMH

P <sub>c</sub> , psia MR T <sub>c</sub> , °R Combustion Gases	100		100		100		100		100			
	Chamber Thrust	ε = 35	Chamber Thrust	ε = 42	Chamber Thrust	ε = 53	Chamber Thrust	ε = 54	Mole Fraction	Mole Fraction		
CO	0.1684	0.1688	0.1002	0.1388	0.1374	0.0979	0.1112	0.1073	0.0453	0.0891	0.0839	0.0076
CO <sub>2</sub>	0.0178	0.0191	0.0905	0.0347	0.0387	0.0893	0.0490	0.0555	0.1381	0.0589	0.0665	0.1622
H	0.0355	0.0233	-	0.0553	0.0467	-	0.0476	0.0412	0.0018	0.0367	0.0314	0.0009
HF	0.0902	0.0911	0.0925	0.1173	0.1192	0.1272	0.1388	0.1413	0.1601	0.1565	0.1593	0.1811
H <sub>2</sub>	0.2776	0.2841	0.3678	0.1398	0.1370	0.1708	0.0787	0.0738	0.0327	0.0495	0.0452	0.0043
H <sub>2</sub> O	0.2132	0.2197	0.1582	0.2712	0.2891	0.3274	0.2718	0.2903	0.4354	0.2555	0.2720	0.4097
NO	0.0008	0.0004	-	0.0064	0.0049	-	0.0133	0.0113	0.0002	0.0182	0.0159	0.0018
N <sub>2</sub>	0.1857	0.1877	0.1907	0.1703	0.1737	0.1873	0.1536	0.1571	0.1833	0.1389	0.1423	0.1689
F	0.0001	-	-	0.0005	0.0004	-	0.0011	0.0008	-	0.0015	0.0011	-
O	0.0007	0.0003	-	0.0107	0.0077	-	0.0257	0.0215	-	0.0362	0.0310	0.0013
OH	0.0097	0.0053	-	0.0466	0.0385	-	0.0739	0.0661	0.0023	0.0847	0.0767	0.0088
O <sub>2</sub>	0.0002	-	-	0.0082	0.0065	-	0.0352	0.0338	0.0005	0.0743	0.0747	0.0535

Table E-II. Propellant System: FLOX (40 F<sub>2</sub> - 60 O<sub>2</sub>)/MMH

P <sub>c</sub> , psia MR T <sub>c</sub> , °R Combustion Gases	100		100		100		100	
	Chamber	Throat	Chamber	Throat	Chamber	Throat	Chamber	Throat
	Mole Fraction ε = 38		Mole Fraction ε = 47		Mole Fraction ε = 54		Mole Fraction ε = 54	
CO	0.1462	0.1465	0.1240	0.1222	0.1056	0.1023	0.1056	0.1023
CO <sub>2</sub>	0.0187	0.0209	0.0275	0.0318	0.0337	0.0393	0.0337	0.0393
H	0.0694	0.0569	0.0681	0.0588	0.0572	0.0492	0.0572	0.0492
HF	0.2228	0.2266	0.2617	0.2669	0.2929	0.2991	0.2929	0.2991
H <sub>2</sub>	0.1664	0.1678	0.0940	0.0906	0.0582	0.0546	0.0582	0.0546
H <sub>2</sub> O	0.1666	0.1805	0.1665	0.1829	0.1490	0.1636	0.1490	0.1636
NO	0.0040	0.0028	0.0099	0.0083	0.0150	0.0131	0.0150	0.0131
N <sub>2</sub>	0.1629	0.1660	0.1465	0.1499	0.1318	0.1351	0.1318	0.1351
F	0.0012	0.0007	0.0028	0.0020	0.0044	0.0033	0.0044	0.0033
O	0.0075	0.0048	0.0240	0.0193	0.0400	0.0341	0.0400	0.0341
OH	0.0313	0.0244	0.0581	0.0516	0.0716	0.0655	0.0716	0.0655
O <sub>2</sub>	0.0030	0.0021	0.0168	0.0156	0.0405	0.0406	0.0405	0.0406

Table E-III. Propellant System: FLOX (60 F<sub>2</sub> - 40 O<sub>2</sub>)/MMH

Combustion Gases	100		100		100		100		100	
	Chamber	Throat	Chamber	Throat	Chamber	Throat	Chamber	Throat	Chamber	Throat
P <sub>c</sub> , psia	100		100		100		100		100	
MR	1.4		1.8		2.2		2.6		2.6	
T <sub>c</sub> , °R	6178		6520		6670		6742		6742	
	Mole Fraction ε = 35		Mole Fraction ε = 42		Mole Fraction ε = 48		Mole Fraction ε = 52			
CO	0.1502	0.1517	0.1310	0.1322	0.1325	0.1152	0.1172	0.1164	0.0826	0.1051
CO <sub>2</sub>	0.0068	0.0076	0.0352	0.0114	0.0135	0.0432	0.0145	0.0177	0.0688	0.0164
H	0.0847	0.0659	-	0.0959	0.0818	-	0.0864	0.0746	0.0012	0.0718
HF	0.3179	0.3234	0.3385	0.3703	0.3787	0.4151	0.4105	0.4213	0.4846	0.4416
H <sub>2</sub>	0.1934	0.2018	0.2626	0.1059	0.1067	0.1410	0.0610	0.0596	0.0480	0.0359
H <sub>2</sub> O	0.0691	0.0764	0.0666	0.0745	0.0861	0.1269	0.0621	0.0727	0.1631	0.0463
NO	0.0017	0.0010	-	0.0059	0.0047	-	0.0105	0.0091	-	0.0142
N <sub>2</sub>	0.1561	0.1588	0.1662	0.1406	0.1437	0.1585	0.1265	0.1295	0.1514	0.1143
F	0.0019	0.0010	-	0.0059	0.0039	-	0.0112	0.0080	-	0.0178
O	0.0035	0.0019	-	0.0178	0.0134	-	0.0376	0.0315	-	0.0569
OH	0.0141	0.0101	-	0.0348	0.0305	-	0.0473	0.0443	0.0003	0.0508
O <sub>2</sub>	0.0005	0.0003	-	0.0049	0.0043	-	0.0151	0.0152	-	0.0288

Table E-IV. Propellant System: FLOX (80 F<sub>2</sub> - 20 O<sub>2</sub>)/MMH

P <sub>c</sub> , psia MR T <sub>c</sub> , °R Combustion Gases	100		100		100		100		100	
	Chamber	Throat	Chamber	Throat	Chamber	Throat	Chamber	Throat	Chamber	Throat
	Mole Fraction ε = 35		Mole Fraction ε = 39		Mole Fraction ε = 44		Mole Fraction ε = 49			
CO	0.1364	0.1386	0.1241	0.1257	0.1138	0.1151	0.1048	0.1057	0.1048	0.1057
CO <sub>2</sub>	0.0003	0.0004	0.0017	0.0022	0.0024	0.0032	0.0031	0.0041	0.0031	0.0041
H	0.1377	0.1140	0.1315	0.1151	0.1060	0.0925	0.0767	0.0639	0.0767	0.0639
HF	0.4647	0.4781	0.5024	0.5230	0.5216	0.5476	0.5285	0.5565	0.5285	0.5565
H <sub>2</sub>	0.1064	0.1178	0.0500	0.0525	0.0242	0.0232	0.0118	0.0100	0.0118	0.0100
H <sub>2</sub> O	0.0020	0.0026	0.0057	0.0077	0.0044	0.0055	0.0030	0.0033	0.0030	0.0033
N	0.0001	-	0.0002	0.0001	0.0003	0.0002	0.0003	0.0002	0.0003	0.0002
NO	0.0003	0.0002	0.0025	0.0023	0.0048	0.0046	0.0067	0.0066	0.0067	0.0066
N <sub>2</sub>	0.1366	0.1389	0.1244	0.1268	0.1137	0.1159	0.1044	0.1064	0.1044	0.1064
F	0.0129	0.0074	0.0344	0.0232	0.0646	0.0493	0.0994	0.0827	0.0994	0.0827
O	0.0010	0.0007	0.0133	0.0114	0.0296	0.0278	0.0444	0.0429	0.0444	0.0429
OH	0.0014	0.0012	0.0092	0.0093	0.0123	0.0126	0.0125	0.0121	0.0125	0.0121
O <sub>2</sub>	-	-	0.0006	0.0007	0.0021	0.0026	0.0044	0.0055	0.0044	0.0055

Table E-V. Propellant System: F<sub>2</sub>/MMH

P <sub>c</sub> , psia MR T <sub>c</sub> , °R Combustion Gases	100		100		100		100		100							
	Chamber	Throat														
C	0.0003	0.0002	-	-	0.0027	0.0018	-	-	0.0032	0.0023	-	-	0.0034	0.0025	-	-
C <sub>2</sub>	0.0003	0.0001	-	-	0.0018	0.0014	-	-	0.0019	0.0015	-	-	0.0017	0.0014	-	-
C <sub>3</sub>	0.0010	0.0005	-	-	0.0025	0.0029	-	-	0.0020	0.0023	-	-	0.0015	0.0017	-	-
CH	0.0001	-	-	-	0.0002	0.0001	-	-	0.0001	0.0001	-	-	0.0001	0.0001	-	-
CH <sub>2</sub>	0.0005	0.0004	-	-	0.0002	0.0001	-	-	0.0001	0.0001	-	-	0.0001	-	-	-
C <sub>2</sub> H <sub>2</sub>	0.0278	0.0211	-	-	0.0034	0.0042	-	-	0.0016	0.0020	-	-	0.0008	0.0008	-	-
CH <sub>3</sub>	0.0001	0.0001	-	-	-	-	-	-	-	-	-	-	-	-	-	-
CN	0.0302	0.0218	-	-	0.0594	0.0564	-	-	0.0581	0.0560	0.0001	0.0001	0.0546	0.0526	0.0002	0.0002
C <sub>2</sub> N <sub>2</sub>	0.0005	0.0003	-	-	0.0003	0.0003	-	-	0.0002	0.0002	-	-	0.0002	0.0002	-	-
CF	0.0001	0.0001	-	-	0.0019	0.0013	-	-	0.0025	0.0019	-	-	0.0031	0.0024	-	-
CF <sub>2</sub>	0.0001	0.0001	-	-	0.0017	0.0014	-	-	0.0025	0.0021	-	-	0.0034	0.0031	0.0008	0.0008
C <sub>2</sub> F <sub>2</sub>	0.0024	0.0013	-	-	0.0130	0.0146	-	-	0.0154	0.0179	-	-	0.0175	0.0207	0.0184	0.0184
CF <sub>3</sub>	-	-	-	-	-	-	-	-	-	-	-	-	-	-	0.0001	0.0001
F	0.0041	0.0028	-	-	0.0468	0.0341	-	-	0.0701	0.0548	0.0002	0.0002	0.0970	0.0804	0.0038	0.0038
HF	0.5539	0.5629	0.5959	0.7059	0.6365	0.6590	0.7992	0.8407	0.6367	0.6612	0.8407	0.8407	0.6313	0.6566	0.8369	0.8369
H	0.0691	0.0641	-	-	0.0866	0.0725	0.0004	0.0023	0.0789	0.0689	0.0028	0.0028	0.0703	0.0609	0.0001	0.0001
H <sub>2</sub>	0.1268	0.1399	0.2285	0.1316	0.0620	0.0628	0.1316	0.0479	0.0185	0.0172	0.0111	0.0111	0.0124	0.0110	-	-
FCN	0.0008	0.0005	-	-	0.0016	0.0013	-	-	0.0027	0.0025	-	-	0.0029	0.0028	0.0003	0.0003
HCN	0.0632	0.0554	0.0001	0.0007	0.0409	0.0447	0.0007	0.0015	0.0147	0.0154	0.0012	0.0012	0.0104	0.0104	0.0001	0.0001
N	-	-	-	-	0.0001	0.0001	-	-	0.0002	0.0001	-	-	0.0002	0.0001	-	-
N <sub>2</sub>	0.1186	0.1284	0.1754	0.1614	0.1008	0.1043	0.1614	0.1490	0.0904	0.0934	0.1438	0.1438	0.0889	0.0922	0.1392	0.1392
Graphite % W/W	0	2.73	10.85	9.27	0	0.01	9.27	8.06	0	0	7.59	7.59	0	0	5.26	5.26

Table E-VI. Propellant System: F<sub>2</sub>/MMH

P <sub>c</sub> , psia MR T <sub>c</sub> , °R Combustion Gases	300		300		300		300		300	
	Chamber	Throat								
C	0.0016	0.0010	0.0022	0.0015	0.0026	0.0018	0.0028	0.0021	0.0028	0.0021
C <sub>2</sub>	0.0013	0.0009	0.0015	0.0012	0.0016	0.0012	0.0015	0.0012	0.0015	0.0012
C <sub>3</sub>	0.0019	0.0021	0.0018	0.0020	0.0014	0.0016	0.0011	0.0012	0.0011	0.0012
CH	0.0002	0.0001	0.0002	0.0001	0.0002	0.0001	0.0002	0.0001	0.0002	0.0001
CH <sub>2</sub>	0.0004	0.0003	0.0002	0.0002	0.0002	0.0001	0.0001	0.0001	0.0001	0.0001
C <sub>2</sub> H <sub>2</sub>	0.0083	0.0103	0.0044	0.0053	0.0022	0.0025	0.0011	0.0011	0.0011	0.0011
CN	0.0507	0.0458	0.0530	0.0496	0.0522	0.0497	0.0491	0.0468	0.0491	0.0468
C <sub>2</sub> N <sub>2</sub>	0.0005	0.0005	0.0004	0.0004	0.0003	0.0003	0.0002	0.0002	0.0002	0.0002
CF	0.0013	0.0008	0.0020	0.0014	0.0028	0.0020	0.0034	0.0026	0.0034	0.0026
CF <sub>2</sub>	0.0014	0.0011	0.0022	0.0018	0.0032	0.0027	0.0044	0.0039	0.0044	0.0039
C <sub>2</sub> F <sub>2</sub>	0.0120	0.0129	0.0151	0.0169	0.0178	0.0205	0.0200	0.0235	0.0200	0.0235
CF <sub>3</sub>	-	-	-	-	-	-	0.0001	0.0001	0.0001	0.0010
CF <sub>4</sub>	-	-	-	-	-	-	-	-	-	0.0003
F	0.0264	0.0177	0.0424	0.0303	0.0634	0.0485	0.0883	0.0718	0.0883	0.0004
HF	0.6361	0.6551	0.6451	0.6668	0.6469	0.6708	0.6430	0.6680	0.6430	0.8394
H	0.0748	0.0627	0.0735	0.0628	0.0687	0.0593	0.0617	0.0529	0.0617	-
H <sub>2</sub>	0.0472	0.0468	0.0324	0.0314	0.0219	0.0204	0.0148	0.0131	0.0148	-
FCN	0.0025	0.0022	0.0029	0.0027	0.0033	0.0031	0.0036	0.0034	0.0036	0.0001
HCN	0.0345	0.0377	0.0250	0.0271	0.0177	0.0186	0.0124	0.0125	0.0124	-
N	0.0001	0.0001	0.0002	0.0001	0.0002	0.0001	0.0003	0.0002	0.0003	-
N <sub>2</sub>	0.0985	0.1016	0.0953	0.0983	0.0933	0.0964	0.0919	0.0953	0.0919	0.1398
Graphite % W/W	0	0	0	0	0	0	0	0	0	5.25

Table E-VII. Propellant System:  $F_2/N_2H_4$

Combustion Gases	Mole Fraction			Mole Fraction		
	Chamber	Throat	$\epsilon = 78$	Chamber	Throat	$\epsilon = 81$
$P_c$ , psia	100			100		
MR	1.6			1.8		
$T_c$ , °R	7112			7326		
F	0.0278	0.0173	-	0.0500	0.0348	-
H	0.1519	0.1315	-	0.1484	0.1320	-
$H_2$	0.0741	0.0813	0.1496	0.0469	0.0491	0.1067
HF	0.5369	0.5569	0.6205	0.5552	0.5810	0.6720
N	0.0003	0.0001	-	0.0004	0.0002	-
$N_2$	0.2091	0.2127	0.2299	0.1991	0.2027	0.2213

Combustion Gases	Mole Fraction			Mole Fraction		
	Chamber	Throat	$\epsilon = 85$	Chamber	Throat	$\epsilon = 89$
$P_c$ , psia	100			100		
MR	2.0			2.2		
$T_c$ , °R	7474			7566		
F	0.0782	0.0602	-	0.1093	0.0906	-
H	0.1367	0.1222	-	0.1213	0.1071	-
$H_2$	0.0303	0.0297	0.0668	0.0203	0.0186	0.0298
HF	0.5640	0.5938	0.7198	0.5666	0.5980	0.7643
N	0.0005	0.0003	-	0.0006	0.0004	-
$N_2$	0.1901	0.1937	0.2134	0.1818	0.1854	0.2060

Combustion Gases	Mole Fraction		
	Chamber	Throat	$\epsilon = 92$
$P_c$ , psia	100		
MR	2.4		
$T_c$ , °R	7616		
F	0.1411	0.1223	0.0095
H	0.1048	0.0900	-
$H_2$	0.0139	0.0119	-
HF	0.5654	0.5977	0.7924
N	0.0006	0.0004	-
$N_2$	0.1742	0.1777	0.1981

Table E-VIII. Propellant System:  $F_2/NH_3$

P <sub>c</sub> , psia	300			300		
	MR	2.6		2.8		
T <sub>c</sub> , °R	7430			7590		
Combustion Gases	Mole Fraction			Mole Fraction		
	Chamber	Throat	ε = 55	Chamber	Throat	ε = 57
F	0.0344	0.0216	-	0.0520	0.0360	-
H	0.1079	0.0914	-	0.1044	0.0899	-
H <sub>2</sub>	0.0614	0.0648	0.1057	0.0432	0.0435	0.0753
HF	0.6495	0.6730	0.7363	0.6587	0.6864	0.7711
N	0.0002	0.0001	-	0.0003	0.0002	-
N <sub>2</sub>	0.1466	0.1490	0.1580	0.1414	0.1438	0.1536

P <sub>c</sub> , psia	300			300		
	MR	3.0		3.2		
T <sub>c</sub> , °R	7706			7784		
Combustion Gases	Mole Fraction			Mole Fraction		
	Chamber	Throat	ε = 59	Chamber	Throat	ε = 61
F	0.0729	0.0549	-	0.0958	0.0769	-
H	0.0969	0.0835	-	0.0872	0.0739	-
H <sub>2</sub>	0.0305	0.0289	0.0465	0.0217	0.0192	0.0191
HF	0.6627	0.6935	0.8040	0.6629	0.6953	0.8353
N	0.0004	0.0002	-	0.0004	0.0003	-
N <sub>2</sub>	0.1366	0.1390	0.1495	0.1320	0.1345	0.1456

P <sub>c</sub> , psia	300			300		
	MR	3.4		3.6		
T <sub>c</sub> , °R	7829			7846		
Combustion Gases	Mole Fraction			Mole Fraction		
	Chamber	Throat	ε = 61	Chamber	Throat	ε = 55
F	0.1197	0.1008	0.0135	0.1439	0.1256	0.0602
H	0.0764	0.0629	-	0.0655	0.0515	-
H <sub>2</sub>	0.0155	0.0127	-	0.0110	0.0084	-
HF	0.6601	0.6932	0.8456	0.6554	0.6882	0.8052
N	0.0004	0.0003	-	0.0005	0.0003	-
N <sub>2</sub>	0.1277	0.1301	0.1409	0.1236	0.1259	0.1342

Table E-IX. Propellant System:  $F_2/H_2$

P <sub>c</sub> , psia	100			100		
	MR			MR		
T <sub>c</sub> , °R	5517			6917		
Combustion Gases	Mole Fraction			Mole Fraction		
	Chamber	Throat	ε = 60	Chamber	Throat	ε = 60
H	0.0537	0.0325	-	0.1962	0.1687	-
H <sub>2</sub>	0.5383	0.5550	0.5807	0.1837	0.1997	0.3067
HF	0.4076	0.4123	0.4193	0.6050	0.6222	0.6932
F	0.0003	0.0001	-	0.0150	0.0093	-

P <sub>c</sub> , psia	100			100		
	MR			MR		
T <sub>c</sub> , °F	7753			7819		
Combustion Gases	Mole Fraction			Mole Fraction		
	Chamber	Throat	ε = 66	Chamber	Throat	ε = 63
H	0.1700	0.1556	0.0037	0.1295	0.1139	-
H <sub>2</sub>	0.0289	0.0270	0.0497	0.0150	0.0128	-
HF	0.6602	0.6967	0.9466	0.6466	0.6836	0.9424
F	0.1408	0.1207	-	0.2088	0.1897	0.0575

Table E-X. Propellant System: F<sub>2</sub>/H<sub>2</sub>

P <sub>c</sub> , psia	300			300		
	MR	1.0		6.0		
T <sub>c</sub> , °R	1668			6116		
Combustion Gases	Mole Fraction			Mole Fraction		
	Chamber	Throat	ε = 65	Chamber	Throat	ε = 65
H	-	-	-	0.0699	0.0466	-
H <sub>2</sub>	0.8992	0.8992	0.8992	0.4643	0.4818	0.5171
HF	0.1008	0.1008	0.1008	0.4649	0.4711	0.4829
F	-	-	-	0.0009	0.0004	-

P <sub>c</sub> , psia	300			300		
	MR	8.0		10.0		
T <sub>c</sub> , °R	6775			7274		
Combustion Gases	Mole Fraction			Mole Fraction		
	Chamber	Throat	ε = 65	Chamber	Throat	ε = 65
H	0.1277	0.0998	-	0.1691	0.1426	-
H <sub>2</sub>	0.3158	0.3348	0.4041	0.2013	0.2167	0.3067
HF	0.5517	0.5628	0.5959	0.6149	0.6318	0.6933
F	0.0048	0.0026	-	0.0147	0.0089	-

P <sub>c</sub> , psia	300			300		
	MR	12.0		14.0		
T <sub>c</sub> , °R	7668			7956		
Combustion Gases	Mole Fraction			Mole Fraction		
	Chamber	Throat	ε = 65	Chamber	Throat	ε = 67
H	0.1872	0.1660	-	0.1828	0.1666	0.0001
H <sub>2</sub>	0.1213	0.1298	0.2220	0.0720	0.0738	0.1476
HF	0.6561	0.6806	0.7780	0.6766	0.7083	0.8523
F	0.0353	0.0236	-	0.0686	0.0512	-

Table E-XI. Propellant System:  $\text{OF}_2/\text{B}_2\text{H}_6$

$P_c$ , psia	300		
MR	3.5		
$T_c$ , °R	7760		
	Mole Fraction		
Gas	Chamber	Throat	$\epsilon = 90$
HF	0.25	0.26	0.27
H	0.23	0.22	0.02
BOF	0.17	0.18	0.30
$\text{H}_2$	0.16	0.17	0.37
BF	0.08	0.07	0.04
BO	0.02	0.02	-
$\text{H}_2\text{O}$	0.02	0.02	-
OH	0.02	0.01	-
O	0.01	0.01	-
F	0.01	0.01	-
Others	0.03	0.03	0

APPENDIX F  
EQUILIBRIUM CHEMICAL COMPATIBILITY EVALUATIONS

In this Appendix are presented the results of detailed equilibrium thermochemical calculations of 1) the compatibility of carbon, silicon carbide and boron nitride residual resin products with specific exhaust products and 2) the compatibility of alumina, magnesia, calcia, beryllia, titania, zirconia and tungsten with the combustion products of the  $\text{OF}_2/\text{B}_2\text{H}_6$  (MR=3.5) propellant system. In addition the predominant chemical reactions that occur in these systems are identified.

## F. 1 COMPATIBILITY OF CANDIDATE RESIN PRODUCTS

The results of equilibrium chemical calculations to determine the compatibility of carbon and silicon carbide with the combustion products of the  $\text{OF}_2/\text{B}_2\text{H}_6$  propellant system at MR=3.5 at 100 psia are listed in terms of the amount of solid removed per unit weight of propellant gas as a function of temperature in Table F-I. Carbon was removed at increased amounts at higher temperatures reaching about one-third pound of carbon per pound of propellant gas at  $7000^\circ\text{R}$ . The silicon carbide solid is more complex in its reactions. In reactions with SiC, the carbon is preferentially removed to the gas phase leaving liquid elemental silicon and unreacted silicon carbide at low temperatures (below about  $5300^\circ\text{R}$ ) or carbon at the higher temperatures. At  $7000^\circ\text{R}$ , the propellant gases will remove more than an equal weight of solid which was the highest ratio included in the calculations. The potential for chemical reactions between the propellant gases and the ablator residue is seen to be present at all temperatures studied. Definition of the important reactions was conducted to provide the basis for continued analysis.

## F. 2 REACTIONS WITH INDIVIDUAL PROPELLANT GASES

The propellant exhaust gases for the systems under consideration contain one or several of the following major species: BOF, HF,  $\text{H}_2$ ,  $\text{H}_2\text{O}$ , CO, and  $\text{CO}_2$ . Minor species, particularly at the higher temperatures, are primary dissociation species or gaseous elemental species from the propellant or the ablator, for example: H, F, C<sub>3</sub>, Si, Si<sub>2</sub>, and B. Because of the high potential reactivity, BOF and HF were singled out for investigation.

Table F-1. Equilibrium Reactions of Carbon and Silicon Carbide with  $OF_2/B_2H_6$  Gases at MR = 3.5, P = 100 psia

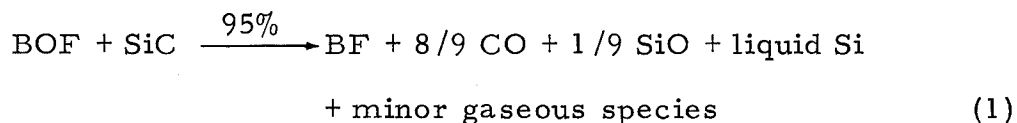
Temperature, °R	Solid Removed Per Unit Weight of Propellant Gas			
	C	SiC		
	Total	Total	Liquid	Gas
4500	0.177	0.505	0.251	0.254
5000	0.188	0.575	0.320	0.255
5500	0.206	0.902	0.601	0.301
6000	0.232	0.930	0.483	0.447
6500	0.269	0.974	0.054	0.920
7000	0.360	1.000	0.0	1.000

### F.2.1 REACTION OF SOLID RESIDUES WITH BOF

Previously it was noted that boron oxyfluoride species could react either as an oxygen source or as a fluorine source. Boron oxyfluoride is expected to be the most reactive of the major exhaust gases (HF, H<sub>2</sub> and BOF) present in the  $OF_2/B_2H_6$  system. Table F-I shows the weight of solid removed per unit weight of BOF gas.

The calculations for BOF/C showed that the gas was composed almost entirely of equimolar quantities of BF and CO. Theoretically, one part, by weight, of BOF could react with 0.262 parts of carbon. The data of Table F-II show that the reaction is almost quantitative.

A similar examination of the gas composition for the BOF/SiC systems shows a nearly complete reaction of BOF with SiC according to Equation (1) at 4500°R.



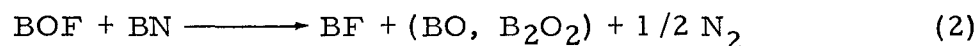
As the temperature was increased the extent of reaction approached 100% and the CO:SiO ratio approaches 1:0. Under these conditions, one part, by weight, of BOF theoretically reacts with 0.877 parts, by weight, of SiC.

Table F-II. Equilibrium Reaction of Carbon, Silicon Carbide and Boron Nitride with BOF

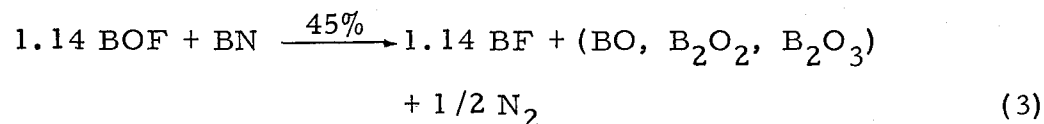
Temp., °R	Solid Removed per Unit Weight of BOF						
	C	SiC			BN		
	Total	Total	Liquid	Gas	Total	Liquid	Gas
4500	0.254	0.737	0.548	0.189	0.379	0	0.379
5000	0.260	0.803	0.528	0.275	0.575	0	0.575
5500	0.261	0.951	0.650	0.301	0.670*	(liquid + gas)	
6000	0.263	0.953	0.580	0.373	0.670	(liquid + gas)	
6500	0.270	0.963	0.322	0.641	0.670	(liquid + gas)	
7000	0.314	1.000*	(all gas)		0.670	(all gas)	

\*These are the largest weight ratios included in the study.

The reactions occurring in the BOF/BN systems are somewhat more complex with a stoichiometry approaching that given in Equation (2) at high temperatures.



At 4500°R, higher oxides of boron are present in the gas phase and the extent of reaction is much less. An approximation to the overall chemistry is given by Equation (3).



#### F.2.2 Reactions of Solid Residues with HF

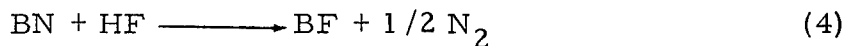
Hydrogen fluoride is an exhaust gas present in all of the fluorine oxidized systems under consideration. Considerable experimental data generally show low reactivity of HF with carbon.

The calculations located in Table V, Section 2.4 of this report verified the lack of reactivity between carbon and HF. It may be seen that even at 7000°R, HF reacted with only 18 percent, by weight, of carbon. The reaction products were principally C<sub>2</sub>F<sub>2</sub> and C<sub>2</sub>H<sub>2</sub> with

small amounts of CF and CF<sub>2</sub>. At 4500°R, where the amount of reaction was about 0.4%, C<sub>2</sub>F<sub>2</sub> was the only significant reaction product.

Silicon carbide was found to be much more reactive with HF than ~~with~~ carbon. The HF preferentially removes the silicon with the carbon remaining in the residue. At 4500°R, HF is 87% reacted giving SiF<sub>4</sub> and SiHF<sub>3</sub> at a 1.7:1 ratio. As the temperature is increased, the SiF<sub>4</sub> and SiHF<sub>3</sub> became less stable and HF was reformed. At 7000°R, HF was about 53% reacted. At this temperature, all of the silicon was removed from the solid residue as Si, SiF, SiF<sub>2</sub> and SiF<sub>4</sub> in the ratio of about 7.5:4.5:4.5:1.

The BN chemistry was not fully defined since the highest solid-gas weight ratio included in this study was 1:1. At this ratio BN was entirely removed to the gas phase by HF. An examination of the gas composition showed that the predominant reaction, Equation (4), was between equimolar amounts of BN and HF.



On the basis of this stoichiometry, hydrogen fluoride would theoretically react with 1.24 times its weight of BN.

It is tentatively concluded that BN is probably the poorest of all residues considered for use in fluorine oxidized systems, while carbon is probably best.

### F.3 COMPATIBILITY OF CANDIDATE ADDITIVES WITH THE OF<sub>2</sub>/B<sub>2</sub>H<sub>6</sub> COMBUSTION PRODUCTS

Equilibrium compositions of the products of combustion of OF<sub>2</sub>/B<sub>2</sub>H<sub>6</sub> (MR=3.5) and of these gases in contact with excess alumina, beryllia and magnesia are shown in Table F-III and for excess silica, zirconia, tungsten and titania in Table F-IV. Calculations in these tables are for a temperature of 5500°R and 100 psia. These conditions were chosen to represent the center of the temperature and pressure ranges considered and the temperature is within about 1000°R of the wall temperature.

Table F-III. Gas Composition for 50 Grams of Propellant Gas Only and in Equilibrium with 50 Grams of Metal Oxides at 5500°R and 100 psia

Gas	OF <sub>2</sub> /B <sub>2</sub> H <sub>6</sub> (MR=3.5) Moles	OF <sub>2</sub> /B <sub>2</sub> H <sub>6</sub> <sup>a</sup> + MgO Moles	OF <sub>2</sub> /B <sub>2</sub> H <sub>6</sub> <sup>a</sup> + Al <sub>2</sub> O <sub>3</sub> Moles	OF <sub>2</sub> /B <sub>2</sub> H <sub>6</sub> <sup>a</sup> + BeO Moles		
BO	0.00423	0.00516	0.00579	0.00934		
BF	0.12417	0.01895	0.03625	0.00058		
BF <sub>2</sub>	0.00745	0.00098	0.00168	0.00000		
B <sub>2</sub> O <sub>2</sub>	0.00021	0.00027	0.00036	0.00077		
BF <sub>3</sub>	0.00856	0.00096	0.00151	0.00000		
B <sub>2</sub> O <sub>3</sub>	0.00026	0.00240	0.00175	0.03526		
F	0.00061	0.00061	0.00049	0.00006		
H	0.09644	0.09067	0.09451	0.00626		
H <sub>2</sub>	0.77447	0.60813	0.72295	0.28235		
HF	0.64814	0.52348	0.43940	0.03397		
H <sub>2</sub> O	0.04101	0.22020	0.13886	0.52562		
HBO	0.01589	0.01613	0.02065	0.01856		
HOBO	0.01452	0.10078	0.06843	0.59660		
H <sub>3</sub> BO <sub>3</sub>	0.00000	0.00001	0.00000	0.00009		
O	0.00014	0.00104	0.00051	0.00622		
OH	0.00184	0.01187	0.00657	0.04460		
BOF	0.62679	0.65429	0.66401	0.10535		
O <sub>2</sub>	0.00002	0.00016	0.00005	0.00466		
Metal Species	Mg	0.27104	Al	0.00066	Be	0.00009
	MgF	0.00104	AlF	0.12696	BeF	1.29956
	MgF <sub>2</sub>	0.11857	AlF <sub>2</sub>	0.02404	BeF <sub>2</sub>	0.00040
	MgH	0.00753	AlF <sub>3</sub>	0.02039	BeO	0.00009
	MgO	0.00708	AlOF	0.00209	Be <sub>2</sub> O <sub>2</sub>	0.00046
	MgOH	0.00061	AlO	0.00015	Be <sub>3</sub> O <sub>3</sub>	0.00132
			Al <sub>2</sub> O	0.00010	Be <sub>4</sub> O <sub>4</sub>	0.00009
			AlH	0.00005	BeOH	0.03060
		HOAlO	0.00021	Be(OH) <sub>2</sub>	0.00043	
Moles of Oxide Consumed	MgO(s)	0.40587	Al <sub>2</sub> O <sub>3</sub> (1)	0.08752	BeO(1)	1.33650

a. Mixture Ratio = 3.5

Table F-IV. Gas Composition for 50 Grams of Propellant Gas Only  
and in Equilibrium with 50 Grams of Ablator  
at 5500°R and 100 psia

Gas	OF <sub>2</sub> /B <sub>2</sub> H <sub>6</sub> <sup>a</sup> Moles	OF <sub>2</sub> /B <sub>2</sub> H <sub>6</sub> <sup>a</sup> + CaO Moles	OF <sub>2</sub> /B <sub>2</sub> H <sub>6</sub> <sup>a</sup> + ZrO <sub>2</sub> Moles	OF <sub>2</sub> /B <sub>2</sub> H <sub>6</sub> <sup>a</sup> + W Moles	OF <sub>2</sub> /B <sub>2</sub> H <sub>6</sub> <sup>a</sup> + TiO Moles			
BO	0.00457	0.01560	0.00573	0.00457	0.00409			
BF	0.11912	0.00424	0.07795	0.11913	0.01585			
BF <sub>2</sub>	0.00275	0.00000	0.00148	0.00275	0.00043			
B <sub>2</sub> O <sub>2</sub>	0.00024	0.00312	0.00038	0.00024	0.00019			
BF <sub>3</sub>	0.00810	0.00000	0.00361	0.00810	0.00150			
B <sub>2</sub> O <sub>3</sub>	0.00031	0.03758	0.00080	0.00031	0.00202			
F	0.00059	0.00004	0.00049	0.00059	0.00071			
H	0.09691	0.08439	0.09795	0.09691	0.08422			
H <sub>2</sub>	0.78087	0.66164	0.80493	0.78088	0.58773			
HF	0.65510	0.05407	0.54731	0.65509	0.67235			
H <sub>2</sub> O	0.03076	0.23782	0.05035	0.03076	0.18417			
HBO	0.01719	0.05715	0.02204	0.01719	0.01336			
HOBO	0.01305	0.39599	0.02657	0.01305	0.08061			
H <sub>3</sub> BO <sub>3</sub>	0.00000	0.00006	0.00000	0.00000	0.00000			
O	0.00014	0.00112	0.00021	0.00014	0.00112			
OH	0.00189	0.01497	0.00303	0.00189	0.01302			
BOF	0.63496	0.20566	0.65977	0.63495	0.67221			
O <sub>2</sub>	0.00000	0.00023	0.00000	0.00000	0.00019			
BOHF <sub>2</sub>	0.00038	0.00000	0.00033	0.00038	0.00040			
BO <sub>2</sub>	0.00136	0.04248	0.00272	0.00136	0.00972			
Metal Species	Ca	0.21884	ZrO	0.00002	WO	0.00001 <sup>7</sup>	TiO	0.00090
	Ca <sup>+1</sup>	0.00006	ZrO <sub>2</sub>	0.00005	WO <sub>2</sub>	0.00000 <sup>3</sup>	TiO <sub>2</sub>	0.00166
	CaH	0.00172	ZrF <sub>2</sub>	0.00007			TiOF	0.00057
	CaF	0.00006	ZrF <sub>3</sub>	0.02561			TiOF <sub>2</sub>	0.00119
	CaO	0.08250	ZrF <sub>4</sub>	0.01582			TiF <sub>2</sub>	0.01507
	CaOH	0.00032					TiF <sub>3</sub>	0.01255
	e <sup>-</sup>	0.00004					TiF <sub>4</sub>	0.00057
	CaF <sub>2</sub> (1)	0.58809					Ti <sub>2</sub> O <sub>3</sub> (1)	0.29664
Moles of Ablator Consumed	CaO (1)	0.89158 <sup>b</sup>	ZrO <sub>2</sub> (1)	0.04159	W (s)	0.00002	TiO <sub>2</sub> (1)	0.62578 <sup>b</sup>

a. Mixture Ratio = 3.5  
b. Completely consumed.

It should be noted that the results of calculations shown in Table F-IV were obtained using new JANAF thermochemical data, whereas those data reported in Table F-III used the older information. Because the amounts of the combustion species that are present in  $\text{OF}_2/\text{B}_2\text{H}_6$  system did not vary too much, it is believed the overall results of the compatibility studies would not be appreciably affected using either the old or new data. Consequently, the information listed in Table F-III was not recalculated.

The predominant reactions occurring may be determined by investigating the net changes in gaseous species after equilibrium of propellant gases and ablator has been attained. These changes normalized to 1 mole of ablator are shown in Tables F-V through F-XI.

Table F-V. Net Reactions of Alumina with OF<sub>2</sub>/B<sub>2</sub>H<sub>6</sub> Propellant Gas (MR = 3.5) at 5500°R and 100 psia

Reactants, moles		Products, moles	
AlO <sub>1.5</sub> <sup>(1)</sup>	1.000	BO	0.009
BF	0.502	B <sub>2</sub> O <sub>2</sub>	0.001
BF <sub>2</sub>	0.033	B <sub>2</sub> O <sub>3</sub>	0.009
BF <sub>3</sub>	0.040	H <sub>2</sub> O	0.559
F	0.001	HBO	0.027
H	0.011	HOBO	0.308
H <sub>2</sub>	0.294	O	0.002
HF	0.884	OH	0.027
		BOF	0.212
		Al	0.004
		AlF	0.725
		AlF <sub>2</sub>	0.137
		AlF <sub>3</sub>	0.117
		AlOF	0.012
		AlO	0.001
		Al <sub>2</sub> O	0.001
		AlH	0.001
		HOAlO	0.001

Approximate Stoichiometry for the Principal Net Reactions

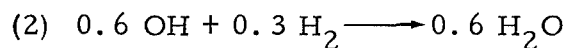
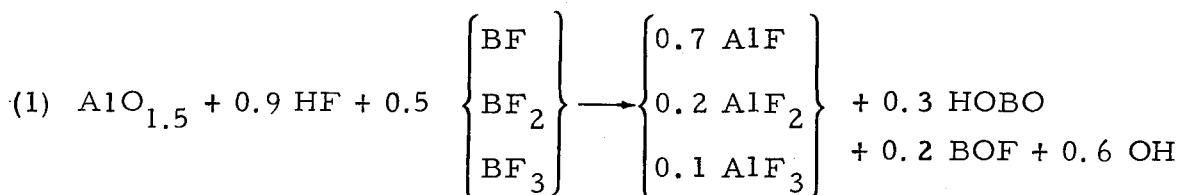


Table F-VI. Net Reactions of Magnesia with OF<sub>2</sub>/B<sub>2</sub>H<sub>6</sub> Propellant Gas (MR = 3.5) at 5500°R and 100 psia

Reactants, moles		Products, moles	
MgO(s)	1.000	BO	0.002
BF	0.259	B <sub>2</sub> O <sub>3</sub>	0.005
BF <sub>2</sub>	0.015	H <sub>2</sub> O	0.441
BF <sub>3</sub>	0.020	HOBO	0.212
H	0.015	O	0.002
H <sub>2</sub>	0.409	OH	0.025
HF	0.308	BOF	0.069
		Mg	0.666
		MgF	0.002
		MgF <sub>2</sub>	0.293
		MgH	0.020
		MgO	0.017
		MgOH	0.002

Approximate Stoichiometry for the Principal Net Reactions

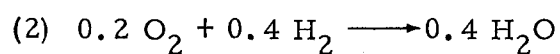
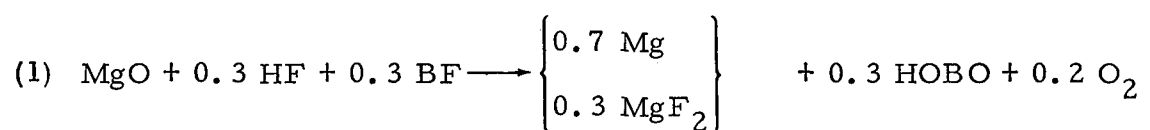


Table F-VII. Net Reactions of Beryllia with OF<sub>2</sub>/B<sub>2</sub>H<sub>6</sub> Propellant Gas (MR = 3.5) at 5500°R and 100 psia

Reactants, moles		Products, moles	
BeO(l)	1.000	BO	0.004
BF	0.093	B <sub>2</sub> O <sub>3</sub>	0.026
BF <sub>2</sub>	0.006	H <sub>2</sub> O	0.362
BF <sub>3</sub>	0.006	HBO	0.002
H	0.023	HOBO	0.436
H <sub>2</sub>	0.368	O	0.005
HF	0.460	OH	0.032
BOF	0.390	O <sub>2</sub>	0.003
		BeF	0.972
		Be <sub>3</sub> O <sub>3</sub>	0.001
		BeOH	0.023

Approximate Stoichiometry for the Principal Net Reactions

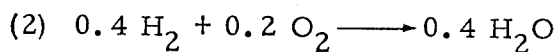
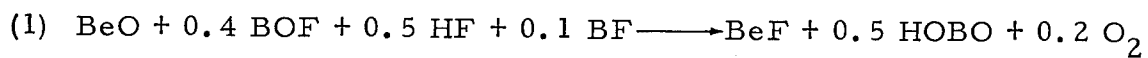


Table F-VIII. Net Reactions of Calcia with  $\text{OF}_2/\text{B}_2\text{H}_6$  Propellant Gas (MR = 3.5) at  $5500^\circ\text{R}$  and 100 psia

Reactants	Moles	Products	Moles
CaO	1.000	BO	0.012
BF	0.129	$\text{B}_2\text{O}_2$	0.003
$\text{BF}_2$	0.003	$\text{B}_2\text{O}_3$	0.042
$\text{BF}_3$	0.009	$\text{H}_2\text{O}$	0.232
F	0.001	HBO	0.045
H	0.014	HOBO	0.430
$\text{H}_2$	0.135	O	0.001
HF	0.674	OH	0.015
BOF	0.482	$\text{BO}_2$	0.046
		Ca	0.245
		CaH	0.002
		CaO (g)	0.093
		$\text{CaF}_2$ (l)	0.660

Since the CaO was completely consumed it is not possible to estimate the stoichiometry of the principal net reactions.

Table F-IX. Net Reactions of Zirconia with  $\text{OF}_2/\text{B}_2\text{H}_6$   
Propellant Gas (MR = 3.5) at  
5500°R and 100 psia

Reactants	Moles	Products	Moles
$\text{ZrO}_2$ (l)	1.000	BO	0.028
BF	0.990	$\text{B}_2\text{O}_2$	0.003
$\text{BF}_2$	0.031	$\text{B}_2\text{O}_3$	0.012
$\text{BF}_3$	0.108	H	0.025
F	0.002	$\text{H}_2$	0.579
HF	2.591	$\text{H}_2\text{O}$	0.471
$\text{BOHF}_2$	0.001	HBO	0.117
		HOBO	0.325
		O	0.002
		OH	0.027
		BOF	0.597
		$\text{BO}_2$	0.033
		$\text{ZrO}_2$ (g)	0.001
		$\text{ZrF}_2$	0.002
		$\text{ZrF}_3$	0.616
		$\text{ZrF}_4$	0.380

Approximate Stoichiometry for Principal Net Reactions:

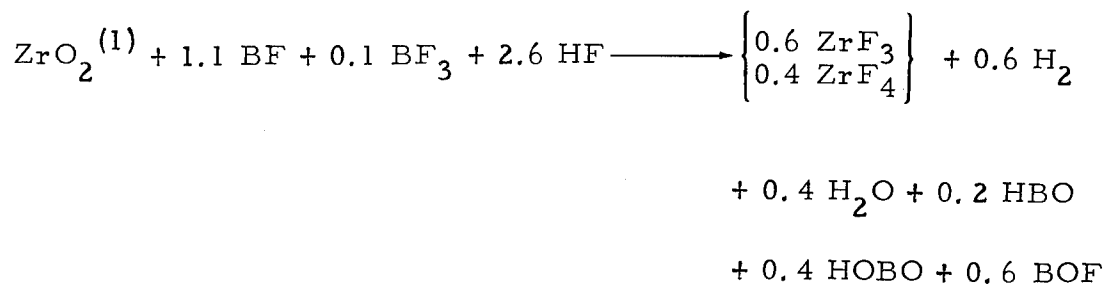


Table F-X. Net Reactions of Tungsten with  $\text{OF}_2/\text{B}_2\text{H}_6$   
Propellant Gas (MR = 3.5) at  
5500°R and 100 psia

Reactants	Moles	Products	Moles
W (s)	1.0	BF	0.5
BOF	0.5	H <sub>2</sub>	0.5
H <sub>2</sub> O	0.3		
HOBO	0.2	WO	0.8
HF	0.3	WO <sub>2</sub>	0.2

Approximate Stoichiometry for Principal Net Reactions:

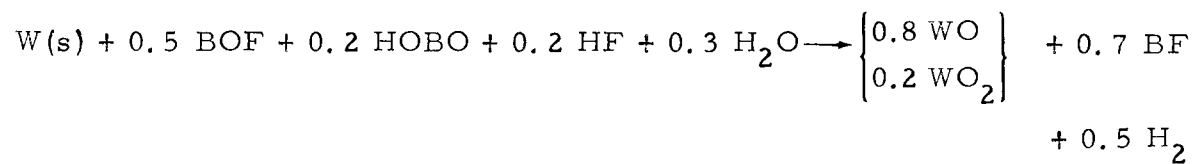


Table F-XI. Net Reactions of Titania with  $\text{OF}_2/\text{B}_2\text{H}_6$  Propellant Gas (MR = 3.5) at 5500°R at 100 psia

Reactants	Moles	Products	Moles
$\text{TiO}_2$ (l)	1.000	$\text{B}_2\text{O}_3$	0.003
BO	0.001	HF	0.028
BF	0.165	$\text{H}_2\text{O}$	0.245
$\text{BF}_2$	0.004	HOBO	0.108
$\text{BF}_3$	0.011	O	0.001
H	0.020	OH	0.018
$\text{H}_2$	0.309	BOF	0.060
HBO	0.006	$\text{BO}_2$	0.013
		TiO	0.001
		$\text{TiO}_2$ (g)	0.003
		TiOF	0.001
		$\text{TiOF}_2$	0.002
		$\text{TiF}_2$	0.024
		$\text{TiF}_3$	0.020
		$\text{TiF}_4$	0.001
		$\text{Ti}_2\text{O}_3$ (l)	0.414

Since the  $\text{TiO}_2$  (l) is completely consumed, it is not possible to estimate stoichiometry of the principal net reactions.

## APPENDIX G

### SYNTHESIS OF CANDIDATE ABLATIVE RESINS

In this Appendix detailed descriptions of the synthesis studies conducted on candidate resin systems are presented. The systems described are high carbon epoxy resins, poly (cyclized 1,2-polybutadiene) tolyl urethane, poly alkaline earth metal acrylates, and phosphate bonded oxides.

#### G.1 HIGH CARBON EPOXY RESINS

Seven unfilled and 36 carbon-filled epoxy formulations were prepared for property evaluation. The majority of these preparations were carbon-filled variations of a DMP-30 catalyzed Novalac-methyl nadic anhydride formulation.

##### G.1.1 Experimental

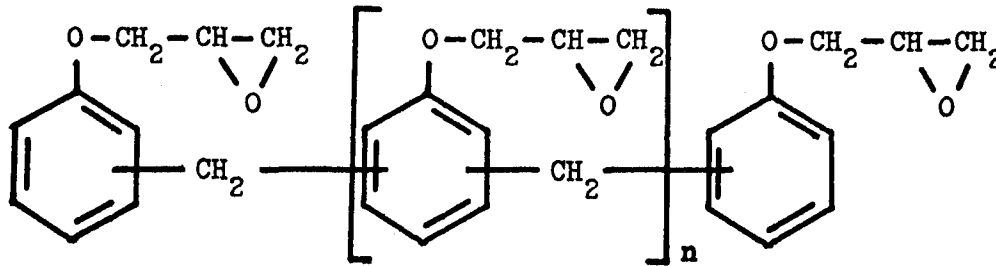
###### G.1.1.1 Procedure

The standard procedure for preparation of bubble-free specimens is described below:

Fixed amounts of epoxy, organic acid anhydride, hardner and carbon filler are stirred to a homogeneous consistency. For convenience in preparation, disposable ice cream cartons are used to contain the mixture. The mixture is degassed at 100°C for one to two hours at a pressure of 5 torr. Then the catalyst, if required, is added and blended into the mixture. The mixture is then cured, first at 100°C for 4 hours and finally at 170°C for eighteen hours. At the end of the curing cycle, the epoxide preparations are machined into samples suitable for subsequent property determination.

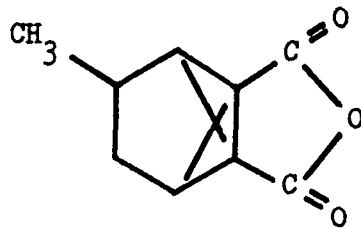
###### G.1.1.2 Materials

The Novalac epoxide (Formula G-1) was obtained as Novalac:D.E.N. 438 from the Dow Chemical Company.



(G-1)

Methyl nadic anhydride (Formula G-2) was obtained from the Allied Chemical Company.

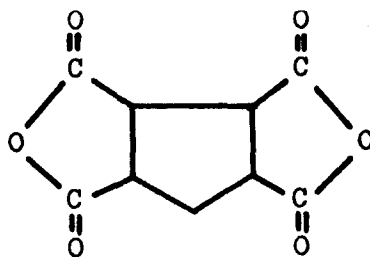


(G-2)

DMP-30, [2, 4, 6-tri(dimethylaminomethyl)phenol],  $\text{HO-C}_6\text{H}_2$   
 $[\text{CH}_2\text{-N}(\text{CH}_3)_2]_3$  was obtained from the Rohm and Haas Company.

Chlorendic anhydride, 1, 4, 5, 6, 7, 7-hexachlorobicyclo-[2, 2, 1]-5-heptene-2, 3-dicarboxylic anhydride, was obtained from the Hooker Chemical Corporation.

C. P. D. A. - cyclopentane tetracarboxylic acid anhydride (Formula G-3) was obtained from Copolymer Rubber and Chemical Company.



(G-3)

Epon 828, a standard material of epoxy formulations, and the Epon curing agent M(2 ethyl-4 methyl-imidazole) were obtained from The Shell Chemical Company.

### G.1.2 Results

The exploratory epoxides that have been prepared are listed in Table XI, Section 3.5 and Table G-I, together with pertinent physical properties. An extensive study of the effect of various types of carbon blacks has been made using the Novalac-methyl nadic anhydride-DMP-30 epoxy formulation (Table XI, Section 3.5). The carbon blacks selected for this study have a broad distribution of particle diameter, surface area and shape, and serve as reference points for advanced carbon-filled resin classes.

The preparations listed in Table G-I show the results of various modified Novalac formulations. The last three formulations of the new cyclopentane dianhydride were prepared with 828 epoxide, while of no direct value as an ablative resin, provides an interesting reference point for comparison of the effectiveness of both the hardener and Novalac epoxide.

Novalac epoxides containing methyl nadic anhydride hardeners are transparent and brownish in color. Chlorendic anhydride hardeners yield epoxides which are similar in appearance, however, compositions of equivalent amounts of epoxide and chlorendic hardener show some settling of hardener which did not dissolve in Novalac upon reaction. Mixtures of chlorendic and methyl nadic anhydride mitigate the settling problem. The cyclopentane tetracarboxylic acid dianhydride hardener yields epoxides which are opaque; they are milk white, and have the appearance and feel of ivory.

### G.2 POLY (CYCLIZED 1,2-POLYBUTADIENE) TOLYL URETHANES

Over ninety exploratory preparations of poly (cyclized 1,2-polybutadiene) tolyl urethanes have been investigated. These studies permitted determination and optimization of the relative amounts of the constituents of the resin: prepolymer, catalyst, and chain extender. The objective was to prepare materials that were tough, stiff, thermally stable, and free of olefinic bonds, yet utilized a minimum amount of catalyst.

Table G-I. Modified Novalac Epoxy Formulations

Anhydride	Weight Ratio <sup>a</sup>	Carbon Filler % W/W	Density, g/ml	Barcol Surface Hardness
Chlorendic	2.06	0	1.699	45
Methyl Nadic/ Chlorendic	0.50:1.03	0	1.504	54
	0.50:1.23	0	1.541	50
	0.33:1.38	0	1.620	53
	0.25:1.55	1	1.587	57
	0.25:1.55	5	1.582	57
Cyclopentane di-	0.58	0	1.482	52
		1		58
		5	1.432	59
Cyclopentane di-/Curing Agent M	0.4:0.0035 <sup>b</sup>	0	1.374	54
		1		
		5		

- a. Weight ratio of indicated anhydride with Novalac epoxide taken as 1.0.  
b. Weight ratio of cyclopentane dianhydride with respect to Epon 828 as 1.0. Novalac was not used in this formulation.

### G.2.1 Experimental

Exploratory samples were made from 1,2-polybutadiene diol (prepolymer) prepared upon request by the U. S. Industrial Chemical Company. The prepolymer was characterized as follows:

#### Microstructure Configuration

1,2 Vinyl, %	82.5
1,4 Trans, %	4.2
1,4 Cis, %	13.3
Hydroxyl, No.	53.8
Acid, No.	0.07
Viscosity, poise; 23°C	855

Although a prepolymer having a microstructure consisting of 100% vinyl 1,2 was considered to be preferable, the above prepolymer had the highest vinyl 1,2 content of various preparations available for

investigation. The prepolymer, a honey-colored, homogeneous liquid, did not contain chemical stabilizers or antioxidants.

Di-t-butyl peroxide, t-butyl peroxide and lauroyl peroxide (Alperox C) were obtained from Ram Chemicals, Inc.

2,5-Dimethyl 2,5-di(t-butylperoxy) hexane, Lupersol 101, was obtained from the Lucidol Division of Wallace and Tiernan Co., Inc.

Toluene diisocyanate, (4-methyl-m-phenylene diisocyanate) was obtained from Matheson, Coleman and Bell.

### G.2.2 Mode of Polymerization

The extent of cyclization of pure prepolymer, and peroxide catalyzed prepolymer after heating in air for 24 hours at 120°C and one week at 170°C was estimated by inspecting the hardness and resistance to bending of the samples. The non-catalyzed prepolymer remained liquid, although oxidation caused the formation of a hard surface scum. Prepolymer containing catalyst hardened to fairly tough, stiff resins. Although the surface of the sample darkened because of air oxidation, the material below the surface essentially retained the color of the prepolymer.

When the prepolymer was combined with an equivalent amount of toluene diisocyanate (TDI) and heated at 100°C for 24 hours, elastomers instead of plastics were formed. Further heating of the elastomers at 170°C did not cause any further hardening in the bulk, although surface hardening due to oxidation was observed. When peroxide catalysts were added to the composition of the elastomers, the elastomeric stage was noticed as an intermediate to the formation of hard, stiff, plastics. Inspection of the samples containing TDI showed that they were much tougher than those without TDI. The formation of tougher plastics were ascribed to chain extension of the prepolymer with TDI to form high molecular weight linear polymers prior to cyclization and cross-linking. It was clear that this mode of polymerization, chain extension and peroxide catalysis, produced better products.

### G. 2.3 Catalysis of Cyclization

Four catalysts were selected for evaluation: 1) di-t-butyl peroxide, 2) t-butyl perbenzoate, 3) 2,5-dimethyl-2,5-di(t-butylperoxy) hexane, and 4) lauroyl peroxide. The first three are liquids; the last is a solid. Sample mixtures of 2% w/w of lauroyl peroxide presented difficulties in handling since the peroxide was not readily soluble in the resin at room temperature. Cured samples of cyclic polybutadiene containing lauroyl peroxide were not as hard as those containing liquid catalysts, hence, this peroxide was eliminated from further consideration. The liquid peroxides were evaluated at 2 and 5% w/w levels. The order of catalytic activity was determined to be t-butyl-perbenzoate > 2,5 dimethyl-2,5-di (t-butylperoxy) hexane > di-t-butyl peroxide. Inspection of the cured products indicated that di-t-butyl peroxide catalyst yielded the hardest and toughest product.

When samples of 50 g or more, were placed directly into a 120°C oven, an exotherm was generated, which was sufficient to char and fracture the cured material. The actual site of initiation and subsequent boundary of the cured-uncured interface could be visually observed.

This effect arose from localization of the exothermic reaction. Variations in reaction-initiation time was found to depend on the particular catalyst employed and its concentration. The rapid curing reaction was not observed to take place at temperatures below 105°C; a procedure consisting of curing for three to four days at 105°C, with subsequent curing at 120°C produced well-defined uniform resins.

Poly (cyclized 1, 2-polybutadiene) tolyl urethane samples were also prepared using 2% w/w peroxide and 10% w/w toluene diisocyanate. A cure schedule of eight days at 105°C followed by one to two days at 120°C was utilized, thus allowing for chain extension of polybutadiene by the lower temperature prior to cyclization at 120°C.\* Carbon-filled samples of 5% and 10% w/w also were prepared using the same formulation.

---

\*Polyurethananation catalysts were not employed in the present study.

The poly (cyclized 1,2-polybutadiene) tolyl urethane preparations were darker in color than the samples containing only peroxide, however, all samples were transparent. These samples were also harder and exhibited more resilience.

A three-ply laminate was prepared employing this resin matrix with a high silica-reinforcing fabric. Inspection of the laminate showed that it was stiff and tough. In addition, a ten-ply laminate and a one-half-inch composite plug were prepared.

#### G.2.4 Infrared Studies of Poly (Cyclized 1,2-Polybutadiene) Tollyl Urethane

Infrared spectroscopy provides an excellent means to determine the extent and mechanism of poly (cyclized 1,2-polybutadiene) tolyl urethane cure reaction. The rate of chain extension can be observed by monitoring the disappearance of isocyanate group and the appearance of the urethane group, whereas the cyclization reaction can be followed by monitoring the disappearance of the vinyl group and appearance of a ring structure. Because a detailed investigation of this sort is outside the scope of the current ablative resin program, only cursory studies were undertaken to establish that the polymer was formed according to the mechanism outlined in Figure G-1 and to provide a semi-quantitative estimate of the extent of polymerization.

##### G.2.4.1 Chain Extension

In the majority of formulations examined, the isocyanate hydroxyl ratio was set at 1.19. However, in the finished chain-extended and cyclized material excess isocyanate was not observed by infrared spectroscopy. In past studies, it has been shown that the infrared method is capable of detecting quantities of free isocyanate of at least 1% of the total amount taken. The consumption of the originally taken excess of toluene diisocyanate (TDI) can be attributed to either one or a combination of several reactions:

- Reaction with trace quantities of water to form substituted amines which, in turn, continue to react with additional isocyanate groups to form ureas;
- Reactions with the urethane link to form allophanates which may serve as a point of cross-linking;

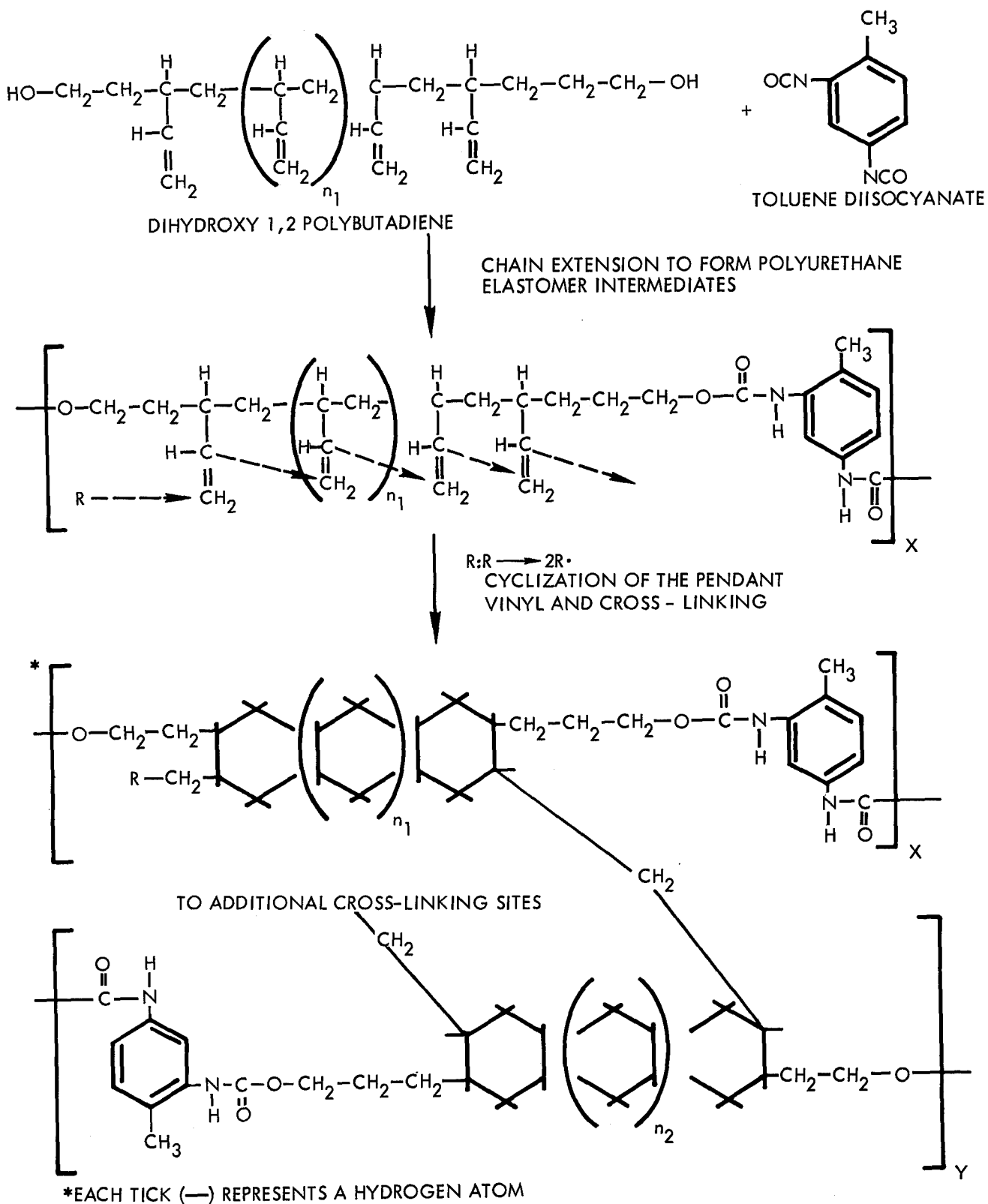


Figure G-1. Synthesis of Poly (Cyclized 1,2-Polybutadiene) Toly Urethane

- Reaction with other isocyanate groups to form isocyanurates which may also serve as a point of cross-linking.

Because of the high degree of reactivity of the para isocyanate group, it is believed that nearly all the toluene diisocyanate molecules react through the para position with the diol in a relatively short time. Consequently, it is unlikely that the excess free TDI is lost through volatilization from the mixture during curing. Detailed studies would be required to establish which of the postulated reactions predominates in consumption of the excess isocyanate.

#### G.2.4.2 Cyclization

The degree of cyclization of the 1,2 vinyl groups was examined by infrared spectroscopy for two standard formulations and for one formulation in which chain extension was eliminated. In particular, the  $910\text{ cm}^{-1}$  vinyl infrared band was observed in these cured products. For a semi-quantitative measurement of the amount of vinyl groups consumed, it was necessary to determine the absorbancy index of the vinyl group. This was obtained from the spectra of the prepolymer dissolved in carbon tetrachloride and by assumption of Lambert-Beer-Bouger Law validity, e. g.,

$$A = abc = \log I_0/I \quad (\text{G-4})$$

where:

- A = absorbance of a particular infrared active band;
- a = absorbance index, ml/meq-cm;
- b = optical path length through the specimens, cm; and
- c = concentration of the infrared active group, meq/ml.

$I/I_0$  = infrared transmittance

From the characterization of the prepolymer by the vendor in which an end group analysis of 0.959 meq OH/g was provided, a molecular weight of 2086 is calculated. From the structure of the prepolymer, it is estimated that, on the average, 37.0 butadiene groups are linked together to form the prepolymer. From the vendor's analysis that 82.5% of the double bonds (i. e., 30.5) are vinyl groups, the vinyl unsaturation concentration of the prepolymer was calculated

to be 14.6 meq/g. The infrared spectrum obtained from a 0.205 g/ml solution of the prepolymer in carbon tetrachloride, using 0.025 mm fixed thickness cells is shown in Figure G-2. From this analysis, an absorbancy index for the  $910\text{ cm}^{-1}$  vinyl band of 139 ml/meq-cm was obtained from use of Equation G-4.

The cured, chain-extended and cyclized products are tough enough to permit sampling by grinding and preparation of clear KBr pellets for subsequent infrared analysis. Ground specimens of material synthesized having an initial NCO/OH ratio of 1.19 and 1% and 2% ditertiary butyl peroxide, and a specimen that has not been chain-extended (e.g., the initial NCO/OH ratio was 0.00) were prepared and KBr pellets were pressed. The infrared curves obtained from these samples are presented in Figures G-3, G-4 and G-5.

For solid pellet infrared studies, the Lambert-Beer-Bouguer relationship (Equation G-4) reduces to:

$$A = \frac{aw_p c}{sd} \quad (\text{G-5})$$

where:

- A = absorbance arising from specific group;
- a = absorbance index, ml/meq-cm;
- $w_p$  = total weight of the pellet, g;
- c = concentration of the specific group in the pellet, meq/ml;
- s = surface area of pellet,  $\text{cm}^2$ ; and
- d = density of pellet,  $\text{g}/\text{cm}^3 = 2.75\text{ g}/\text{cm}^3$  for KBr.

The concentration of specific group in the sample,  $c_r$ , is obtained from

$$c_r = \frac{w_p}{w_r d} c \quad (\text{G-6})$$

where:

- $w_r$  = the weight of the sample in the KBr pellet.

Combining Equations G-5 and G-6

$$c_r = \frac{sA}{aw_r} \quad (\text{G-7})$$

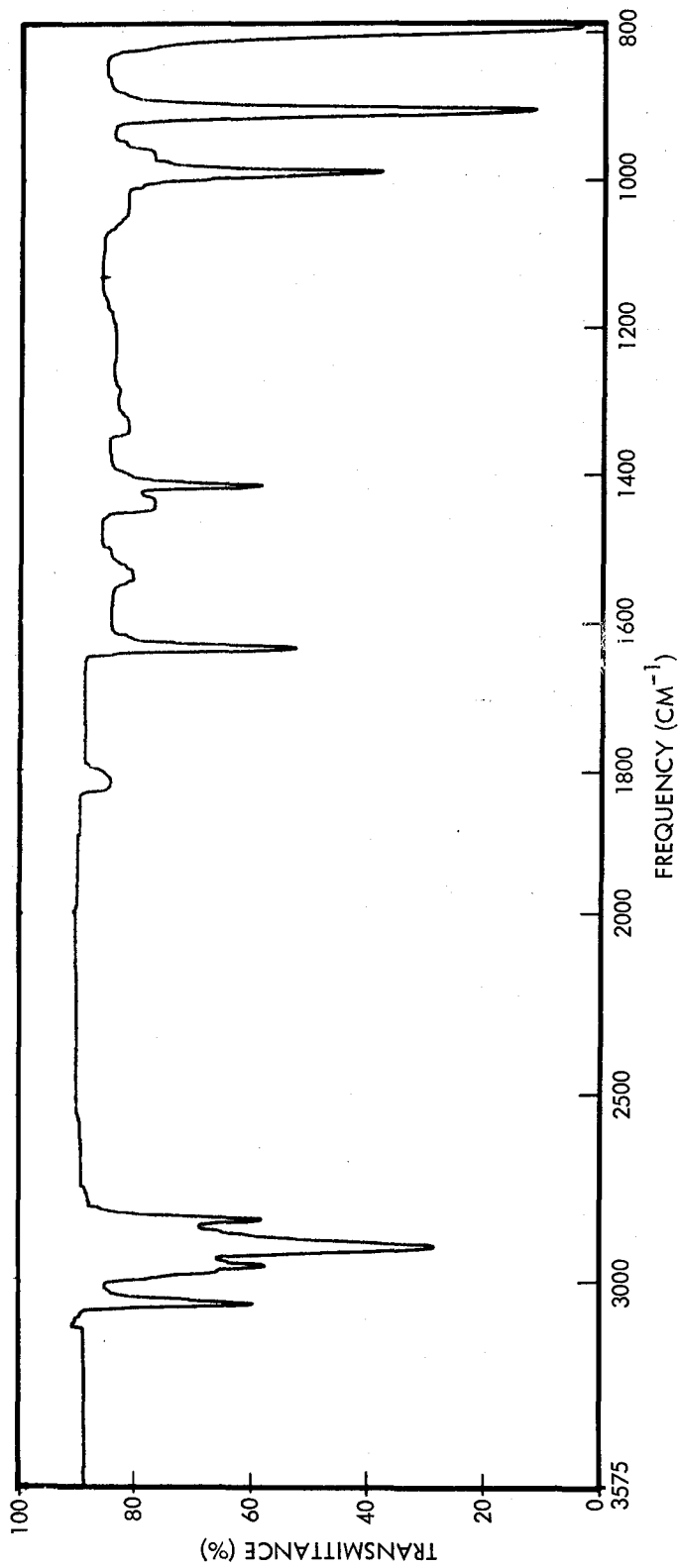


Figure G-2. Infrared Spectrum of 1, 2-Polybutadiene Diol (0.205 g/ml in Carbon Tetrachloride)

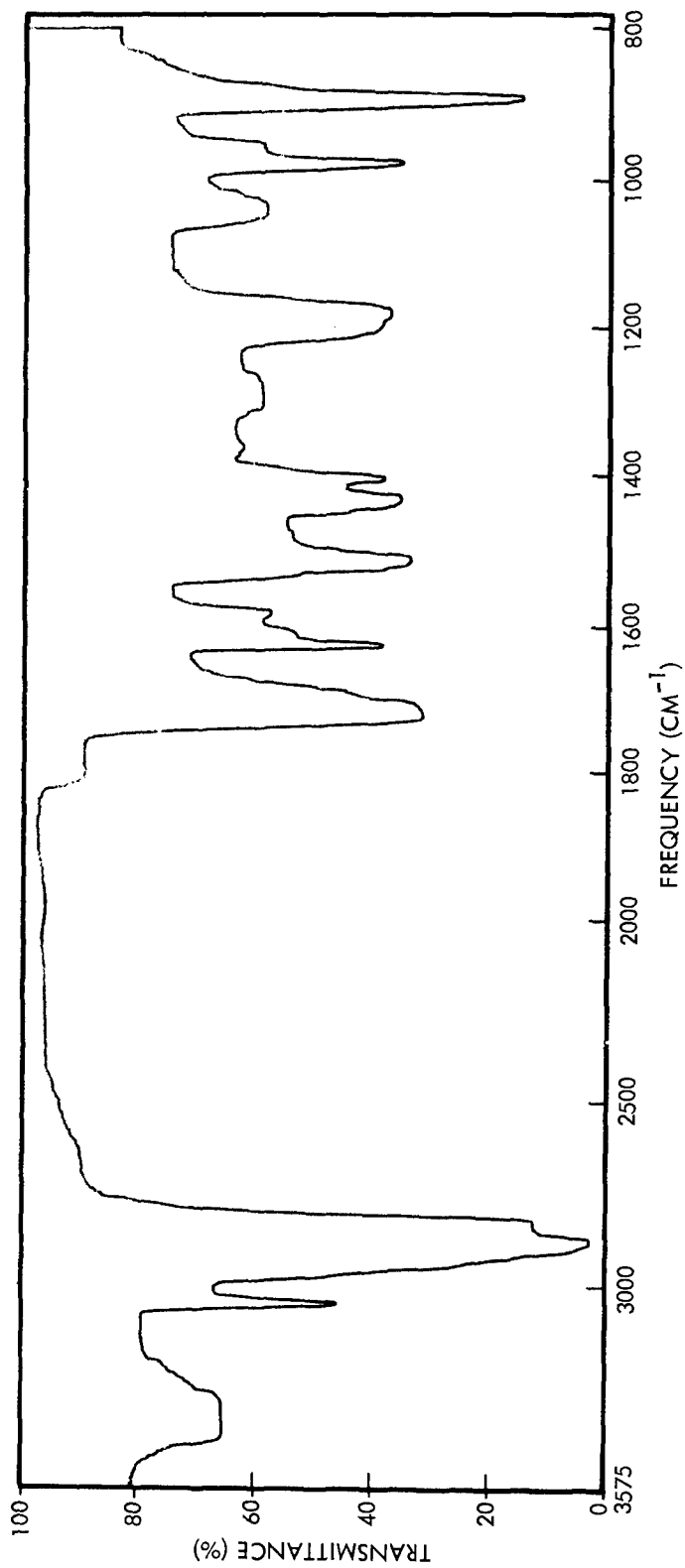


Figure G-3. Infrared Spectrum of Poly (Cyclized 1, 2- Polybutadiene)  
Tolly Urethane Mixture No. 28C

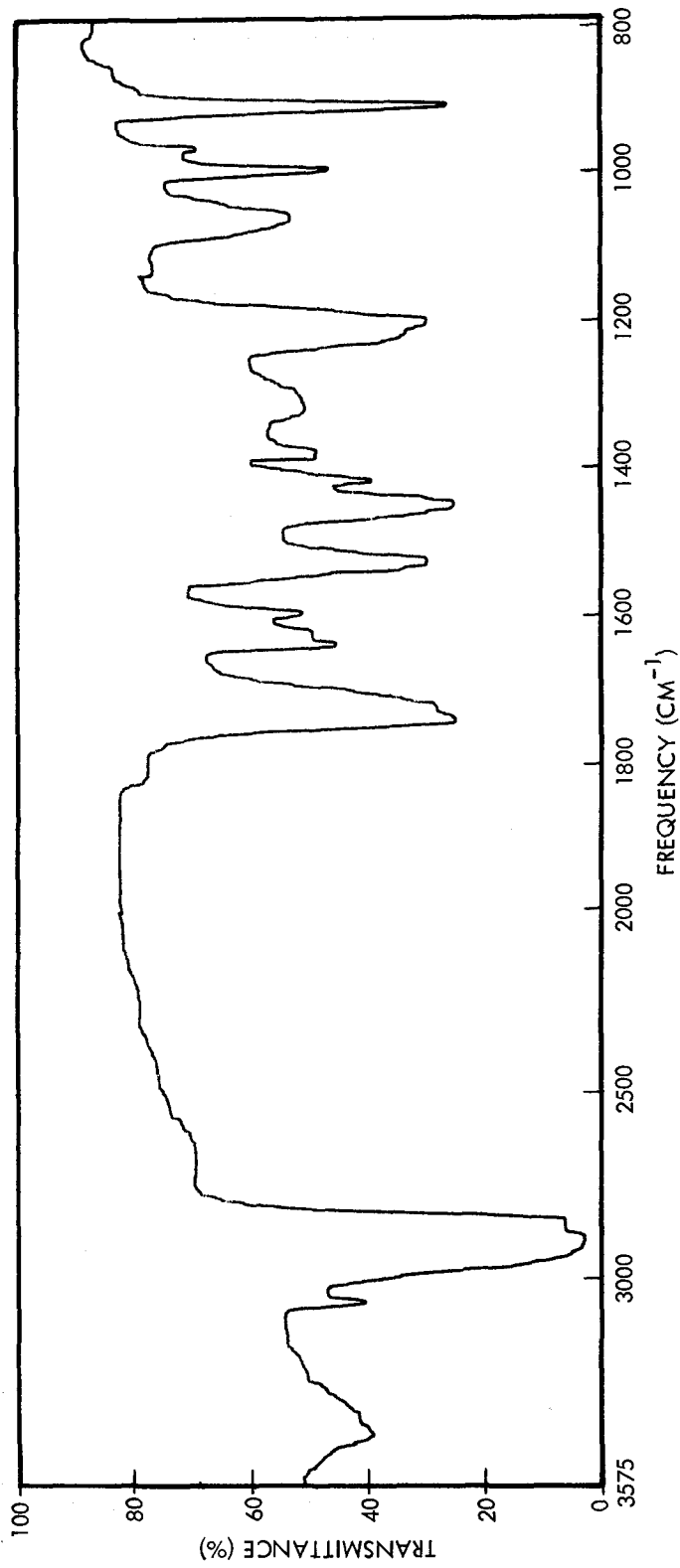


Figure G-4. Infrared Spectrum of Poly (Cyclized 1, 2-Polybutadiene)  
Toly Urethane Mixture No. 25B

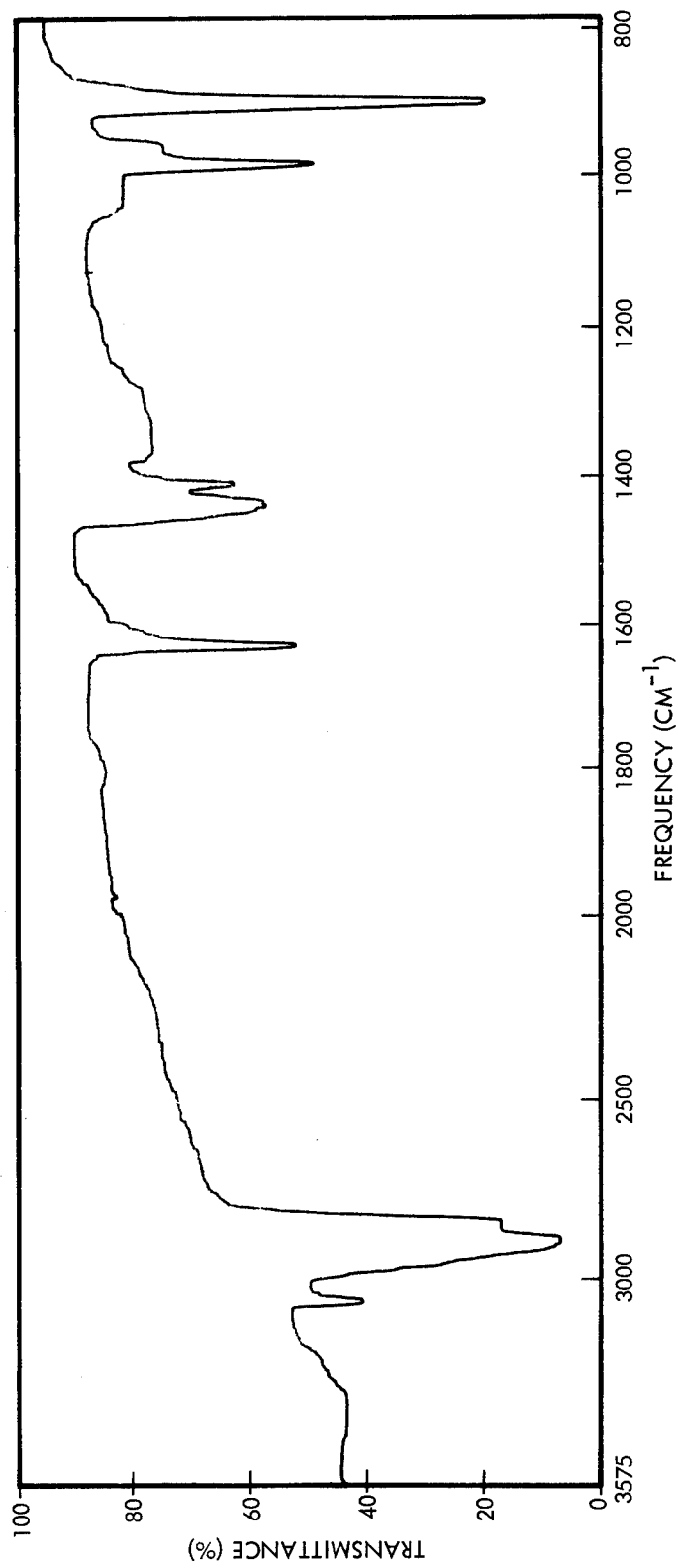


Figure G-5. Infrared Spectrum of Poly (Cyclized 1, 2-Polybutadiene)  
Toluene Mixture No. 18A

The initial concentration of vinyl double bonds in the resin,  $c_r^0$ , is calculated from the dilution of the concentration of vinyl unsaturation in the prepolymer (14.6 meq/g) with the diisocyanate and catalyst.

Calculations of the fraction of vinyl unsaturation remaining,  $c_r/c_r^0$ , after curing the three formulations are listed in Table G-II. From these data it is indicated that the unreacted vinyl unsaturation, which is essentially the same as that expected theoretically (e.g., 14%, see Appendix G.2.6), is attained at a catalyst/prepolymer ratio of 0.02. Also, it is indicated that the presence of the isocyanate promotes the consumption of the vinyl groups. The isocyanate can promote the vinyl reaction through chain extension by increasing the viscosity of the mixture, and hence, reducing the vapor pressure of the catalyst which will permit a larger concentration to remain in the mixture at the curing temperature.

#### G.2.5 Physical Properties of Poly (Cyclized 1,2-Polybutadiene) Tollyl Urethane

The physical properties of poly (cyclized 1,2-polybutadiene) tolyl urethane are given in Table G-III. This polymer is dimensionally stable in vacuum at 400°C (Note: cyclized polybutadiene prepared by Gaylord (Reference 8) was found to be stable at 405°C). The amount of volatiles released by heating poly (cyclized 1,2-polybutadiene) tolyl urethane at 400°C is negligible, and is comparable to that released by commercially available polyimides.

The differential calorimetric scan of this material is shown in Figure G-6. This curve indicates that gross decomposition occurs at 457°C (854°F). The observed gradual endothermic baseline drift after 350°C occurs because of differences between the calorimeter constants of the sample and reference containers. This variation is greatest at the high temperature end of the programmed scan.

Poly (cyclized 1,2-polybutadiene) tolyl urethane is relatively stable in air at 300°C, having a weight loss of only 0.079%/hr. Under the same test conditions, an epoxide prepared from Epon 828 (diglycidyl ether of bisphenol-A) and CPDA (cyclopentane dianhydride) has a weight loss of 2.3%/hr.

Table G-II. Infrared Examination of Vinyl Consumption in Various Poly (Cyclized 1,2-Polybutadiene) Toly Urethane Formulations

Mixture Number	Catalyst/Prepolymer Ratio	(NCO/OH) <sub>o</sub> Ratio	c <sub>r</sub> <sup>o</sup> meq/g	w <sub>r</sub> , mg	A, at 910 cm <sup>-1</sup>	c <sub>r</sub> , meq/g	c <sub>r</sub> /c <sub>r</sub> <sup>o</sup>
28C	0.01	1.19	13.2	2.28	0.900	3.76	0.285
25B	0.02	1.19	13.1	2.60	0.515	1.89	0.144
18A	0.02	0.00	14.3	1.60	0.714	4.25	0.296

Pellet Surface Area = 1.33 cm<sup>2</sup>.

Absorbency Index = 139 ml/meq-cm for 910 cm<sup>-1</sup> vinyl band.

#### G.2.6 Related Work (Literature)

Gaylord, et al (Reference 8) have polymerized butadiene with aluminum triethyl titanium tetrachloride catalyst system at an Al/Ti molar ratio of 0.5 to yield insoluble, powdery polymers which contained absorption peaks similar to those observed in cyclic Balata (trans-1,4-polyisoprene), Hevea (cis-1,4-polyisoprene) and 3,4-polyisoprene. The solid cyclopolymers, having an estimated cyclic structure content that ranges from 60 to 90%, obtained directly from the monomer (butadiene) was found to revert irreversibly to liquids at 405°C. Further cyclization of the cyclopolymers by acid treatment was reported to increase the decomposition temperature.

The extent of the fused sequences of cyclic structure in the polymer chain was presumed to depend upon the number of isotactic or syndiotactic units in sequence, and to be interrupted by the presence of an alternative 1,2, or a cis-, or trans-1,4 unit. The isotactic sequences yield ladder structures containing fused cyclohexane rings (Equation G-9).

Table G-III. Poly (Cyclized 1,2-Polybutadiene) Tollyl Urethane Properties

<u>STRUCTURE:</u>	
Empirical Formula	$C_{84}H_{120}O_2N$
Weight % Carbon	85.9
Weight % Hydrocarbon	96.1
<u>PHYSICAL PROPERTIES:</u>	
Thermal Stability	Stable at 400°C
Differential Scan Calorimetry Decomposition Temperature	457°C
Density	1.02 - 1.09 g/cm <sup>3</sup>
Specific Heat	0.47 cal/g
N <sub>2</sub> O <sub>4</sub> Resistance	Excellent
Stability in Air at 300°C	0.079% weight loss/hour
Hardness	30-40 Barcol
Thermal Conductivity	$7.54 \times 10^{-4}$ cal/cm-sec-°C
F <sub>2</sub> /H <sub>2</sub> Exposure Loss	0.0354 g/cm <sup>2</sup> -sec
<u>PROCESSING FEATURES:</u>	
Viscous Liquid at Room Temperature	
Cure Temperature	90 - 120°C
Catalyzed Reaction	

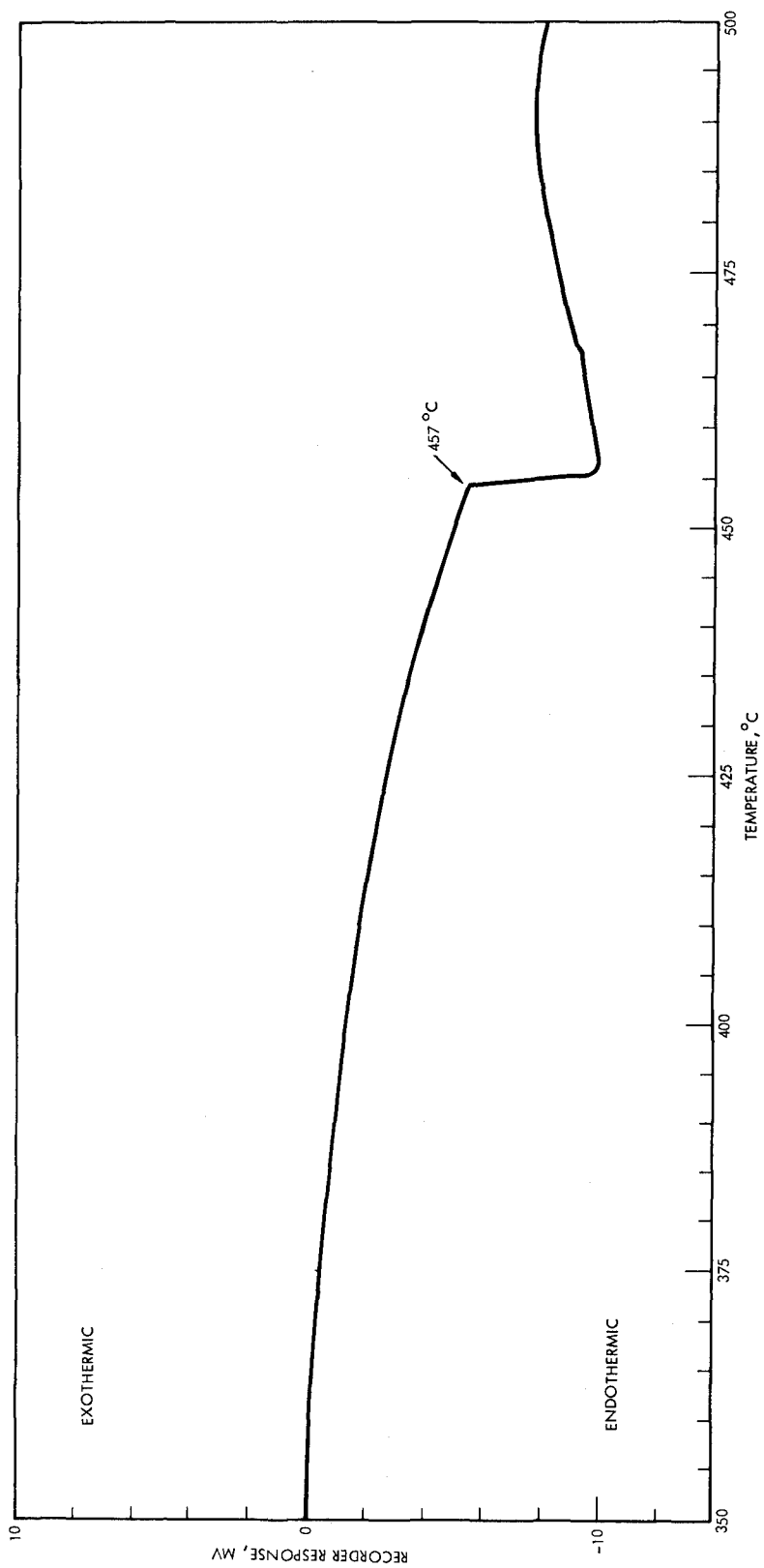
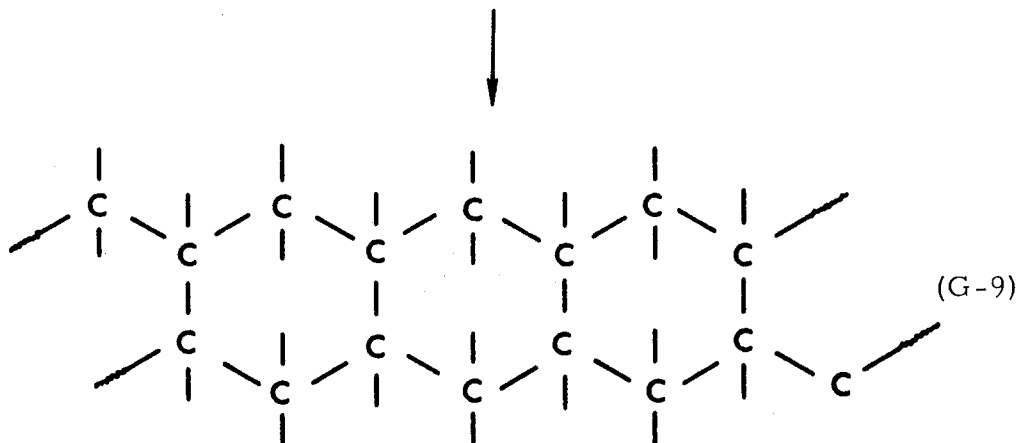
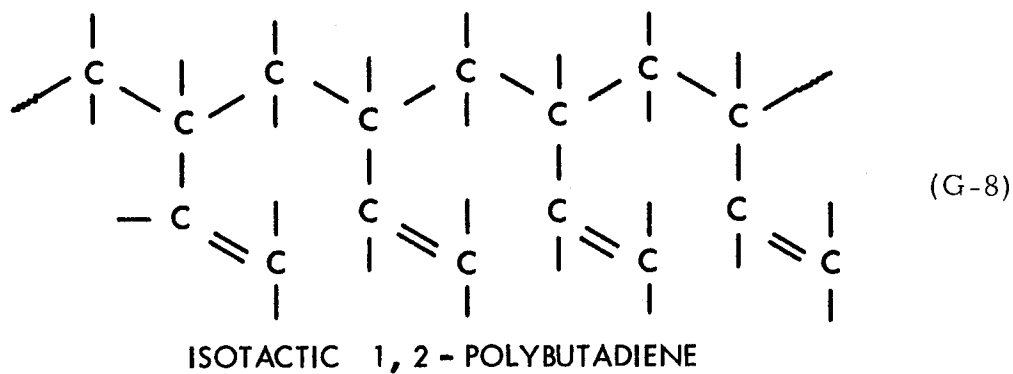


Figure G-6. Differential Calorimetric Scan of Poly  
(Cyclized 1,2-Polybutadiene) Toly1 Urethane



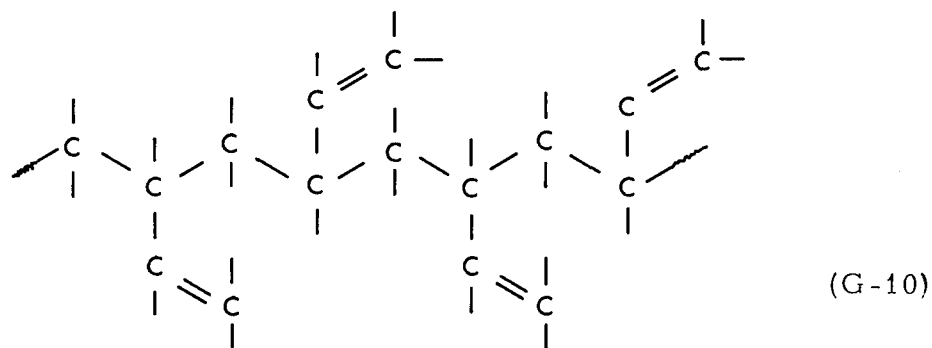
EACH TICK REPRESENTS A HYDROGEN ATOM

The fused cyclohexane rings may exist as one of two isomers wherein the 1, 3 junctures are cis (diaxial) and the 1, 2 junctures are either trans (axial-equatorial), or the 1, 2 junctures are cis.

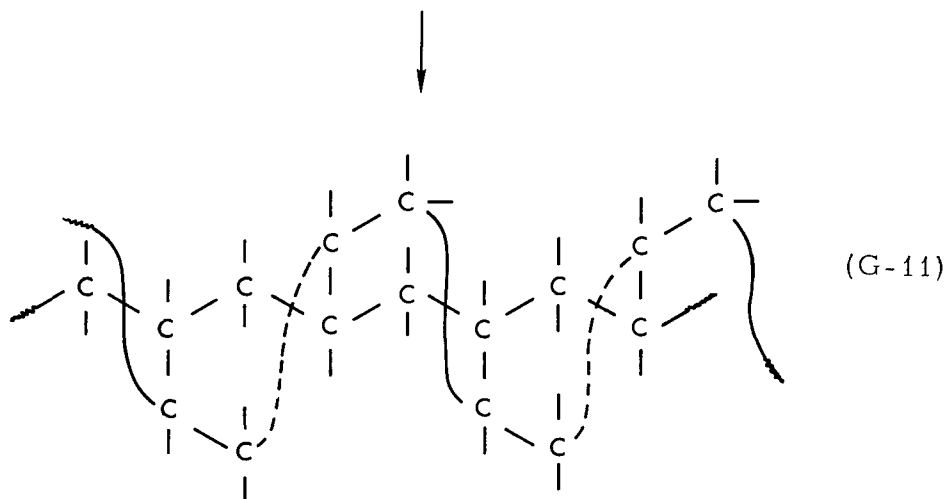
The syndiotactic sequence yields spiral ladder structures containing fused cyclohexane rings in which one chain spirals around the backbone, but is connected to every third carbon (Equation G-11).

The spiral ladder cyclohexane fused ring structure may yield 1, 3-trans-1, 2-cis or 1, 3-trans-1, 2-trans products. Doubt remains, however, as to which of the above possible structures characterize the cyclopolymers prepared by Gaylord.

C. S. Marvel (Reference 9) postulated that the preparations of Gaylord were polymers wherein cyclization was incomplete because of mathematical probabilities associated with cyclization reactions. These probabilities indicate cyclization proceeds to the extent of 86.4% of



SYNDIOTACTIC 1, 2 - POLYBUTADIENE



\*EACH TICK REPRESENTS A HYDROGEN ATOM

the pendant groups. The isolated groups are potential points of cleavage of the polymer. Consequently, the average molecular weight of a cyclized polymer will be about the same, no matter how large a pre-polymer molecule taken.

#### G. 2.7 Mechanism of Peroxide-Catalyzed Cyclization of 1, 2 - Polybutadiene

Cyclization of 1, 2-polybutadiene by peroxide occurs from a free radical mechanism rather than an ionic mechanism. In contrast, cyclized 1, 2-polybutadiene prepared by Gaylord's method, which utilizes the Ziegler catalyst, is formed by a cationic or anionic mechanism - although general agreement exists that Ziegler catalysis is an ionic mechanism, disagreement exists concerning the electrical charge on the growing chain. The important consequence of this difference in mechanism is that the ring closure reaction, which is

homogeneously catalyzed by peroxide, will not be interrupted by alternate stereoconfigurations of vinyl groups. In other words, the free radical mechanism may be considered to be able to cyclize all adjacent vinyl groups even though they may exist in both 'd' and 'l' stereoconfigurations. In contrast, the Ziegler catalyst (due to the heterogeneous nature of its catalytic action) will cyclize vinyl sequences in either the 'd' or 'l' configurations, however, the polymerization will be interrupted by the alternative configurations. Cyclization is expected to be interrupted by the 1, 4 configuration, no matter whether an ionic or free radical mechanism is operating.

The stereoconfiguration of 1, 2-polybutadiene diol investigated in this program is that of an atactic polymer i. e., the vinyl groups are disposed randomly along the chain backbone in 'd' and 'l' configurations. The stereoconfiguration of the cyclized chain, therefore, is complex because of the stereochemistry associated with the closure of isotactic structures (all 'd' or 'l') and syndiotactic structures (alternate 'd' and 'l'). Considering the various stereoconfigurations arising from the closure of each of the above structures, it may not be possible to characterize the final configuration of the cyclized chain. Nevertheless, the most important consequence of cyclization irrespective of structure is that it results in a 'stiff' chain.

In addition to cyclization, it may be reasonable to expect some cross-linking of the polymer molecules. It is believed that the relative amount of cross-linking to that of cyclization will not be significant because reaction with an unreacted vinyl group on a given polymer chain by a free radical on an adjacent polymer chain will not be the most probable event. The more probable event is the reaction of the free radical on the polymer chain with the vinyl group in the immediate vicinity, i. e., the adjacent vinyl groups on the chain, thus favoring cyclization. Nevertheless, some tendency for cross-linking will occur when the free radical has progressed to the end of its polymer chain (see Figure G-1) and therefore must seek out the vinyl groups of other polymer chains for further reaction. Crosslinking from radical abstractions of ~~tertiary~~<sup>ALLYL</sup> hydrogens, although important in the curing of rubber gum stock, is considered to be of minor significance in this case because the preponderance of the unsaturation is vinyl.

### G. 3 POLY ALKALINE EARTH METAL ACRYLATES

The chemistry of poly alkaline earth metal acrylates was investigated in order to prepare hard compact resins suitable for use in ablaters. The specific poly alkaline earth metal acrylates selected for synthesis and evaluation were the magnesium, calcium, and barium salts of poly acrylic acid. The poly alkaline earth metal acrylates have an equivalent oxide content of 24.2, 30.8 and 54.9% for the magnesium, calcium and barium compounds, respectively.

#### G. 3.1 Preparation of Calcium Acrylate

Anhydrous crystalline calcium acrylate was prepared from crude calcium acrylate by the following procedure:

Crude calcium acrylate was prepared by combining calcium carbonate with an aqueous solution of acrylic acid (calcium carbonate 10% equivalent XS), allowing carbon dioxide to evolve, and then heating the mixture. The salt was precipitated from the supernatant with acetone, isolated by filtration, washed with acetone, and dried.

Saturated aqueous solutions of the precipitated calcium acrylate were prepared at 90°C and the salt was crystallized on gradual cooling of the solutions to 0°C. The crystalline salt was isolated by filtration, washed with ice water, and dried under vacuum to constant weight at 90°C.

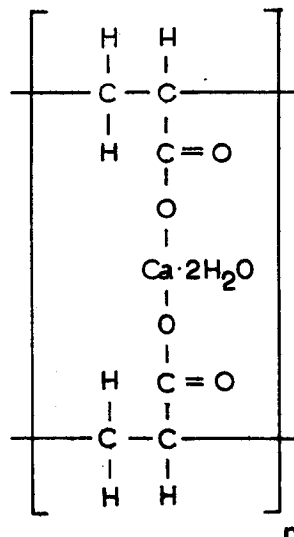
Pyrolysis of the salt at 800°C to constant weight indicated that the material was anhydrous, i. e., the average weight of the ignited residue to weight of sample was 0.305, whereas the gravimetric factor for anhydrous calcium acrylate ( $\text{CaO}/\text{Ca}(\text{C}_3\text{H}_3\text{O}_2)_2$ ) is 0.308.

Drying the calcium acrylate isolated from aqueous solution at 90°C without vacuum yielded the monohydrate, because in this case the average weight of ignited residue to weight of sample ratio was 0.279, whereas the gravimetric factor for the calcium acrylate monohydrate  $\left[ \text{CaO}/\text{Ca}(\text{C}_3\text{H}_3\text{O}_2) \cdot \text{H}_2\text{O} \right]$  is equal to 0.280.

G. 3.2 Polymerization of Calcium Acrylate

Poly-calcium acrylates were prepared by the addition of peroxide catalysts to aqueous solutions of calcium acrylate. Various polymerization conditions were investigated, e. g., catalyst concentration, monomer concentration and temperatures. The best yield of polymer (30%) after a 45-minute reaction period was obtained by adding *t*-butyl perbenzoate (2.0% w/w salt) to a refluxing 2-molal solution of calcium acrylate. The polymer was insoluble and precipitated from solution upon formation. On standing for a few seconds, the precipitate swelled. The swollen particles interlaced to form a continuous gel suspended in the mother liquor. Unreacted calcium acrylate was extracted from the gel by leeching it with distilled water, i. e., the gel was resuspended in distilled water until the aqueous supernatant yielded no precipitate upon addition of phosphoric acid. The gel was then dried to constant weight at 115°C. A chalk-white powder was obtained after grinding the dried gel. When the white powder was dispersed in water it was found to regenerate the gel, thereby showing that the drying procedure did not depolymerize the polymer.

From results obtained by igniting the polymers under the same conditions employed for the analysis of the calcium acrylate, it was possible to deduce that the water/calcium molar ratio in the polymer was two. The experimentally determined residue/sample weight ratio of 0.250 agrees well with the theoretical gravimetric factor of 0.257 of the poly-calcium acrylate dihydrate structure shown below:



(G-12)

The anhydrous polymer was obtained by drying the leached gel to constant weight under vacuum at 90°C. Pyrolysis of the polymer at 800°C to constant weight indicated that the anhydrous material had been prepared, i. e., the average weight of the ignited residue to weight of sample was 0.292, whereas the gravimetric factor for anhydrous poly-calcium acrylate ( $\text{CaO}/\text{Ca}(\text{C}_3\text{H}_3\text{O}_2)_2$ ) is equal to 0.308.

### G. 3.3 Preparation of Poly-Magnesium Acrylate and Poly-Barium Acrylate

Poly-magnesium acrylate and poly-barium acrylate were prepared in the same manner described above for poly-calcium acrylate.

Poly-magnesium acrylate, after drying at 115°C was determined to be the monohydrate. The anhydrous polymer was prepared by heating the monohydrate under vacuum at 90°C or in air at 170°C.

Poly-barium acrylate, after drying at 115°C, was determined to be the dihydrate. The anhydrous polymer was prepared by heating the dihydrate under vacuum at 90°C or in air at 175°C. Pyrolysis of poly-barium acrylate was found to yield barium carbonate in contrast to poly-calcium acrylate and poly-magnesium acrylate which yielded, upon pyrolysis, calcium oxide and magnesium oxide, respectively.

### G. 3.4 Hygroscopic and Physical Properties of Poly Alkaline Earth Acrylates

Poly-magnesium acrylate monohydrate was found to be hygroscopically stable in air. The anhydrous polymer in air increases to constant weight which corresponds to that expected for the formula of the monohydrate.

Calcium acrylate monohydrate was found to be hygroscopically stable in air. The anhydrous salt increased in weight to a value corresponding to that expected for the monohydrate.

Similarly, poly-calcium acrylate dihydrate was stable in air. The anhydrous polymers in air increased in weight until the dihydrate was formed. In the cases of poly-magnesium acrylate and poly-barium acrylate the monohydrate, and the dihydrate, respectively, were found to be the stable form of the polymers in air.

Infrared spectra of the calcium salt of acrylic acid and the polymer of the calcium salt of acrylic acid obtained using the KBr pellet

techniques have provided confirmatory evidence concerning the existence of the polymer.

### G. 3. 5 Preparation of Compact Alkaline Earth Acrylate Resin Specimens

In order to prepare compact resin masses of neat poly alkaline earth metal acrylates it was necessary to press powdered polymers under vacuum at high mechanical pressure and heat. In order to accomplish this task it was necessary to design and fabricate a special hot press die apparatus for use on this program.

The completed apparatus is illustrated schematically in Figure G-7. The hot press die assembly consists of a water-cooled vacuum chamber which contains a support for holding and locating the die, the die itself, ceramic heat shields, and a heater. The ceramic heat shields are standard aluminum oxide discs, and the heater is a Hevi-Duty assembly rated for 1000°C continuous duty. The die and mandrel are fabricated from Inconel in order to 1) minimize scaling during the heat cycle, and 2) provide maximum strength at the sintering temperatures. A bellows assembly is used at the top in order to allow the necessary linear motions for compaction under vacuum.

The operation consists of loading the specimen material into the die, assembly of the top section and die components, evacuating the system and establishing the desired thermal environment. The entire assembly is then placed into a large hydraulic press, and the requisite loading pressure applied. Utilization of the heat shields and the stainless steel standoffs have been incorporated into the design to minimize the thermal sink of the system.

Figures G-8 and G-9 show a view of the interior of the hot press die assembly and the hot press die assembly in the large Research Incorporated hydraulic press together with the associated controlling and monitoring equipment.

The conditions employed in the preparation of the specimens are 15, 000 psi, 350°C temperature and under a vacuum less than one torr. The poly calcium acrylate resin was machined into property determination specimens. The poly magnesium acrylates and poly barium acrylates, however, were not sufficiently tough to permit machining.

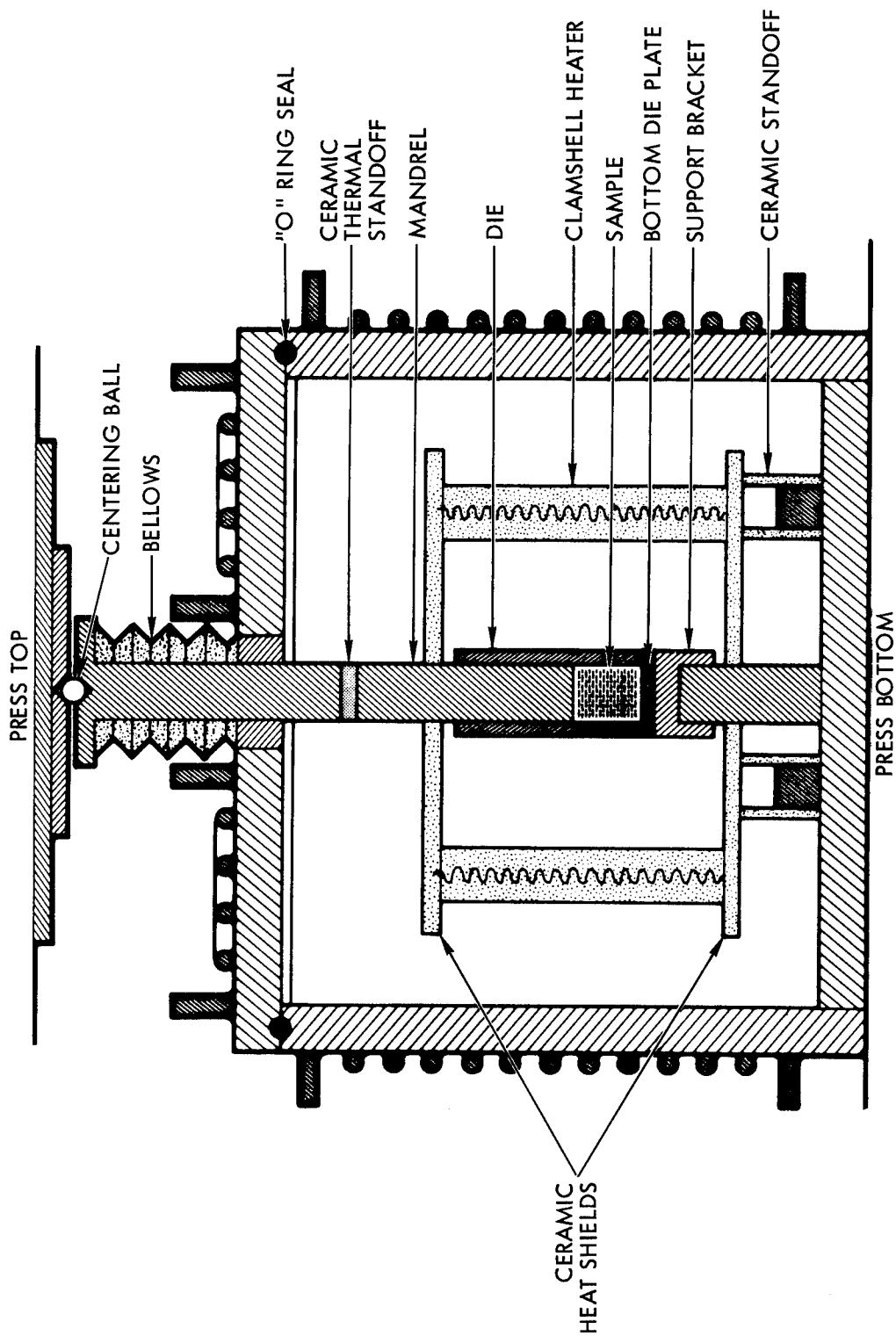


Figure G-7. Schematic Diagram of the Vacuum Hot Press

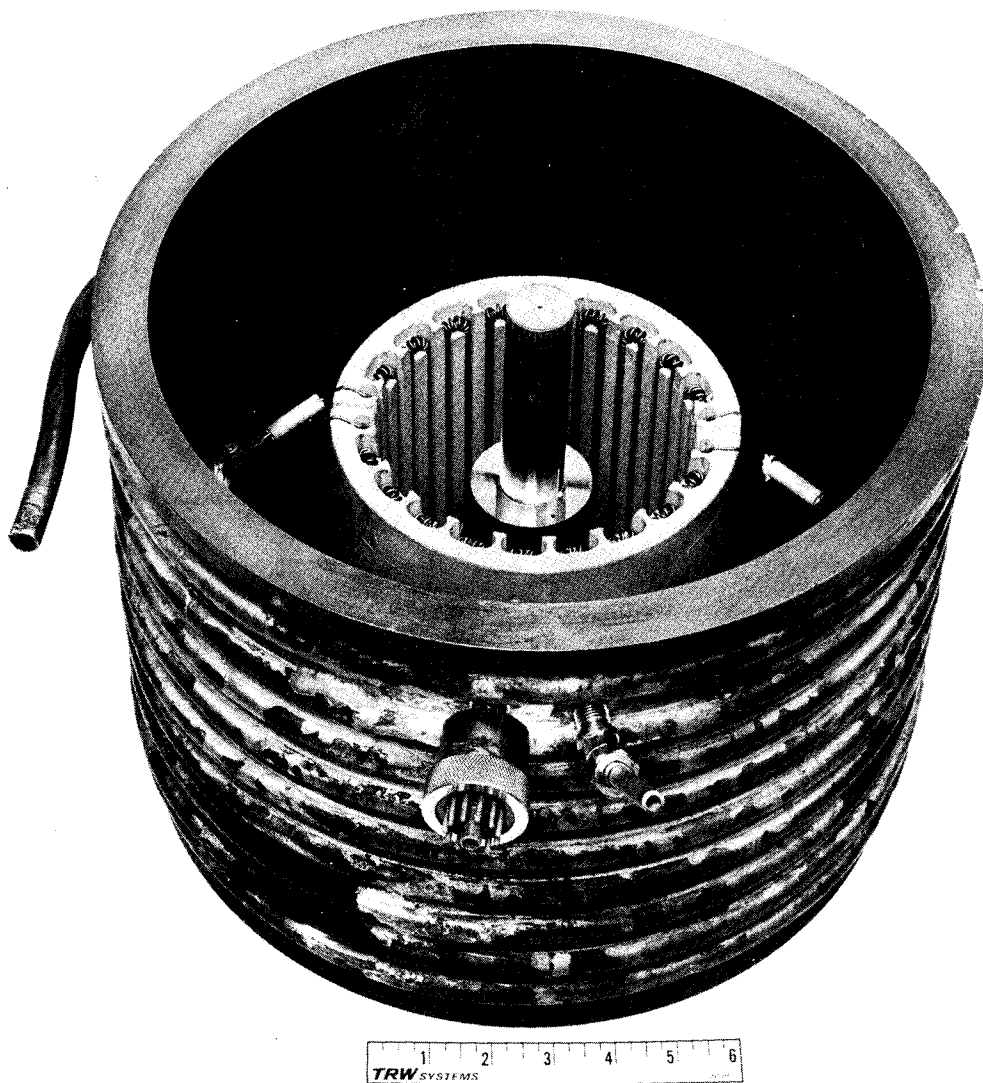


Figure G-8. Interior View of the Hot Press Die Assembly



Figure G-9. Hot Press Die Assembly in the Press and Associated Controlling and Monitoring Equipment

The pressed poly calcium acrylate resin was insensitive to the thermal shock imposed by an oxygen-hydrocarbon and fluorine-hydrogen flame.

#### G.4 PHOSPHATE BONDED OXIDES

Two preparations of phosphate bonded oxides were made according to the procedure of Wehr and Lauchner (Reference 4). A mixture of aluminum oxide, cobalt oxide, and zinc oxide was composed as follows:

$\text{Al}_2\text{O}_3$	225 gms
$\text{Co}_3\text{O}_4$	50 gms
ZnO	5 gms

The composite mixture was ball milled for three hours. Two portions of this composite were mixed with ortho phosphoric acid, at a weight ratio of 50 g to 17 ml. The mixtures were placed in a reaction tube, the tube evacuated, and dry nitrogen gas was introduced into the system. The mixture remained under nitrogen gas for four hours at 300°C. A hard, semi-porous sponge was produced. A screw hammered into the inorganic sponge did not shatter or splinter the material, indicating that the synthesized material had ductility comparable to that found previously (Reference 4).

The sponge was powdered in a ball mill and then screened into several particle size ranges. The ball milling conditions employed gave a 47% yield of -325 mesh powder; however, only 1% was obtained in the -150 to -120 mesh size. To prepare samples of maximum bulk density, a bimodal blend of equal amounts of -325 mesh particles and -150/+170 mesh particles was prepared. The ambient conditions for effective fusing of phosphate bonded oxides was found to be 950°C and 3000 psi. Fusing phosphate bonded oxides at the temperature (650°C) suggested by Wehr and Lauchner (Reference 4) did not yield a compact specimen, but rather a weak and powdery material. Consequently, a study of pressing temperature was undertaken and the 950°C was selected as that at which maximum press deflection occurred.

Fused phosphate bonded oxides were investigated relative to their thermal shock sensitivity. The material cracked when exposed to the



## APPENDIX H PROPERTY DETERMINATION METHODS

In this Appendix are discussions of the property determination methods employed in this program. The properties determined routinely were thermal conductivity, specific heat, decomposition temperature, resistance to a  $F_2/H_2$  flame measured by the Propellant Exhaust Environmental Test (PEET), and density.

### H. 1 THERMAL CONDUCTIVITY

The thermal conductivity of the resins and composite specimens was determined by precise measurement of the temperature gradient across a specimen which was caused by a known heat flow. This measurement was accomplished in the apparatus shown schematically in Figure H-1. The apparatus consisted of a cooled metal plate, main sample heater, guard ring heater, and top heater.

The sample was heated from the top, and the temperature gradient, established across the specimen by the lower temperature of the bottom cooling plate, was determined from thermocouple measurements. The guard and top heaters were operated at the same temperature as the main heater in order to insure that all of the heat from the main heater was applied to the sample. The thermal energy input was calculated from the electrical energy supplied to the main sample heater, and the thermal conductivity was calculated as follows:

$$k = 0.239 \frac{E I \ell}{A \Delta T}$$

where:  $k$  = thermal conductivity in  $\text{cal sec}^{-1} \text{cm}^{-1} \text{deg C}^{-1}$

$E$  = voltage applied to main heater, volts

$I$  = current flow in main heater, amperes

$\ell$  = samples thickness, cm

$A$  = sample area,  $\text{cm}^2$

$\Delta T$  = temperature difference across sample surfaces,  $^{\circ}\text{C}$ .

Figure H-2 shows the thermal conductivity apparatus in position to receive the sample. For convenience in sample preparation, a

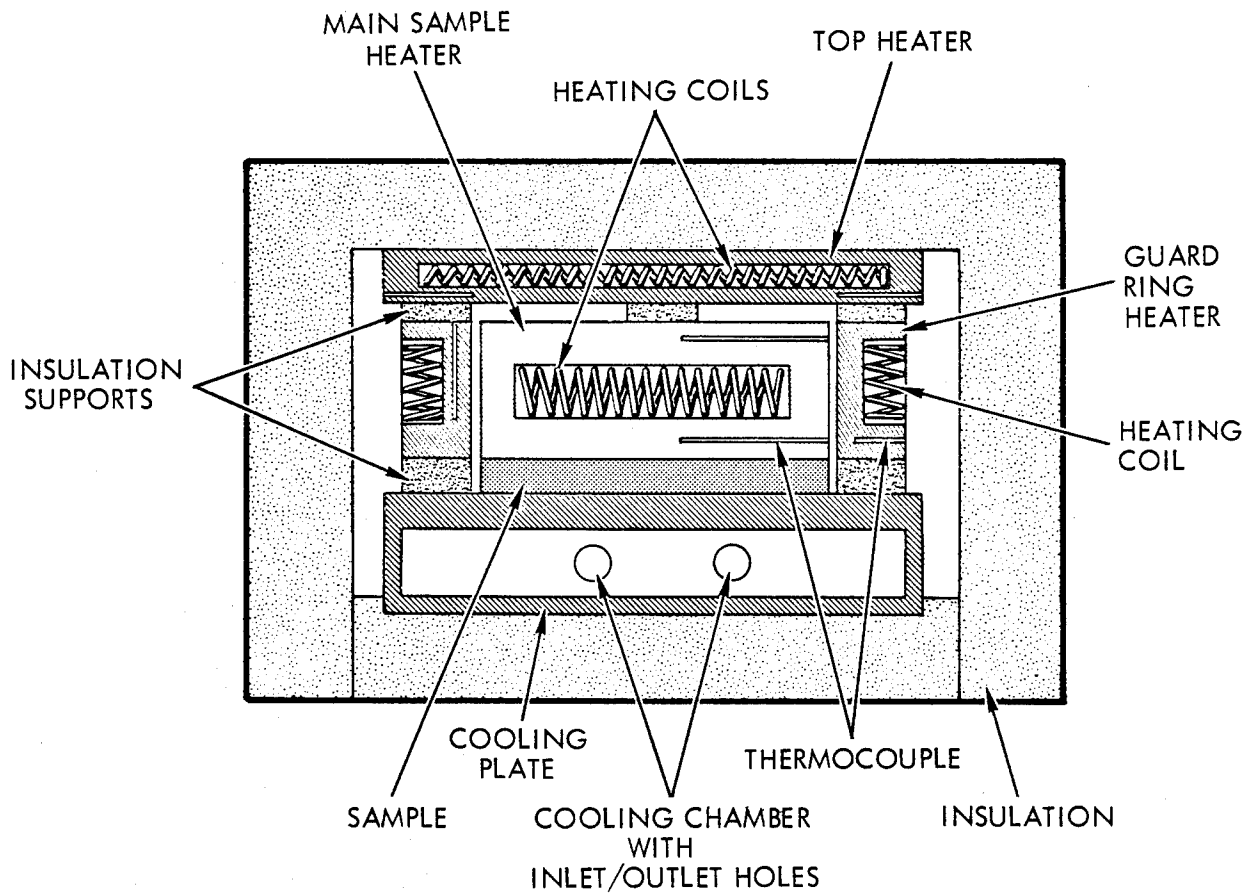


Figure H-1. Schematic Diagram of the Thermal Conductivity Apparatus

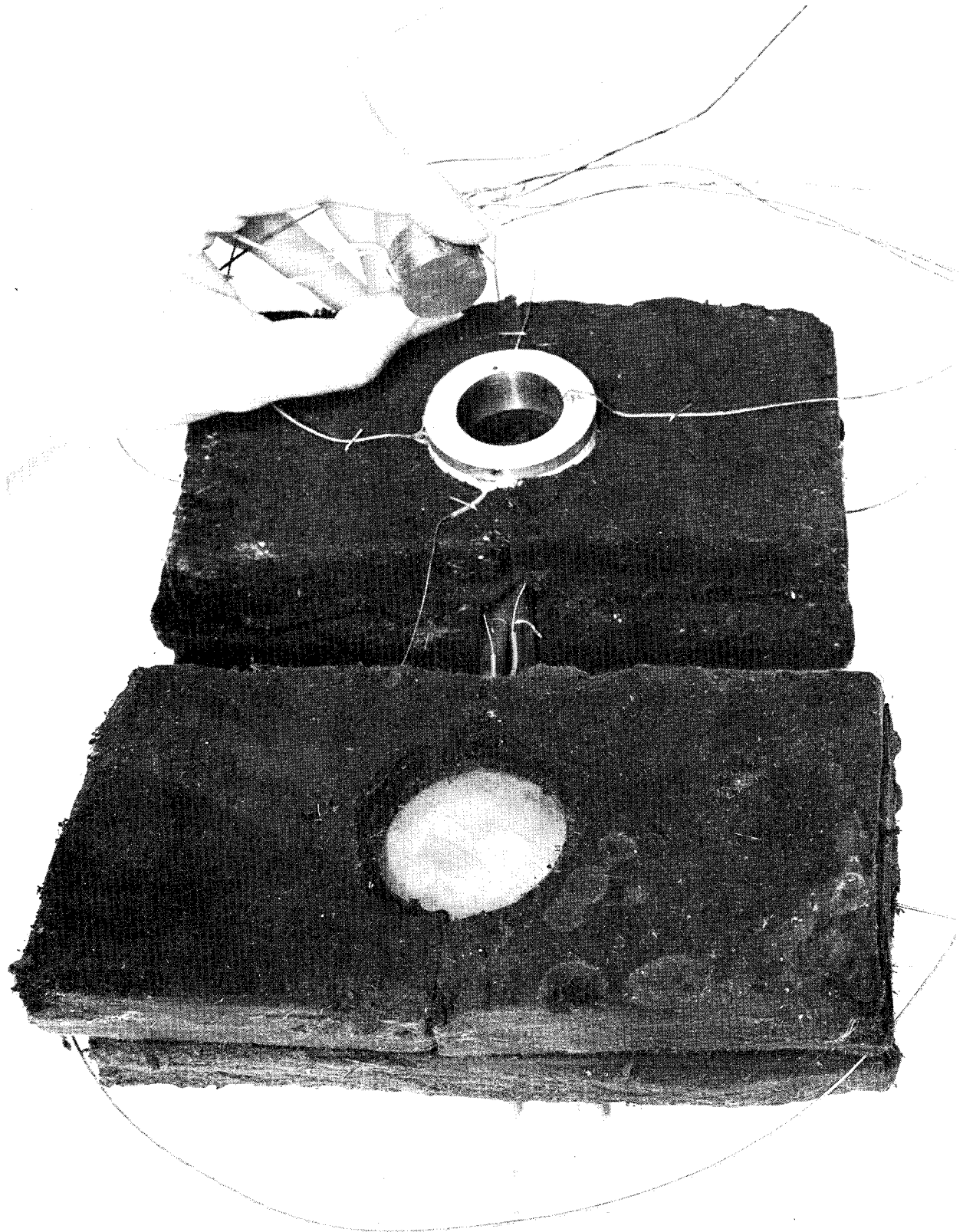


Figure H-2. Thermal Conductivity Apparatus With Top Insulation  
Removed and Main Sample Heater in Hand

cylindrical sample one-half inch thick by one inch in diameter was utilized. The dark material surrounding the device in Figure H-2 is low conductance insulation, Min-K 503 (conductance is  $6 \times 10^{-5}$  cal-sec<sup>-1</sup> cm<sup>-1</sup> °C<sup>-1</sup>, manufactured by Johns Mansville Co.). It was assumed that there was negligible heat loss through the sides of the sample, since the insulation was at least an order of magnitude less conductive than the samples measured. Results of tests made on referee specimens have shown this assumption was valid.

## H. 2 SPECIFIC HEAT

The specific heat of the resins was measured with a Perkin-Elmer Model DSC-1 Differential Scan Calorimeter. This calorimeter provided a rapid and convenient method for the determination of the thermal energy involved in subjecting a sample through a temperature excursion. This excursion could involve the transformation of the material via melting, boiling or decomposition, as well as determination of the specific heat. The operation was as follows:

The DSC-1 as shown in Figure H-3 is programmed to perform a temperature excursion at a desired rate. A sample was placed in one side of a two-container receptacle, which was composed of a heater and temperature sensor for each side. The other side was utilized as a reference cell at the same temperature. By appropriate electronic feedback networks, the increase or decrease in energy required (output of a watt meter) to maintain the equivalent temperature was seen as a displacement on a recording potentiometer. Thus the transition was seen as a peak or valley on the recorded trace. By integrating the area under the curve, the internal energy change of the sample was determined. If the type of transition is known, then the integrated energy (expressed as calories) may be equated to the material per unit weight.

In this manner, the DSC-1 was used to obtain the heat of fusion, heat of formation, heat of decomposition, activation energy, and any other thermal phenomenon which involves the direct measurement of absorbed or evolved thermal energy. For specific heat measurements, the temperature was varied over a small range and the difference in the

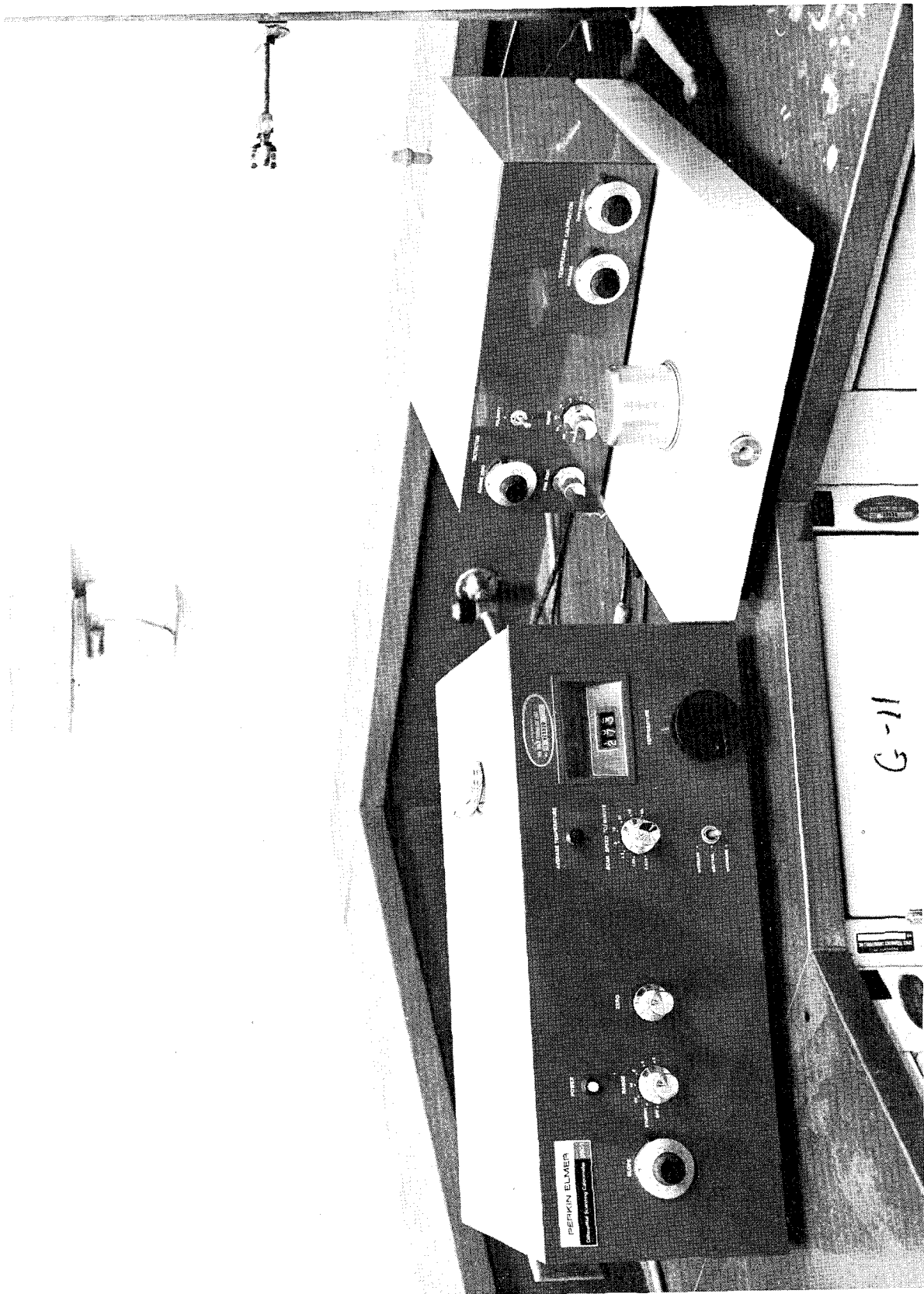


Figure H-3. Perkin-Elmer Model DSC-1 Differential Scan Calorimeter

energy between the sample side and the reference side was measured. The specific heat was calculated readily from the known change in temperature, the mass of the sample, and the calorific energy change.

### H. 3 DECOMPOSITION TEMPERATURE

As described previously, the DSC-1 Differential Scan Calorimeter was capable of determining the endothermic or exothermic energy changes in materials in terms of the energy demand of the sample sensing element. By scanning the entire temperature range (room temperature to 500°C), the thermal history of the sample was obtained. Because the decomposition of a resin was an endothermic reaction, examination of the curve for the final endothermic excursion gives the temperature of decomposition when it falls within the range the instrument. The incipient decomposition temperature was determined as the temperature at which the first indication of significant decomposition occurs.

This method also gives an indication of any other thermal processes occurring prior to the decomposition reaction, e. g., solvent volatilization and secondary curing or rearrangement reactions. A typical example of a decomposition curve obtained with the DSC is shown in Figure G-6 of Appendix G for the candidate poly (cyclized 1, 2 polybutadiene) tolyl urethane resin.

Determination of decomposition temperatures by use of pressure increase in a constant volume chamber was attempted but difficulty in distinction between a true decomposition reaction and one of rearrangement in which the material was still structurally sound, prevented full utilization of this method.

### H. 4 THE PROPELLANT EXHAUST ENVIRONMENTAL TEST (PEET)

The propellant exhaust environmental test (PEET) has been designed to permit preliminary evaluation of the resistance of new candidate ablative resins to exhaust species of advanced propellants such as fluorine-hydrogen propellant combinations. The apparatus, its operation and interpretation are described below.

The experimental arrangement of components for the PEET apparatus is shown in Figure H-4. Shown are the fluorine gas cylinder

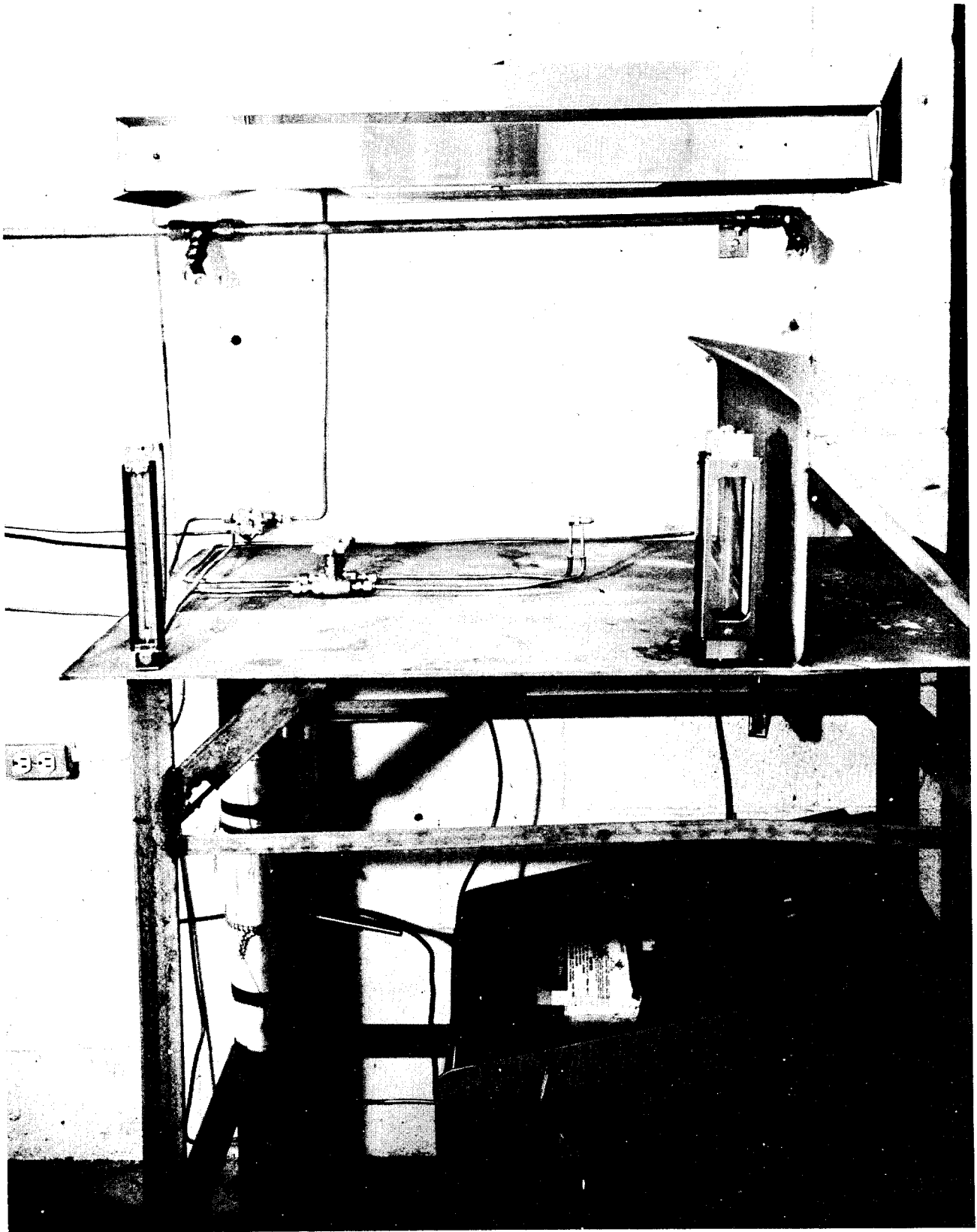


Figure H-4. Propellant Exhaust Environmental Test (PEET) Apparatus

installed in the barracade (lower right), the hydrogen flowmeter (upper left), the HF trap (lower left) and the propellant torch (center of picture). At the top is the stainless steel hood and fire shower heads. The propellant torch assembly is a Beckman Instrument Company flame spectroscopy burner which has been modified in a manner similar to that described by Collier (Reference 10). The modification consisted of incorporation of an internal Monel sleeve to permit a non-reactive, compatible flow of fluorine. Not shown are 1) the hydrogen gas cylinder (located external to the room), 2) the nitrogen purge cylinder (whose lines are seen emerging from the left), 3) the inert atmosphere shield (which provided an argon cover atmosphere to eliminate contamination of the hot combustion products), 4) the argon gas cylinder, and 5) the ablative resin sample holder.

The method of operation for a hydrogen-fluorine exhaust test is as follows:

The HF trap is activated, all the system lines are purged with dry nitrogen, the volume surrounding the sample is purged with argon, and the fluorine flow is started. Then the hydrogen is permitted to flow and the flow rates of the hydrogen and fluorine are adjusted to simulate operational engine mixture ratios. Because the outer gas mantel for laminar flames does not vary appreciably over a large distance (Reference 11), the sample is located so that the flame "mushrooms" and envelopes the face of the sample to insure a relatively constant thermal flux.

Figures H-5 and H-6 show the assembled and disassembled sample holder, respectively. The holder was mounted directly in front of the torch, so that the distance from the torch tip to the sample face was defined precisely. The purge gas (argon) inlet was located to the side, and the long stack was designed to facilitate the discharge of gaseous combustion by-products directly into the exhaust system. The torch projects into the sample cavity, and the area around the torch was sealed with aluminum foil. The required sample geometry was a one-half inch diameter cylinder having a nominal height of one-half inch. A hole was drilled into the sample such that the copper standoff post was one-quarter inch from the front surface of the sample. The sample was inserted in the sample post on the back cover plate (shown in Figure H-6), and the cover plate was installed. This technique

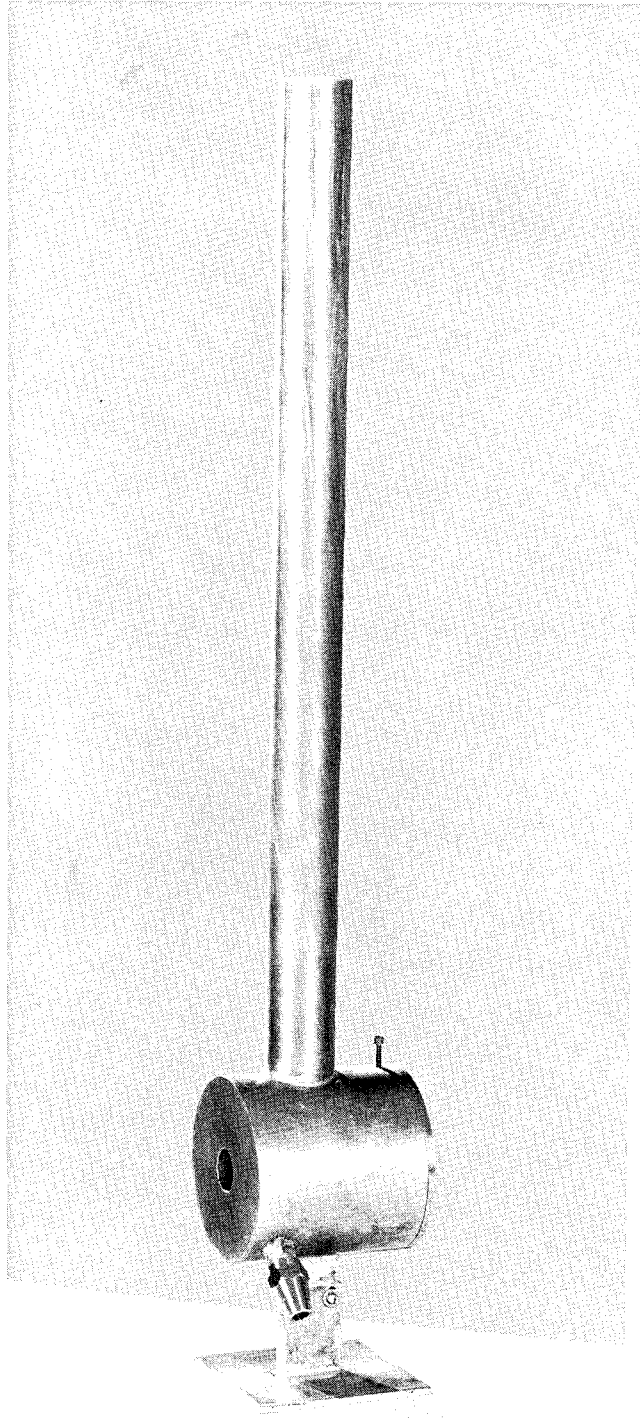


Figure H-5. Assembled PEET Sample Holder and Inert Gas Chamber

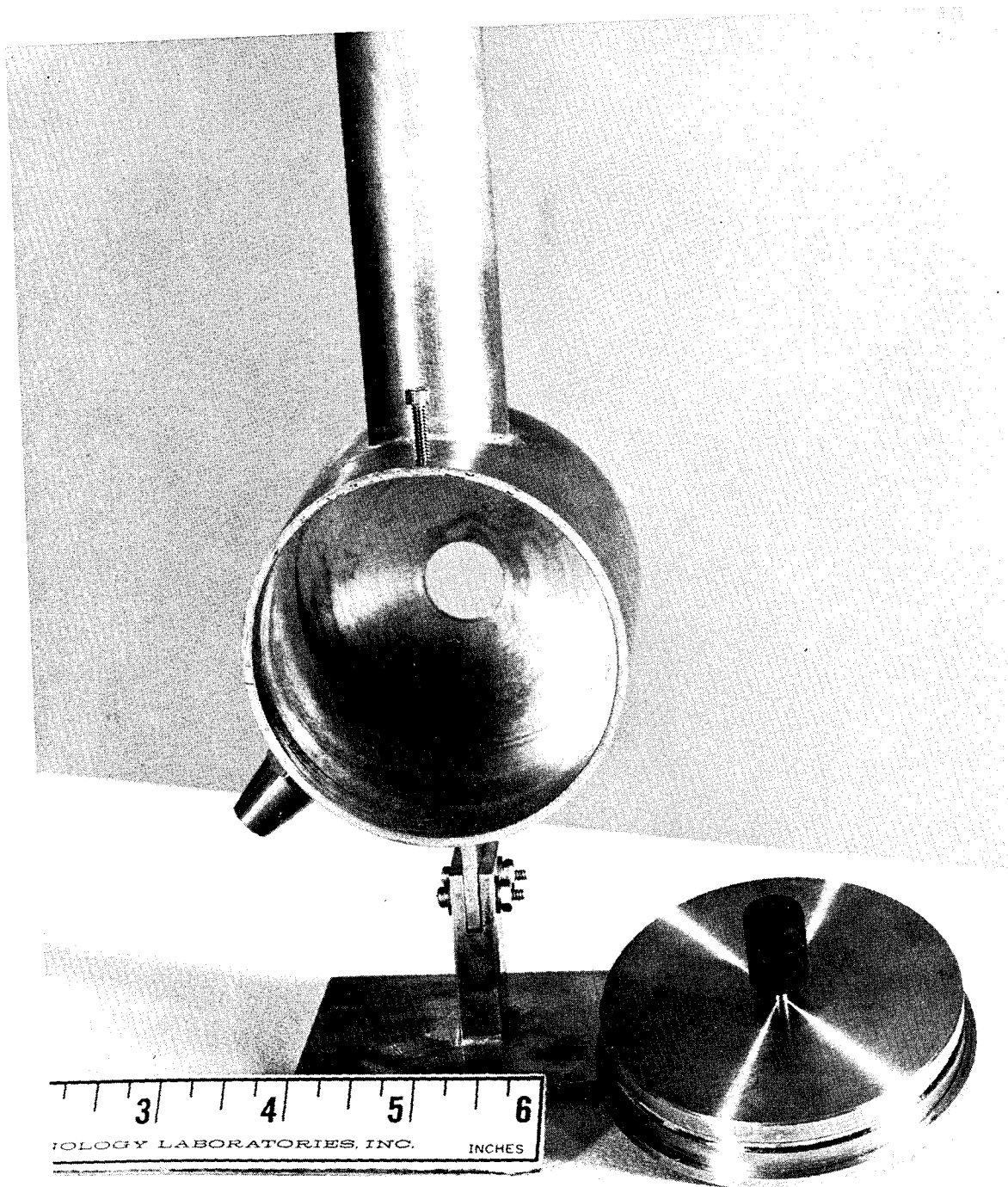


Figure H-6. Disassembled PEET Sample Holder and Inert Gas Chamber Showing a Target Specimen

insured that the face of the sample was always at the same initial distance from the torch tip (one and one-quarter inches).

Table H-I shows the results of a series of  $F_2/H_2$  thermochemical performance calculations obtained using the TRW AP2A Propellant Computer Program. Figure H-7 shows the plot of calculated flame temperature vs. volume mixture ratio. Present state of the art fluorine-hydrogen engines have optimum performance in the 0.5-0.6  $F_2/H_2$  volume ratio, with a potential performance goal of around 0.8. Inasmuch as the direction of engine performance is toward higher  $F_2/H_2$  ratios, it was decided to test the samples near the maximum flame temperature calculated for this system. Thus, the materials were exposed to the extreme hostile environment in the initial tests, in order to obtain an indication of any immediate failure trend, if one exists. All the tests were performed at a volume ratio of 1.0 (3984 °K flame temperature).

**Because of erosion of the nozzle and subsequent change in the impinging flame, test samples of a standard Novalac epoxy resin were included with each run, so that any change in ablation rate arising from a change in nozzle tip could be evaluated. Table H-II shows the variation in weight loss of the reference specimen along with the standard deviation, sample deviation, and percent variation within each population. As can be seen, the populations are distinct and represent true differences in thermal input. Inasmuch as only the thermal input has varied, all the data from the PEET facility is comparable provided the runs are normalized to a common reference rate. The base reference point for the data reported in Section 5.10 was selected as a weight loss of 0.55 g for the standard Novalac epoxy resin, because this loss corresponds to the thermal input of the majority of the tests.**

The measurement of the thermal flux of the fluorine hydrogen torch was obtained using a well-defined copper heat sink having the same surface area dimensions as the normal PEET target sample. The heat sink was mounted on a Transite insulating holder. Two thermocouples were installed within the target near the exposed surface with one centered and the other near the edge. In this manner, the thermal variation across the target was measured. Two targets with

Table H-I. Hydrogen-Fluorine Flame Composition and Temperature as a Function of Volume Composition

Volume Ratio, F <sub>2</sub> /H <sub>2</sub>	Principal Species, Mole Fraction					Flame Temperature, °K
	F	H	H <sub>2</sub>	HF	Total	
0.2	-	0.05	0.62	0.32	0.99	2724
0.4	-	0.20	0.28	0.51	0.99	3319
0.6	0.03	0.27	0.09	0.60	0.99	3694
0.8	0.12	0.24	0.03	0.62	1.01	3911
1.0	0.21	0.18	0.01	0.60	1.00	3984
1.2	0.29	0.13	-	0.58	1.00	3991

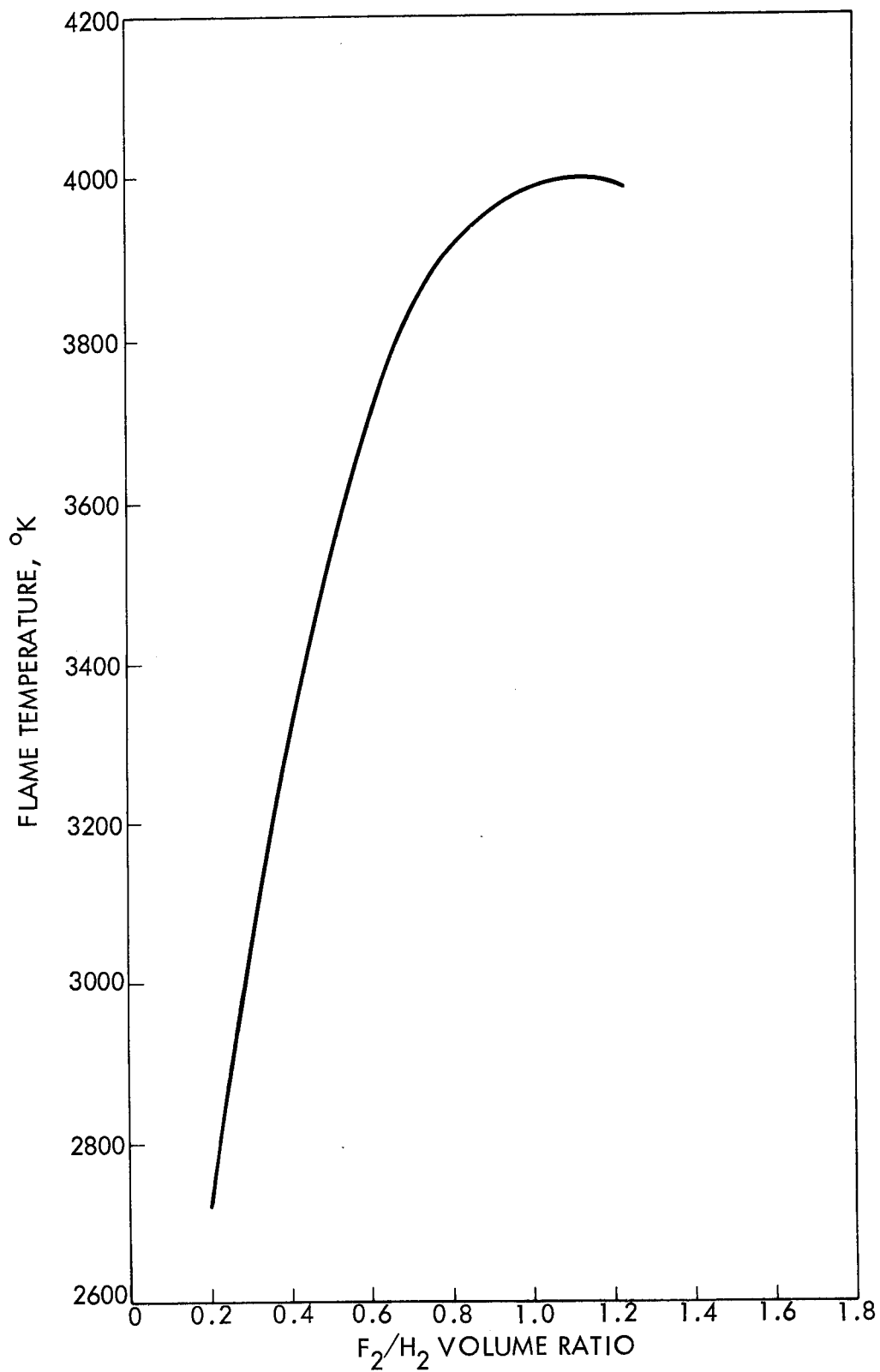


Figure H-7. F<sub>2</sub>/H<sub>2</sub> Flame Temperatures as a Function of Volume Mixture Ratio

Table H-II. Variation of Ablation Parameters in Standard Novalac Resin Samples

Average Weight Loss	Standard Deviation	Range	Percent Standard Deviation
0.55g	0.04g	0.05g	9
0.44g	0.04g	0.05g	9
0.33g	0.03g	0.04g	9

varying mass were used in order to determine whether a significant heat lag occurred in the bulk of the target. The output of the thermocouples was fed into two Bausch and Lomb Model No. VOM5 recorders.

The standard flux measurement procedure was as follows:

The recorders were calibrated, the target was installed in the PEET assembly holder and the F<sub>2</sub>/H<sub>2</sub> torch was initiated using the standard PEET procedure. The temperature rise of the heat sink was monitored visually as it was recorded and when the maximum temperature was observed, the torch was extinguished. The thermal flux of the F<sub>2</sub>/H<sub>2</sub> torch assembly was calculated directly from the rate of temperature rise and the weight and heat capacity of the heat sink. The average thermal flux of the F<sub>2</sub>/H<sub>2</sub> PEET obtained at a volume ratio of 1:1 and a total flow of 8.0 liters/min, gave a temperature rise of 150°F/sec which is equivalent to a flux of 65 BTU/ft<sup>2</sup>-sec.

#### H. 5 DENSITY

The densities of the resins were determined using a Beckman Instruments Company Model 930 Air Comparison Pycnometer. This device measures the volume of solids having almost any geometric or surface configuration. From the mass of the material, together with the determined volume, its density was calculated readily.

A photograph of this apparatus is shown in Figure H-8. The principle of its operation is shown schematically in Figure H-9. The pistons in the sample and reference cylinders are advanced to increase the pressure in both sides of the differential system. When the sample is not present, advancing the pistons to position 2 will not produce a pressure differential between the two chambers. However, when a sample is present, its volume causes an increase higher pressure when both pistons are at position 2. When the sample piston is adjusted to give a zero pressure differential, while the reference piston is at position 2, the sample piston will be located at position 3. In practice, both pistons were advanced keeping a zero pressure differential until the reference piston was situated at position 2. The distance between positions 2 and 3 is proportional to the volume of the sample and when the system was calibrated, the volume was read out directly on a digital counter attached to the linear displacement measuring system. Volumes of irregular solids (in the neighborhood of  $50 \text{ cm}^3$ ) could be determined by this technique with an absolute error of only  $0.1 \text{ cm}^3$ .

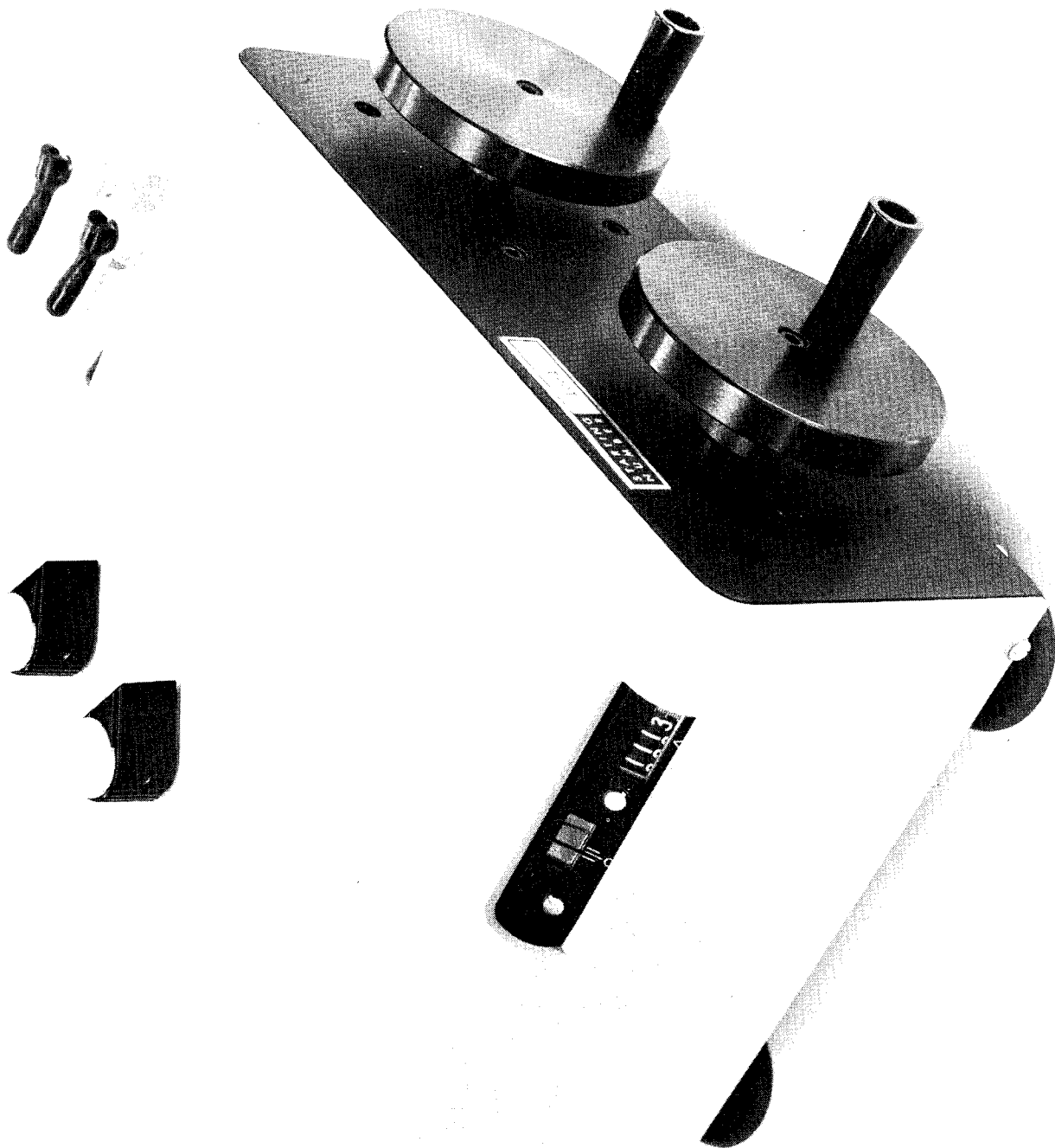


Figure H-8. Beckman Model 930 Air Comparison Pycnometer

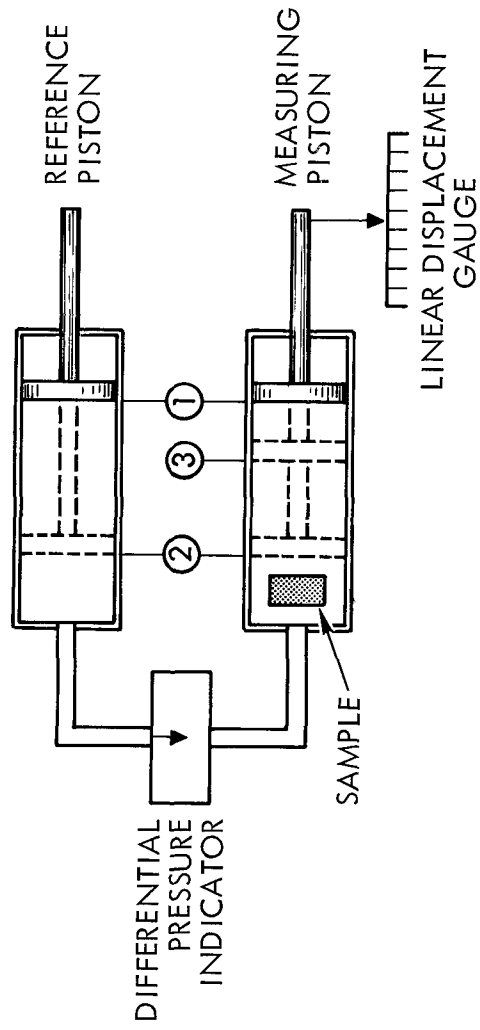


Figure H-9. Principle of Operation of the Air Comparison Pycnometer

APPENDIX I

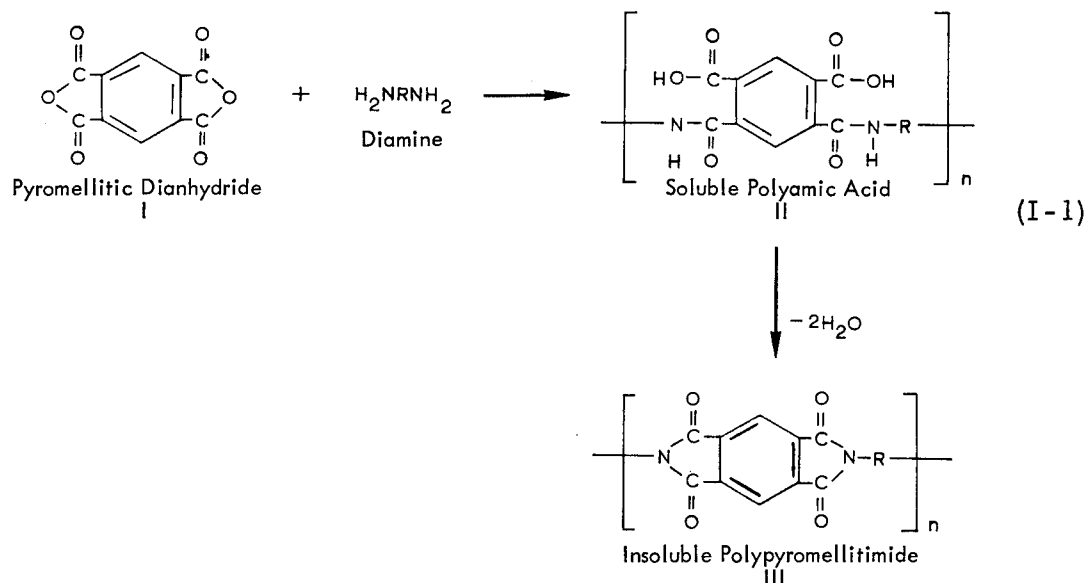
SYNTHESIS ROUTES AND STRUCTURE  
OF SELECTED STIFF POLYMERS

This appendix describes synthesis routes and structures of selected "stiff" polymers which satisfy the parameters presented in Appendix B concerning advanced thermally and dimensionally stable organic resins. Polymeric systems which are discussed include polypyromellitimides (polyimides), polyimide-amide homopolymers, polybenzimidazoles and polyquinoxalines.

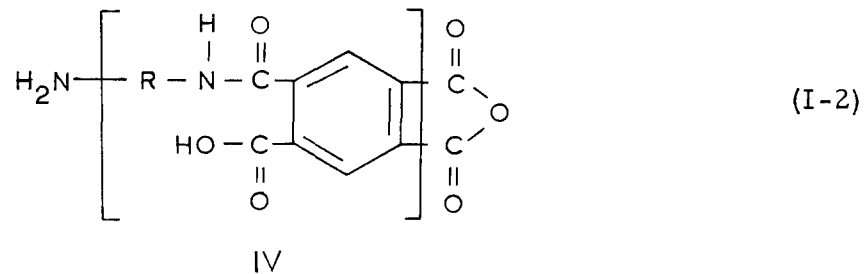
It is interesting to compare the synthesis routes of these polymers with those described for the polyimide esters and ethers (see Section 3.4). The polymers described in this appendix are prepared by the formation of cyclic groups through the elimination of water and/or phenol in intermolecular and/or intramolecular condensation reactions. The polyimide esters and polyimide ethers are prepared by abstraction of hydrogen gas from cyclic groups in the backbone in precursors. Consequently, the polyimide esters and polyimide ethers are expected to have distinct processing advantages over the stiff polymers described here.

I. 1 POLYPYROMELLITIMIDES (POLYIMIDES)

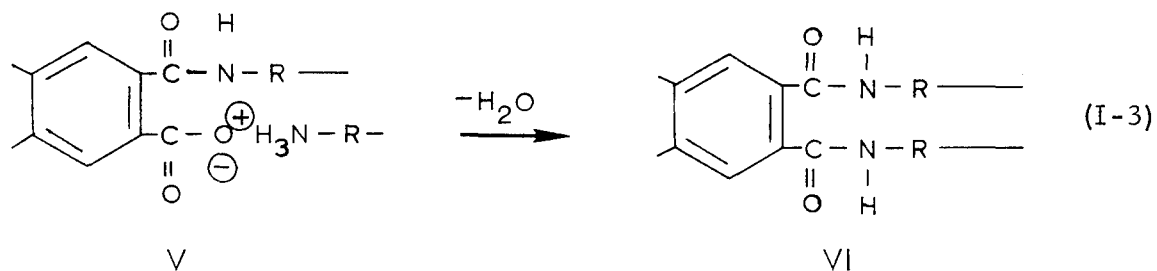
Polypyromellitimides (polyimides) are formed according to reaction (I-1)



Pyromellitic dianhydride is reacted with an equivalent amount of diamine in dimethylformamide to form the soluble polyamic acid. Because it is desirable to prepare high molecular weight polypyromellitimides, the molecular weight of its precursor, polyamic acid, should be as high as possible. As a result, polyamic acid is formed in relatively dilute solutions in order to prevent fractionation of polymer molecules by precipitation. Polyamic acids, however, are hydrolytically sensitive. Consequently, anhydrous conditions must be invoked in order to achieve maximum polymerization. Ideally, infinite molecular weight can be attained with stoichiometric reaction, however, in practice, complete reaction is not realized, and the product may be characterized as follows:



The remaining free amine reacts with the carboxylic acid groups of IV to form a nylon-type salt, V.



The concentration of the nylon-type salt is dependent on the dynamic competition of carboxylic groups and acid anhydride groups for free amine. Because salt formation requires lower activation energy than amide formation, the latter forming through the opening of the anhydride group, higher temperatures favor the amine-anhydride reaction. On the other hand, the increased energy favors disruption of the molecular weight of polyamic acid polymer to lower molecular weight species. Thus, it is apparent that the preparation of polyamic acid of high molecular weight requires careful programming. Refrigeration of polyamic acid solution in storage becomes necessary, and the optimum reaction temperature for its formation and retention of molecular weight must be determined.

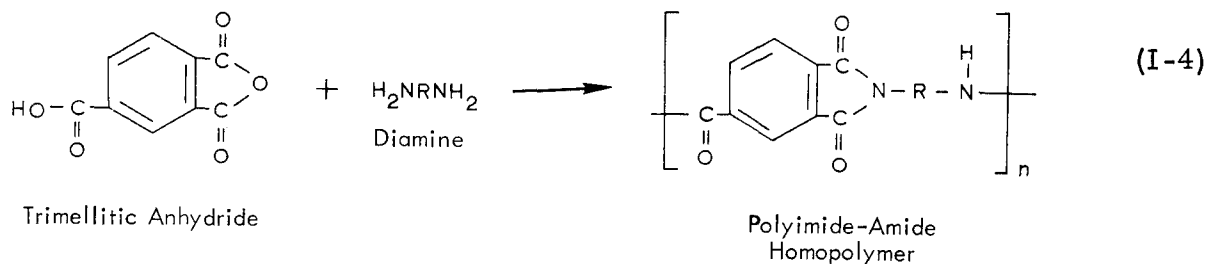
On heating polyamic acid, intermediate VI is obtained in addition to the product III. Intermediate VI can rearrange to yield III by elimination of a free primary amine which, in turn, could react with unreacted anhydride remaining from incomplete reaction in the initial formation of polyamic acid. However, the very viscous resin which results with formation of the polypyromellitimide occurs concurrently with the formation of amide groups through the elimination of water, and it may become a medium in which diffusion of unreacted chemical groups necessary for subsequent reaction becomes exceedingly difficult. In contrast, free carboxyl groups in the polyamic acid chain are fixed in the vicinity of unreacted amide groups, and their reaction with the neighboring unreacted amide groups to form the corresponding imide is not diffusion limited. This fact reinforces the requirement for high molecular weight polyamic acids prior to cyclization to polypyromellitimides.

It becomes apparent that the preparation of polypyromellitimide films must be carefully programmed. The polyamic acid formed in dilute solution (to prevent precipitation of polymer) must be concentrated at relatively low temperatures. During this step, cyclization of polyamic acid to polypyromellitimides must be prevented because the intractable polyimide promotes premature precipitation of the polymer. Films consisting essentially of solvent free, high molecular weight polyamic acid should be obtained prior to cyclization. The film thickness must not be too large to prevent the elimination of water of reaction and remaining solvent. The heating of the film must favor the formation of imides over the formation of amides obtained by the elimination of

water. Diamines employed in the synthesis of polypyromellitimides are listed in Table I-I.

## I. 2 POLYIMIDE-AMIDE HOMOPOLYMERS

Polyimide-amide homopolymers are prepared by the reaction of trimellitic anhydride which contains a carboxyl group and an acid anhydride group with a primary diamine:

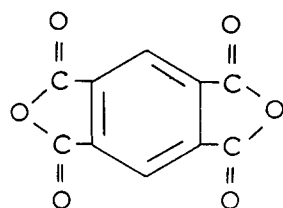


Polyimide-amide homopolymers contain alternating imide and amide chemical linkages in its backbone. In contrast, the copolymers, or interpolymers, have these linkages distributed randomly. Half of the nitrogen atoms in the homopolymer (those in the amide groups) are not in ring configurations, in contrast to polypyromellitimides wherein all the nitrogen atoms are members of heterocyclic rings. Consequently, it may be presumed that the glass transition temperature of the polyimide-amide homopolymer will be less than that of polypyromellitimides because of greater "flexibility" of the backbone of the homopolymer. The resin, therefore, may be more readily processed in laminates than polypyromellitimides (see Appendix J).

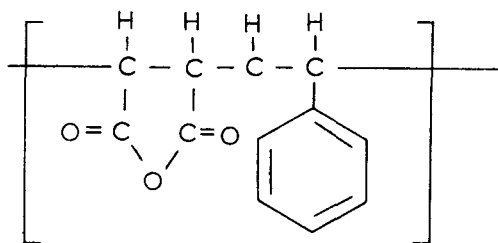
Polyimide-amide homopolymers are of particular interest because the amide linkages of the homopolymer may facilitate its adhesion to glass fabrics, thereby yielding tough laminates. Tenacious adhesion of the homopolymers to fabrics in laminates may greatly increase their resistance to the abrasive action of exhaust gases of rocket motors. The diamines employed in conjunction with trimellitic anhydride for the preparation of polyimide-amide homopolymers are the same as those given in Table I-I for use in the preparation of polypyromellitimides.

Table I-I. Monomers for Polypyromellitimide Preparations

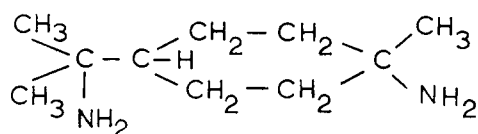
Acid Anhydrides



Pyromellitic Dianhydride

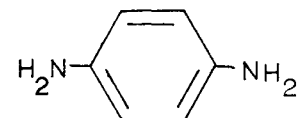


Maleic Anhydride - Styrene  
Copolymer

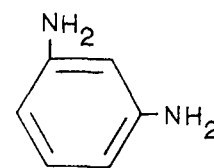


Mentane Diamine

Diamines



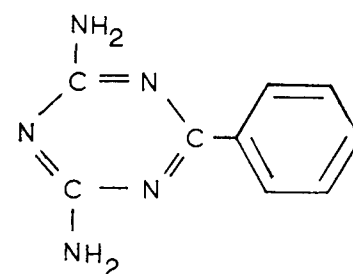
p-Phenylene Diamine



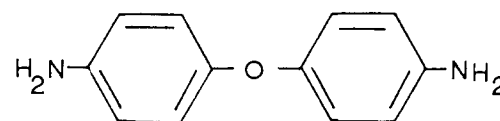
m-Phenylene Diamine



Benzidine



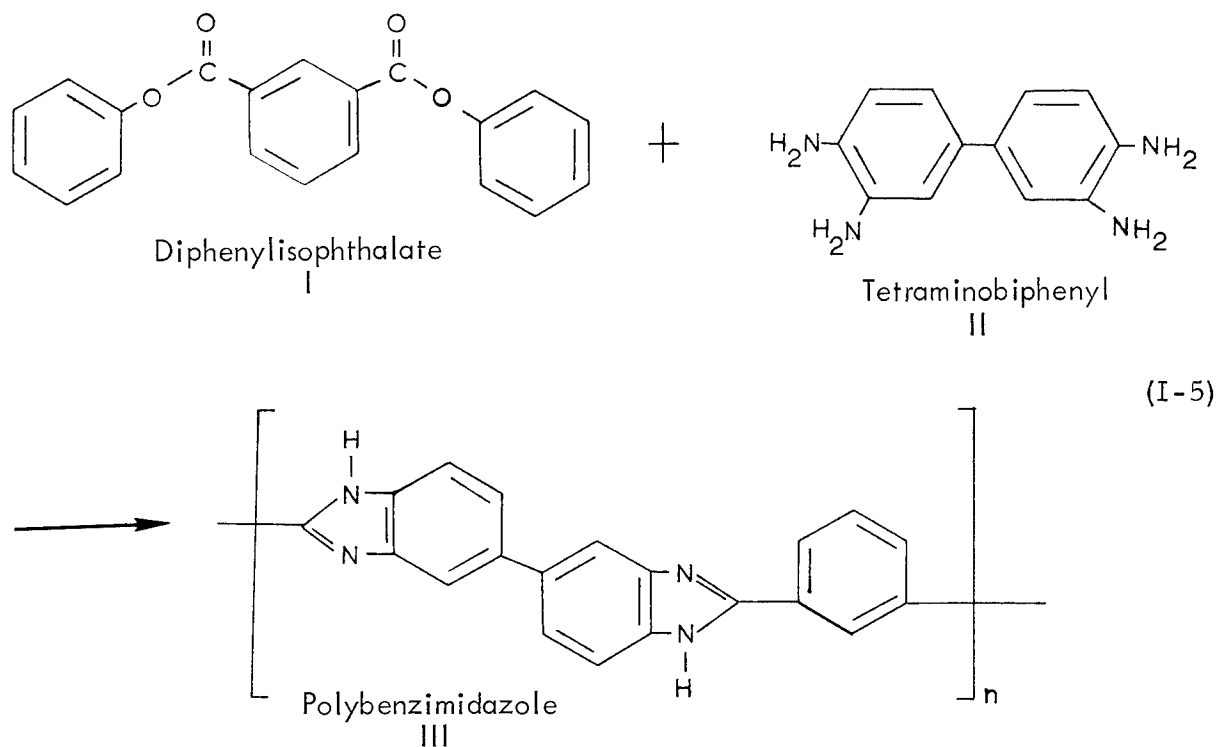
2,4 Diamino-6-Phenyl-s-Triazine



bis (4-Aminophenyl) Ether

### I. 3 POLYBENZIMIDAZOLES

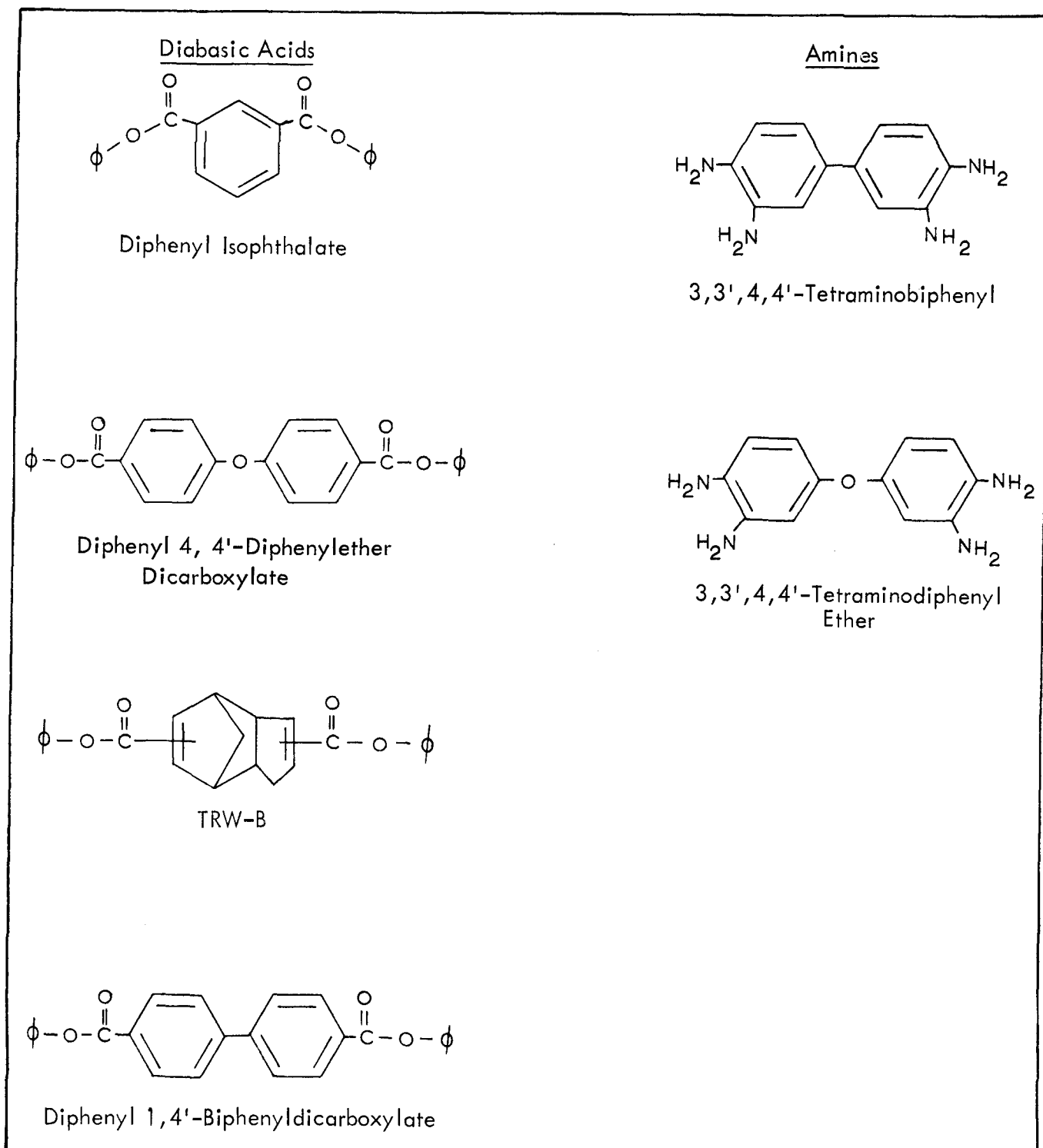
Polybenzimidazoles are made by condensation of a dibasic acid and a tetramine:



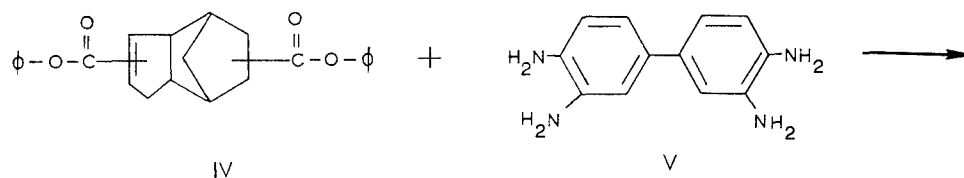
The above-polymer developed by C. S. Marvel (Reference 9) exhibits unusual thermal stability because of its conjugated structure.

Table I-II shows other basic and acidic monomers suitable for the preparation of polybenzimidazoles. All of the resulting polymers may not have backbones wherein all of their chemical double bonds are contiguously conjugated as shown in structure III, thus presumably having lower heat stability (see Section B.1 "Thermal and Oxidative Stability of Polymers"); however, they have other features which make them interesting for investigation, e. g., lower thermal conductivity, easier processing properties, etc. An example of a polybenzimidazole which is not described in the literature and may exhibit high thermal stability combined

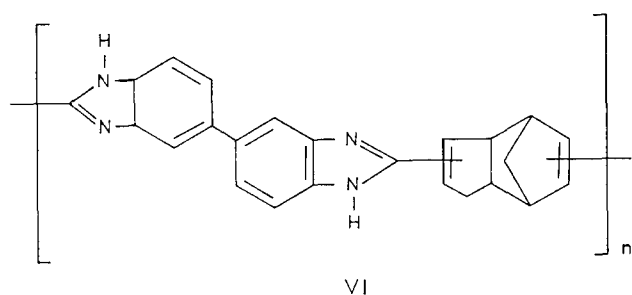
Table I-II. Monomers for Polybenzimidazoles



with low thermal conductivity is the condensation product of the following:



(I-6)

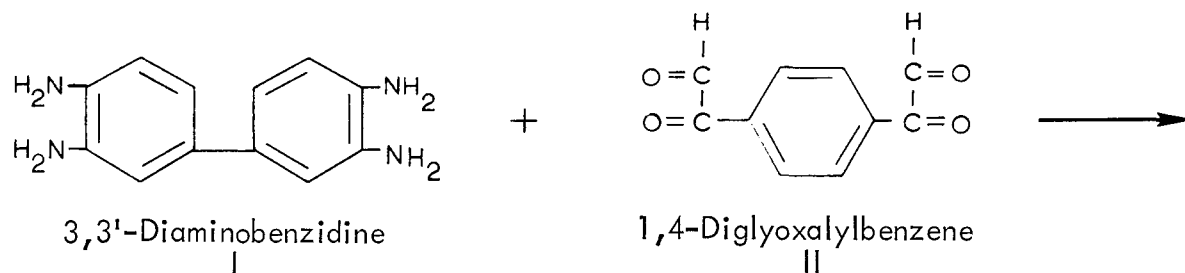


Structure VI, similar to structure III of C. S. Marvel, shows all the double bonds to be conjugated. However, the polymer molecule is not conjugated contiguously because alternating double and single bonds do not characterize the polymer backbone. Single bonds connecting rings in VI, however, are stabilized by conjugation as in III. The remaining single bonds, although unstabilized by conjugation are the components of a condensed ring configuration, thus yielding a grouping of carbon atoms similar to that in thermally stable "ladder" polymers. All single bonds of the polymer are either in the conjugated or "ladder" configuration.

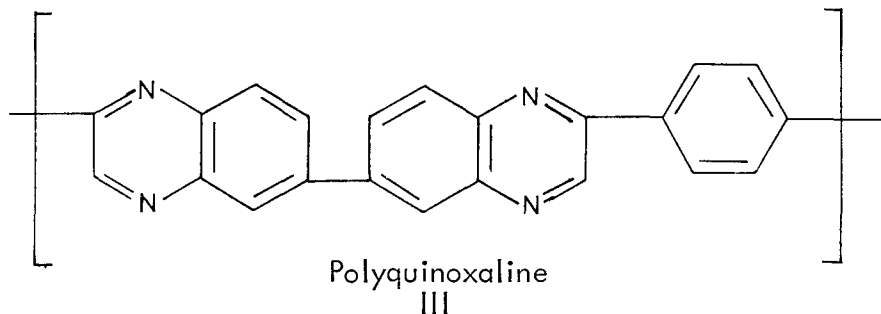
It appears that VI will be stable thermally. However, the thermal conductivity of VI may be less than III, because it does not exhibit the contiguously conjugated backbone - a property which enhances thermal conductivity.

#### I. 4 POLYQUINOXALINES

Polyquinoxalines are prepared by reacting 3, 3'-diaminobenzidine with 1, 4-diglyoxalylbenzene (Equation I-7).



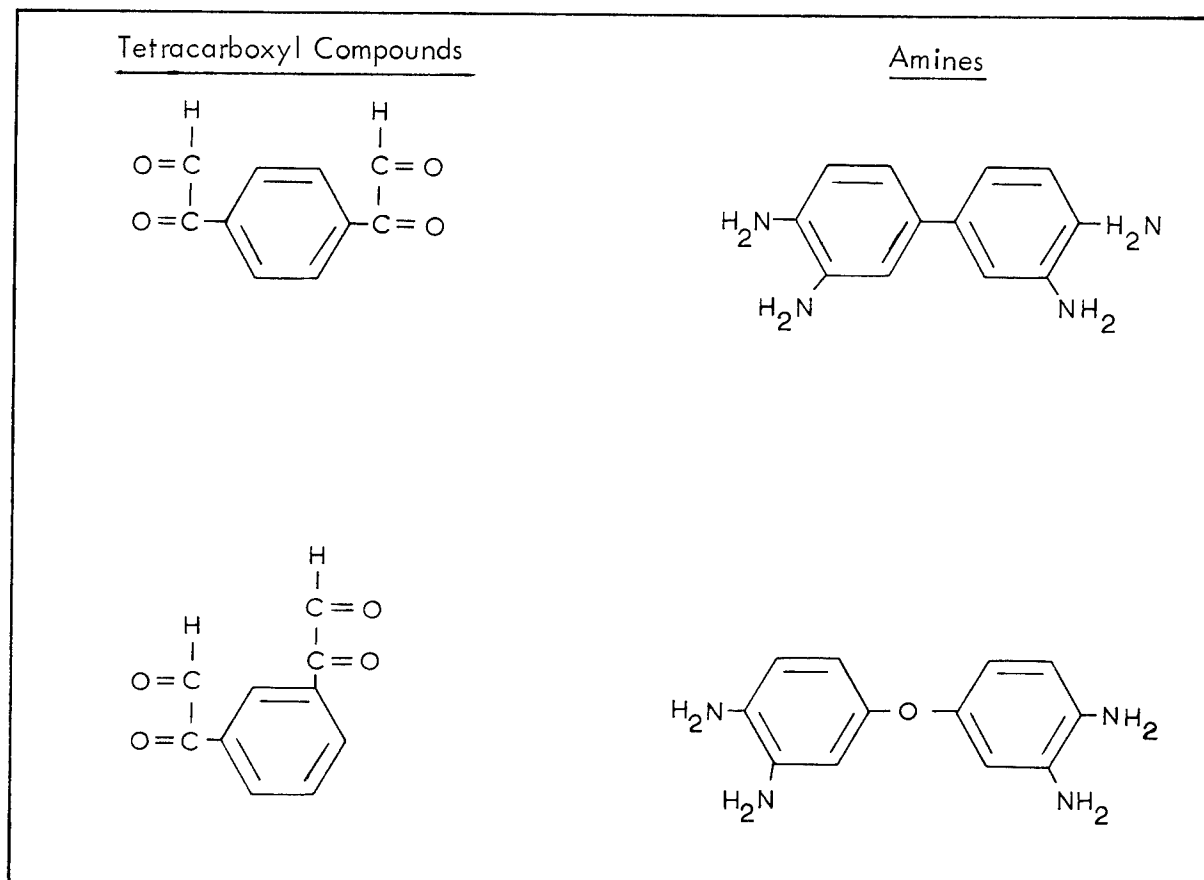
(I-7)



Other starting materials used in the preparation of polyquinoxalines are shown in Table I-III.

Because polyquinoxalines are contiguously conjugated aromatic polymers, they show thermally stable properties similar to polybenzimidazoles. In contrast to the polypyromellitimides, polyimide-amide homopolymers and polybenzimidazoles, where organic or inorganic acid anhydrides are employed in their synthesis, the synthesis of polyquinoxalines requires tetracarboxyl containing compounds as the acidic component. The tetracarboxyl compounds must have their ketone and aldehyde groups in two alpha sets on each side of an aromatic nucleus.

Table I-III. Monomers for Polyquinoxalines



APPENDIX J  
PARAMETERS AFFECTING DRY BONDING ADHESION

This appendix is presented in response to the request to review the parameters which affect adhesion, particularly with respect to employing new heat stable organic polymers, "stiff" polymers, in the fashioning of laminates through the technique of "dry bonding." Because the basis of the lamination process is adhesion, new concepts concerning methods for obtaining improved adhesion are described together with a discussion of the limitations in laminating "stiff" polymers. "Dry bonding" is proposed as a method for the preparation of laminates with "stiff" polymers. The rationale in this section provides the basis for TRW Systems' approach for effecting adhesion between polymers by "dry bonding."

J. 1 APPLICABILITY OF SELECTED POLYMER TYPES TO DRY BONDING

The polymer types selected for evaluation as ablative resins were from the first two of the three general classes of polymers:

- Cross-linked, e.g., phenols, furans, epoxides and melamines;
- Linear with "stiff" backbones, ("stiff" polymers), e.g., polyimides, polybenzimidazoles and polyquinoxalines;
- Linear with 'flexible' backbones, e.g., nylons, polyesters and polyacrylates.

The first class includes most of the current polymers employed as high temperature adhesives. The second class is composed of polymers which were recently introduced to polymer art, and exhibit significantly higher heat distortion temperatures (HDT), stiffness, and 'toughness' than those of the first class. The third class was not preferred because the HDT and "stiffness" of polymers in this class are usually significantly lower than those of the other two classes. In addition, these polymers tend to flow at elevated temperatures.

Representative of the first class of polymers selected for evaluation were epoxide and cyclic 1,2-polybutadiene systems. These systems can be fashioned into laminates by conventional means, e.g., wet lay-ups,

prepregs, etc., because they are fluid at convenient processing temperatures.

From the many candidate 'stiff' polymers, polyimides, and polybenzimidazoles were chosen for evaluation. The polymers are attractive because they exhibit higher HDT's, increased toughness, and greater oxidative stability than that of conventional polymers. Unfortunately, however, the 'stiff' polymers are difficult to use as laminating resins because they are higher melting solids. In this case, the formation of laminates by "dry bonding" becomes attractive. The resin parameters affecting dry bonding are discussed in the following sections.

## J.2 DRY BONDING ADHESION

Candidate ablative resins must be evaluated as adhesives because their composites will not exhibit optimum mechanical strength if "proper" adhesion is not affected between the filler and the resin. Sharpe (Reference 12) and Bikerman (Reference 13) postulate that wetting of the adherend by the adhesive is the overriding parameter affecting the formation of the "proper" adhesive bond. Wetting in general is determined by the relative surface energetics of the adhesive and the adherend. The strength of the "proper" adhesive bond is limited only by the strength of the weakest material.

Wetting, however, is a kinetic effect. As a result, although surface energetics dictate that a particular pair of materials is amenable to bonding in the conventional manner, a strong joint may not always result if the adhesive becomes solid before extensive and proper interfacial contact occurs. Thus, when an adhesive cures too quickly, before intimate interfacial contact is effected, the strength of the adhesive joint will be low since an "improper" adhesive bond is formed. Nevertheless, strong joints are made when the cure temperature promoting rapid solidification of the adhesive is sufficiently high to produce the onset of the macromobile polymer motion (melting) of the adherend. Thus, intimate and extensive interfacial contact is facilitated by motion of adherend molecules.

In addition to macromobile polymer motion, however, micromobile polymer motion in the adherend at the glass transition temperature,  $T_g$ , facilitates wetting, and hence, the formation of strong adhesive joints. The utilization of micromobile polymer motion to facilitate the formation of an adhesive bond is the phenomenon which makes "dry bonding" possible.

The effect of forming adhesive joints at the glass transition temperature and the melting temperature of the adherend upon the strength of the joints was shown by Sharpe and Schonhorn (Reference 14). The results of their work are given in Figures J-1 and J-2. Significantly stronger joint strengths were obtained when the adhesive bond was formed at the melting temperature or at the glass transition temperature of the adherend. Between these temperatures poorer strengths were observed as a result of too rapid cure of the adhesive. The glass transition temperature was the lowest allowable cure temperature for obtaining strong adhesive joints because it facilitated micromobility in the adherend and minimal cure rate. A significant increase in the strength of the adhesive joint occurred at this temperature. At lower temperatures, the "frozen" molecules of the adherend did not readily participate in the wetting phenomenon; although the adhesive cured at a lower rate, solidification occurred before extensive and intimate contact between the adhesive and adherend was effected. This resulted in weak adhesive joints. On the other hand, macromobile polymer motion in the adherend at the melting point yielded strong adhesive bonds despite the rapid curing of the adhesive at the elevated temperature.

"Stiff" polymers cannot be employed as adhesives in the same manner as conventional polymers, because they are high melting solids, rather than fluids at room temperature or moderately high temperatures. Nevertheless, solid polymers effect an adhesive bond at temperatures greater than  $T_g$  of the polymers.

The establishment of  $T_g$  of the polymer as the minimum temperature at which an adhesive bond may be effected with stiff polymers was the result of the work J.H. Freeman, et al (Reference 15). In practice, temperatures 15 to 20°C above the corresponding  $T_g$  value were found to give the most satisfactory results.

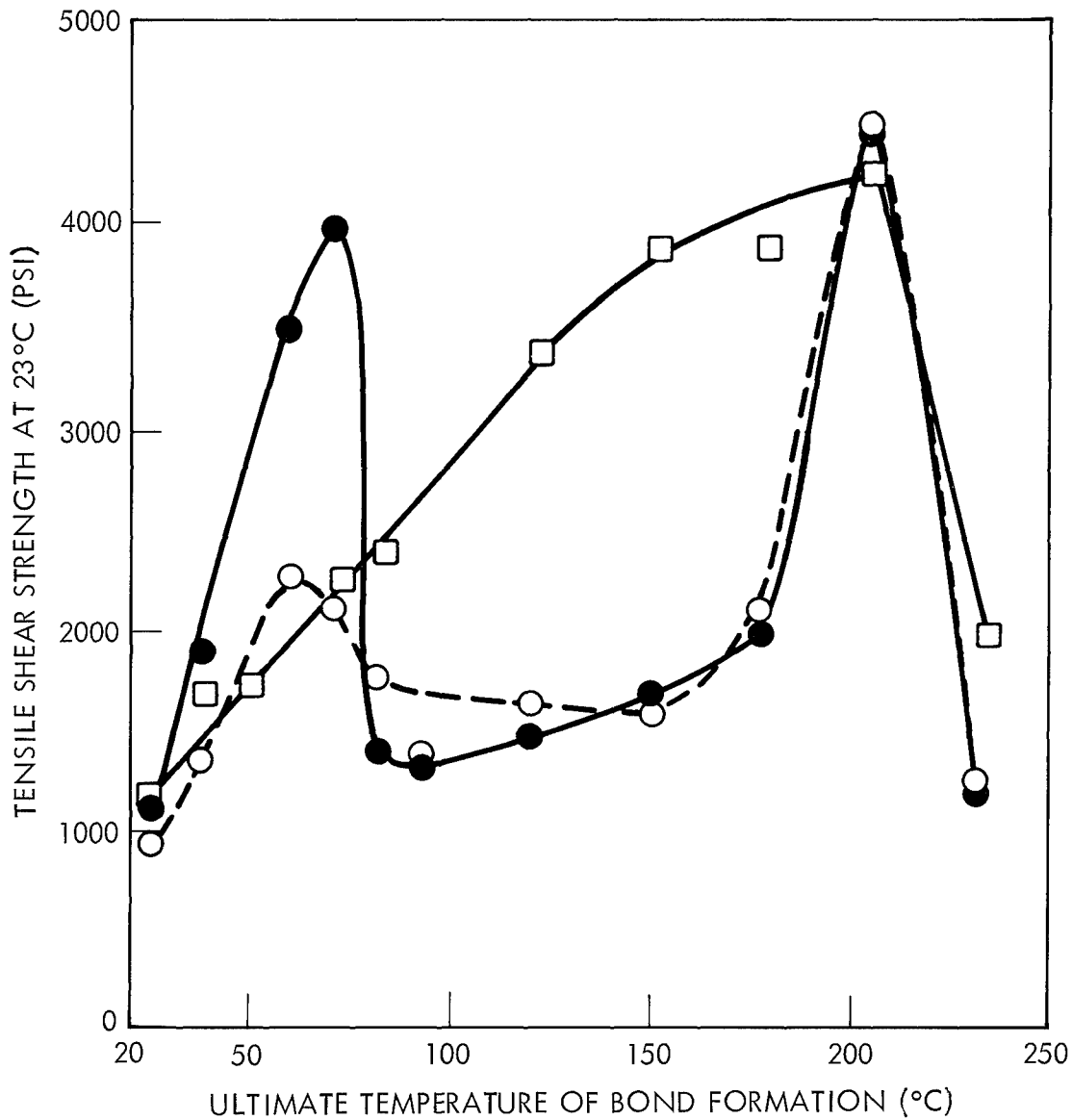


Figure J-1. Dependence of Joint Strength on Temperature of Joint Formation -- (□) Aluminum-epoxy-aluminum composite; (○) Aluminum-epoxy-crystalline chlorotrifluoroethylene-vinylidene fluoride copolymer-epoxy-aluminum composite; (●) Aluminum-epoxy-amorphous chlorotrifluoroethylene-vinylidene fluoride copolymer-epoxy-aluminum composite.

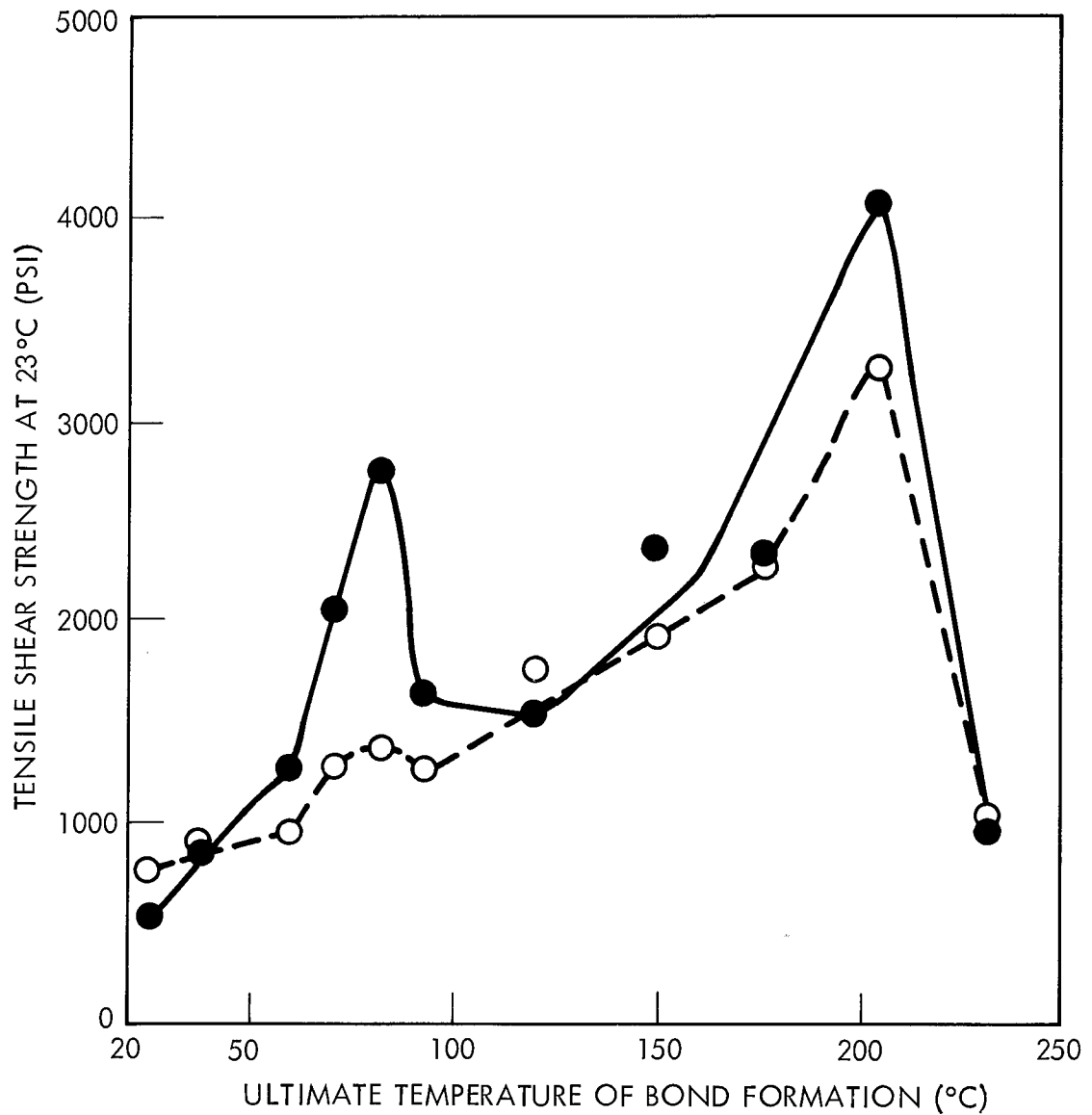


Figure J-2. Dependence of Joint Strength on Temperature of Joint Formation -- (○) Aluminum-epoxy-crystalline chlorotrifluoroethylene homopolymer-epoxy-aluminum composite; (●) Aluminum-epoxy-amorphous chlorotrifluoroethylene homopolymer-epoxy-aluminum composite.

"Stiff" polymers can be modified in order to obtain materials having lower  $T_g$  values so that processing may be expedited. It is apparent, however, that processing is thereby accomplished at the expense of polymer properties because  $T_g$  determines the upper limit of the dimensional stability of the polymer. Nevertheless, this approach is employed in the preparation of composites with "stiff" polymers. Solutions of precursors of "stiff" polymers are employed to wet the adherend. The solvent is evaporated, and the remaining solid is "dead" cured upon the surface of the adherend. The adherends are bonded to each other through this process, which is termed "dry bonding."

In practice, however, this approach is often compromised in the hope of obtaining resin matrices in the composite with heat distortion temperatures greater than the processing temperatures. The compromise involves volatilization of some solvent and/or advancing partially formed polymers upon extended heating of the composite in the mold. The escape of volatiles may result in voids in the composite however, thereby reducing the strength of the composition. The method for preparing suitable composites is determined by carrying out a systematic exploratory program pertaining to the particular resin under study.

### J.3 DRY BONDING: A PRACTICAL APPROACH TO LAMINATING WITH "STIFF" POLYMERS

The shortcomings of aromatic, heat-stable polymers ("stiff" polymers) as laminating resins lie in the difficulty to fashion these polymers into a so-called "B" stage, the formable intermediate which permits processing of the laminate. Polymers like polypyromellitimides, polybenzimidazoles, and polyquinoxalines, which are thermally stable at temperatures higher than 700°C, 650°C, and 800°C, respectively, present unusual laminating problems because the temperatures at which these materials exhibit formable character necessary for laminating (macromobile and micromobile polymer motion) are prohibitively high.

Some "stiff" polymers are not soluble in solvents that can be handled conveniently in laminating. The polypyromellitimides, for example, are difficult resins in laminating because of their insolubility in suitable volatile solvents. Only fuming nitric acid has been found to be a general solvent for polypyromellitimides as a group, while

concentrated sulfuric acid is effective for some (Reference 16). Although the precursors of polypyromellitimides, polyamic acids, are solvent soluble, thus providing a probable "B" stage, they also are unsuitable for laminating uses. The formation of polypyromellitimides from polyamic acids occur with the liberation of water of reaction which, in turn, cannot be readily removed from the resin masses or laminates. Our attempts to prepare a thick mass of polypyromellitimides by casting film upon film (i. e., casting a film, evaporating the solvent, curing, and then repeating the process), were not successful. Instead of a homogeneous mass of plastic, layers of plastic film were obtained which easily peeled apart.

Polybenzimidazoles, in contrast to polypyromellitimides can be dissolved as "finished" polymers into volatile solvents, e. g., dimethylformamide. Although a thick mass of plastic can be made by casting film on film, the absorption of solvent into the solvent-free precast film, in effect, makes the process similar to concentrating the polymer solution by evaporation. In laminating, the removal of residual solvent from the laminate becomes a difficult problem.

If low molecular polymer is employed to hot-melt coat the fabric of the laminate, then the laminating temperature must be high and applied for an extended period of time in order to complete the polymer-forming condensation reaction. Condensation reactions of low molecular weight polymers yield volatile compounds which are unable to escape from the intractable resin mass, and therefore, must be constrained and molecularly dispersed through the laminate by application of high pressures in order to prevent porosity. Similar problems arise when solvent remains in resin coated fabrics and removal of residual solvent from the laminate is attempted.

Although "stiff" polymers are intractable, particularly to laminating techniques, in contrast, their formation into films and coatings can be accomplished with relative ease. Films and coatings allow transpiration readily of solvents and/or volatiles due to polymer formation. In "dry bonding" the laminate fabrics are coated with the thermally stable polymer, either by wetting the fabric with a solution of the "finished" polymer, or with solution of its precursor. After

heating, the fabric contains a solvent-free "finished" or "dead cured" polymer resin coating. The fabric is assembled in layers (plys) and heated under pressure at a temperature greater than the glass transition temperature of the thermally stable polymer to form the finished laminate.

Laminates made by the "dry bonding" technique do not exhibit the usual flow characteristic of molten stage materials. Nevertheless, a good bond can be achieved. This method is not accompanied with evolution of volatile matter, and consequently, greatly reduces any tendency for blistering in the laminate during cure or post cure (which frequently affects laminated products intended for high temperature use.)

REFERENCES

1. Romie, F. E., "A Theory for Erosion of Phenolic-Silica Nozzle Throats," TRW Systems Interoffice Correspondence, dated 14 August 1964.
2. Crank, J., and P. Nicholson, "A Practical Method for Numerical Evaluation for Solutions of Partial Differential Equations of the Heat Conduction Type," Proceedings of the Cambridge Philosophical Society, Vol. 43, pgs. 50-67, (1947).
3. Duff, R. E., and S. H. Bauer, "Equilibrium Composition of the C/H System at Elevated Temperatures," J. Chem. Phys., 36, 1754 (1962).
4. Wehr, A. G., and J. H. Launcher, "Inorganic Matrix Materials," Conference on Structural Plastics, Adhesives, and Filament Wound Composites, Vol. 1, Dec. 11-13 (1962) Plastics and Components Branch, Nonmetallic Materials Laboratory, Materials Control.
5. Glaser, F. W., and B. Post, "System Zirconium-Boron," J. Metals, 5, 1117 (1953).
6. Post, B., and F. W. Glaser, "Borides of Some Transition Metals," J. Chem. Phys., 20, 1050 (1952).
7. Post, B., and F. W. Glaser, "Crystal Structure of  $ZrB_{12}$ ," J. Metals, 4, 631 (1952).
8. Gaylord, N. G., M. Stofka, and J. Vodeharal, "Polymerization of Conjugated Dienes to Ladder Polymers and the Cyclization of Stereoregular Diene Polymers," J. Am. Chem. Soc., 85, 641 (1963).
9. Marvel, C. S., "Polyaromatic Heterocycles," Polymer Preprint of the 147th American Chemical Society Meeting, held in Philadelphia, April 1964.
10. Collier, H. E. Jr., "The Mechanism of Spectral Excitation of Metallic Ions by a New High Temperature Source," Doctoral Dissertation, Lehigh University, 1955.
11. Lewis, B., and G. von Elbe, "Combustion, Flames, and Explosions of Gases," Academic Press, New York, 1961, p. 284.
12. Sharpe, L. H., "Adhesion Reduction to Practice," Presented at the Modern Theories of Adhesion and Their Application Symposium, University of Southern California, November 6, 1964.

13. Bikerman, J. J., "Fundamentals of Adhesion," Presented at the Modern Theories of Adhesion and Their Application Symposium, University of Southern California, November 6, 1964.
14. Sharpe, L. H., and H. Schonhorn, "Adsorption Theory of Adhesion" presented at the 144th American Chemical Society Meeting, held in Los Angeles, April 1963.
15. Freeman, J. H., L. W. Frost, G. M. Bower, and E. J. Traynor, "Resins and Reinforced Plastic Laminates for Continuous Use at 650<sup>o</sup>F," "Conference on Structural Plastics, Adhesives, and Filament Wound Composites, Vol. 1, Dec. 11-13, (1962). Plastics and Composites Branch Nonmetallic Materials Laboratory, Materials Control, Wright Patterson Air Force Base.
16. Stogg, C. E., S. V. Abrams, C. E. Berr, W. M. Edwards, A. L. Endrey and K. L. Olivier, "Aromatic Polypyromellitimides from Aromatic Polyamic Acids," Polymer Reprints from the 147th American Chemical Society Meeting, held in Philadelphia, April 1964, p. 132.

DISTRIBUTION LIST

	<u>COPIES</u>
National Aeronautics and Space Administration Lewis Research Center 21000 Brookpark Road Cleveland, Ohio 44135	
Attn: Contracting Officer, MS 500-210	1
Liquid Rocket Technology Branch, MS 500-209	8
Technical Report Control Office, MS 5-5	1
Technology Utilization Office, MS 3-16	1
Air Force Systems Command Liaison Office, MS 4-1	2
Library	2
Office of Reliability and Quality Assurance, MS 500-203	1
Dr. Murray Pinns, MS 6-1	1
Mr. Jerry Winter, MS 100-1	1
National Aeronautics and Space Administration Washington, D. C. 20546	
Attn: Code RRM	1
Code RPL	2
Code SV	1
Code MT	1
National Aeronautics and Space Administration Scientific and Technical Information Facility P. O. Box 33 College Park, Maryland 20740	
Attn: NASA Representative Code CRT	6
National Aeronautics and Space Administration Ames Research Center Moffett Field, California 94035	
Attn: Library	1
Dr. John Parker	1
National Aeronautics and Space Administration Flight Research Center P. O. Box 273 Edwards, California 93523	
Attn: Library	1
National Aeronautics and Space Administration Goddard Space Flight Center Greenbelt, Maryland 20771	
Attn: Library	1

NASA CR-54471  
4176-6014-S0000

	<u>COPIES</u>
National Aeronautics and Space Administration Langley Research Center Langley Station Hampton, Virginia 23365	
Attn: Library	1
William Brooks	1
G. F. Pezdirtz	1
National Aeronautics and Space Administration Manned Spacecraft Center Houston, Texas 77001	
Attn: Library	1
J. G. Thibodaux, Code EP	1
National Aeronautics and Space Administration George C. Marshall Space Flight Center Huntsville, Alabama 35812	
Attn: Library	1
National Aeronautics and Space Administration Western Operations 150 Pico Boulevard Santa Monica, California 90406	
Attn: Library	1
National Aeronautics and Space Administration John F. Kennedy Space Center Cocoa Beach, Florida 32931	
Attn: Library	1
Jet Propulsion Laboratory 4800 Oak Grove Drive Pasadena, California 91103	
Attn: Library	1
Office of the Director of Defense Research and Engineering Washington, D. C. 20301	
Attn: Dr. H. W. Schulz, Office of Asst. Dir. (Chem. Technology)	1
Defense Documentation Center Cameron Station Alexandria, Virginia 22314	1
Research and Technology Division Bolling Air Force Base Washington, D. C. 20332	
Attn: Code RTNP	1

COPIES

Arnold Engineering Development Center Air Force Systems Command Tullahoma, Tennessee 37389 Attn: AEOIM	1
Air Force Systems Command Andrews Air Force Base Washington, D. C. 20332 Attn: SCLT/Captain S. W. Bowen	1
Air Force Rocket Propulsion Laboratory Edwards, California 93523 Attn: RPM	1
Air Force Flight Test Center Edwards Air Force Base, California 93523 Attn: FTAT-2	1
Office of Research Analyses Holloman Air Force Base, New Mexico 88330 Attn: RRRT	1
Air Force Office of Scientific Research Washington, D. C. 20333 Attn: SREP, Dr. J. F. Masi	1
Air Force Rocket Propulsion Laboratory Edwards Air Force Base, California 93523 Attn: RPC	1
Air Force Materials Laboratory Wright-Patterson Air Force Base, Ohio 45433 Attn: Code MAAE	1
Air Force Materials Laboratory Wright-Patterson Air Force Base, Ohio 45433 Attn: Code MAAM	1
Commanding Officer Ballistic Research Laboratories Aberdeen Proving Ground, Maryland 21005 Attn: AMXBR-I	1
Department of the Army U. S. Army Materiel Command Washington, D. C. 20315 Attn: AMCRD-RC	1

	<u>COPIES</u>
Commanding Officer U. S. Army Research Office Box CM, Duke Station Durham, North Carolina 27706	1
U. S. Army Missile Command Redstone Scientific Information Center Redstone Arsenal, Alabama 35808 Attn: Chief, Document Section	1
Bureau of Naval Weapons Department of the Navy Washington, D. C. 20360 Attn: DLI-3	1
Bureau of Naval Weapons Department of the Navy Washington, D. C. 20360 Attn: RMMP-2	1
Bureau of Naval Weapons Department of the Navy Washington, D. C. 20360 Attn: RMMP-4	1
Bureau of Naval Weapons Department of the Navy Washington, D. C. 20360 Attn: RRRE-6	1
Commander U. S. Naval Missile Center Point Mugu, California 93041 Attn: Technical Library	1
Commander U. S. Naval Ordnance Laboratory White Oak Silver Spring, Maryland 20910 Attn: Library	1
Commander U. S. Naval Ordnance Test Station China Lake, California 93557 Attn: Code 45	1

	<u>COPIES</u>
Commander (Code 753) U. S. Naval Ordnance Test Station China Lake, California 93557 Attn: Technical Library	1
Superintendent U. S. Naval Postgraduate School Naval Academy Monterey, California 93900	1
Commanding Officer Office of Naval Research 1030 E. Green Street Pasadena, California 91101	1
Director (Code 6180) U. S. Naval Research Laboratory Washington, D. C. 20390 Attn: H. W. Carhart	1
Director Special Projects Office Department of the Navy Washington, D. C. 20360	1
Commanding Officer U. S. Naval Underwater Ordnance Station Newport, Rhode Island 02844 Attn: W. W. Bartlett	1
Commander U. S. Naval Weapons Laboratory Dahlgren, Virginia 22448 Attn: Technical Library	1
Aerojet-General Corporation P. O. Box 296 Azusa, California 91703 Attn: Librarian	1
Aerojet-General Corporation 11711 South Woodruff Avenue Downey, California 90241 Attn: F. M. West, Chief Librarian	1
Aerojet-General Corporation P. O. Box 1947 Sacramento, California 95809 Attn: Technical Library 2484-2015A	1

	<u>COPIES</u>
Aeronutronic Division Philco Corporation Ford Road Newport Beach, California 92600 Attn: Dr. L. H. Linder, Manager Technical Information Department	1
Aeroprojects, Inc. 310 East Rosedale Avenue West Chester, Pennsylvania 19380 Attn: C. D. McKinney	1
Aerospace Corporation P. O. Box 95085 Los Angeles, California 90045 Attn: Library-Documents	1
Allied Chemical Corporation General Chemical Division P. O. Box 405 Morristown, New Jersey 07960 Attn: Security Office	1
Celanese Corporation of America Box 3049 Asheville, North Carolina 28802	1
American Cyanamid Company 1937 W. Main Street Stamford, Connecticut 06902 Attn: Security Officer	1
IIT Research Institute Technology Center Chicago, Illinois 60616 Attn: C. K. Hersh, Chemistry Division	1
ARO, Inc. Arnold Engineering Dev. Center Arnold Air Force Station, Tennessee 37389 Attn: Dr. B. H. Goethert Chief Scientist	1
Atlantic Research Corporation Shirley Highway and Edsall Road Alexandria, Virginia 22314 Attn: Security Office for Library	1

	<u>COPIES</u>
University of Denver Denver Research Institute P. O. Box 10127 Denver, Colorado 80210 Attn: Security Office	1
Battelle Memorial Institute 505 King Avenue Columbus, Ohio 43201 Attn: Report Library, Room 6A	1
Bell Aerosystems Box 1 Buffalo, New York 14205 Attn: T. Reinhardt	1
Chemical Propulsion Information Agency Applied Physics Laboratory 8621 Georgia Avenue Silver Spring, Maryland 20910	1
Propulsion Engineering Division (D. 55-11) Lockheed Missiles and Space Company 1111 Lockheed Way Sunnyvale, California 94087	1
Douglas Aircraft Company, Inc. Santa Monica Division 3000 Ocean Park Boulevard Santa Monica, California 90405 Attn: Mr. J. L. Waisman	1
Dow Chemical Company Security Section Box 31 Midland, Michigan 48641 Attn: Dr. R. S. Karpiuk, 1710 Building	1
E. I. duPont deNemours and Company Eastern Laboratory Gibbstown, New Jersey 08027 Attn: Mrs. Alice R. Steward	1
Esso Research and Engineering Company Special Projects Unit P. O. Box 8 Linden, New Jersey 07036 Attn: Mr. D. L. Baeder	1

NASA CR-54471  
4176-6014-S0000

COPIES

Ethyl Corporation Research Laboratories 1600 West Eight Mile Road Ferndale, Michigan 48220 Attn: E. B. Rifkin, Assistant Director, Chemical Research	1
General Dynamics/Astronautics P. O. Box 1128 San Diego, California 92112 Attn: Library and Information Services (128-00)	1
Hercules Powder Company Allegany Ballistics Laboratory P. O. Box 210 Cumberland, Maryland 21501 Attn: Library	1
Institute for Defense Analyses 400 Army-Navy Drive Arlington, Virginia 22202 Attn: Classified Library	1
Lockheed Propulsion Company P. O. Box 111 Redlands, California 92374 Attn: Miss Belle Berlad, Librarian	1
Marquardt Corporation 16555 Saticoy Street Box 2013 - South Annex Van Nuys, California 91404	1
Minnesota Mining and Manufacturing Company 900 Bush Avenue St. Paul, Minnesota 55106 Attn: Code 0013 R and D VIA: H. C. Zeman, Security Administrator	1
North American Aviation, Inc. Space and Information Systems Division 12214 Lakewood Boulevard Downey, California 90242 Attn: Technical Information Center D/096-722 (AJOI)	1
Rocket Research Corporation 520 South Portland Street Seattle, Washington 98108	

COPIES

Rocketdyne 6633 Canoga Avenue Canoga Park, California 91304 Attn: Library, Department 596-306	1
Rohm and Haas Company Redstone Arsenal Research Division Huntsville, Alabama 35808 Attn: Librarian	1
Texaco Experiment Incorporated P. O. Box 1-T Richmond, Virginia 23202 Attn: Dr. Gordon Miller	1
Thiokol Chemical Corporation Alpha Division, Huntsville Plant Huntsville, Alabama 35800 Attn: Technical Director	1
Thiokol Chemical Corporation Elkton Division Elkton, Maryland 21921 Attn: Librarian	1
Thiokol Chemical Corporation Reaction Motors Division Denville, New Jersey 07834 Attn: Librarian	1
Thiokol Chemical Corporation Rocket Operations Center P. O. Box 1640 Ogden, Utah 84401 Attn: Librarian	1
Thiokol Chemical Corporation Wasatch Division P. O. Box 524 Brigham City, Utah 84302 Attn: Library Section	1
United Aircraft Corporation Corporation Library 400 Main Street East Hartford, Connecticut 06118 Attn: Dr. David Rix	1

COPIES

United Aircraft Corporation Pratt and Whitney Fla. Res. and Dev. Ctr. P. O. Box 2691 W. Palm Beach, Florida 33402 Attn: Library	1
United Aircraft Corporation United Technology Center P. O. Box 358 Sunnyvale, California 94088 Attn: Librarian	1
General Electric Company Apollo Support Department P. O. Box 2500 Daytona Beach, Florida 32015 Attn: C. Day	1
Office of Advanced Research and Technology Mission Analysis Division Moffett Field, California 94035 Attn: Mr. Fred Casal	1
General Technologies Corporation 708 North West Street Alexandria, Virginia Attn: Mr. H. M. Childers	1
Plastics Technical Evaluation Center Picatinny Arsenal Dover, New Jersey Attn: SMUPA-VP3	1
Sandia Corporation Livermore Laboratory P. O. Box 969 Livermore, California 94551 Attn: Technical Library (RPT)	1
Monsanto Research Corporation Dayton Laboratory Station B, Box 8 Dayton, Ohio 45407 Attn: Library	1
Boeing Company Missile and Information Systems Division P. O. Box 3985 Seattle, Washington 98124 Attn: Robert H. Jewett for Ruth E. Peerenboom (520) Technical Library, Processes Supervisor	1

General Electric Company  
Valley Forge STC  
P. O. Box 8555  
Philadelphia, Pennsylvania 19101

COPIES

Attn: Library

1

Aerotherm Corporation  
800 Welch Road  
Palo Alto, California 94304

Attn: Mr. Roald Rindal

1